Universidade do Estado do Rio de Janeiro
Centro de Tecnologia e Ciências
Instituto de Física Armando Dias Tavares

Duive Maria van Egmond

Working towards a gauge-invariant description of the Higgs model: from local composite operators to spectral density functions

Rio de Janeiro
2020

Duive Maria van Egmond

Working towards a gauge-invariant description of the Higgs model: from local composite operators to spectral density functions

Tese apresentada, como requisito parcial para obtenção do título de Doutor, ao Programa de Pós-Graduação em Física, da Universidade do Estado do Rio de Janeiro.

Orientador: Prof. Dr. Marcelo Santos Guimarães

Rio de Janeiro

2020

CATALOGAÇÃO NA FONTE
UERJ/ REDE SIRIUS / BIBLIOTECA CTC/D

E31w Egmond, Duive Maria van.
Working towards a gauge-invariant description of the Higgs model: from local composite operators to spectral density functions / Duive Maria van Egmond. – 2020.
206 f. : il.

Orientador: Marcelo Santos Guimarães.
Tese (doutorado) - Universidade do Estado do Rio de Janeiro, Instituto de Física Armando Dias Tavares.

1. Teoria quântica de campos – Teses. 2. Yang-Mills, Teoria de – Teses. 3. Campos de calibre (Física) – Teses. 4. Higgs, Bósons de – Teses. 5. Simetria (Física) – Teses. I. Guimarães, Marcelo Santos (Orient.). II. Universidade do Estado do Rio de Janeiro. Instituto de Física Armando Dias Tavares. III. Título.

CDU 530.145

Bibliotecária: Teresa da Silva CRB7/5209

_____ _____

Assinatura Data

Duive Maria van Egmond

Working towards a gauge-invariant description of the Higgs model: from local composite operators to spectral density functions

Tese apresentada, como requisito parcial para obtenção do título de Doutor, ao Programa de Pós-Graduação em Física, da Universidade do Estado do Rio de Janeiro.

Aprovada em 11 de agosto de 2020.

Banca Examinadora:

Prof. Dr. Marcelo Santos Guimarães (Orientador)
Instituto de Física Armando Dias Tavares– UERJ

Prof. Dr. David Dudal
KU Leuven - Campus Kortrijk

Profa. Dra. Tereza Christina da Rocha Mendes
Universidade de São Paulo

Prof. Dr. Silvio Sorella
Instituto de Física Armando Dias Tavares - UERJ

Prof. Dr. Rudnei de Oliveira Ramos
Instituto de Física Armando Dias Tavares - UERJ

Prof. Dr. Antonio Duarte Perreira
Universidade Federal Fluminense

Rio de Janeiro

2020

DEDICATÓRIA

This thesis is dedicated to my father, Dr. Jacob Jan van Egmond (1949-2017). He saw this work before I did.

ACKNOWLEDGMENTS

This thesis was supposed to be written during my last months as a PhD student in Rio de Janeiro. Unfortunately, the COVID-19 pandemic kept me in my hometown in the Netherlands, where I have been reminiscing about my time in Brazil while writing this thesis. All of this under the fantastic care of my mother Marieke, and for this and many more reasons I want to thank her first and foremost.

I want to thank my parents for providing a home in which education was valued above everything else. I also want to thank my brothers Isaac and Jac and my sister Marie Beth for always, and tirelessly, challenging me with their great intelligence.

Since I went to Rio de Janeiro four years ago, I have had nothing but support from my friends and family in the Netherlands. I want to thank my family and all my friends in the Netherlands for their love and friendship. All the visits and phone calls have made me feel connected with you throughout this time. I would also like to thank my friends and colleagues at UERJ, with whom I have shared a lot of nice moments, during and after work. A special thanks to Ozório, for all the great discussions, for his encouragement and for supporting me during difficult moments.

In the four years of my PhD at UERJ, I have learned what it means to be a researcher. There are four people I would like to especially thank for that. First of all, prof. dr. Marcelo Guimarães, who taught me to trust myself and follow my curiosity. Then, prof. dr. Silvio Sorella, from whom I learned the art of writing an article, and whose phrase "fecha os olhos e vai" (close your eyes and go) has helped me in many moments during my research. Prof. dr. David Dudal, with whom I share a passion for the connection between small details and the greater picture. Prof. dr. Urko Reinosa, who taught me that you can never be sure enough about a calculation, and that there is sheer pleasure in that.

Finally, I would like to thank prof. dr. Leticia Palhares and prof. dr. Marcela Peláez for showing me what women in physics can achieve.

The present work was carried out with the support of the Coordination for the Improvement of Higher Education Personnel - Brazil (CAPES) - Financing Code 001.

All language is but a poor translation.

Franz Kafka

ABSTRACT

EGMOND, D.M. *Working towards a guage-invariant description of the Higgs model*: from local composite operators to spectral density functions. 2020. 206 f. Tese (Doutorado em Física) - Instituto de Física Armando Dias Tavares, Universidade do Estado do Rio de Janeiro, Rio de Janeiro, 2020.

We analyze different BRST invariant solutions for the introduction of a mass term in Yang-Mills (YM) theories. First, we analyze the non-local composite gauge-invariant field $A^h_\mu(x)$, which can be localized by the Stueckelberg-like field $\xi^a(x)$. This enables us to introduce a mass term in the $SU(N)$ YM model, a feature that has been indicated at a non-perturbative level by both analytical and numerical studies. The configuration of $A^h(x)$, obtained through the minimization of $\int d^4x A^2$ along the gauge orbit, gives rise to an all orders renormalizable action, a feature which will be illustrated by means of a class of covariant gauge fixings which, as much as 't Hooft's R_ξ-gauge of spontaneously broken gauge theories, provide a mass for the Stueckelberg-like field. Then, we consider the unitary Abelian Higgs model and investigate its spectral functions at one-loop order. This analysis allows to disentangle what is physical and what is not at the level of the elementary particle propagators, in conjunction with the Nielsen identities. We highlight the role of the tadpole graphs and the gauge choices to get sensible results. We also introduce an Abelian Curci-Ferrari action coupled to a scalar field to model a massive photon which, like the non-Abelian Curci-Ferarri model, is left invariant by a modified non-nilpotent BRST symmetry. We clearly illustrate its non-unitary nature directly from the spectral function viewpoint. This provides a functional analogue of the Ojima observation in the canonical formalism: there are ghost states with nonzero norm in the BRST-invariant states of the Curci-Ferrari model. Finally, the spectral properties of a set of local gauge-invariant composite operators are investigated in the $U(1)$ and $SU(2)$ Higgs model quantized in the 't Hooft R_ξ gauge. These operators enable us to give a gauge-invariant description of the spectrum of the theory, thereby surpassing certain incommodities when using the standard elementary fields. The corresponding two-point correlation functions are evaluated at one-loop order and their spectral functions are obtained explicitly. It is shown that the spectral functions of the elementary fields suffer from a strong unphysical dependence from the gauge parameter ξ, and can even exhibit positivity violating behaviour. In contrast, the BRST invariant local operators exhibit a well defined positive spectral density.

Keywords: Quantum Field Theory. Gauge-Higgs systems. Mass generation.

RESUMO

EGMOND, D.M. *Investigando em direção de uma descrição invariante de gauge*: de operadores compostos locais a funções de densidade espectral. 2020. 206 f.
Tese (Doutorado em Física) - Instituto de Física Armando Dias Tavares, Universidade do Estado do Rio de Janeiro, Rio de Janeiro, 2020.

Analisamos diferentes soluções invariantes do BRST para a introdução de um termo de massa nas teorias de Yang-Mills (YM). Primeiro, analisamos o campo invariante de calibre composto não local $A^h_\mu(x)$, que pode ser localizado pelo campo tipo Stueckelberg $\xi^a(x)$. Isto nos permite introduzir um termo de massa no modelo $SU(N)$ YM, uma característica que foi indicada em um nível não perturbativo por estudos analíticos e numéricos. A configuração de $A^h(x)$, obtida através da minimização de $\int d^4x A^2$ ao longo da órbita de calibre, dá origem a uma ação renormalizável de todas as ordens, uma característica que será ilustrada por meio de uma classe de fixações de calibre covariantes que, como tanto quanto o R_ξ-gauge de 't Hooft de teorias de calibre quebradas espontaneamente, fornecem uma massa para o campo do tipo Stueckelberg. Em seguida, consideramos o modelo unitário de Abelian Higgs e investigamos suas funções espectrais na ordem de um loop. Esta análise permite desembaraçar o que é físico e o que não é ao nível dos propagadores de partículas elementares, em conjunto com as identidades Nielsen. Destacamos o papel dos gráficos de girinos e das escolhas de medidores para obter resultados sensatos. Também introduzimos uma ação Abeliana de Curci-Ferrari acoplada a um campo escalar para modelar um fóton massivo que, como o modelo não-Abeliano de Curci-Ferrari, é deixado invariante por uma simetria BRST não-nilpotente modificada. Ilustramos claramente sua natureza não unitária diretamente do ponto de vista da função espectral. Isso fornece um análogo funcional da observação de Ojima no formalismo canônico: existem estados fantasmas com norma diferente de zero nos estados invariantes do BRST do modelo Curci-Ferrari. Finalmente, as propriedades espectrais de um conjunto de operadores compostos invariantes de calibre locais são investigadas no modelo $U(1)$ e $SU(2)$ de Higgs quantizado no medidor 't Hooft R_ξ. Esses operadores nos permitem fornecer uma descrição invariante de calibre do espectro da teoria, superando assim certas comodidades ao usar os campos elementares padrão. É mostrado que as funções espectrais dos campos elementares sofrem de uma forte dependência não física do parâmetro de calibre ξ, e podem até exibir comportamento de violação de positividade. Em contraste, os operadores locais invariantes do BRST exibem uma densidade espectral positiva bem definida.

Palavras-chave: Teoria quântica de campos. Sistemas de Gauge-Higgs. Geração de massa.

LIST OF FIGURES

LIST OF TABLES

CONTENTS

INTRODUCTION

Fundamental forces and field theory: a historical overview

Four fundamental forces seem to constitute nature: Electromagnetic force, Gravitational force and the Strong and Weak nuclear forces.

The electromagnetic force was at the heart of the development of modern physics. Classically, it is described by Maxwell's equations from 1862 (MAXWELL, 1865) in terms of electric charges that generate an electromagnetic field, which in turn exerts a force on other electric charges within that field. At the end of the nineteenth century, this picture was challenged by several experimental observations such as blackbody radiation and the photoelectric effect, which did not have an explanation within the Maxwell equations. In 1900, Max Planck introduced the idea that energy is quantized in order to derive, heuristically, a formula for the energy emitted by a black body. Planck's law (PLANCK; MASIUS, 1914) marked the beginning of quantum physics. Subsequently, Einstein explained the photoelectric effect by stating that the energy of an electromagnetic field is quantized in discrete units that were called *photons*. The photon is a *force carrier* or *messenger particle*, neutrally charged and massless, that mediates the electromagnetic force between electrically charged matter particles. The phenomenological theories of Planck and Einstein were followed by more rigorous descriptions of quantum-mechanical sytems, with the Schrödinger wave equation as the main postulate of modern quantum physics (SCHRÖDINGER, 1926).

Simultaneously to the emergence of quantum physics, Einstein's theory of special relativity (EINSTEIN et al., 1905), built on Maxwell's equations, meant a revolution in the perception of space and time. However, the concepts of relativity seemed incompatible with quantum physics: relativity theory treats time and space on an equal footing, while in quantum physics spatial coordinates are promoted to operators, with time a label. In 1928, Dirac succeeded in writing a relativistic wave equation for the electron (DIRAC, 1928), which however hypothesized negative energy solutions, pointing to the existence of anti-particles (we now know the antiparticle of the electron to be the positron). This eventually led to the development of the first quantum field theory, dubbed Quantum Electrodynamics (QED) by Dirac. In QED, electrons and other matter particles are pictured as excited states of an underlying field, just as photons are excited states of the electromagnetic field. In the associated field operator $\varphi(x,t)$, position and time are both labels, in line with relativity theory. Moreover, QED naturally incorporates negative energy states.

In order to understand the classical electromagnetic field in the light of quantum field theory, we take the classical magnetic vector potential A, whose curl is equal to the

magnetic field. This quantity had been known from Maxwell's equations but within the Schrödinger picture it overtook the electromagnetic field as the fundamental quantity. By construction, the vector potential can be changed by terms that have a vanishing curl without changing the magnetic field. This "gauge symmetry" became central to QED, where the potential was promoted to a relativistic four-vector $A_\mu(x,t)$, the photon field, and interactions of fields were summarized in a Lagrangian that is invariant under transformations of the local $U(1)$ group, called gauge transformations.

QED gives the most accurate predictions quantum physics currently has to offer. For example, the calculation of the electron's magnetic moment in QED agrees with experimental data up to ten digits. The success of QED can be attributed to the fact that many of the phenomena in our visible (low-energy) world can be approximated by perturbing the electromagnetic quantum vacuum, known as perturbation theory. Feynman diagrams are the visual representation of the perturbative contributions. However, QED is not well-defined as a quantum field theory to arbitrarily high energies, because the coupling constant (interaction strength) runs to infinity at finite energy. This divergence at high energy scale is known as the Landau pole (LANDAU et al., 1955). Other questions concerning the electromagnetic force, such as the existence of a magnetic monopole, still remain open problems today.

QED has served as the model and template for quantum field theories that try to describe the other three fundamental forces. Attempts to fit Einstein's gravity theory of curved spacetime (EINSTEIN, 2019) into the concepts of quantum field theory have not been an unqualified success. For example, the hypothetical force carrier of the gravitational force, the *graviton*, has never been detected. Moreover, the description of gravity as a field theory has been shown to fail at Planck length. Most modern research in quantum gravity is conducted in the framework of String Theory, which takes a different approach to unite quantum phyics and relativity: instead of making time and space both labels, they are both operators. Today, it is even disputed if gravitational force is truly a fundamental force, or an emergent effect of deeper quantum mechanical processes (VERLINDE, 2017).

In 1954, Yang and Mills extended the abelian $U(1)$ gauge group of QED to non-abelian gauge groups (YANG; MILLS, 1954). Their goal was to find an explanation for the strong interaction which holds subatomic particles together. Today, we know the Yang-Mills (YM) $SU(3)$ theories as the quantum field theory describing the strong interactions. The matter particles for this force are *quarks*, while the strong interaction is mediated by force carriers called *gluons*. Particles that interact under the strong force carry a *color charge*, and the YM theory of strong interactions is therefore also called Quantum Chromodynamics (QCD). Different from QED, the gauge fields themselves carry color and can thus interact with eachother. Therefore the gauge boson A_μ is displayed as $A^a_\mu T^a$, with a the color charge and T^a the $SU(3)$ generators. There are as many A^a_μ's as there

are generators, and because the number of generators for an $SU(N)$ group is $N^2 - 1$, we have eight differently colored gluons.

The fact that gluons carry color has dramatic consequences for the relation between QCD interactions and energy scale. In QED, the fact that charged particles interact less when they get further away is explained by *charge screening*. A charged particle like the electron is surrounded by the vacuum, a cloud of virtual photons and electron-positron pairs continuously popping in and out of existence. Because of the attraction between opposite charges, the virtual positrons tend to be closer to the electron and screen the electron charge. Thus, the effective charge becomes smaller at large distances (low energies, also called the infrared (IR) region), and grow stronger at small distances (high energies, also called the ultraviolet (UV) region). This is completely intuitive to us: the further away, the less interaction. It is also how Feynman diagrams are designed: a free particle comes in from the distance, interacts, and vanishes into the distance again.

In QCD, quark-antiquark pairs screen the color charged particles in the same way as the electron-positron pairs screen the electrically charged particles. However, the QCD vacuum also contains pairs of the charged gluons, which do not only carry color but also an anti-color magnetic moment. The net effect is not the screening of the color charged particle, but the augmentation of its charge. This means that the particles will interact more at larger distances, or lower energies, and vice versa. This was also observed in experiments: when high energies were applied to quarks, they hardly interacted with eachother. This means a theoretical model should have a coupling constant descreasing to zero in the UV limit. In 1973, Gross, Wilczek and Politzer proved that this is indeed the case for YM theories (GROSS; WILCZEK, 1973; POLITZER, 1973). This behaviour, called *asymptotic freedom*, is seemingly counterintuitive and can be best explained by imagining particles inside an elastic rod: in rest, there is no force between them, but the further you try to pull it apart, the more they will try to get back together. It also reminds of a superconductor: if a magnetic field is forced to run through the superconductor, the energy associated with the created flux tube grows with distance. This has led to some QCD models based on superconductivity, known as dual superconductor models (RIPKA, 2004).

Asymptotic freedom means that for QCD, the relation between energy scale and interaction strength is inverted with reference to QED. This means that it should be possible to use perturbation theory in the UV limit. Indeed, for high energy phenomena the perturbative QCD models are in excellent agreement with the experiments (JEGERLEHNER; KALMYKOV; VERETIN, 2002; JEGERLEHNER; KALMYKOV; VERETIN, 2003; MARTIN, 2015a; MARTIN, 2015b). In order to be quantized, these perturbative models demand a gauge-fixing, or choosing a gauge, in the Faddeev-Popov (FP) procedure. This introduces in YM theories so-called *ghost fields*, which are Grassmann fields that violate spin-statistics and can therefore not be physical. After gauge-fixing

there is no longer a local gauge-invariance, but there is still a residual symmetry, known as Becchi-Rouet-Stora-Tyutin (BRST) symmetry. BRST symmetry guarantees the unitarity of the quantized YM theories and can be used to derive the Slavnov-Taylor identities, which are fundamental to renormalization methods such as Algebraic Renormalization (PIGUET; SORELLA, 1995). Important is that the BRST symmetry is nilpotent, which means the BRST variation s applied on another BRST variation is zero, $s^2 = 0$. Kugo and Ojima (KUGO; OJIMA, 1978, 1978) used this to distinguish between two types of states that are annihilated by a BRST transformation: those that trivially do so because they themselves are a BRST transformations of another state, and those that are not BRST transformations of another states. Physical states are of the second type and are said to be in the BRST *cohomology*. Non-physical states, such as the ghost fields, are of the first type and are outside the BRST cohomology. BRST symmetry therefore is an important tool for the definition of physical space.

The UV regime of QCD is well described by perturbative YM theories with a FP gauge fixing. However, the standard perturbation theory is unable to access the IR regime because it presents a Landau pole. This may be related to the fact that for large coupling constants the FP procedure is not valid because the gauge-fixing is no longer unique, leading to an infinite number of copies of the gauge field in the model. This was first observed by Gribov in 1978, and is called the *Gribov ambiguity*. Over the years, various attempts have been made to deal with this problem, see for example (ZWANZIGER, 1989; ZWANZIGER, 1993; DUDAL et al., 2008a; SERREAU; TISSIER, 2012; CAPRI et al., 2016c; ZWANZIGER, 2002). Until today, no coherent analytical model for the IR region in non-abelian gauge theories is available. Nonetheless, we have learned several things about the IR physics of QCD from lattice simulations. It was found (BOWMAN et al., 2007; CUCCHIERI; MENDES; TAURINES, 2005; STRAUSS; FISCHER; KELLERMANN, 2012; DUDAL; OLIVEIRA; SILVA, 2014; DUDAL et al., 2020b), in lattice simulations for the minimal Landau gauge, that the spectral function of the gluon propagator is not non-negative everywhere, which means that in the IR there is no physical interpretation for this propagator like there is for the photon propagator in QED. This behaviour of the gluon spectral function is commonly associated with the concept of confinement (CORNWALL, 2013; KREIN; ROBERTS; WILLIAMS, 1992; ROBERTS; WILLIAMS, 1994; LOWDON, 2018), which means that quarks and gluons clump together under the strong force to form composite particles called *hadrons*. Because they are confined, we do not see isolated quarks and gluons in nature. The non-positivity of the spectral function then becomes a reflection of the inability of the gluon to exist as a free physical particle. A further important observation in lattice QCD is that the gluon propagator shows massive behaviour in the non-perturbative region. This has prompted research into massive analytical models for the QCD confinement region, which we will discuss in further detail in section 1.3.1, as well as in chapter 2, where we will discuss a

BRST invariant solution for the massive QCD model.

Through experiments in the 1950s the weak interaction, responsible for radioactive decay of the atoms, was predicted to be carried by three gauge bosons: two W bosons and one Z boson. This fits with the three generators of the $SU(2)$ YM model. Because the W bosons carry electric charge, the weak and electromagnetic force are described together in an $SU(2)\times U(1)$ theory, called electroweak theory. However, the W, Z bosons are massive, unlike the photon. In the Lagrangian, a mass term for the gauge boson would take the form

$$\mathcal{L} \supset \frac{1}{2}m^2 A_\mu A_\mu, \tag{1}$$

which is not gauge-invariant and can not be implemented into the Lagrangian by hand. We now know that the solution for this problem is given by the spontaneous symmetry breaking (SSB) due to the non-zero vacuum value of the scalar $SU(2)$ Higgs field $\Phi(x)$, and the Higgs mechanism[1] that gives mass to the gauge bosons. The $SU(2)$ gauge theory with a scalar field is referred to as Yang-Mills-Higgs (YMH) theory. The Glashow-Weinberg-Salam (GWS) model of electroweak symmetry breaking (GLASHOW, 1961; WEINBERG, 1967; SALAM, 1968), based on the Higgs mechanism, gives mass to the W, Z bosons, while keeping the photon massless. Together with QCD, the electroweak theory constitutes the Standard Model (SM) of particle physics.

The electroweak sector can be shown to be both unitary and renormalizable by employing a class of gauge-fixing called 't Hooft or R_ξ gauge, which introduces the gauge parameter ξ. Different choices of ξ highlight different properties of the model. In the formal limit $\xi \to \infty$, we end up in the unitary gauge, which is considered the physical gauge as it decouples the non-physical particles. However, this gauge is known to be non-renormalizable (PESKIN; SCHROEDER, 1995). For any finite choice of ξ, the model is renormalizable because the R_ξ gauge cancels an unrenormalizable mixing term between the gauge boson and an unphysical Goldstone boson. For $\xi \to 0$, we end up in the Landau gauge, a very useful gauge choice that picks out the transverse part of the gauge boson. Of course, any physical process or quantity should be independent of the ξ parameter. Therefore, the R_ξ gauge provides a powerful check on practical calculations.

[1] A more accurate name is the Higgs-Brout-Englert-Guralnik-Hagen-Kibble mechanism (HIGGS, 1964; ENGLERT; BROUT, 1964; GURALNIK; HAGEN; KIBBLE, 1964)

Higgs mechanism without spontaneous symmetry breaking

In most textbook accounts, the mass generation of gauge bosons through the Higgs mechanism is displayed in terms of the notion of spontaneous symmetry breaking (SSB) of the local gauge symmetry. However, the meaning of SSB in connection to the Higgs mechanism is ambiguous, since it was established already in 1975 by Elitzur (ELITZUR, 1975) that local gauge symmetries can never be spontaneously broken. In this section, I will try to make sense of these contradictory accounts and discuss the solution provided by the gauge-invariant composite local operators of 't Hooft (HOOFT et al., 1980) and Fröhlich, Morchio and Strocchi (FROHLICH; MORCHIO; STROCCHI, 1980; FROHLICH; MORCHIO; STROCCHI, 1981), which are the central subject of this thesis.

The term "spontaneous symmetry breaking" originated in the statistical physics of phase transitions. One of the best known examples is that of SSB in a ferromagnet. Above the Curie temperature T_C, the ground state of the ferromagnet is rotationally symmetric because of the random spin orientation of the atoms. Below T_C however, the ground state consists of spins which are aligned within a certain domain, thus breaking the rotational symmetry. The orientation of this alignment is random in the sense that each direction is equally likely to occur, but nevertheless one direction is chosen. So, even though the system still has a rotational symmetry, the ground state is not invariant under this symmetry and we say the symmetry is spontaneously broken.

Any situation in physics in which the ground state of a system has less symmetry than the system itself, exhibits SSB. Two different configurations of the ground state are seperated by an energy barrier, and the phenomenon of SSB therefore goes accompanied by a discontinuous change of a physical quantity related to the free energy, called the order parameter, as a function of another quantity, the control parameter. In the case of a ferromagnet, the magnetic susceptibility (order parameter) goes to infinity at the critical temperature (control parameter). Symmetry breaking of the ground state is always connected with mass generation: movement of the ground state in direction of the energy barrier has an energy cost and as is therefore "massive", while a movement in the direction perpendicular to the energy barrier costs zero energy, i.e. it is a "massless" mode. These concepts become more explicit in field theory, where the massive and massless modes correspond to genuine massive and massless bosons. This was first described by Nambu (NAMBU, 1960) for the spontaneous breaking of the chiral symmetry of massless fermions and was subsequently elucidated by Goldstone (GOLDSTONE, 1961). We can illustrate the occurrence of massless and massive SSB bosons in the simple model of a complex scalar field $\varphi(x)$ with $U(1)$ symmetry. The Lagrangian

$$\mathcal{L} \;=\; \partial_\mu \varphi^\dagger \partial_\mu \varphi - V(\varphi^\dagger \varphi) \quad \text{with} \quad V(\varphi\varphi^\dagger) = \frac{\lambda}{2}\left(\varphi^\dagger\varphi - \frac{v^2}{2}\right)^2, \;\; \lambda > 0 \tag{2}$$

Figure 1 - Higgs potential

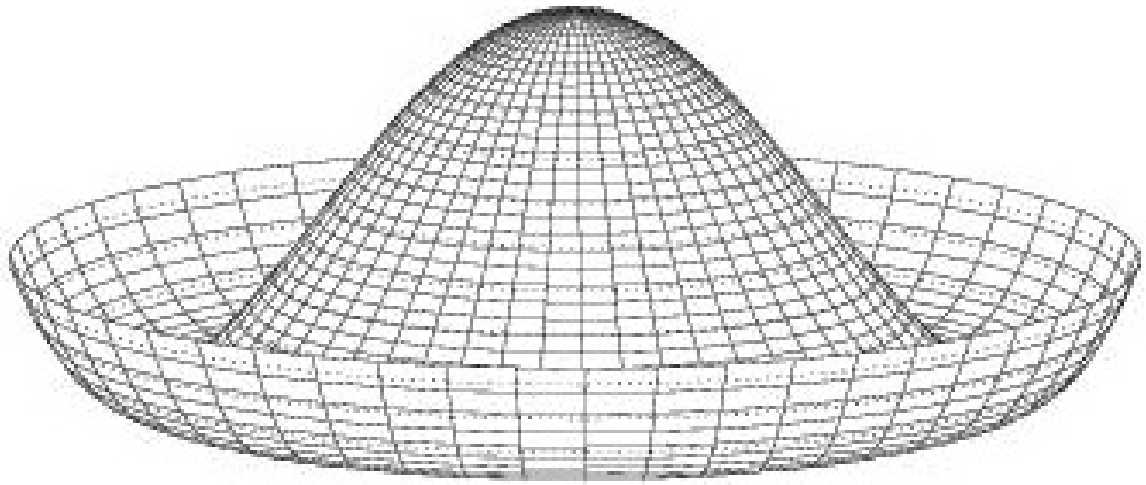

Legend: Representation of the potential for the global $U(1)$ symmetry.
Source: The author, 2020.

is invariant under the global $U(1)$ transformation $\varphi \to e^{i\alpha}\varphi$. The minimum of the potential is degenerate, because any configuration of the vacuum expectation value (vev) $\langle\varphi\rangle = \frac{v}{\sqrt{2}}e^{i\theta}$, with θ an arbitrary phase, minimizes the potential. This is the famous "Mexican hat" potential depicted in Figure 1. Any choice for θ will lead to the same $U(1)$ invariant Langrangian. However, after choosing a particular θ, the vev $\langle\varphi\rangle$ is not $U(1)$ invariant since under a global $U(1)$ transformation $\theta \to \theta + \alpha$. Thus, the $U(1)$ symmetry is spontaneously broken by the vev of the scalar field. Let us now choose one vacuum orientation, e.g. $\theta = 0$ so that $\langle\varphi\rangle = \frac{v}{\sqrt{2}}$. We can define two new real scalar field $\rho(x)$ and $\chi(x)$ with zero vev, $\langle\rho\rangle = \langle\chi\rangle = 0$, and set $\varphi = \frac{1}{\sqrt{2}}(v+\rho)\,e^{-i\chi/v}$. Then, in the Lagrangian (2) the ρ field acquires a mass $m_\rho = \lambda v$, while the field χ remains massless. The massless boson is called the Nambu-Goldstone (NG) boson, and the $U(1)$ case is the simplest example of the *Goldstone theorem*, which states that for every broken generator there is one massless Goldstone boson. For the $U(1)$ model, the SSB breaks the complete symmetry, but for more complex systems, SSB can break the symmetry group down to a subgroup under which the ground state is invariant. For example, the SSB of the chiral symmetry in QCD breaks a global $SU(3) \times SU(3)$ chiral flavor symmetry down to the diagonal $SU(3)$ group, generating eight NG bosons.

As is well-known, the global $U(1)$ symmetry can be promoted to a local $U(1)$ gauge symmetry by changing the derivative $\partial_\mu\varphi$ in (2) to the covariant derivative $D_\mu\varphi = \partial_\mu\varphi - ieA_\mu\varphi$, with A_μ the gauge boson. The Lagrangian

$$\mathcal{L} \;=\; F_{\mu\nu}F_{\mu\nu} + (D_\mu\varphi)^\dagger D_\mu\varphi - V(\varphi^\dagger\varphi) \;\text{ with }\; V(\varphi\varphi^\dagger) = \frac{\lambda}{2}\left(\varphi^\dagger\varphi - \frac{v^2}{2}\right)^2,\ \lambda > 0, \qquad (3)$$

with $F_{\mu\nu} = \partial_\mu A_\nu - \partial_\nu A_\mu$, is invariant under the local $U(1)$ transformations $\varphi \to e^{ie\alpha(x)}\varphi$ and $A_\mu \to A_\mu + \partial_\mu\alpha(x)$. Naturally, the global $U(1)$ transformations form a subgroup of the local $U(1)$ transformations, namely when $\alpha(x)$ is constant for every point in spacetime, $\alpha(x) = \alpha$. At first glance, it looks like we can repeat the SSB mechanism described for the global $U(1)$ symmetry by taking $\langle\varphi\rangle = \frac{v}{\sqrt{2}}$. The field configuration $\varphi = \frac{1}{\sqrt{2}}(v + h)\, e^{-i\chi/v}$ then will give a mass to the gauge boson, $m_A = ev$. While the Lagrangian is still invariant under a $U(1)$ gauge transformation, the vev of the scalar field is not; we seem to have a SSB of the local gauge symmetry. The $\chi(x)$ field would be the NG boson for the broken $U(1)$ gauge theory, but for gauge theories this is not a physical degree of freedom since we can use the gauge freedom to set $\chi(x) = 0$; this gauge choice is called unitary gauge.

The process described above is how the Higgs mechanism is displayed in most introductory text on the subject. It can easily be generalized to non-abelian gauge theories, and it is used to describe the $SU(2)_L \times U(1)_Y \to U(1)_{EM}$ local symmetry breaking which explains mass generation for the W and Z bosons, as well as for several fermion fields. In section 1.1 we will go further into the details of the Higgs mechanism in the electroweak sector.

Despite the phenomological success, however, there are some important objections to be made against the concept of SSB of a local gauge symmetry. The most important result in this context is Elitzur's theorem, which states that *local gauge symmetries can never be broken spontaneously.* The theorem is rigorously proven on the lattice (ELITZUR, 1975), but can be understood by the 2-D Ising model, a simple lattice configuration with two symmetry-breaking ground states: all $\uparrow$ and all $\downarrow$. In this system, to go from one ground state to the other there is an extensive energy cost, i.e. there is an energy barrier to overcome, because a change in the ground state configuration encompasses the whole system. Therefore, at low temperature the system gets stuck in a particular spin alignment and the symmetry is broken. In constrast, for local symmetries this argument does not apply. Imagine a local transformation, only acting on a very small subset of the system: this will change a ground state configuration into another ground state configuration at zero energy cost. As a consequence, there is no energy barrier between any two ground states, because they are always related by a sequence of local transformations. The system will be able to explore the entire space of ground states and there is no symmetry breaking. In the case of the local gauge symmetry, this means that $\phi(x)$, rather than being stuck in a certain gauge configuration, can move around freely around the "gauge orbit". This means that when you compute the average value of the operator over the group it must be zero; Elitzur's theorem is also stated as that

all gauge non-invariant operators must have a vanishing vev. For a more formal treatment of Elitzur's theorem in lattice theory, see for example (ITZYKSON; DROUFFE, 1991).

Of course, local gauge symmetries can be broken *explicitly* by adding a symmetry breaking term to the Lagrangian. In fact, for the quantization of a field theory we have to break the local gauge symmetry by choosing a specific gauge configuration, i.e. by gauge fixing. It seems that gauge fixing offers a way out of Elitzur's theorem. Say, for example, that in the $U(1)$ model (3) we fix the gauge in the Landau gauge, $\partial_\mu A_\mu = 0$. Since the very purpose of a gauge fixing constraint is to restrict the domain of field configurations, the constraint itself is of course not invariant under a local gauge transformation. Exceptions are the so-called Gribov copies, which appear when the gauge fixing constraint is preserved under local gauge transformations. Gribov copies jeopardize the field description of non-abelian theories in the low-energy (non-perturbative) regime. For small coupling constants, however, the Gribov copies can be ignored and it can be shown that e.g. the Landau gauge does not allow for local gauge transformations in the perturbative region. Even so, it is easy to see that $\partial_\mu A_\mu = 0$ is still invariant under the global subgroup of the $U(1)$ gauge transformation, $\alpha(x) = \alpha$. The residual global symmetry which remains after gauge fixing is called the *remnant global gauge symmetry* (CAUDY; GREENSITE, 2008). There is no theorem that forbids the SSB of *this* symmetry. We can then state that the Higgs mechanism is in fact the breaking of the remnant global symmetry by setting $\langle\phi\rangle = \frac{v}{\sqrt{2}}$ after gauge fixing. This is in fact what is done in some modern takes on the Higgs mechanism (ENGLERT, 2011).

However, there are some important distinction to be made between the SSB of the global gauge symmetry and the original formulation of SSB. In the ferromagnet, the SSB of the spin alignment means that out of all *physically* distinct configurations, one is actually realised. In contrast, the choice of a particular configuration within the global gauge symmetry does not reflect any physical outcome, and we therefore do not expect an accompanying abrupt change in any physical properties, in particular those related to the free energy. This is in agreement with findings on the lattice (FRADKIN; SHENKER, 1979) that there is no order parameter which varies discontinuously along the path going from the "confinement phase" (strong coupling) to the "Higgs phase" (weak coupling), at least in the fundamental representation of the Higgs field. This absence of a phase boundary is known as "Higgs complementarity".

A further observation about remnant global gauge symmetry is that it is ambiguous because different gauge choices will lead to different global subgroups after fixing the gauge. For example, the aforementioned unitary gauge leaves no global symmetry, while the Coulomb gauge $\partial_i A_i = 0$ leaves a large invariance, $\alpha(x) = \alpha(t)$. The question is then to decide which, if any, of these gauge-symmetry breakings is associated with a transition between physically different phases. In (CAUDY; GREENSITE, 2008), it was

found on the lattice that for SSB of the global remnant symmetry, the Landau gauge and the Coulomb gauge show distinct transition lines. Moreover, they both show a SSB at points where there is no actual phase change, making their role in the confinement-Higgs transition highly doubtful.

Another, often forgotten problem with the approach of gauge-fixing to surpass Elitzur's theorem is that choosing a gauge leaves a residual local symmetry: the BRST symmetry. The vacuum should, even after gauge-fixing, always be BRST invariant because it is a physical quantity. It thus seems there is no way around using gauge-invariant fields to represent physical particles. In non-abelian theories, these fields are necessarily composite. In (HOOFT et al., 1980), 't Hooft defined composite operators for the $SU(2)$ Higgs model. These operators are gauge-invariant combinations of the elementary YM fields, the gauge boson and the fermion fields, with the Higgs field. They are constructed in such a way that for a constant value of the Higgs field, we regain the elementary field. The gauge-invariant composite extension of the neutral Z-boson is defined as $\Phi^\dagger D_\mu \Phi$, while that of the charged $W^\pm$ bosons is given by $\varepsilon_{ij}\Phi_i D_\mu \Phi_j$ and its complex conjugate.[2] The Higgs field itself can be obtained from $\Phi^\dagger\Phi$. 't Hooft's definitions incorporate the Higgs complementarity, because there is no fundamental difference between the particle in the Higgs phase and the confining phase. In the confinement phase, the composite operators are bound states of the fundamental field with extremely strong confining forces. In the Higgs phase, the perturbative expansion of these composite operators will lead to gauge-invariant descriptions of the expected weakly-interacting degrees of freedom.

In (FROHLICH; MORCHIO; STROCCHI, 1980; FROHLICH; MORCHIO; STROCCHI, 1981), Fröhlich, Morchio and Strocchi (FMS) further formalized the role of gauge-invariant local composite operators in the Higgs mechanism. Because of their gauge invariance, the composite operators cover the whole gauge orbit, and a non-zero vev for these operators cannot break the local or global gauge invariance. Thus, taking for example the gauge-invariant extension of the Higgs field, $\mathcal{O} = \Phi^\dagger\Phi$, we can assign this field a vev $\langle\mathcal{O}\rangle = \frac{v^2}{2}$. Now, we can achieve the usual dynamics of the Higgs mechanism by taking $\Phi = \frac{1}{\sqrt{2}}(v+\rho)\, e^{-i\chi/v}$, with $\langle\rho\rangle = \langle\chi\rangle = 0$, without having to impose $\langle\Phi\rangle = v$. This is the Higgs mechanism without a symmetry breaking order parameter. The FMS mechanism gives a simple relation between the correlation functions of the gauge-invariant fields $\tilde{\mathcal{O}}(x)$ and the corresponding gauge dependent ones $\varphi = (A^a_\mu, h)$ calculated in the standard perturbation expansion. Expanding the two-point function of the composite operator we

[2] While they do not play a role in this work, fermions can also be given a gauge-invariant extension, e.g. $\Phi^\dagger\Psi$ for the neutrino and $\varepsilon_{ij}\Phi_i\Psi_j$ for the electron.

find

$$\langle \tilde{\mathcal{O}}(x)\tilde{\mathcal{O}}(y)\rangle \;\sim\; \langle \varphi(x)\varphi(y)\rangle_{\text{1-loop}} + \dots , \tag{4}$$

where ... denote higher-order loop corrections, combinations of the elementary fields which make the sum of correlation functions gauge-invariant.

In QCD, the use of composite operators is common in the description of hypothetical composite bound states in the confinement (IR) region. For example, glueballs, bound states solely composed of gluons, have a field theoretical description as the gauge-invariant operator $F_{\mu\nu}^2$ (VANDERSICKEL, Thesis (Ph.D. in Physics) - Faculty of Sciences, Universiteit Gent, Gent, 2011). There are however some important differences between configurations like glueballs and the local composite gauge-invariant operators. The local composite gauge-invariant operators have a clear connection to elementary fields: the first transforms into the latter when the Higgs field acquires a constant value. As a consequence, these operators can be analyzed in the Higgs phase by perturbative loop calculations.

The gauge-invariant FMS construction has gained little attention throughout the years. In most texts where it appears, it serves mainly as a justification of the Higgs mechanism, while for practical matters the SSB of the gauge symmetry is used. The question is whether the FMS mechanism serves a purpose outside this formal role. To try and answer that question, let us look at the gauge boson propagator

$$\langle A_\mu(x)A_\mu(y)\rangle \, , \tag{5}$$

which plays a fundamental role in QED, describing the quantum dynamical path that a photon takes when it travels from x to y, calculated by means of Feynman-diagrams. In $U(1)$ theory, the transversal part of the propagator is gauge-invariant and can therefore be associated with physically observable quantities. However, in $SU(N)$ theory the (transverse) propagator is not gauge-invariant (or BRST invariant after gauge fixing) and it is therefore impossible that this object would describe a physical quantity. Nevertheless, the propagator (5) is a much used quantity in electroweak theory, and succesfully so: the higher order calculations of the pole masses and cross sections derived from the propagator (5) are in very accurate agreement with the experimental data (JEGERLEHNER; KALMYKOV; VERETIN, 2002; JEGERLEHNER; KALMYKOV; VERETIN, 2003; MARTIN, 2015a; MARTIN, 2015b). This apparent paradox can be explained by the FMS construction. Looking at eq. (4), we can see that the pole mass of the elementary field $\varphi(x)$ should coincide with the pole mass of the gauge-invariant composite operator $\tilde{\mathcal{O}}(x)$. This was confirmed in preliminary lattice result (MAAS; MUFTI, 2014; MAAS, 2015). This means the pole mass of the gauge-dependent propagator (5) is gauge-invariant and can be interpreted as a physical quantity. The gauge-invariance of the pole

mass of (5) can also be proven by the so-called Nielsen identities (NIELSEN, 1975; GAMBINO; GRASSI; MADRICARDO, 1999; GAMBINO; GRASSI, 2000; GRASSI; KNIEHL; SIRLIN, 2001) which follow from the Slavnov-Taylor identities. The Nielsen identities ensure that the pole masses of the propagators of the transverse gauge bosons and Higgs field do not depend on the gauge parameter ξ entering the R_ξ gauge fixing condition.

Nevertheless, as one can easily figure out, the use of the non-gauge-invariant fields has its own limitations which show up in several ways. For example, the spectral density function of the elementary two-point correlation function $\langle\varphi(x)\varphi(y)\rangle$ in terms of the Källén-Lehmann (KL) representation is not protected from gauge-dependence, because the higher-order loop correction in (4) will contribute to the gauge-invariance of the $\tilde{\mathcal{O}}(x)$ spectral density function. These higher-order loop corrections are the main subject of the present work. We will show how the local gauge invariant composite operators can be introduced in the Higgs model and analyzed by perturbative loop calculations. The main goal is to gain insight in the spectral properties of the gauge bosons and Higgs fields. Calculations of spectral properties of elementary fields are plagued by an unphysical gauge-dependency, but through the use of the gauge-invariant composite operators, these feautures can be made visible.

Outline of this thesis

This thesis is organized as follows. In chapter 1, we will discuss existing massive solutions for YM theories. First, we will discuss in detail the GWS model of electroweak symmetry breaking of the Standard Model (SM) in section 1.1.1. We will also discuss other examples of the Higgs mechanism, that are not part of the SM, in 1.2. Massive solutions for the QCD sector are discussed in section 1.3.1. Chapter 2 is based on (CAPRI et al., 2018b) and was also treated in (HOLANDA, 2019). In this chapter, we will look at renormalizable gauge class for the non-local gauge invariant configuration $A^h_\mu(x)$, which can be localized by the dimensionless auxiliary Stueckelberg field ξ. In chapter 3, which is based on (DUDAL et al., 2019), we will discuss the spectral properties of the $U(1)$ Higgs model. The main purpose of this chapter is to establish the dependence of the spectral properties for the elementary fields on the gauge parameter. This analysis allows to disentangle what is physical and what is not at the level of the elementary particle propagators. In chapter 4, the gauge-invariant spectral description of the $U(1)$ Higgs model from local gauge-invariant composite operators will be discussed, as was done in (DUDAL et al., 2020a). In 5, we will extend this analysis to the $SU(2)$ Higgs model, as done in (DUDAL et al.,). The Conlusion summarizes our conclusions and discusses some ideas for future projects, based on the results of this work.

Throughout this thesis, we shall work in Euclidean four-dimensional space-time,

unless otherwise indicated.

1 MASS GENERATION WITHIN AND BEYOND THE STANDARD MODEL

1.1 The Higgs mechanism in the Standard Model

The SM describes the strong interactions, weak interactions and hypercharge in an $SU(3)_c \times SU(2)_L \times U(1)_Y$ gauge theory, where c stands for color, L for the left-handed fermions it couples to and Y for the hypercharge. Here, we will discuss the Georgi-Weinberg-Salam (GWS) model, where $SU(2)_L \times U(1)_Y \to U(1)_{\mathrm{EM}}$. Before engaging in the Higgs mechanism for this model, we will first discuss the gauge sector and the Higgs sector for the SM. We will not discuss the fermion sector here, but it is important to realize that quark and lepton masses are also generated through coupling with the Higgs field, known as Yukawa coupling. For a nice complete overview, see (LOGAN, 2014).

1.1.1 The SM gauge sector

The four-dimensional action of the SM is described in terms of field strength tensors by:

$$S_{gauge} = \int d^4x \frac{1}{4} G^a_{\mu\nu} G^a_{\mu\nu} + \frac{1}{4} W^a_{\mu\nu} W^a_{\mu\nu} + \frac{1}{4} B_{\mu\nu} B_{\mu\nu}, \tag{6}$$

with repeated indices taken as summed.

For $SU(3)_c$ we have the following field strength tensor

$$G^a_{\mu\nu} = \partial_\mu G^a_\nu - \partial_\nu G^a_\mu + g_s \, f^{abc} G^b_\mu G^c_\nu, \tag{7}$$

with g_s the strong interaction coupling strength and f^{abc} the antisymmetric structure constant. There are eight different color charges, corresponding to the eight generators T^a of $SU(3)$, given in matrix representation by $\lambda^a/2$, with λ^a the Gell-Mann matrices.

For the $SU(2)_L$ interaction, the field strength tensor is given by

$$W^a_{\mu\nu} = \partial_\mu W^a_\nu - \partial_\nu W^a_\mu + g \, \epsilon^{abc} W^b_\mu W^c_\nu, \tag{8}$$

with g the weak interaction coupling strength. There are three different charges, so the structure constant is equal to the Levi-Civita tensor $f^{abc} = \epsilon^{abc}$. The generators t^a are given in matrix representation by $\tau^a/2$, with τ^a the Pauli matrices.

For both $SU(3)_c$ and $SU(2)_L$, and any non-abelian group, the relation between the group generators is given by

$$[t^a, t^b] = if^{abc}t^c. \tag{9}$$

Finally, we have the abelian field strength tensor for the $U(1)_Y$ interaction

$$B_{\mu\nu} = \partial_\mu B_\nu - \partial_\nu B_\mu. \tag{10}$$

The gauge transformations which leave the Lagrangian (6) invariant are

$$\begin{aligned} SU(3)_c: \; G_\mu &\rightarrow U_c(x)G_\mu U_c^{-1}(x) + \frac{i}{g_c}U_c(x)\partial_\mu U_c^{-1}(x), \\ U_c &= \exp(-ig_c\theta_c^a(x)T^a) \end{aligned}$$

$$\begin{aligned} SU(2)_L: \; W_\mu &\rightarrow U_L(x)W_\mu U_L^{-1}(x) + \frac{i}{g}U_L(x)\partial_\mu U_L^{-1}(x), \\ U_c &= \exp(-ig\theta_L^a(x)t^a) \end{aligned}$$

$$\begin{aligned} U(1)_Y: \; B_\mu &\rightarrow U_Y(x)B_\mu U_Y^{-1}(x) + \frac{i}{g'Y}U_Y(x)\partial_\mu U_Y^{-1}(x), \\ U_Y(x) &= \exp\left(-ig'\theta_Y(x)Y\right) \end{aligned} \tag{11}$$

with $G_\mu = G_\mu^a T^a$, $W_\mu = W_\mu^a t^a$ and g' the coupling strength of the hypercharge interaction. In infinitesimal form, this gives

$$\begin{aligned} G_\mu^a &\rightarrow G_\mu^a - \partial_\mu\omega_c^a(x) - gf^{abc}G_\mu^b\theta_c^c(x) \\ W_\mu^a &\rightarrow W_\mu^a - \partial_\mu\theta_L^a(x) - g\epsilon^{abc}W_\mu^b\theta_L^c(x) \\ B_\mu &\rightarrow B_\mu - \partial_\mu\omega_Y(x) \end{aligned} \tag{12}$$

1.1.2 The SM Higgs sector

Clearly, the gauge sector does not allow for a massive term of the gauge bosons to be inserted in by hand, since this would violate gauge-invariance. To explain the experimentally-observed nonzero mass of the $SU(2)_L$ gauge bosons, the SM requires a new ingredient. We therefore introduce a single $SU(2)_L$-doublet scalar field, which will

lead to a mass generation of the gauge bosons by means of the Higgs mechanism.

The Higgs field Φ is given by an $SU(2)_L$-doublet of complex scalar fields that can be written as

$$\Phi = \frac{1}{\sqrt{2}} \begin{pmatrix} \phi^+ \\ \phi^0 \end{pmatrix} = \frac{1}{\sqrt{2}} \begin{pmatrix} \phi_1 + i\phi_2 \\ \phi_3 + i\phi_4 \end{pmatrix}, \tag{13}$$

with ϕ_i properly normalized real scalar fields. The Lagrangian for the Higgs sector is given by

$$\mathcal{L}_\Phi = (\mathcal{D}_\mu \Phi)^\dagger (\mathcal{D}_\mu \Phi) - V(\Phi), \tag{14}$$

with the covariant derivative

$$\mathcal{D}_\mu = \partial_\mu - ig' B_\mu Y - igW_\mu. \tag{15}$$

The Lagrangian (14) is invariant under the gauge transformations (11) in combination with

$$\begin{aligned} \Phi &\to U_Y(x)\Phi \\ \Phi &\to U_L(x)\Phi, \end{aligned} \tag{16}$$

with $U_L(x)$ and $U_Y(x)$ as defined in (11). We assign a hypercharge $Y = 1/2$ to the Higgs field, and make it a color singlet.

The most general gauge invariant potential energy function is given by

$$V(\Phi) = \frac{\lambda}{2} \left(\Phi^\dagger \Phi - \frac{v^2}{2} \right)^2, \tag{17}$$

where we will choose λ and v to be real and positive numbers.

1.1.3 The SM Higgs mechanism

In the introductory chapter, we have seen that the Higgs mechanism cannot be caused by a non-zero vev of the Higgs field $\Phi(x)$, because this field is not gauge-invariant.

However, this is not contradictory with the statement that the potential (17) is minimized by the configuration

$$\Phi_0 = \frac{1}{\sqrt{2}} \begin{pmatrix} 0 \\ v \end{pmatrix}, \tag{18}$$

as long as we do not attribute it any physical meaning, such as vacuum expectation values. In fact, eq. (18) is effectively expressing the attribution of a non-zero vev to the composite local gauge-invariant operator, namely $\langle \Phi^\dagger \Phi \rangle = \Phi_0^\dagger \Phi_0 = \frac{v^2}{2}$.

We can establish the configuration (18) by choosing

$$\phi_{3,0} = v, \qquad \phi_{1,0} = \phi_{2,0} = \phi_{4,0} = 0. \tag{19}$$

We can also define a new scalar field h defined by

$$\phi_3 = h + v \tag{20}$$

so that $h_0 = 0$, while renaming

$$\phi_1 \;\; = \;\; \rho_2, \;\; \phi_2 = \rho_1, \;\; \phi_4 = -\rho_3. \tag{21}$$

The Higgs field then becomes

$$\Phi = \frac{1}{\sqrt{2}} \begin{pmatrix} i\rho_1 + \rho_2 \\ v + h - i\rho_3 \end{pmatrix} = \frac{1}{\sqrt{2}} \left((v + h)\, 1 + i\rho^a \tau^a \right) \cdot \begin{pmatrix} 0 \\ 1 \end{pmatrix}. \tag{22}$$

Putting this configuration into the potential function (17), we find that h gains a mass $m_h = \sqrt{\lambda} v$, while the ρ^a fields are massless. We can rewrite (22) up to first order in the fields as

$$\Phi = \frac{1}{\sqrt{2}} \exp\left(\frac{i\rho^a \tau^a}{v} \right) \begin{pmatrix} 0 \\ v + h \end{pmatrix}, \tag{23}$$

and "gauge away" the fields ρ^a by making the appropriate $SU(2)$ gauge transformation. This means the ρ^a fields are no physical fields; they are "would-be" Goldstone bosons.

This gauge choice is the unitary gauge, and the Higgs field after gauge fixing becomes

$$\Phi = \frac{1}{\sqrt{2}} \begin{pmatrix} 0 \\ v + h \end{pmatrix}. \tag{24}$$

The minimizing configuration (18) is not invariant under the gauge transformations (16), because $\tau^a \Phi_0 \neq 0$ and $1\Phi_0 \neq 0$. Thus, all the generators of $SU(2)_L \times U(1)_Y$ are broken by the configuration (18). However, one linear combination of these generators remains unbroken

$$(t^3 + Y)\Phi_0 \;=\; \frac{1}{2\sqrt{2}} \left(t^3 + 1\right) \begin{pmatrix} 0 \\ v \end{pmatrix} = 0. \tag{25}$$

This is the electric charge operator

$$Q = t^3 + Y = \begin{pmatrix} 1/2 & 0 \\ 0 & -1/2 \end{pmatrix} + \begin{pmatrix} 1/2 & 0 \\ 0 & 1/2 \end{pmatrix} = \begin{pmatrix} 1 & 0 \\ 0 & 0 \end{pmatrix} \tag{26}$$

and we see from (13) that ϕ^+ is charged, while ϕ^0 is uncharged. Thus, the electromagnetic $U(1)$ symmetry group is unbroken, and the Higgs mechanism for the GWS model gives $SU(2)_L \times U(1)_Y \to U(1)_{EM}$.

1.1.4 Mass generation for gauge bosons

Let us look at the gauge-kinetic term of the Lagrangian (14). The terms quadratic in the gauge fields are

$$\left(\mathcal{D}_\mu \Phi\right)^\dagger \left(\mathcal{D}_\mu \Phi\right) \supset \frac{g^2 v^2}{8} W_\mu^a W_\mu^a + \frac{g'^2 v^2}{8} B_\mu B_\mu - \frac{g g' v^2}{4} B_\mu W^{3\mu}, \tag{27}$$

and we can write this in matrix form in the basis (W^1, W^2, W^3, B):

$$M^2 = \frac{v^2}{4} \begin{pmatrix} g^2 & 0 & 0 & 0 \\ 0 & g^2 & 0 & 0 \\ 0 & 0 & g^2 & -gg' \\ 0 & 0 & -gg' & g'^2 \end{pmatrix}, \tag{28}$$

so that for the pure $SU(2)$ theory, $g' = 0$, there is a symmetry under the rotation $W^1 \leftrightarrow W^2 \leftrightarrow W^3$, i.e. it is invariant under $W^a_\mu \to W^a_\mu + \varepsilon^{abc}\omega^b W^c_\mu$. This symmetry is called the *custodial symmetry*, and we will discuss its origin in section 1.1.5.

We can diagonalize the mass matrix by defining

$$\begin{pmatrix} Z_\mu \\ A_\mu \end{pmatrix} = \begin{pmatrix} \cos\theta_\theta & -\sin\theta_\theta \\ \sin\theta_\theta & \cos\theta_\theta \end{pmatrix} \begin{pmatrix} W^3_\mu \\ B_\mu \end{pmatrix}, \tag{29}$$

with $\cos\theta_\theta = \frac{g}{\sqrt{g^2+g'^2}}$ and $\sin\theta_\theta = \frac{g'}{\sqrt{g^2+g'^2}}$. θ_ω is called weak mixing angle. In the basis (W^1, W^2, Z, A), we have the mass matrix

$$M^2 = \frac{v^2}{4}\begin{pmatrix} g^2 & 0 & 0 & 0 \\ 0 & g^2 & 0 & 0 \\ 0 & 0 & g^2+g'^2 & 0 \\ 0 & 0 & 0 & 0 \end{pmatrix}. \tag{30}$$

We identify A_μ as the photon and Z as the neutral weak boson, while the charged weak bosons are given by the combinations

$$W^\pm = W_1 \mp iW_2. \tag{31}$$

The masses of the W and Z bosons are related by

$$\frac{M_W}{M_Z} = \cos\theta_\theta, \tag{32}$$

and for $g' \to 0$, we have $\cos\theta_\theta = 1$ and the custodial symmetry is restored.

The mass matrix (30) allows for the masses of W boson and Z boson to be determined in terms of three experimentally well known quantities. First, we have the Fermi coupling constant $G = 1.16 \times 10^{-5} GeV^-2$, which gives the minimizing constant $v = \left(G\sqrt{2}\right)^{-1/2}$. Then, the parameters g and g' can be expressed in terms of electric charge and weak mixing angle as $g\sin\theta_\theta = g\cos\theta_\theta = e$, where e is related to the fine-structure constant as $\alpha = \frac{e^2}{4\pi} = \frac{1}{137.04}$. The weak mixing angle, finally, has been determined from neutrino scattering experiments to be $\sin^2\theta_\theta = 0.235 \pm 0.005$. We have

$$M_W = \left(\frac{\alpha\pi}{G\sqrt{2}}\right)^{1/2}\frac{1}{\sin\theta_\theta}, \qquad M_Z = \left(\frac{\alpha\pi}{G\sqrt{2}}\right)^{1/2}\frac{2}{\sin 2\theta_\theta} \tag{33}$$

which gives

$$M_W \approx 77\,\mathrm{GeV}, \qquad M_Z \approx 88\,\mathrm{GeV} \tag{34}$$

which is a reasonable, but not perfect, approximation of the experimentally determined values

$$M_W = 80.22 \pm 0.26\,\mathrm{GeV}, \qquad M_Z = 91.17 \pm 0.02\,\mathrm{GeV}. \tag{35}$$

The approximation can be further improved by taking into account renormalization corrections.

1.1.5 Custodial symmetry

We can see the origin of the custodial symmetry by writing out the potential energy function

$$V(\phi) = \lambda \left(\phi_1^2 + \phi_2^2 + \phi_3^2 + \phi_4^2 - \frac{v^2}{2} \right)^2 . \tag{36}$$

This potential is cleary invariant under a larger symmetry than $SU(2)_L \times U(1)_Y$: it preserves a global $O(4)$ symmetry under which the vector $(\phi_1, \phi_2, \phi_3, \phi_4)$ transforms. The global $O(4)$ corresponds to a global $SU(2)_L \times SU(2)_R$ symmetry, as can be seen by writing Φ in the form of a bidoublet

$$\Phi = \frac{1}{\sqrt{2}} \begin{pmatrix} \phi^{0*} & \phi^+ \\ -\phi^{+*} & \phi^0 \end{pmatrix} \tag{37}$$

so that

$$V(\phi) = \frac{\lambda}{2} \left(\frac{1}{2} \mathrm{Tr}\, \Phi^\dagger \Phi - \frac{v^2}{2} \right)^2 , \tag{38}$$

is invariant under the global $SU(2)_L \times SU(2)_R$ symmetry

$$\begin{aligned} \Phi &\rightarrow M_L \Phi M_R^{-1} \\ W_\mu &\rightarrow M_L W_\mu M_R^{-1} \end{aligned} \tag{39}$$

with $M_{R,L} = \exp\left(i a^a_{R,L} \frac{\sigma^a}{2}\right)$ two independent global $SU(2)$ matrices. The minimizing configuration for Φ is the bidoublet

$$\Phi_0 = \frac{1}{\sqrt{2}} \begin{pmatrix} v & 0 \\ 0 & v \end{pmatrix}, \tag{40}$$

which breaks the global $SU(2)_L \times SU(2)_R$ symmetry down to subgroup where $M_L = M_R$. This is the *diagonal subgroup* $SU(2)_{\text{diag}}$, and it is preserved thanks to the fact that we were able to write Φ_0 proportional to the unit matrix.

In order to have the dynamical term in the Lagrangian invariant under $SU(2)_L \times SU(2)_R$, we need a covariant derivative such that

$$\mathcal{D}_\mu \Phi \rightarrow M_L \mathcal{D}_\mu \Phi M_R^{-L}, \tag{41}$$

while preserving the form of the dynamical part of the Lagrangian around the vev eq. (27). Let us start by switching off the hypercharge gauge interaction $U(1)_Y$, i.e. $g' = 0$. In this case, we can easily meet the requirements (27) and (41) by promoting $SU(2)_L$ to a local gauge symmetry, $\alpha^a_L \rightarrow \omega^a_L(x)$. Thus, the Lagrangian

$$\mathcal{L}_\Phi = \text{Tr}\left(\mathcal{D}_\mu \Phi\right)^\dagger \left(\mathcal{D}_\mu \Phi\right) - \lambda \left(\text{Tr}\, \Phi^\dagger \Phi - \frac{v^2}{2}\right)^2, \tag{42}$$

with

$$\mathcal{D}_\mu = \partial_\mu - i \frac{g}{2} W^a_\mu \sigma^a, \tag{43}$$

has an $SU(2)_{L,local} \times SU(2)_{R,global}$ symmetry. The minimizing configuration (40) breaks this symmetry down to the global symmetry of the diagonal subgroup $SU(2)_{\text{diag}}$, defined by $M_L = M_R$ in eq. (39). Under this symmetry, the gauge field transforms in infinitesimal form as $W^a_\mu \rightarrow W^a_\mu + \varepsilon^{abc} \omega^b W^c_\mu$. The diagonal subgroup $SU(2)_{\text{diag}}$ is the custodial symmetry.

Switching on g', we see from (27) that the custodial symmetry is broken. We can see this in the Lagrangian when we try to add the $U(1)_Y$ gauge symmetry, while preserving

the $SU(2)_{L,local} \times SU(2)_{R,global}$ symmetry. If we change the covariant derivative to the full $SU(2)_L \times U(1)_Y$ covariant derivative in eq. (15) while using the bioublet Higgs field (37) , we would get an erroneous, 'custodial' result

$$\mathrm{Tr}\left(\mathcal{D}_\mu \Phi\right)^\dagger \left(\mathcal{D}_\mu \Phi\right) \supset \frac{g^2 v^2}{8} W_\mu^a W_\mu^a + \frac{g'^2 v^2}{8} B_\mu B_\mu. \tag{44}$$

We could also define a new covariant derivative

$$\mathcal{D}_\mu \;=\; \partial_\mu - i\frac{g}{2}\left(W_\mu^a \sigma^a\right)_L + i\frac{g'}{2}\left(B_\mu \sigma^3\right)_R, \tag{45}$$

which gives the right result (27) at $\Phi = \Phi_0$. We then have to gauge the third generator of M_R and identify it with the hypercharge generator, $\alpha_R^3 \to \theta_Y(x)$. The generator of the custodial symmetry would be the electric charge $Q = t^3 + Y$, which remains unbroken because Φ_0 is not charged and therefore $Q = 0$ at this point. However, gauging only one component of a global symmetry violates the global symmetry. Thus, the custodial symmetry is only an approximate global symmetry of the SM, violated by hypercharge gauge interactions.

The custodial symmetry is important because it rules out some possible scalar field configurations. The ρ parameter

$$\rho \equiv \frac{M_W^2}{\cos^2\theta_\theta M_Z^2} \tag{46}$$

was experimentally measured to be very close to its 'custodial' value $\rho = 1$. Now imagine a complex triplet X with $Y = 1$ and a minimizing configuration

$$X_0 = \begin{pmatrix} 0 \\ 0 \\ v_X \end{pmatrix} \tag{47}$$

so that

$$\left(\mathcal{D}_\mu X\right)^\dagger \left(\mathcal{D}_\mu X\right) \supset g^2 v_X^2 W_\mu^+ W_\mu^- + g^2 v_X^2 W_\mu^3 W_\mu^3 + g'^2 v_X^2 B_\mu B_\mu - 2gg' v_X^2 B_\mu W^{3\mu}. \tag{48}$$

The mass matrix is therefore, in the basis (W^1, W^2, W^3, B)

$$M_X^2 = v_X^2 \begin{pmatrix} g^2 & 0 & 0 & 0 \\ 0 & g^2 & 0 & 0 \\ 0 & 0 & 2g^2 & -2gg' \\ 0 & 0 & -2gg' & 2g'^2 \end{pmatrix}, \tag{49}$$

which we can diagonalize this in the same way as the Φ mass matrix by using the weak mixing angle matrix (29), so that in the basis (W^1, W^2, Z, A)

$$M_X^2 = v_X^2 \begin{pmatrix} g^2 & 0 & 0 & 0 \\ 0 & g^2 & 0 & 0 \\ 0 & 0 & 2(g^2 + g'^2) & 0 \\ 0 & 0 & 0 & 0 \end{pmatrix}. \tag{50}$$

The photon is still massless, but the custodial symmetry for $g' \to 0$ is no longer present.

In the presence of both the Φ doublet and the X triplet we have

$$M_W^2 = \frac{g^2}{4}(v^2 + 4v_X^2), \qquad M_Z^2 = \frac{g^2 + g'^2}{4}(v^2 + 8v_X^2) \tag{51}$$

so that

$$\rho = \frac{v^2 + 4v_X^2}{v^2 + 8v_X^2}, \tag{52}$$

so that v_X has to be very small compared to v to meet the experimental value of ρ. Thus, the existence of a scalar boson X with a significant minimizing value X_0 is ruled out by the custodial symmetry. However, combinations of X with other triplets can restore the custodial symmetry, and make for some interesting beyond-the-SM phenomenology (LOGAN, 2014).

1.1.6 R_ξ gauge class

In the previous sections, we have restricted ourselves to a specific gauge choice, the unitary gauge. Even though the gauge choice should never affect any physical outcome, different gauge choices help us to understand different aspects of our model. For example, in the unitary gauge all fields are physical, which proves the unitarity of the S-matrix.

On the other hand, using e.g. the Landau gauge, we can prove the renormalizability of the Higgs model.

Instead of using different gauge fixing models, we can combine several gauge choices into a *gauge class*. Gauge classes can go through different gauge choices by means of an unphysical *gauge parameter*. For example, the Linear Covariant Gauges (LCG) is a gauge class given by $\partial_\mu A_\mu = \alpha\, b$, with b an auxiliary field and α the gauge parameter. For $\alpha = 0$, we end up in the Landau gauge, while for finite α the gauge field acquires a longitudinal component. Of course, physical quantities should never depend on α; the gauge parameter is therefore also an important check of the physicality of our outcome.

In this section, we will discuss the R_ξ gauge class, introduced by 't Hooft to prove the renormalizability of the Higgs model. It is therefore an important gauge class for the GWS model, but can be understood in the $U(1)$ Higgs model. In the action

$$S = \int d^4x \left\{ \frac{1}{4} F_{\mu\nu} F_{\mu\nu} + (D_\mu \varphi)^\dagger D_\mu \varphi + \frac{\lambda}{2} \left(\varphi^\dagger \varphi - \frac{v^2}{2} \right)^2 \right\}, \tag{53}$$

we can parametrize $\varphi(x) = \frac{1}{\sqrt{2}}(v + h(x)) e^{-i\chi(x)/v}$, and then make the unitary gauge choice $\chi(x) = 0$. This decouples the non-physical "would-be" NG boson. However, expanding the Lagrangian we have for the squared gauge boson terms

$$\mathcal{L} \supset -\frac{1}{2} A_\mu \partial^2 A_\mu + \frac{1}{2} A_\mu \partial_\mu \partial_\nu A_\nu + \frac{1}{2} m^2 A_\mu A_\mu, \tag{54}$$

with $m = ev$. The two-point function for the gauge boson is then given by

$$\langle A_\mu(p) A_\nu(-p) \rangle = \frac{1}{p^2 + m^2} \mathcal{P}_{\mu\nu}(p^2) + \frac{1}{m^2} \mathcal{L}_{\mu\nu}(p^2), \tag{55}$$

with $\mathcal{P}_{\mu\nu}(p^2) = \delta_{\mu\nu} - \frac{p_\mu p_\nu}{p^2}$ and $\mathcal{L}(p^2) = \frac{p_\mu p_\nu}{p^2}$ the transversal and longitudinal projectors. The longitudinal part does not vanish for large values of the momentum p, and we cannot prove renormalizability.

The problem with renormalizability can be made more explicit by adapting another parametrization of the scalar field in eq. (53), namely $\varphi(x) = \frac{1}{\sqrt{2}}(v + h(x) + i\rho(x))$. This will lead to a term in the Lagrangian

$$\mathcal{L} \supset m\, A_\mu \partial_\mu \rho, \tag{56}$$

and this mixing term between the gauge boson and the would-be NG boson will lead to

unrenormalizable results. We therefore employ the gauge-fixing action

$$S_{gf} = \int d^4x \left\{ \frac{1}{2\xi} \left(\partial_\mu A_\mu + \xi m \rho\right)^2 \right\}, \tag{57}$$

known as the R_ξ gauge class with the gauge parameter ξ. The mixing term in (57) will cancel exactly the unwanted mixing term (56). The two-point function for the gauge boson is now given by

$$\langle A_\mu(p) A_\nu(-p) \rangle \;=\; \frac{1}{p^2 + m^2} \mathcal{P}_{\mu\nu}(p^2) + \frac{\xi}{p^2 + \xi m^2} \mathcal{L}_{\mu\nu}(p^2), \tag{58}$$

and we can show that this gauge is renormalizable for all finite values of ξ. Notice that for $\xi = 0$ we end up in the Landau gauge, while in the limit $\xi \to \infty$ we find back eq. (55), the unitary gauge. This means the R_ξ-gauge is both unitary and renormalizable. The would-be Goldstone remains in the Lagrangian and has a two-point function

$$\langle \rho(p) \rho(-p) \rangle = \frac{1}{p^2 + \xi m^2}, \tag{59}$$

but the very fact that its mass depends on the ξ-parameter brands it as unphysical. The same thing happens for the ghost field.

Another important feature of the R_ξ-gauge is that we can show, in non-abelian and abelian gauge theories, that the pole masses of the two-point function of both the gauge boson $A_\mu(x)$ and the Higgs field $h(x)$ do not depend on the gauge parameter ξ (GAMBINO; GRASSI, 2000). This property, contained in the Nielsen Identities (NIELSEN, 1975), is important because it allows to give a physical meaning to the polemass of the otherwise gauge-dependent (and therefore unphysical) correlation functions.

Even though the R_ξ-gauge is unique to the Higgs model because it requires the Goldstone boson ρ^a, the concepts of this gauge class can be used to define a renormalizable class of gauge-fixing also outside of the Higgs environment, as we will see in chapter 2.

1.2 Higgs beyond the Standard Model

The Higgs mechanism for the electroweak sector has been firmly established as the mechanism that gives mass to the W, Z bosons, as well as some fermions, while leaving the photons massless. In 2012, the Higgs boson was discovered at the CERN Large Hadron Collidor (LHC) (AAD et al., 2012; CHATRCHYAN et al., 2012), in full agreement with

the SM predictions.

It is nonetheless important to realize that there is no *a priori* reason that the Higgs mechanism only occurs in the version $SU(2) \times U(1) \to U(1)$. The Higgs mechanism can be described for any gauge theory, such as the simple example $U(1) \to$ nothing that we discussed in the introduction. However, the photon is massless, so we know that nature did not provide for a $U(1)$ Higgs boson. Still, the $U(1)$ Higgs model is a useful toy model to study several properties of the Higgs model, as we will see in chapter 3 and 4 . Another useful model is $SU(2) \to$ nothing, the Higgs-Yang-Mills (HYM) model which can be achieved by setting $g' = 0$ in the electroweak model. This model will be central to chapter 5. As we have seen in the previous section, the pure $SU(2)$ model will exhibit a full custodial symmetry.

Since the discovery of the Higgs mechanism, several symmetry breaking models have been proposed besides the GWS model. We will discuss two of them, both proposed by Georgi and Glashow. Then, we will also disuss how the Higgs mechanism would occur in QCD in the presence of an $SU(3)$ Higgs boson.

It is important to mention that while all the examples of the Higgs mechanism in this section are variations of the Higgs mechanism in the electroweak sector, the same mechanism of a non-zero minimizing value is also widely used in other areas such as condensed matter physics, where it was first established by Anderson (ANDERSON, 1962) as an analogy to the Landau-Ginzburg effective model of superconductivity.

1.2.1 $\underline{SU(2) \to U(1)}$

This model, proposed in (GEORGI; GLASHOW, 1972), provides an alternative Higgs model in the electroweak sector. Since $SU(2)$ is homeomorphic to $SO(3)$, we will use the Hermitian traceless generators

$$\tau^1 = \begin{pmatrix} 0 & 0 & 0 \\ 0 & 0 & -i \\ 0 & i & 0 \end{pmatrix} \quad \tau^2 = \begin{pmatrix} 0 & 0 & i \\ 0 & 0 & 0 \\ -i & 0 & 0 \end{pmatrix} \quad \tau^3 = \begin{pmatrix} 0 & -i & 0 \\ i & 0 & 0 \\ 0 & 0 & 0 \end{pmatrix}, \tag{60}$$

so that $(\tau^a)^{bc} = -i\epsilon^{abc}$. This is a real representation, so the Lagrangian is given by

$$\mathcal{L} = -\frac{1}{4} F^a_{\mu\nu} F^a_{\mu\nu} + \frac{1}{2} (\mathcal{D}_\mu \phi)^2 - \frac{\lambda}{8} \left(\phi\phi^\dagger - v^2 \right)^2, \tag{61}$$

and the minimizing value of $\phi(x)$ is

$$\phi = \begin{pmatrix} 0 \\ 0 \\ v \end{pmatrix} \tag{62}$$

so that the mass matrix is given by

$$M^2 = \begin{pmatrix} m^2 & 0 & 0 \\ 0 & m^2 & 0 \\ 0 & 0 & 0 \end{pmatrix}, \tag{63}$$

which means two gauge bosons, A^1_μ and A^2_μ, are massive, while A^3_μ is massless.

The above model does not account for the neutral Z-boson and is therefore not the correct theory for the electroweak mass generation. However, as was shown in (HOOFT, 1974), identifying the photon with the massless A^3_μ does provide for a radial magnetic field which indicates the existence of a magnetic monopole. The magnetic monopole, often hypothesized but never found, is not present in the GWS model.

1.2.2 $SU(5) \to SU(3) \times SU(2) \times U(1)$

It would be aesthetically nice if the standard model was the low-energy phenomenology of a larger gauge theory. This is the idea of a Grand Unified Theory (GUT). Georgi and Glashow proposed a model to this effect in (GEORGI; GLASHOW, 1974). The required Higgs field transforms under the adjoint representation of SU(5) and can be represented by 5×5 hermitian traceless matrix. The Higgs field transforms under the adjoint representation as

$$\Phi^a \to \Phi^a + f^{abc}\omega^b\Phi^c \tag{64}$$

or, adding a generator t^a on both sides

$$\Phi \to \Phi - i\omega^a[t^a, \Phi], \tag{65}$$

so that configurations of Φ that commute with a (sub)group with generators t^a are invariant under the gauge transformation related to this (sub)group.

As for any non-abelian gauge theory, the covariant derivative in the adjoint repre-

sentation is given by

$$D_\mu^{ab} = \delta^{ab}\partial_\mu - g f^{abc} A_\mu^c \tag{66}$$

with $N^2 - 1 = 24$ different color charges, corresponding to the 24 generators t^a of $SU(5)$. We can use eq. (9) and the normalization $[t^a, t^b] = \frac{\delta^{ab}}{2}$ to write the mass term of the Lagrangian as

$$\mathcal{L}_m = \frac{g^2}{2}(f^{abc} A_\mu^b \Phi_0^c)^2 = -g^2 \mathrm{Tr}[[t^a, \Phi_0][t^b, \Phi_0]] A_\mu^a A_\mu^b, \tag{67}$$

which means, from eq. (65), that gauge bosons corresponding to unbroken symmetries remain massless.

If we choose

$$\Phi_0 = v \begin{pmatrix} 2 & 0 & 0 & 0 & 0 \\ 0 & 2 & 0 & 0 & 0 \\ 0 & 0 & 2 & 0 & 0 \\ 0 & 0 & 0 & -3 & 0 \\ 0 & 0 & 0 & 0 & -3 \end{pmatrix}, \tag{68}$$

this commutes with the $SU(3)$ subgroup $\begin{pmatrix} T^a & 0 \\ 0 & 0 \end{pmatrix}$, the $SU(2)$ subgroup $\begin{pmatrix} 0 & 0 \\ 0 & t^a \end{pmatrix}$ and the $U(1)$ subgroup corresponding to the generator proportional to Φ_0. We then have twelve massless gauge bosons, corresponding to the unbroken generators of $SU(3)\times SU(2)\times U(1)$, and twelve massive gauge bosons. This adjoint Higgs particle would only accomplish the seperation of the different interactions. Another Higgs field, in the fundamental representation, would provide electroweak symmetry breaking.

The attractiveness of the $SU(5)$ model, besides its simplicity, lies in the fact that matter particles fit neatly into representations of $SU(5)$. A single generation of the standard model fits perfectly into two irreducible representations of $SU(5)$, the $\overline{5}$ and 10. However, the model predicts many unobserved phenomena such as proton decay, and quark-to-lepton mass ratios that don't agree with experiment. It also predicts particles so heavy ($M_{GUT} \approx 10^{15}$ GeV) that they cannot be detected.

1.2.3 $\underline{SU(3) \to SU(2) \times U(1)}$

The $SU(3)$ Higgs mechanism works in a similar way as that of $SU(5)$. In the adjoint representation, the minimizing configuration

$$\Phi_0 = v \begin{pmatrix} 1 & 0 & 0 \\ 0 & 1 & 0 \\ 0 & 0 & -2 \end{pmatrix}, \tag{69}$$

commutes with the $SU(2)$ subgroup $\begin{pmatrix} t^a & 0 \\ 0 & 0 \end{pmatrix}$, the Gell-Mann matrices $\lambda_{1,2,3}$, and the $U(1)$ subgroup corresponding to the generator proportional to Φ_0, i.e. λ_8. This amounts to four massless gauge bosons, corresponding to the unbroken generators of $SU(2) \times U(1)$, and four massive gauge bosons, corresponding to $\lambda_{4,5,6,7}$. From (67) one can then find the mass of the gauge bosons, $m = 3gv$.

It is well-known that gluons in the high-energy (perturbative) regime are massless. Therefore, we do not expect a Higgs boson for the strong interaction. However, in non-perturbative regimes there are indications of massive behaviour, as we will discuss in the next section.

1.3 **Massive solutions for the QCD sector**

In the high-energy regime, the FP procedure gives the gauge-fixed YM action for the massless QCD sector:

$$S = \int d^4x \left\{ \frac{1}{4} F^a_{\mu\nu} F^a_{\mu\nu} + b^a \partial_\mu A^a_\mu + \overline{c}^a \partial_\mu D^{ab}_\mu c^b \right\}, \tag{70}$$

with the covariant derivative D^{ab}_μ in the adjoint representation of the gauge group as in eq. (66), the fields $(\overline{c}^a, c^a)$ denoting the FP ghosts and b^a the Lagrange multiplier implementing the Landau gauge condition $\partial_\mu G^a_\mu = 0$. The gauge-fixed Lagrangian is invariant under the nilpotent BRST symmetry

$$\begin{aligned} sA^a_\mu &= -D^{ab}_\mu c^b \\ sc^a &= \frac{1}{2} g f^{abc} c^b c^c \\ s\overline{c}^a &= b^a \\ sb^a &= 0, \end{aligned} \tag{71}$$

with $s^2 = 0$. Notice that the Lagrangian in eq. (70) describes any $SU(N)$ theory. As we will see in what follows, in some cases an $SU(2)$ theory is used as a simplification of the $SU(3)$ theory to describe the gluon dynamics of the strong interaction. Notice also that we use the denotation for the gluon field strength tensor $F^a_{\mu\nu}$ and for the vector field A^a_μ, instead of $G^a_{\mu\nu}$ and G^a_μ from section 1.1.1 [3].

The predictions in the QCD sector derived from the Lagrangian in eq. (223) through perturbation theory agree with what has been observed in high-energy experiments. However, when extending this analysis to finite energies, the coupling constant g_c diverges and hits a Landau pole. In early studies of QCD, this behaviour was seen as responsible for the IR counterpart of asymptotic freedom, the "IR slavery" that keeps the gluons and quarks confined (ALKOFER; SMEKAL, 2001). In other words, confinement was seen as a direct consequence of the Landau pole. However, the modern view based on lattice simulations is that the Landau pole is not an expression of confinement, but rather a sign that some non-perturbative effect, such as the Gribov ambiguity, invalidates the extension of the perturbative results to the IR regime.

The Gribov ambiguity or Gribov problem, first described by Gribov in (GRIBOV, 1978), demonstrates the non-uniqueness of the FP gauge-fixing beyond the perturbative level. To explain this, let us consider the Landau gauge, although an analogous argument can be cast in other gauges. If two gluon fields A^a_μ and A'^a_μ connected by a gauge transformation

$$A'^a_\mu = A^a_\mu - D^{ab}_\mu \alpha^b, \tag{72}$$

they are said to be on the same *gauge orbit*. Now if both fields are satisfying the same gauge fixing condition, i.e. $\partial_\mu A_\mu = \partial_\mu A'_\mu = 0$, so that

$$-\partial_\mu D^{ab}_\mu \alpha^b = 0, \tag{73}$$

this means that the FP procedure failed to fully eliminate the multiple counting of physical states in the path integral due to gauge invariance. So, when eq. (73) has solutions for certain values of the gauge field, so-called *zero modes*, this means the model still contains different gauge configurations, known as *Gribov copies*. Notice that for small values of the coupling constant g_c, the LHS of eq. (73) reduces to $\partial^2\alpha$, which has only positive eigenval-

[3] This is in line with most articles written on the subject of YM theories, since for pure YM theories there is no danger of confusion with the photon field A_μ.

ues. Therefore, the Gribov problem does not exist in the UV regime, and the FP procedure is valid there. Over the years, various attempts have been made to deal with this problem in the continuum functional approach, mainly by trying to evaluate the path integral in such a way that it contained no zero modes. The most notable attempts in this direction are the Gribov-Zwanziger (GZ) approach (ZWANZIGER, 1989; ZWANZIGER, 1993; ZWANZIGER, 2002) and the Refined Gribov-Zwanziger (RGZ) approach (DUDAL et al., 2008b; DUDAL et al., 2008a; DUDAL; SORELLA; VANDERSICKEL, 2011; CAPRI et al., 2016c), recently formulated in a BRST invariant fashion (CAPRI et al., 2015; CAPRI et al., 2016c; CAPRI et al., 2016a; CAPRI et al., 2017a; CAPRI et al., 2017b). For a nice overview of the Gribov problem and the (R)GZ approach, see (VANDERSICKEL; ZWANZIGER, 2012).

The breakdown of the FP procedure and the existence of a Landau pole demonstrate the necessity of non-perturbative components that break with the standard FP gauge-fixed YM picture. This has lead to analytical QCD models that fundamentally differ from the model in eq. (70) in the IR, but preserves the standard FP predictions in the UV. Interestingly, the problem of the Landau pole in asymptotically free theories is in some cases circumvented by the introduction of an infrared gluon mass. Still, however, we want to recover the massless character of the FP gauge fixing theory in the perturbative UV region. A model which implements an effective mass only in the IR region was first proposed in (CORNWALL, 1982) based on the idea of a momentum-dependent or dynamical gluon mass (PARISI; PETRONZIO, 1980; BERNARD, 1982). For this, the Schwinger-Dyson (SD) equations are employed in order to get a suitable gap equation that governs the evolution of the dynamical gluon mass $m(p)$, which vanishes for $p^2 \to \infty$. This setup preserves both renormalizability and gauge invariance.

The SD equations give relations between Green's functions that go beyond perturbation theory. In principle this would make them the most important analytical tool to get insight in the gluon propagator in the IR regime, and they are often employed as such (BINOSI; IBANEZ; PAPAVASSILIOU, 2012; AGUILAR; BINOSI; PAPAVASSILIOU, 2014; CYROL et al., 2016; HUBER, 2018; BOUCAUD et al., 2012). However, in practice the SD equations are hard to work with because they entail an infinite set of coupled equations for the vertex functions, which somehow needs to be truncated. This requires involved techniques and calculations, with in some cases an important numerical part. Numerically, the IR regime of the gluon propagator is more rigorously described by lattice simulations. One important observation on the lattice is that the gluon propagator reaches a finite positive value in the deep IR for space-time Euclidean dimensions $d > 2$, see e.g. (CUCCHIERI; MENDES, 2007; CUCCHIERI; MENDES, 2008; BOGOLUBSKY et al., 2009; MAAS, 2009; CUCCHIERI; MENDES; SANTOS, 2009; CUCCHIERI; MENDES, 2010; CUCCHIERI; MENDES, 2009; CUCCHIERI et al., 2012; BORNYAKOV; MITRJUSHKIN; MULLER-PREUSSKER, 2010; OLIVEIRA;

Figure 2 - Lattice gluon propagator.

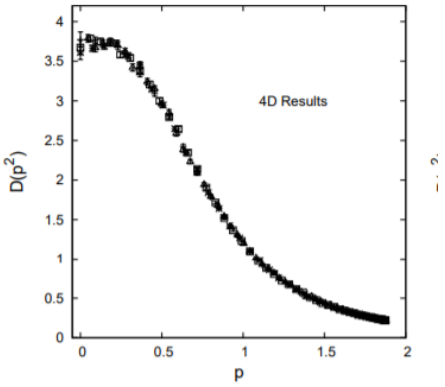

Legend: The gluon propagator $D(p^2)$ as a function of the lattice momenta p, with p given in GeV.
Source: CUCCHIERI, MENDES; 2009, p.09.

SILVA, 2012; BICUDO et al., 2015; CUCCHIERI et al., 2016; DUARTE; OLIVEIRA; SILVA, 2016; DUDAL; OLIVEIRA; SILVA, 2018; BOUCAUD et al., 2018). This saturation of the gluon propagator for small momenta p, see Figure 2, indicates massive behavior of the gluon in the IR regime. Massive-like behavior for the gluon propagator, known as the decoupling solution, has also emerged within other approaches, as the study of the Schwinger-Dyson equations, the Renormalization Group and other techniques, see for instance (AGUILAR; BINOSI; PAPAVASSILIOU, 2008; AGUILAR; BINOSI; PAPAVASSILIOU, 2016; FISCHER; MAAS; PAWLOWSKI, 2009; AGUILAR; BINOSI; PAPAVASSILIOU, 2015; HUBER, 2015; FISCHER; PAWLOWSKI, 2009; WEBER, 2012; FRASCA, 2008; SIRINGO, 2016) and references therein.

1.3.1 Massive Yang-Mills model

The lattice results, as well as the fact that the Landau pole can be circumvented by an effective gluon mass, has stimulated research into effective massive models for the IR region of QCD. The aforementioned RGZ theory is an example of such a model. In this section we will discuss another example: the massive YM model from (TISSIER; WSCHEBOR, 2010), which is a particular case of the Curci-Ferrari (CF) model (CURCI; FERRARI, 1976a). The action for this theory is

$$S = \int d^4x \left\{ \frac{1}{4} G^a_{\mu\nu} G^a_{\mu\nu} + b^a \partial_\mu A^a_\mu + \overline{c}^a \partial_\mu D^{ab}_\mu c^b + \frac{1}{2} m^2 A^a_\mu A^a_\mu \right\}, \tag{74}$$

which is a Landau gauge FP Euclidean Lagrangian for pure gluodynamics, supplemented with a gluon mass term. This term modifies the theory in the IR but preserves the FP perturbation theory for momenta $p \gg m$. It was argued that this model could be part of a complete gauge-fixing in the Landau gauge, since a CF gluon mass term may arise after the Gribov copies have been accounted for via an averaging procedure (SERREAU; TISSIER, 2012), see also (TISSIER, 2018) for a related discussion in a different gauge. The mass term breaks the BRST symmetry of the model, which means the unitarity of the model can be no longer proven (BOER et al., 1996), although it is debatable whether some non-perturbative effect could restore unitarity. However, since the BRST breaking is soft, it does not spoil renormalizability. The Lagrangian (74) turns out to be still invariant under a modified BRST symmetry

$$\begin{aligned} s_m A^a_\mu &= -D^{ab}_\mu c^b \\ s_m c^a &= \frac{1}{2} g f^{abc} c^b c^c \\ s_m \overline{c}^a &= b^a \\ s_m b^a &= i m^2 c^a, \end{aligned} \tag{75}$$

which is however not nilpotent since $s_m^2 \overline{c}^a \neq 0$.

The massive YM model is not justified *a priori* from first principles. Instead, its legitimacy is measured by how well it accounts for lattice results. In (TISSIER; WSCHEBOR, 2010; TISSIER; WSCHEBOR, 2011; GRACEY et al., 2019), it has been shown that, both at one and two-loop order, the model reproduces very well the lattice predictions for the gluon and ghost propagator, see Figure 3. It was also shown that with an adequate renormalization scheme, dubbed the Infrared Safe (IS) scheme, there is no Landau pole.

The analysis of the gluon propagator in (TISSIER; WSCHEBOR, 2010; TISSIER; WSCHEBOR, 2011; GRACEY et al., 2019) was done by perturbative loop calculations. How can the non-perturbative region be accessed with perturbative methods? In (TISSIER; WSCHEBOR, 2011; GRACEY et al., 2019), it is claimed that higher loop corrections for this model seem to be rather small, even for a significantly high coupling constant ($g = 7.5$ in (TISSIER; WSCHEBOR, 2011)). The reason for this, as explaind in (TISSIER; WSCHEBOR, 2011), lies in the massive gluons. When momenta are much smaller than the gluon mass, all diagrams that include internal gluon lines are suppressed by inverse powers of the gluon mass. This means that higher order loop terms, which naturally possess more internal gluon lines, will be surpressed. Thus, using an effective mass term makes perturbative loop calculations possible in an otherwise non-perturbative region.

Figure 3 - Gluon propagator

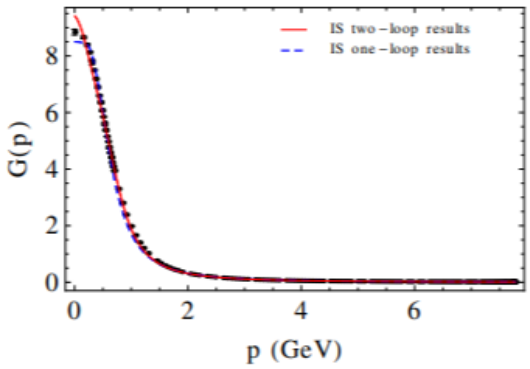

Legend: The gluon propagator in the IS scheme compared with the lattice result from (CUCCHIERI; MENDES, 2009) for one- and two-loop corrections.

Source: GRACEY et al.,2019, p. 09.

1.3.2 Positivity violation and complex poles

The CF model is capable of reproducing, to high accuracy, the lattice results of the gluon propagator. This is despite the fact that the gluon propagator as derived from eq. (74) is not gauge-invariant and the model has no nilpotent BRST invariance. It should be emphasized here, however, that the goal of (TISSIER; WSCHEBOR, 2010) and follow-up works was not to introduce a theory for massive gauge bosons, but to discuss a relatively simple and useful effective description of some non-perturbative aspects of QCD. Also, in this respect the CF model is not in a worse position than other models that try to go beyond standard perturbation theory, such as the GZ model, which also breaks BRST symmetry. One could even argue that unitarity of the gauge bosons sector, secured by a nilpotent BRST symmetry, is not so much an issue here as one expects the gauge bosons to be undetectable anyhow, due to confinement.

An interesting question is whether the massive YM model is also capable of reproducing other aspects of QCD observed on the lattice. One of the most intriguing observations of lattice QCD in recent years is *positivity violation*. Positivity violation means that in the KL spectral representation of the propagator

$$G(p^2) = \int_0^\infty \frac{\rho(t)}{t + p^2} dt, \tag{76}$$

the spectral density function $\rho(t)$ is not positive everywhere. The spectral density function displays, for a certain two-point function such as the gluon propagator, the different states (1-particle states, bound states and multiparticle states) associated with different energy

Figure 4 - Lattice real space propagator

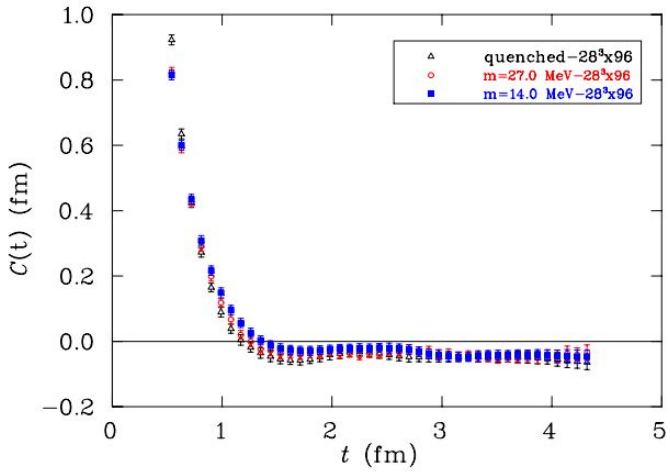

Legend: Lattice results for the real space propagator related to the gluon propagator, for the quenched case (no quarks) and light sea quark masses. The quenched approximation corresponds to the pure gauge theory for QCD.

Source: BOWMAN et al. , 2007, p. 05.

values. If the spectral density function violates positivity, the states it describes cannot be part of the physical state space. Positivity violation is therefore attributed to confinement (CORNWALL, 2013; KREIN; ROBERTS; WILLIAMS, 1992; ROBERTS; WILLIAMS, 1994; LOWDON, 2018): the non-positivity of the spectral function is seen as a reflection of the inability of the gluon to exist as a free physical particle.

Positivity violation for the gluon propagator has been confirmed in both analytical studies of the SD equations (SMEKAL; HAUCK; ALKOFER, 1997; SMEKAL; HAUCK; ALKOFER, 1998; ALKOFER et al., 2004) and in lattice simulations (CUCCHIERI; MENDES; TAURINES, 2005; BOWMAN et al., 2007). In (ALKOFER; SMEKAL, 2001), a complete overview of evidence for positivity violation is given. On the lattice, positivity violation is detected through the real space propagator $C(t)$ related to the gluon propagator, see Figure 4. The real space propagator is defined by

$$C(t) = \int_{-\infty}^{\infty} \frac{dp}{2\pi} e^{ipt} G(p), \tag{77}$$

that is, $C(t)$ is the Fourier transform of the gluon propagator $G(p)$. It can be shown, see for example (CUCCHIERI; MENDES; TAURINES, 2005), that positivity of the real space propagator implies positivity of the spectral density function.

In (TISSIER; WSCHEBOR, 2010), the real space propagator for the gluon prop-

Figure 5 - Real space propagator

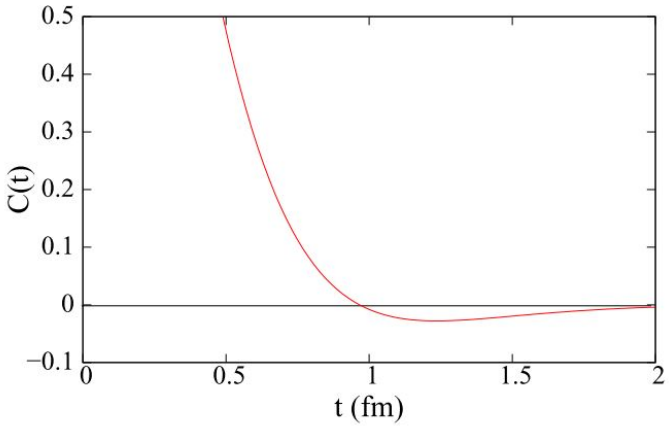

Legend: Real space propagator related to the one-loop corrected gluon propagator for the massive YM model.
Source: TISSIER; WSCHEBOR, 2010, p. 03.

agator in the CF model was obtained by inserting the one-loop gluon propagator derived from the action (74) into eq. (77), and it was found that the curve of $C(t)$ as observed on the lattice was reproduced, including the positivity violation, see Figure 5. On the one hand, it is remarkable that the CF model seems capable of reproducing the lattice results of the real space propagator. On the other hand, we should distinguish between the significance of positivity violation on the lattice and in the CF model. In lattice simulations, one starts out with a unitary (physical) YM model and subsequently observes positivity violation, i.e. non-physical behavior. In the CF model however, one starts out with a model without a nilpotent BRST symmetry. From the Kugo-Ojima criterion (KUGO; OJIMA, 1979), it is known that nilpotency of the BRST symmetry is indispensable to formulate suitable conditions for the construction of the states of the BRST invariant physical (Fock) sub-space, providing unitarity of the S-matrix. Indeed, in (OJIMA, 1982; BOER et al., 1996) the existence of negative norm states in the s_m-invariant subspace ("the would-be physical subspace") was confirmed, see also section 3.5 for a detailed example. Therefore, to find non-physical behavior for a model without BRST symmetry is somewhat of a self fulfilling prophecy.

In fact, the non-physical behaviour of the CF model can be detected in a step prior to the spectral density function. As was established in (KONDO et al., 2020), and recently in (FISCHER; HUBER, 2020) in the context of SD equations, the use of the Landau gauge in the massive YM model (74) leads to complex pole masses, which will obstruct the calculation of the KL spectral function. Indeed, if at some order in perturbation theory

(one-loop as in (KONDO et al., 2020) for example) a pair of Euclidean complex pole masses appear, at higher order these poles will generate branch points in the complex p^2-plane at unwanted locations, i.e. away from the negative real axis, deep into the complex plane, thereby invalidating a KL spectral representation. This can be appreciated by rewriting the Feynman integrals in terms of Schwinger or Feynman parameters, whose analytic properties can be studied through the Landau equations (EDEN et al., 1966). Let us also refer to (BAULIEU et al., 2010; WINDISCH; HUBER; ALKOFER, 2013) for concrete examples. In chapter 2 we will develop some methods to avoid complex poles in the unitary Higgs model.

Finally, it must be pointed out that also lattice simulations of the gluon propagator are not free of "built-in" non-physical features that could attribute to positivity violation. In all studies that show a violation of positivity, both in the context of SD equations and on the lattice, a gauge-dependent and therefore *a priori* non-physical Landau-gauge gluon propagator is used. Indeed, even while on the lattice it is in principle possible to work only with gauge-invariant quantities, in (CUCCHIERI; MENDES; TAURINES, 2005; BOWMAN et al., 2007) a gauge-dependent environment was created, including a lattice gauge-fixing. This gauge-dependent environment also provided the opportunity to test the naturally gauge-dependent GZ proposal on the lattice, see for example (CUCCHIERI; MENDES, 2009; CUCCHIERI; MENDES, 2013; DUDAL; OLIVEIRA; VANDERSICKEL, 2010; CUCCHIERI et al., 2012; CUCCHIERI; DUDAL; VANDERSICKEL, 2012). The use of the gauge-dependent propagator is justified in literature because for an unconfined field, the propagator presumably has a normal KL representation (CORNWALL, 2009), in line with the fact that predictions made from the perturbative gluon propagator of the gauge-fixed YM model agree with experimental observations (JEGERLEHNER; KALMYKOV; VERETIN, 2002; JEGERLEHNER; KALMYKOV; VERETIN, 2003; MARTIN, 2015a; MARTIN, 2015b). This motivated the hypothesis that gauge dependent propagators could give some piece of information about confinement. Nonetheless, the question can be asked whether the gauge field in its elementary, gauge-dependent form gives a complete representation of the gauge boson in all ranges of the energy scale. It can be hypothesized that these elementary fields are in fact part of a greater gauge-invariant configuration, which shares with the gauge-dependent field some essential, but not all, properties. In the next chapters, we will discuss two proposals to this effect: the non-local composite configuration A^h in chapter 2 and the local gauge-invariant composite operators proposed by 't Hooft (HOOFT et al., 1980) in chapters 3 and 4. The latter are unique to the Higgs model, but they are not less relevant to the above question since the W, Z bosons are also expected to be confined in the low-energy regime.

2 ON A RENORMALIZABLE CLASS OF GAUGE FIXINGS FOR THE GAUGE INVARIANT OPERATOR $A^2_{\mathbf{MIN}}$

In this chapter we pursue the investigation (CAPRI et al., 2016b) of the dimension two gauge invariant operator $A^2_{\min}$, obtained by minimizing the functional $\mathrm{Tr}\int d^4x\, A^u_\mu A^u_\mu$ along the gauge orbit of A_μ (ZWANZIGER, 1990; DELL'ANTONIO; ZWANZIGER, 1989; DELL'ANTONIO; ZWANZIGER, 1991; BAAL, 1992), namely

$$\begin{aligned} A^2_{\min} &\equiv \min_{\{u\}} \mathrm{Tr}\int d^4x\, A^u_\mu A^u_\mu \,, \\ A^u_\mu &= u^\dagger A_\mu u + \frac{i}{g} u^\dagger \partial_\mu u \,. \end{aligned} \tag{78}$$

As highlighted in (CAPRI et al., 2016b), the functional $A^2_{\min}$ enables us to introduce a non-local gauge invariant field configuration A^h_μ (LAVELLE; MCMULLAN, 1997) which turns out to be helpful to construct renormalizable BRST invariant YM theories which can be employed as effective massive theories to study non-perturbative infrared aspects of confining YM theories in Euclidean space. As we will see, the massive YM model discussed in 1.3.1 is deeply related to $A^2_{\min}$, because A^h_μ and A_μ are equal in the Landau gauge, see eq. (82) below. See also (CAPRI et al., 2018c) for a supersymmetric extension of the composition $A^h_\mu(x)$. In the present chapter we extend the analysis of the operator $A^2_{\min}$ to a general class of covariant gauges which share great similarity with 't Hooft's R_ζ-gauge discussed in section 1.1.6. In fact, as shown in (CAPRI et al., 2016b), the localization procedure for both $A^2_{\min}$ and A^h_μ requires the introduction of a dimensionless auxiliary Stueckelberg field ξ which, as much as the Higgs field of 't Hooft's R_ζ-gauge, will now enter explicitly the gauge condition through the appearance of a gauge massive paramater μ^2. This property will enable us to provide a fully BRST invariant mass for the auxiliary field ξ, a feature which might have helpful consequences in explicit loop calculations involving ξ in order to keep control of potential infrared divergences associated to its dimensionless nature. Moreover, as in the case of R_ζ-gauge, also the Faddeev-Popov ghosts will acquire a mass through the gauge-fixing. Of course, setting $\mu^2 = 0$, the linear covariant gauges discussed in (CAPRI et al., 2016b) will be recovered. The chapter is organized as follows. In section 2.1 we give a short presentation of the main properties of $A^2_{\min}$ and of the gauge invariant configuration A^h_μ, reminding to Appendix (A) for more specific details. Sections 2.2,2.3,2.4,2.5 are devoted to the presentation of the local BRST invariant action for $A^2_{\min}$ and A^h_μ as well as of the main properties of the aforementioned gauge-fixing. In section 2.6 we establish the set of Ward identities fulfilled by the resulting action. These identities will be employed to characterize the most general allowed invariant counterterm through the procedure of the algebraic renormalization (PIGUET; SORELLA, 1995). In

section 2.7 a detailed analysis of the counterterm will be presented together with the renormalization factors needed to establish the all order renormalizability of the model. Section 2.8 contains our conclusion. Finally, in Appendix B, a second, equivalent, proof of the renormalizability of the model will be outlined by making use of a generalised gauge fixing and ensuing Ward identities.

2.1 Brief review of the operator $A^2_{\min}$ and construction of a non-local gauge invariant and transverse gauge field A^h_μ

Here we will give a short overview of the operator $A^2_{\min}$, eq.(78), reminding to the more complete Appendix A for details.

In particular, looking at the the stationary condition for the functional (78), one gets a non-local transverse field configuration A^h_μ, $\partial_\mu A^h_\mu = 0$, which can be expressed as an infinite series in the gauge field A_μ, see Appendix A, *i.e.*

$$\begin{aligned} A^h_\mu &= \left(\delta_{\mu\nu} - \frac{\partial_\mu\partial_\nu}{\partial^2}\right)\phi_\nu \ , \qquad \partial_\mu A^h_\mu = 0 \ , \\ \phi_\nu &= A_\nu - ig\left[\frac{1}{\partial^2}\partial A, A_\nu\right] + \frac{ig}{2}\left[\frac{1}{\partial^2}\partial A, \partial_\nu\frac{1}{\partial^2}\partial A\right] + O(A^3) \ . \end{aligned} \tag{79}$$

Remarkably, as shown in Appendix A, the configuration A^h_μ turns out to be left invariant by infinitesimal gauge transformations order by order in the gauge coupling g (LAVELLE; MCMULLAN, 1997):

$$\begin{aligned} \delta A^h_\mu &= 0 \ , \\ \delta A_\mu &= -\partial_\mu\omega + ig\left[A_\mu, \omega\right] \ . \end{aligned} \tag{80}$$

Making use of (79), the gauge invariant nature of expression (78) can be made manifest by rewriting it in terms of the field strength $F_{\mu\nu}$. In fact, as proven in (ZWANZIGER, 1990), it turns out that

$$\begin{aligned} A^2_{\min} = \int d^4x A^h_\mu A^h_\mu &= -\frac{1}{2}\mathrm{Tr}\int d^4x \left(F_{\mu\nu}\frac{1}{D^2}F_{\mu\nu} + 2i\frac{1}{D^2}F_{\lambda\mu}\left[\frac{1}{D^2}D_\kappa F_{\kappa\lambda}, \frac{1}{D^2}D_\nu F_{\nu\mu}\right]\right. \\ &\left. -2i\ \frac{1}{D^2}F_{\lambda\mu}\left[\frac{1}{D^2}D_\kappa F_{\kappa\nu}, \frac{1}{D^2}D_\nu F_{\lambda\mu}\right]\right) + O(F^4) \ , \end{aligned} \tag{81}$$

from which the gauge invariance becomes apparent. The operator $(D^2)^{-1}$ in expression (81) denotes the inverse of the Laplacian $D^2 = D_\mu D_\mu$ with D_μ being the covariant derivative (ZWANZIGER, 1990). Let us also underline that, in the Landau gauge $\partial_\mu A_\mu = 0$,

the operator $(A^h_\mu A^h_\mu)$ reduces to the operator A^2

$$(A^{h,a}_\mu A^{h,a}_\mu)\Big|_{\text{Landau}} = A^a_\mu A^a_\mu \,. \tag{82}$$

This feature, combined with the gauge invariant nature of $(A^{h,a}_\mu A^{h,a}_\mu)$, implies that the anomalous dimension of $(A^{h,a}_\mu A^{h,a}_\mu)$ equals (CAPRI et al., 2016b), to all orders, that of the operator $A^a_\mu A^a_\mu$ of the Landau gauge, *i.e.*

$$\gamma_{(A^h)^2} = \gamma_{A^2}\Big|_{\text{Landau}} \,. \tag{83}$$

Moreover, as proven in (DUDAL; VERSCHELDE; SORELLA, 2003), $\gamma_{A^2}\Big|_{\text{Landau}}$ is not an independent parameter, being given by

$$\gamma_{A^2}\Big|_{\text{Landau}} = \left(\frac{\beta(a)}{a} + \gamma_A^{\text{Landau}}(a)\right) \,, \qquad a = \frac{g^2}{16\pi^2} \,, \tag{84}$$

where $(\beta(a), \gamma_A^{\text{Landau}}(a))$ denote, respectively, the β-function and the anomalous dimension of the gauge field A_μ in the Landau gauge. This relation was conjectured and explicitly verified up to three-loop order in (GRACEY, 2003).

2.2 A local action for A^h_μ

Following (CAPRI et al., 2016b), a fully local framework for the gauge invariant operator A^h_μ can be achieved. To that end, we consider the local, BRST invariant, action

$$S_{inv} = \int d^4x \, \frac{1}{4} \, F^a_{\mu\nu} F^a_{\mu\nu} + \int d^4x \left(\tau^a \, \partial_\mu A^{h,a}_\mu + \frac{m^2}{2} \, A^{h,a}_\mu A^{h,a}_\mu + \bar{\eta}^a \partial_\mu D^{ab}_\mu(A^h)\eta^b\right) \,, \tag{85}$$

where

$$A^h_\mu \equiv A^{h,a}_\mu \, T^a = h^\dagger A_\mu h + \frac{i}{g} h^\dagger \partial_\mu h. \tag{86}$$

with

$$h = e^{ig\xi} = e^{ig\xi^a T^a}. \tag{87}$$

The matrices $\{T^a\}$ are the generators of the gauge group $SU(N)$ and ξ^a is an auxiliary localizing Stueckelberg field. By expanding (86), one finds an infinite series whose first terms are

$$(A^h)^a_\mu = A^a_\mu - \partial_\mu \xi^a - g f^{abc} A^b_\mu \xi^c - \frac{g}{2} f^{abc} \xi^b \partial_\mu \xi^c + \text{higher orders} \,. \tag{88}$$

That the action S_{inv} gives a local setup for the nonlocal operator A^h_μ of eq.(79) follows by noticing that the Lagrange multiplier τ implements precisely the transversality condition

$$\partial_\mu A^h_\mu = 0 \,, \tag{89}$$

which, when solved iteratively for the Stueckelberg field ξ^a, gives back the expression (79), see Appendix A. In addition, the extra ghosts $(\bar{\eta}, \eta)$ account for the Jacobian arising from the functional integration over τ which gives a delta-function of the type $\delta(\partial A^h)$. Finally, the term $\frac{m^2}{2}\, A^{h,a}_\mu A^{h,a}_\mu$ accounts for the inclusion of the gauge invariant operator $A^{h,a}_\mu A^{h,a}_\mu$ through the mass parameter m^2 which, as mentioned before, can be used as an effective infrared parameter whose value can be estimated through comparison with the available lattice simulations on the two-point gluon correlation function, see (DUDAL et al., 2008b; DUDAL et al., 2008a; DUDAL; SORELLA; VANDERSICKEL, 2011; TISSIER; WSCHEBOR, 2010; TISSIER; WSCHEBOR, 2011; AGUILAR; BINOSI; PAPAVASSILIOU, 2008; AGUILAR; BINOSI; PAPAVASSILIOU, 2016; FISCHER; MAAS; PAWLOWSKI, 2009; AGUILAR; BINOSI; PAPAVASSILIOU, 2015; HUBER, 2015; FISCHER; PAWLOWSKI, 2009; WEBER, 2012; FRASCA, 2008; SIRINGO, 2016; CUCCHIERI; MENDES, 2007; CUCCHIERI; MENDES, 2008; CUCCHIERI et al., 2012; OLIVEIRA; SILVA, 2012; CUCCHIERI; MENDES; SANTOS, 2009; CUCCHIERI et al., 2011; BICUDO et al., 2015; CUCCHIERI et al., 2016)

The local action S_{inv}, eq.(85), enjoys an exact BRST symmetry:

$$sS_{inv} = 0 \,, \tag{90}$$

where the nilpotent BRST transformations are given by

$$\begin{aligned}
sA^a_\mu &= -D^{ab}_\mu c^b \,, \\
sc^a &= \frac{g}{2} f^{abc} c^b c^c \,, \\
s\bar{c}^a &= ib^a \,, \\
sb^a &= 0 \,, \\
s\tau^a &= 0 \,, \\
s\bar{\eta}^a &= s\eta^a = 0 \,, \\
s^2 &= 0 \quad .
\end{aligned} \tag{91}$$

For the Stueckelberg field one has (DRAGON; HURTH; NIEUWENHUIZEN, 1997), with i, j indices associated with a generic representation,

$$sh^{ij} = -igc^a (T^a)^{ik} h^{kj} \,, \qquad s(A^h)^a_\mu = 0 \,, \tag{92}$$

from which the BRST transformation of the field ξ^a can be evaluated iteratively, yielding

$$s\xi^a = g^{ab}(\xi)c^b = -c^a + \frac{g}{2}f^{abc}c^b\xi^c - \frac{g^2}{12}f^{amr}f^{mpq}c^p\xi^q\xi^r + O(\xi^3)\ . \tag{93}$$

2.3 Introducing the gauge fixing term S_{gf}

As it stands, the action (85) needs to be equipped with the gauge fixing term, S_{gf}, which we choose as

$$\begin{aligned} S_{gf} &= \int d^4x\ s\left(\bar{c}^a(\partial_\mu A^a_\mu - \mu^2\xi^a) - i\frac{\alpha}{2}\bar{c}^a b^a\right) \\ &= \int d^4x\left(ib^a\partial_\mu A^a_\mu + \frac{\alpha}{2}b^a b^a - i\mu^2 b^a\xi^a + \bar{c}^a\partial_\mu D^{ab}_\mu(A)c^b + \mu^2\bar{c}^a g^{ab}(\xi)c^b\right)\ . \end{aligned} \tag{94}$$

Besides the traditional gauge parameter α, we have now introduced a second gauge massive parameter μ^2. As it will be clear in the next section, this massive parameter will provide a fully BRST invariant regularizing mass for the Stueckelberg field ξ^a, a feature which has helpful consequences when performing explicit loop calculations involving ξ^a. Setting $\mu^2 = 0$, the gauge fixing (94) reduces to that of the usual linear covariant gauge (CAPRI et al., 2016b). Moreover, when $\mu^2 = \alpha = 0$, the Landau gauge, $\partial_\mu A^a_\mu = 0$, is recovered. Nevertheless, it is worth underlining that both μ^2 and α appear only in the gauge fixing term, which is an exact BRST variation. As such, μ^2 and α are pure gauge parameters which will not affect the correlation functions of local BRST invariant operators.

Though, before going any further, let us provide a few remarks related to the explicit presence of the Stueckelberg field ξ^a in eq. (94). As it is easily realized, the field ξ^a is a dimensionless field, a feature encoded in the fact that the invariant action S_{inv} itself is an infinite series in powers of ξ^a. As in any local quantum field theory involving dimensionless fields, one has the freedom of performing arbitrary reparametrization of these fields as, for instance, in the case of the two-dimensional non-linear sigma model (BLASI; DELDUC; SORELLA, 1989; BECCHI; PIGUET, 1989) and of $N = 1$ super YM in superspace (PIGUET; SIBOLD, 1982, 1982). In the present case, this means that we have the freedom of replacing ξ^a by an arbitrary dimensionless function of ξ^a, namely

$$\xi^a \to \omega^a(\xi) = \xi^a + a_1^{abc}\xi^b\xi^c + a_2^{abcd}\xi^b\xi^c\xi^d + a_3^{abcde}\xi^b\xi^c\xi^d\xi^e + ... \tag{95}$$

This freedom, inherent to the dimensionless nature of ξ^a, is clearly evidentiated at the quantum level by the fact that the Stueckelberg field renormalizes in a non-linear way (CAPRI et al., 2016b), i.e. like eq. (95), expressing precisely the freedom one has in the

choice of a reparametrization for ξ^a.

In our context, in eq.(94), we could have been equally started with a term like

$$s\left(\bar{c}^a\xi^a\right) \to s\left(\bar{c}^a\omega^a(\xi)\right) = s\left(\bar{c}^a(\xi^a + a_1^{abc}\xi^b\xi^c + a_2^{abcd}\xi^b\xi^c\xi^d + ...)\right) \ . \tag{96}$$

Of course, as much as μ^2 and α, all coefficients $(a_1^{abc}, a_2^{abcd}, a_3^{abcde}, ...)$ are gauge parameters, not affecting the correlation functions of the gauge invariant quantities. Equation (96) expresses the freedom which one always has when dealing with a gauge fixing term which depends explicitly from a dimensionless field, as the term (94). In particular, this freedom will persist through the renormalization analysis, meaning that the renormalization of the gauge fixing itself has to be determined modulo an exact BRST terms of the kind $s\left(\bar{c}^a\omega^a(\xi)\right)$. Alternatively, one could start directly with the generalized gauge-fixing

$$\begin{aligned} S_{gf}^{gen} &= \int d^4x \ s\left(\bar{c}^a(\partial_\mu A_\mu^a) - \mu^2\omega^a(\xi)) - i\frac{\alpha}{2}\bar{c}^a b^a\right) \\ &= \int d^4x \left(ib^a\partial_\mu A_\mu^a + \frac{\alpha}{2}b^a b^a - i\mu^2 b^a\omega^a(\xi) + \bar{c}^a\partial_\mu D_\mu^{ab}(A)c^b + \mu^2\bar{c}^a\frac{\partial\omega^a(\xi)}{\partial\xi^c}g^{cd}(\xi)c^d\right) \ , \end{aligned} \tag{97}$$

and take into account the renormalization of the quantity $\omega^a(\xi)$, encoded in the infinte set of gauge parameters $(a_1^{abc}, a_2^{abcd}, a_3^{abcde}, ...)$. In the following, we shall make use of the gauge-fixing (94) and identify in the final counterterm the term which corresponds to the reparametrization (96). Moreover, in the Appendix B, we shall provide a second proof of the renormalizability of the model by deriving the generalized Slavnov-Taylor identities corresponding to the gauge fixing term (97).

In summary, as starting point, we shall take the local, BRST invariant action

$$S = S_{inv} + S_{gf} \ , \tag{98}$$

with

$$sS = 0 \ , \tag{99}$$

where the BRST transformations are given by eqs.(91),(92),(93).

Let us proceed now by giving a look at the propagators of the elementary fields.

2.4 **A look at the propagators of the elementary fields**

The propagators of the elementary fields are easily evaluated from the quadratic part of the action, eq.(98), *i.e.*

$$
\begin{aligned}
S_{quad.} &= \int d^4x \, \left(\frac{1}{4}(\partial_\mu A^a_\nu - \partial_\nu A^a_\mu)^2 + i b^a \partial_\mu A^a_\mu + \frac{\alpha}{2} b^a b^a + \bar{c}^a \partial^2 c^a - \mu^2 \bar{c}^a c^a \right. \\
&\quad + \frac{m^2}{2} A^a_\mu A^a_\mu - m^2 A^a_\mu \partial_\mu \xi^a + \frac{m^2}{2} \left(\partial_\mu \xi^a\right) \left(\partial_\mu \xi^a\right) \\
&\quad \left. + \tau^a \partial_\mu A^a_\mu - \tau^a \partial^2 \xi^a + \bar{\eta}^a \partial^2 \eta^a - i\mu^2 b^a \xi^a \right) \\
&= \int d^4x \, \frac{1}{2} \left[\begin{array}{cccc} A^a_\mu & b^a & \xi^a & \tau^a \end{array} \right] \times \\
&\quad \times \left[\begin{array}{cccc} (-\delta_{\mu\nu}\partial^2 + \partial_\mu \partial_\nu + m^2) & -i\partial_\mu & -m^2 \partial_\mu & -\partial_\mu \\ i\partial_\nu & \alpha & -i\mu^2 & 0 \\ m^2 \partial_\nu & -i\mu^2 & -m^2 \partial^2 & -\partial^2 \\ \partial_\nu & 0 & -\partial^2 & 0 \end{array} \right] \left[\begin{array}{c} A^a_\mu \\ b^a \\ \xi^a \\ \tau^a \end{array} \right] \\
&\quad + \int d^4x \, \left(\bar{c}^a \partial^2 c^a + \bar{\eta}^a \partial^2 \eta^a - \mu^2 \bar{c}^a c^a \right) \, . \qquad (100)
\end{aligned}
$$

Thus, for the propagators we get

$$
\begin{aligned}
\left\langle A^a_\mu(p) \, A^b_\nu(-p) \right\rangle &= \delta^{ab} \left(\frac{P_{\mu\nu}}{p^2 + m^2} + \frac{\alpha p^2 L_{\mu\nu}}{\left(p^2 + \mu^2\right)^2} \right) \\
\left\langle A^a_\mu(p) \, b^b(-p) \right\rangle &= \delta^{ab} \left(\frac{p_\mu}{p^2 + \mu^2} \right) \\
\left\langle A^a_\mu(p) \, \xi^b(-p) \right\rangle &= \delta^{ab} \left(\frac{-i\alpha p_\mu}{\left(p^2 + \mu^2\right)^2} \right) \\
\left\langle A^a_\mu(p) \, \tau^b(-p) \right\rangle &= \delta^{ab} \left(\frac{i\mu^2 p_\mu}{p^2 \left(p^2 + \mu^2\right)} \right) \\
\left\langle b^a(p) \, b^b(-p) \right\rangle &= 0 \\
\left\langle b^a(p) \, \xi^b(-p) \right\rangle &= \frac{\delta^{ab} i}{p^2 + \mu^2} \\
\left\langle b^a(p) \, \tau^b(-p) \right\rangle &= 0 \\
\left\langle \xi^a(p) \, \xi^b(-p) \right\rangle &= \frac{\delta^{ab} \alpha}{\left(p^2 + \mu^2\right)^2} \\
\left\langle \xi^a(p) \, \tau^b(-p) \right\rangle &= \frac{\delta^{ab}}{p^2 + \mu^2} \\
\left\langle \tau^a(p) \, \tau^b(-p) \right\rangle &= -\frac{\delta^{ab} m^2}{p^2} \\
\left\langle \bar{c}^a(p) \, c^b(-p) \right\rangle &= \frac{\delta^{ab}}{p^2 + \mu^2} \\
\left\langle \bar{\eta}^a(p) \, \eta^b(-p) \right\rangle &= \frac{\delta^{ab}}{p^2} \qquad (101)
\end{aligned}
$$

where, $P_{\mu\nu} = \left(\delta_{\mu\nu} - \frac{p_\mu p_\nu}{p^2} \right)$ and $L_{\mu\nu} = \frac{p_\mu p_\nu}{p^2}$ are the transverse and longitudinal projectors. We see that all propagators have a nice ultraviolet behavior, fully compatible with

the power-counting. Moreover, the role of the massive gauge parameter μ^2 becomes now apparent: it gives a BRST invariant regularizing mass for the Stueckelberg field ξ^a. Observe in fact that, when $\mu^2 = 0$, the propagator of the Stueckelberg field is given by $\langle \xi(p)\xi(-p)\rangle_{\mu^2=0} = \frac{\alpha}{p^4}$ which might give rise to potential infrared divergences in some class of Feynman diagrams. Notice also that, as expected, the mass parameter m^2 appears in the transverse part of the gluon propagator, a feature which exhibits its physical meaning. In fact, being coupled to the gauge invariant operator $(A^{h,a}_\mu A^{h,a}_\mu)$, the parameter m^2 will enter the correlation functions of physical operators, *i.e.* gauge invariant operators, allowing thus to parametrize in an effective way their infrared behavior.

2.5 $A^2_{\min}$ versus the conventional Stueckelberg mass term

As done in (CAPRI et al., 2016b), before facing the analysis of the renormalizability of the action S, eq. (98), let us make a short comparison with the standard Stueckelberg mass term (RUEGG; RUIZ-ALTABA,), corresponding to the action

$$S_{Stueck} = \int d^4x \left(\frac{1}{4} F^a_{\mu\nu} F^a_{\mu\nu} + \frac{m^2}{2} A^{h,a}_\mu A^{h,a}_\mu \right) + S_{gf} \ , \tag{102}$$

where S_{gf} is given by eq. (94). One sees that the conventional Stueckelberg action corresponds to the addition of the gauge invariant operator $(A^{h,a}_\mu A^{h,a}_\mu)$ without taking into account the transversality constraint $\partial_\mu A^{h,a}_\mu = 0$, implemented in the action (98) through the Lagrange multiplier τ^a and the corresponding ghosts $(\bar\eta^a, \eta^a)$. The removal of the constraint $\partial_\mu A^{h,a}_\mu = 0$ gives rise to the conventional Stueckelberg propagator, namely

$$\langle \xi^a(p)\, \xi^b(-p)\rangle_{Stueck} = \frac{\delta^{ab} p^2}{m^2(p^2+\mu^2)^2} + \frac{\delta^{ab}\alpha}{(p^2+\mu^2)^2} \ . \tag{103}$$

From this expression one easily understand the cause of the bad ultraviolet behavior of the Stueckelberg mass term, giving rise to its nonrenormalizability (FERRARI; QUADRI, 2004). We see in fact that the mass parameter m^2 enters the denominator of expression (103). As one easily figures out, this property jepardizes the renormalizability of the standard Stueckelberg formulation (FERRARI; QUADRI, 2004). Due to the presence of the parameter m^2 in the denominator of expressions (103), non-renormalizable divergences in the inverse of the mass m^2 will show up, invalidating thus the perturbative loop expansion based on expression (102).

The role of the term $\int d^4x \ \tau^a \, \partial_\mu A^{h,a}_\mu$, implementing the constraint $\partial_\mu A^{h,a}_\mu = 0$, becomes now clear. It gives rise to a deep modification of the Stueckelberg propagator, removing precisely the first problematic term, $\frac{\delta^{ab}p^2}{m^2(p^2+\mu^2)^2}$, from expression (103). We are left therefore only with the second piece, *i.e.* $\frac{\delta^{ab}\alpha}{(p^2+\mu^2)^2}$, which does not pause any problem

with the ultraviolet power-counting. It is this nice feature which will ensure the all order renormalizability of the action S, eq.(98), as we shall discuss in details in the next sections.

2.6 Algebraic characterization of the counterterm

We are now ready to start the analysis of the renormalizability of the action S, eq. (98). Following the setup of the algebraic renormalization (PIGUET; SORELLA, 1995), we proceed by establishing the set of Ward identities which will be employed for the study of the quantum corrections. To that end, we need to introduce a set of external BRST invariant sources (Ω^a_μ, L^a, K^a) coupled to the non-linear BRST variations of the fields (A^a_μ, c^a, ξ^a) as well as sources $(\mathcal{J}^a_\mu, \Xi^a_\mu)$ coupled to the BRST invariant composite operators $(A^{ha}_\mu, D^{ab}_\mu(A^h))$,

$$s\Omega^a_\mu = sL^a = sK^a = s\mathcal{J}^a_\mu = s\Xi^a_\mu = 0 \ . \tag{104}$$

We shall thus start with the BRST invariant complete action Σ defined by

$$\begin{aligned}\Sigma \ = \ & \int d^4x \left(\frac{1}{4} \left(F^a_{\mu\nu}\right)^2 + ib^a \partial_\mu A^a_\mu + \bar{c}^a \partial_\mu D^{ab}_\mu c^b + \frac{\alpha}{2} \left(b^a\right)^2 - iM^{ab} b^a \xi^b \right. \\ & -N^{ab} \bar{c}^a \xi^b + M^{ab} \bar{c}^a g^{bc} \left(\xi\right) c^c + \bar{\eta}^a \partial_\mu D^{ab}_\mu \left(A^h\right) \eta^b + \frac{m^2}{2} A^{ha}_\mu A^{ha}_\mu \\ & +\tau^a \partial_\mu A^{ha}_\mu - \Omega^a_\mu D^{ab}_\mu c^b + \frac{g}{2} f^{abc} L^a c^b c^c + K^a g \left(\xi\right)^{ab} c^b + \mathcal{J}^a_\mu A^{ha}_\mu \\ & \left. + \Xi^a_\mu D^{ab}_\mu \left(A^h\right) \eta^b \right) \ , \end{aligned} \tag{105}$$

where, for later convenience, we have also introduced the BRST doublet of external sources (M^{ab}, N^{ab})

$$sM^{ab} = N^{ab} \ , \qquad sN^{ab} = 0 \ , \tag{106}$$

so that

$$s\Sigma = 0 \ . \tag{107}$$

Notice that the invariant action S of eq. (98) is immediately recovered from the complete action Σ upon setting the external sources $(\Omega^a_\mu = L^a = K^a = \mathcal{J}^a_\mu = \Xi^a_\mu = 0)$ and $(M^{ab} = \delta^{ab}\mu^2, N^{ab} = 0)$.

It turns out that the complete action Σ obeys the following Ward identities:

- the Slavnov-Taylor identity

$$\mathcal{S}(\Sigma) = \int d^4x \left(\frac{\delta\Sigma}{\delta\Omega^a_\mu}\frac{\delta\Sigma}{\delta A^a_\mu} + \frac{\delta\Sigma}{\delta L^a}\frac{\delta\Sigma}{\delta c^a} + ib^a\frac{\delta\Sigma}{\delta\bar{c}^a} + \frac{\delta\Sigma}{\delta K^a}\frac{\delta\Sigma}{\delta\xi^a} + N^{ab}\frac{\delta\Sigma}{\delta M^{ab}} \right) = 0 \,, \tag{108}$$

- the equation of motion of the Lagrange multiplier b^a and of the antighost $\bar{c}^a$

$$\frac{\delta\Sigma}{\delta b^a} = i\partial_\mu A^a_\mu + \alpha b^a - iM^{ab}\xi^b \,, \tag{109}$$

$$\frac{\delta\Sigma}{\delta\bar{c}^a} + \partial_\mu\frac{\delta\Sigma}{\delta\Omega^a_\mu} - M^{ab}\frac{\delta\Sigma}{\delta K^b} = N^{ab}\xi^b \,, \tag{110}$$

- the ghost-number Ward identity

$$\int d^4x \left(c^a\frac{\delta\Sigma}{\delta c^a} - \bar{c}^a\frac{\delta\Sigma}{\delta\bar{c}^a} - \Omega^a_\mu\frac{\delta\Sigma}{\delta\Omega^a_\mu} - 2L^a\frac{\delta\Sigma}{\delta L^a} - K^a\frac{\delta\Sigma}{\delta K^a} + N^{ab}\frac{\delta\Sigma}{\delta N^{ab}} \right) = 0 \tag{111}$$

- the equation of the Lagrange multiplier τ^a

$$\frac{\delta\Sigma}{\delta\tau^a} - \partial_\mu\frac{\delta\Sigma}{\delta\mathcal{J}^a_\mu} = 0 \,, \tag{112}$$

- the η^a Ward identity

$$\int d^4x \left(\frac{\delta\Sigma}{\delta\eta^a} + gf^{abc}\bar{\eta}^b\frac{\delta\Sigma}{\delta\tau^c} + gf^{abc}\Xi^b\frac{\delta\Sigma}{\delta\mathcal{J}^c_\mu} \right) = 0 \,, \tag{113}$$

- the $\bar{\eta}^a$ antighost equation

$$\frac{\delta\Sigma}{\delta\bar{\eta}^a} - \partial_\mu\frac{\delta\Sigma}{\delta\Xi^a_\mu} = 0 \,, \tag{114}$$

- the $(\eta^a, \bar{\eta}^a)$ ghost number

$$\int d^4x \left(\eta^a\frac{\delta\Sigma}{\delta\eta^a} - \bar{\eta}^a\frac{\delta\Sigma}{\delta\bar{\eta}^a} - \Xi^a\frac{\delta\Sigma}{\delta\Xi^a} \right) = 0 \,. \tag{115}$$

All quantum numbers and dimensions of all fields and sources are displayed in Tables (1) and (2).

Table 1 - Quantum number of the fields.

	A^a_μ	b^a	c^a	$\bar{c}^a$	τ^a	η^a	$\bar{\eta}^a$	ξ^a
dim.	1	2	0	2	2	0	2	0
c gh. number	0	0	1	-1	0	0	0	0
η gh. number	0	0	0	0	0	1	-1	0

Source: The author, 2020.

Table 2 - The quantum numbers of the sources.

	Ω^a_μ	L^a	K^a	$\mathcal{J}^a_\mu$	Ξ^a_μ	M^{ab}	N^{ab}
dim.	3	4	4	3	2	2	2
c gh. number	-1	-2	-1	0	0	0	1
η gh. number	0	0	0	0	-1	0	0

Source: The author, 2020.

In order to characterize the most general invariant counterterm which can be freely added to all order in perturbation theory, we follow the setup of the algebraic renormalization (PIGUET; SORELLA, 1995) and perturb the classical action Σ, eq.(105), by adding an integrated local quantity in the fields and sources, Σ^{ct}, with dimension bounded by four and vanishing ghost number. We demand thus that the perturbed action, $(\Sigma + \varepsilon\Sigma^{ct})$, where ε is an expansion parameter, fulfills, to the first order in ε, the same Ward identities obeyed by the classical action Σ, *i.e.* equations (108), (109), (111), (112), (113) and (114). This amounts to impose the following constraints on Σ:

$$\mathcal{B}_\Sigma \Sigma^{ct} = 0 \,, \tag{116}$$

$$\frac{\delta \Sigma^{ct}}{\delta b^a} = 0 \,, \tag{117}$$

$$\frac{\delta \Sigma^{ct}}{\delta \bar{c}^a} + \partial_\mu \frac{\delta \Sigma^{ct}}{\delta \Omega^a_\mu} - M^{ab} \frac{\delta \Sigma^{ct}}{\delta K^b} = 0 \,, \tag{118}$$

$$\frac{\delta \Sigma^{ct}}{\delta \tau^a} - \partial_\mu \frac{\delta \Sigma^{ct}}{\delta \mathcal{J}^a_\mu} = 0 \,, \tag{119}$$

$$\int d^4x \left(\frac{\delta \Sigma^{ct}}{\delta \eta^a} + g f^{abc} \bar{\eta}^b \frac{\delta \Sigma^{ct}}{\delta \tau^c} + g f^{abc} \Xi^b \frac{\delta \Sigma^{ct}}{\delta \mathcal{J}^c_\mu} \right) = 0 \, , \tag{120}$$

$$\frac{\delta \Sigma^{ct}}{\delta \bar{\eta}^a} - \partial_\mu \frac{\delta \Sigma^{ct}}{\delta \Xi^a_\mu} = 0 \, , \tag{121}$$

where $\mathcal{B}_\Sigma$ is the so-called nilpotent linearized Slavnov-Taylor operator (PIGUET; SORELLA, 1995), defined as

$$\begin{aligned} \mathcal{B}_\Sigma &= \int d^4x \left(\frac{\delta \Sigma}{\delta \Omega^a_\mu} \frac{\delta}{\delta A^a_\mu} + \frac{\delta \Sigma}{\delta A^a_\mu} \frac{\delta}{\delta \Omega^a_\mu} + \frac{\delta \Sigma}{\delta L^a} \frac{\delta}{\delta c^a} + \frac{\delta \Sigma}{\delta c^a} \frac{\delta}{\delta L^a} + \frac{\delta \Sigma}{\delta K^a} \frac{\delta}{\delta \xi^a} \right) \\ &+ \int d^4x \left(\frac{\delta \Sigma}{\delta \xi^a} \frac{\delta}{\delta K^a} + i b^a \frac{\delta}{\delta \bar{c}^a} + N^{ab} \frac{\delta}{\delta M^{ab}} \right) \, , \end{aligned} \tag{122}$$

with

$$\mathcal{B}_\Sigma \mathcal{B}_\Sigma = 0 \, . \tag{123}$$

The first condition, eq. (116), tells us that the counterterm Σ^{ct} belongs to the cohomology of the operator $\mathcal{B}_\Sigma$ in the space of the integrated local polynomials in the fields, sources and parameters, of dimension four and ghost number zero. Owing to the general results on the BRST cohomology of YM theories (PIGUET; SORELLA, 1995) and taking advantage of the analysis already done in (CAPRI et al., 2016b), the most general form for Σ^{ct} can be written as

$$\Sigma^{ct} = \Delta_{cohom} + \mathcal{B}_\Sigma \Delta^{(-1)} \, , \tag{124}$$

where Δ_{cohom} identifies the cohomolgy of $\mathcal{B}_\Sigma$, *i.e.* the non-trivial solution of eq.(116), and $\Delta^{(-1)}$ stands for the exact part, *i.e.* for the trivial solution of (116). Notice that, according to the quantum numbers of the fields, $\Delta^{(-1)}$ is an integrated polynomial of dimension four, c-ghost number -1 and η-number equal to zero.

For Δ_{cohom}, we have

$$\begin{aligned} \Delta_{cohom} &= \int d^4x \left(\frac{a_0}{4} \left(F^a_{\mu\nu} \right)^2 + a_1 \left(\partial_\mu A^{ha}_\mu \right) \left(\partial_\nu A^{ha}_\nu \right) + a_2 \left(\partial_\mu A^{ha}_\nu \right) \left(\partial_\mu A^{ha}_\nu \right) \right. \\ &+ a_3^{abcd} A^{ha}_\mu A^{hb}_\mu A^{hc}_\nu A^{hd}_\nu + \left(\partial_\mu \tau^a + \mathcal{J}^a_\mu \right) F^a_\mu \left(A, \xi \right) + a_5 \left(\partial_\mu \bar{\eta}^a + \Xi^a_\mu \right) \left(\partial_\mu \eta^a \right) \\ &\left. + f^{abc} \left(\partial_\mu \bar{\eta}^a + \Xi^a_\mu \right) \eta^b G^c_\mu \left(A, \xi \right) + m^2 I \left(A, \xi \right) \right) \, , \end{aligned} \tag{125}$$

where $F^a_\mu\left(A,\xi\right)$, $G^c_\mu\left(A,\xi\right)$ and $I\left(A,\xi\right)$ are local functional of A^a_μ and ξ^a, with dimension 1, 1 and 2, respectively. To write expression (125) we have taken into account the constraints (118)–(121). Moreover, from condition (116) one immediately gets

$$\mathcal{B}_\Sigma F^a_\mu\left(A,\xi\right)=\mathcal{B}_\Sigma G^c_\mu\left(A,\xi\right)=\mathcal{B}_\Sigma I\left(A,\xi\right)=0\ . \tag{126}$$

Proceeding as in (CAPRI et al., 2016b), equations (126) are solved by

$$F^a_\mu\left(A,\xi\right)=a_4A^{ha}_\mu\ ,\qquad G^c_\mu\left(A,\xi\right)=a_6A^{ha}_\mu\ ,\qquad I\left(A,\xi\right)=a_7A^{ha}_\mu A^{ha}_\mu\ , \tag{127}$$

where (a_4,a_6,a_7) are free coefficients. Therefore,

$$\begin{aligned}\Delta_{cohom}\ =\ &\int d^4x\left(\frac{a_0}{4}\left(F^a_{\mu\nu}\right)^2+a_1\left(\partial_\mu A^{ha}_\mu\right)\left(\partial_\nu A^{ha}_\nu\right)+a_2\left(\partial_\mu A^{ha}_\nu\right)\left(\partial_\mu A^{ha}_\nu\right)\right.\\&+a_3^{abcd}A^{ha}_\mu A^{hb}_\mu A^{hc}_\nu A^{hd}_\nu+a_4\left(\partial_\mu\tau^a+\mathcal{J}^a_\mu\right)A^{ha}_\mu+a_5\left(\partial_\mu\bar\eta^a+\Xi^a_\mu\right)\left(\partial_\mu\eta^a\right)\\&\left.+a_6f^{abc}\left(\partial_\mu\bar\eta^a+\Xi^a_\mu\right)\eta^bA^{hc}_\mu+a_7m^2A^{ha}_\mu A^{ha}_\mu\right)\ .\end{aligned}$$

Let us discuss now the exact part of the cohomology of $\mathcal{B}_\Sigma$ which, taking into account the quantum numbers of the fields and sources, can be parametrized as

$$\begin{aligned}&\Delta^{(-1)}\\&\int d^4x\left(f^{ab}_1\left(\xi,\alpha\right)\xi^aK^b+f^{ab}_2\left(\xi,\alpha\right)L^ac^b+f^{ab}_3\left(\xi,\alpha\right)\xi^a\left(\partial_\mu\Omega^b_\mu\right)+f^{ab}_4\left(\xi,\alpha\right)\left(\partial_\mu\xi^a\right)\Omega^b_\mu.\right.\\&+f^{ab}_5\left(\xi,\alpha\right)A^a_\mu\Omega^b_\mu+f^{ab}_6\left(\xi,\alpha\right)A^a_\mu\left(\partial_\mu\bar c^b\right)+f^{ab}_7\left(\xi,\alpha\right)\left(\partial_\mu A^a_\mu\right)\bar c^b\\&+f^{ab}_8\left(\xi,\alpha\right)\left(\partial_\mu\xi^a\right)\left(\partial_\mu\bar c^b\right)+f^{ab}_9\left(\xi,\alpha\right)\xi^a\left(\partial^2\bar c^b\right)+f^{ab}_{10}\left(\xi,\alpha\right)\bar c^ab^b\\&+f^{ab}_{11}\left(\xi,\alpha\right)\bar c^a\tau^b+f^{abc}_{12}\left(\xi,\alpha\right)\bar\eta^a\eta^b\bar c^c+f^{abc}_{13}\left(\xi,\alpha\right)\bar c^a\bar c^bc^c\\&\left.+f^{abcd}_{14}\left(\xi,\alpha\right)M^{ab}\xi^c\bar c^d\right)\ ,\end{aligned}$$

where $(f_1,...,f_{14})$ are arbitrary coefficients. Imposing the constraint (117), *i.e.*

$$\frac{\delta}{\delta b^k}\mathcal{B}_\Sigma\Delta^{(-1)}=0\ , \tag{128}$$

and making use of the commutation relation

$$\frac{\delta}{\delta b^k}\mathcal{B}_\Sigma=\mathcal{B}_\Sigma\frac{\delta}{\delta b^k}+i\left(\frac{\delta}{\delta\bar c^k}+\partial_\mu\frac{\delta}{\delta\Omega^k_\mu}-M^{kl}\frac{\delta}{\delta K^l}\right)\ , \tag{129}$$

one finds

$$\frac{\delta\Delta^{(-1)}}{\delta b^k}=f^{ak}_{10}\left(\xi,\alpha\right)\bar c^a\qquad\Rightarrow\qquad\mathcal{B}_\Sigma\frac{\delta\Delta^{(-1)}}{\delta b^k}=\frac{\delta\Sigma}{\delta K^m}\frac{\partial f^{ak}_{10}\left(\xi,\alpha\right)}{\partial\xi^m}\bar c^a+if^{ak}_{10}\left(\xi,\alpha\right)b^a\ .$$

Moreover, from

$$
\begin{aligned}
i\left(\frac{\delta\Delta^{(-1)}}{\delta\bar{c}^k}+\partial_\mu\frac{\delta\Delta^{(-1)}}{\delta\Omega_\mu^k}-M^{kl}\frac{\delta\Delta^{(-1)}}{\delta K^l}\right) &= -i\partial_\mu\left(f_6^{ak}(\xi,\alpha)\,A_\mu^a\right)+if_7^{ak}(\xi,\alpha)\left(\partial_\mu A_\mu^a\right)\\
&\quad -i\partial_\mu\left(f_8^{ak}(\xi,\alpha)\left(\partial_\mu\xi^a\right)\right)+i\partial^2\left(f_9^{ak}(\xi,\alpha)\,\xi^a\right)\\
&\quad +if_{10}^{kb}(\xi,\alpha)\,b^b+if_{11}^{kb}(\xi,\alpha)\,\tau^b\\
&\quad +if_{12}^{abk}(\xi,\alpha)\,\bar{\eta}^a\eta^b+2if_{13}^{kbc}(\xi,\alpha)\,\bar{c}^bc^c\\
&\quad +if_{14}^{abck}(\xi,\alpha)\,M^{ab}\xi^c\\
&\quad -i\partial^2\left(f_3^{ak}(\xi,\alpha)\,\xi^a\right)+i\partial_\mu\left(f_4^{ak}(\xi,\alpha)\left(\partial_\mu\xi^a\right)\right)\\
&\quad +i\partial_\mu\left(f_5^{ak}(\xi,\alpha)\,A_\mu^a\right)-iM^{kl}f_1^{al}(\xi,\alpha)\,\xi^a\,,
\end{aligned}
$$

it follows that

$$
\begin{aligned}
&\frac{\delta}{\delta b^k}\mathcal{B}_\Sigma\Delta^{(-1)}=0\\
&=\left[\frac{\partial f_{10}^{bk}(\xi,\alpha)}{\partial\xi^m}g^{mc}(\xi)-2if_{13}^{kbc}(\xi,\alpha)\right]c^c\bar{c}^b\\
&+i\left[f_{10}^{ak}(\xi,\alpha)+f_{10}^{ka}(\xi,\alpha)\right]b^a\\
&+i\left[-f_6^{ak}(\xi,\alpha)+f_5^{ak}(\xi,\alpha)+f_7^{ak}(\xi,\alpha)\right]\left(\partial_\mu A_\mu^a\right)\\
&-i\left[\left(\partial_\mu f_6^{ak}(\xi,\alpha)\right)-\left(\partial_\mu f_5^{ak}(\xi,\alpha)\right)\right]A_\mu^a\\
&+i\left[-\left(\partial_\mu f_8^{ak}(\xi,\alpha)\right)-\left(\partial_\mu f_3^{ak}(\xi,\alpha)\right)+\left(\partial_\mu f_4^{ak}(\xi,\alpha)\right)+\left(\partial_\mu f_9^{ak}(\xi,\alpha)\right)\right]\left(\partial_\mu\xi^a\right)\\
&+i\left[-f_8^{ak}(\xi,\alpha)-f_3^{ak}(\xi,\alpha)+f_4^{ak}(\xi,\alpha)+f_9^{ak}(\xi,\alpha)\right]\left(\partial^2\xi^a\right)\\
&+i\left[-\left(\partial^2 f_3^{ak}(\xi,\alpha)\right)+\left(\partial^2 f_9^{ak}(\xi,\alpha)\right)\right]\xi^a\\
&+if_{11}^{kb}(\xi,\alpha)\,\tau^b+if_{12}^{abk}(\xi,\alpha)\,\bar{\eta}^a\eta^b+i\left[f_{14}^{abck}(\xi,\alpha)-\delta^{ka}f_1^{cb}(\xi,\alpha)\right]M^{ab}\xi^c\,,
\end{aligned}
$$

form which we can derive relations among the coefficients $(f_1,...,f_{14})$. Let us start with

$$
\left(\partial_\mu f_6^{ak}(\xi,\alpha)\right)-\left(\partial_\mu f_5^{ak}(\xi,\alpha)\right)=0 \qquad \Rightarrow \qquad f_6^{ab}=f_5^{ab}+\delta^{ab}a\,, \tag{130}
$$

where a is a constant. Further

$$
-f_6^{ak}(\xi,\alpha)+f_5^{ak}(\xi,\alpha)+f_7^{ak}(\xi,\alpha)=0 \qquad \Rightarrow \qquad f_7^{ak}(\xi,\alpha)=\delta^{ab}a\,. \tag{131}
$$

Analogously

$$
-\left(\partial^2 f_3^{ak}(\xi,\alpha)\right)+\left(\partial^2 f_9^{ak}(\xi,\alpha)\right)=0 \qquad \Rightarrow \qquad f_9^{ak}(\xi,\alpha)=f_3^{ak}(\xi,\alpha)+b\delta^{ak}\,, \tag{132}
$$

with b a free constant. Next, from

$$\left[-\left(\partial_\mu f_8^{ak}(\xi,\alpha)\right)-\left(\partial_\mu f_3^{ak}(\xi,\alpha)\right)+\left(\partial_\mu f_4^{ak}(\xi,\alpha)\right)+\left(\partial_\mu f_9^{ak}(\xi,\alpha)\right)\right] , \tag{133}$$

we get

$$f_8^{ak}(\xi,\alpha)=f_4^{ak}(\xi,\alpha)+c\delta^{ak} , \tag{134}$$

with c constant. Finally

$$-f_8^{ak}(\xi,\alpha)-f_3^{ak}(\xi,\alpha)+f_4^{ak}(\xi,\alpha)+f_9^{ak}(\xi,\alpha)=0 \qquad \Rightarrow \qquad b=c . \tag{135}$$

Therefore, $\Delta^{(-1)}$ becomes

$$\begin{aligned}\Delta^{(-1)} \;=\; & \int d^4x \left(f_1^{ab}(\xi,\alpha)\left(\xi^a K^b+M^{cb}\xi^a\bar{c}^c\right)\right.\\ & +f_2^{ab}(\xi,\alpha)\,L^a c^b+f_3^{ab}(\xi,\alpha)\,\xi^a\left(\left(\partial_\mu\Omega_\mu^b\right)+\left(\partial^2\bar{c}^b\right)\right)\\ & +f_4^{ab}(\xi,\alpha)\left(\partial_\mu\xi^a\right)\left(\Omega_\mu^b+\left(\partial_\mu\bar{c}^b\right)\right)\\ & +f_5^{ab}(\xi,\alpha)\,A_\mu^a\left(\Omega_\mu^b+\left(\partial_\mu\bar{c}^b\right)\right)\\ & \left.+f_{10}^{ab}(\xi,\alpha)\,\bar{c}^a b^b+\frac{1}{2i}\frac{\partial f_{10}^{ba}(\xi,\alpha)}{\partial\xi^m}g^{mc}(\xi)\,\bar{c}^a\bar{c}^b c^c\right) .\end{aligned}$$

We can now impose the constraint (120)

$$\int d^4x\left(\frac{\delta\Sigma^{ct}}{\delta\eta^m}+gf^{mnp}\bar{\eta}^n\frac{\delta\Sigma^{ct}}{\delta\tau^p}+gf^{mnp}\Xi^n\frac{\delta\Sigma^{ct}}{\delta\mathcal{J}_\mu^p}\right) \;=\; 0 ,$$

$$\Rightarrow\int d^4x\,(a_6+a_4 g)\,f^{mnp}\left(\partial_\mu\bar{\eta}^n+f^{mnp}\Xi^n\right)A_\mu^{hp} \;=\; 0 ,$$

from which we obtain $a_6=-a_4 g$.

As done in (CAPRI et al., 2016b), we can further reduce the number of parameters entering Σ^{ct} by observing that, setting $K^a=M^{ab}=N^{ab}=\mathcal{J}_\mu^a=\Xi_\mu^a=m=0$, the complete action Σ, eq.(105), reduces to that or ordinary YM theory in the linear covarinat gauges, as integration over τ^a, η^a and $\overline{\eta}^a$ gives a unity. As a consequence, making use of the well known renormalization of standard YM theory in the linear covariant gauges (PIGUET; SORELLA, 1995), we get $a_1=a_2=a_3^{abcd}=0$, $a_5=a_4$,

as well as

$$f_2^{ab}(\xi,\alpha)=\delta^{ab}d_1(\alpha)\ ,\qquad f_5^{ab}(\xi,\alpha)=\delta^{ab}d_2(\alpha)\ , \tag{136}$$

with (d_1,d_2) free parameters. In addition, we also have

$$f_3^{ab}(\xi,\alpha)=f_4^{ab}(\xi,\alpha)=f_{10}^{ab}(\xi,\alpha)\ =\ 0\ .$$

Hence

$$\begin{aligned}\Delta_{cohom}\ =\ &\int d^4x\left(\frac{a_0}{4}\left(F_{\mu\nu}^a\right)^2+a_4\left(\left(\partial_\mu\tau^a+\mathcal{J}_\mu^a\right)A_\mu^{ha}+\left(\partial_\mu\bar{\eta}^a+\Xi_\mu^a\right)D^{ab}\left(A^h\right)\eta^b\right)\right.\\&\left.+a_7m^2A_\mu^{ha}A_\mu^{ha}\right),\end{aligned}$$

and

$$\Delta^{(-1)}=\int d^4x\Big(f_1^{ab}(\xi,\alpha)\left(\xi^aK^b+M^{cb}\xi^a\bar{c}^c\right)+d_1(\alpha)L^ac^a+d_2(\alpha)A_\mu^a\left(\Omega_\mu^a+(\partial_\mu\bar{c}^a)\right)\Big)\ .$$

Let us end this section by rewriting the final expression of the most general invariant counterterm Σ^{ct} in its parametric form (PIGUET; SORELLA, 1995), a task that will simplify the analysis of the renormalziation factors, namely

$$\begin{aligned}\Sigma^{ct}\ =\ &-a_0g\frac{\partial\Sigma}{\partial g}+d_2(\alpha)\,2\alpha\frac{\partial\Sigma}{\partial\alpha}+a_7m^2\frac{\partial\Sigma}{\partial m^2}\\&+\int d^4x\left(a_4\left(-\tau^a\frac{\delta\Sigma}{\delta\tau^a}+\mathcal{J}_\mu^a\frac{\delta\Sigma}{\delta\mathcal{J}_\mu^a}-\bar{\eta}^a\frac{\delta\Sigma}{\delta\bar{\eta}^a}+\Xi_\mu^a\frac{\delta\Sigma}{\delta\Xi_\mu^a}\right)\right.\\&-\left(f_1^{ab}(\xi,\alpha)+\frac{\partial f_1^{kb}(\xi,\alpha)}{\partial\xi^a}\xi^k\right)K^b\frac{\delta\Sigma}{\delta K^a}+f_1^{ab}(\xi,\alpha)\,\xi^a\frac{\delta\Sigma}{\delta\xi^b}\\&+d_2(\alpha)\,A_\mu^a\frac{\delta\Sigma}{\delta A_\mu^a}-d_2(\alpha)\,b^a\frac{\delta\Sigma}{\delta b^a}-d_2(\alpha)\,\Omega_\mu^a\frac{\delta\Sigma}{\delta\Omega_\mu^a}-d_2(\alpha)\,\bar{c}^a\frac{\delta\Sigma}{\delta\bar{c}^a}\\&-d_1(\alpha)\,c^a\frac{\delta\Sigma}{\delta c^a}+d_1(\alpha)\,L^a\frac{\delta\Sigma}{\delta L^a}+\left(-f_1^{cb}(\xi,\alpha)+d_2(\alpha)\,\delta^{cb}\right)N^{ab}\frac{\delta\Sigma}{\delta N^{ac}}\\&\left.+\left(d_2(\alpha)\,\delta^{ab}-f_1^{ab}(\xi,\alpha)\right)M^{cb}\frac{\delta\Sigma}{\delta M^{ca}}+\frac{\partial f_1^{ab}(\xi,\alpha)}{\partial\xi^k}M^{cb}\xi^a g(\xi)^{kd}\,c^d\bar{c}^c\right)\ .\end{aligned} \tag{137}$$

2.7 **Analysis of the counterterm and renormalization factors**

Having determined the most general form of the local invariant counterterm, eq.(137), let us turn to its physical meaning. As already mentioned before, in order to determine the renormalization of the fields, sources and parameters, we have to pay attention to the fact that, due to the explicit dependence of the gauge fixing from the Stueckelberg field ξ^a, the renormalization of the gauge fixing itself is determined up to an ambiguity of the type of eq.(96), which would correspond to the renormalization of the quantity $\omega^a(\xi)$, *i.e.* of the gauge parameters $(a_1^{abc}, a_2^{abcd}, a_3^{abcde}, ...)$. To that end, it will be sufficient to analyse the last two terms of the expression for Σ^{ct}, eq.(137), which, upon setting the sources (M^{ab}, N^{ab}) to their physical values, namely $(M^{ab} = \delta^{ab}\mu^2, N^{ab} = 0)$, becomes

$$\begin{aligned} & (d_2(\alpha) - f_1(0,\alpha))\,\mu^2 \frac{\partial \Sigma}{\partial \mu^2} \\ + \quad & \mu^2 \int d^4x \left(\tilde{f}_1^{ab}(\xi,\alpha)(ib^b\xi^a - \bar{c}^b g^{ak}(\xi)c^k) + \frac{\partial \tilde{f}_1^{ab}(\xi,\alpha)}{\partial \xi^k} \bar{c}^b \xi^a g^{kd}(\xi) c^d \right) \end{aligned} \tag{138}$$

where we have set

$$f_1^{ab}(\xi,\alpha) = f_1^{ab}(0,\alpha) + \tilde{f}_1^{ab}(\xi,\alpha)\ , \tag{139}$$

with $f_1^{ab}(0,\alpha) = \delta^{ab} f_1(0,\alpha)$ being the first, ξ^a-independent, term of the Taylor expansion of $f_1^{ab}(\xi,\alpha)$ in powers of ξ^a and $\tilde{f}_1^{ab}(\xi,\alpha)$ denoting the ξ-dependent remaining terms. Of course, $f_1^{ab}(0,\alpha) = \delta^{ab} f_1(0,\alpha)$ is just a constant.

Furthermore, we observe that expression (138) can be rewritten as

$$(d_2(\alpha) - f_1(0,\alpha))\,\mu^2 \frac{\partial \Sigma}{\partial \mu^2} + \mu^2 \int d^4x\ s\left(\tilde{f}_1^{ab}(\xi,\alpha)\bar{c}^b\xi^a \right)\ , \tag{140}$$

or, equivalently

$$(d_2(\alpha) - f_1(0,\alpha))\,\mu^2 \frac{\partial \Sigma}{\partial \mu^2} + \mu^2 \int d^4x\ s\left(\bar{c}^b \tilde{\omega}^b(\xi,\alpha) \right)\ , \tag{141}$$

with $\tilde{\omega}^b(\xi,\alpha) = \tilde{f}_1^{ab}(\xi,\alpha)\xi^a$.

We are now able to unravel the meaning of this term. First, the term $(d_2(\alpha) - f_1^{aa}(0,\alpha))$ corresponds to a multiplicative renormalization of the gauge massive parameter μ^2. This follows by observing that, being μ^2 a space-time independent parameter, its renormalization must be given by a field independent space-time constant factor, *i.e.* precisely by $(d_2(\alpha) - f_1^{aa}(0,\alpha))$. On the other hand, the term $\int d^4x\ s\left(\bar{c}^b\tilde{\omega}^b(\xi,\alpha)\right)$

is of the type of eq.(96), thus corresponding to the ambiguity inherent to the gauge fixing discussed before. As already mentioned, this term can be handled by starting with the generalised gauge fixing (97), whose algebraic renormalization can be faced by employing the Ward identities displayed in Appendix B. Doing so, the term $\int d^4x\; s\left(\bar{c}^b\tilde{\omega}^b(\xi,\alpha)\right)$ will correspond to a renormalization of the gauge fixing function $\omega^a(\xi)$, *i.e.* of the gauge parameters $(a_1^{abc}, a_2^{abcd}, a_3^{abcde}, ...)$.

We can now read off the renormalization factors, *i.e.*

$$\Sigma(\Phi) + \varepsilon\Sigma^{ct}(\Phi) = \Sigma(\Phi_0) + O(\varepsilon^2)\;, \tag{142}$$

with

$$\Phi_0 = Z_\Phi\Phi + O(\varepsilon^2)\;, \tag{143}$$

where Φ stands for a short-hand notation for all fields, sources and parameters. Specifically, for the renormalization factors one finds:

$$\begin{aligned}
A_0 &= Z_A^{1/2}A_\mu\;,\;\; b_0 = Z_b^{1/2}b\;,\;\; c_0 = Z_c^{1/2}c\;,\;\; \bar{c}_0 = Z_{\bar{c}}^{1/2}\bar{c}\;, && (144)\\
\xi_0^a &= Z_\xi^{ab}(\xi)\xi^b \;\;\tau_0 = Z_\tau^{1/2}\tau\;, \Omega_0 = Z_\Omega\Omega\;,\;\; L_0 = Z_L L && (145)\\
K_0^a &= Z_K^{ab}(\xi)K^b\;,\;\; m_0^2 = Z_{m^2}m^2\;,\;\; \mathcal{J}_0 = Z_{\mathcal{J}}\mathcal{J}\;, && (146)\\
g_0 &= Z_g g\;,\;\; \alpha_0 = Z_\alpha\alpha\;,\;\; \bar{\eta}_0 = Z_{\bar{\eta}}^{1/2}\bar{\eta}\;,\;\; \eta_0 = Z_\eta^{1/2}\eta\;, && (147)\\
\Xi_0 &= Z_\Xi\Xi\;,\;\; \mu_0^2 = Z_{\mu^2}\mu^2\;, && (148)
\end{aligned}$$

where

$$\begin{aligned}
Z_g &= 1 - \varepsilon\frac{a_0}{2}\\
Z_A^{1/2} &= Z_\Omega^{-1} = Z_{\bar{c}}^{-1/2} = Z_b^{-1/2} = Z_\alpha^{1/2} = 1 + \varepsilon d_2(\alpha)\\
Z_\xi^{ab} &= \delta^{ab} + \varepsilon f_1^{ab}(\xi,\alpha)\\
Z_L &= Z_c^{-1/2} = 1 + \varepsilon d_1(\alpha)\\
Z_{\bar{\eta}} &= Z_\eta = Z_\Xi^2 = Z_\tau^{1/2} = Z_{\mathcal{J}} = 1 + \varepsilon a_4\\
Z_{m^2} &= 1 + \varepsilon a_7\\
Z_{\mu^2} &= 1 + \varepsilon(d_2 - f_2(0,\alpha))\\
Z_K^{ab} &= \delta^{ab} - \varepsilon\left(f_1^{ab}(\xi,\alpha) + \frac{\partial f_1^{kb}(\xi,\alpha)}{\partial\xi^a}\xi^k\right)\;.
\end{aligned} \tag{149}$$

Notice that, as expected, the dimensionless field ξ^a renormalizes in a non-linear

way through the quantity $f_1^{ab}(\xi,\alpha)$ which is a power series in ξ^a. Equations (142) and (149) establish the renormalizability of the complete action Σ, eq.(105), and thus of the invariant action S of expression (98), up to a BRST exact unphysical ambiguity of the type of eq.(96). As already mentioned, the explicit inclusion of such an ambiguity will be provided in Appendix B.

2.8 **Conclusion**

In this chapter the gauge invariant operator $A^2_{\rm min}$, eq.(78), and corresponding gauge invariant transverse field configuration A^{ah}_μ, eq.(79), have been investigated in a general class of gauge fixings, eq.(94) and eq.(97), which share similarities with 't Hooft's R_ζ-gauge used in the analysis of YM theory with spontaneous symmetry breaking. As shown in (CAPRI et al., 2016b), a local setup can be constructed for both $A^2_{\rm min}$ and A^{ah}_μ, being summarised by the local and BRST invariant action (85). The localization procedure makes use of an auxiliary dimensionless Stueckelberg field ξ^a. However, despite the presence of the field ξ^a and unlike the conventional non-renormalizable Stueckelberg mass term, the present construction gives rise to a perfectly well behaved model in the ultraviolet which turns out to be renormalizable to all orders, as discussed in details in sections (2.6) and (2.7) as well as in Appendix (B). In particular, the pivotal role of the transversality constraint $\partial_\mu A^{ah}_\mu = 0$ has been underlined throughout the paper. It is precisely the direct implementation of this constraint in the local action (85) which makes a substantial difference with respect to the conventional Stueckelberg theory. In fact, as pointed out in section (2.5), it removes exactly the component of the Stueckelberg propagator which gives rise to non-renormalizable ultraviolet divergences, see eq.(103) versus eqs.(101). In particular, form eqs.(101), one sees that, similar to what happens in the case of 't Hooft's R_ζ-gauge, the use of the general class of gauge fixings (94) and (97) provide a mass μ^2 for the dimensionless Stueckelberg field ξ^a. This a welcome feature which can be effectively employed as a fully BRST invariant infrared regularization for ξ^a in explicit higher loop calculations.

3 SOME REMARKS ON THE SPECTRAL FUNCTIONS OF THE ABELIAN HIGGS MODEL

In section 1.3.2, we have discussed the two main observations in lattice QCD in recent years: massive behavior of the gluon propagator, and positivity violation of its spectral density function. In this context, it is worthwhile to investigate the spectral properties of massive gauge models to try and shed some light on the infrared behavior of their fundamental fields in an analytical way. The direct comparison between a massive model that violates BRST, such as the massive YM model from section 1.3.1, and a model that preserves the original nilpotent BRST symmetry, such as the Higgs model, can be particularly enlightening. In any case, the explicit determination of the spectral properties of Higgs theories and the study of the role played by gauge symmetry there is an interesting pursue on its own.

Most articles on massive YM models employ the renormalizable Landau gauge, although it was noticed that this gauge might not be the preferred gauge in non-perturbative calculations (OEHME; ZIMMERMANN, 1980). For the Higgs model, one can fix the gauge by means of 't Hooft R_ξ-gauge, see section 1.1.6. Understanding the different gauges and their influence on the spectral properties is a delicate subject. This gave us further reason to undertake a systematic study of the spectral properties of Higgs models. In this chapter, we present the results for the simplest case: that of the $U(1)$ Abelian Higgs model. In fact, it turned out that this model is already very illuminating on aspects like positivity of the spectral function, gauge-parameter independence of physical quantities and unitarity. Of course, these properties are not unknown in the Abelian case. This chapter should therefore not be seen as giving any new information on the physical properties of the Abelian model. Rather, exactly because these properties are so well-known, we are in a better position to understand the problems that we face when calculating the analytic structure behind some of them within a gauge-fixed setup. This chapter is therefore a first attempt to understand analytically the spectral properties of a Higgs-gauge model in contrast to those of a non-unitary massive model. As such, it is laying the groundwork for the next chapters.

The $U(1)$ Higgs model is known to be unitary (GIERES, 1997; HOOFT et al., 1980) and renormalizable (BECCHI; ROUET; STORA, 1975). In this work, we consider two propagators: that of the photon, and that of the Higgs scalar field. They are obtained through the calculation of the one-loop corrections to the corresponding $1PI$ two-point functions. After adopting the R_ξ-gauge, we are left with an exact BRST nilpotent symmetry. Of course, the correlation function of BRST invariant quantities should be independent of the gauge parameter. Since the transverse component of the photon propagator is gauge invariant, we should find that the one-loop corrected trans-

verse propagator does not depend on the gauge parameter. As a consequence, the photon pole mass will neither. This property has been proven before by the use of the Nielsen identities, (HAUSSLING; KRAUS, 1997), see also (NIELSEN, 1975; PIGUET; SIBOLD, 1985; GAMBINO; GRASSI, 2000), but never in a direct calculation. The same goes for the Higgs particle propagator: the gauge independence of its pole mass was proven in (HAUSSLING; KRAUS, 1997), but never in a direct loop calculation to our knowledge. We underline here the importance of properly taking into account the tadpole contributions (MARTIN, 2015a; MARTIN, 2015b) or, equivalently, the effect on the propagators of quantum corrections of the Higgs vacuum expectation value. Armed with the one-loop results, we are able to calculate the spectral properties of the respective propagators for different values of the gauge parameter. Finally, we compare our results with those of a non-unitary massive Abelian model, to clearly pinpoint at the level of spectral functions the differences (and issues) of both unitary and non-unitary massive vector boson models.

This chapter is organized as follows. In section 3.1, we review the $U(1)$ Higgs model and its gauge fixing, as well as the tree-level field propagators and vertices. In section 3.2, we calculate the one-loop propagator of both the photon field and the Higgs field, showing the gauge-parameter independence of the transverse photon propagator and of the Higgs pole mass up to one-loop order. In section 3.3, we calculate the spectral function of both propagators. In section 3.4 we discuss some subtleties of the Higgs spectral function and in section 3.5 we compare our results with those of a non-unitary massive Abelian model. We also address the residue computation. Section 3.6 collects our conclusions and outlook.

3.1 **Abelian Higgs model: some essentials**

We start from the Abelian Higgs classical action with a manifest global $U(1)$ symmetry

$$S = \int d^4x \left\{ \frac{1}{4} F_{\mu\nu} F_{\mu\nu} + (D_\mu \varphi)^\dagger D_\mu \varphi + \frac{\lambda}{2} \left(\varphi^\dagger \varphi - \frac{v^2}{2} \right)^2 \right\}, \tag{150}$$

where

$$\begin{aligned} F_{\mu\nu} &= \partial_\mu A_\nu - \partial_\nu A_\mu, \\ D_\mu \varphi &= \partial_\mu \varphi + ieA_\mu \varphi \end{aligned} \tag{151}$$

and the parameter v gives the minimizing value of the scalar field to first order in $\hbar$, $\varphi_0 = v$. The spontaneous symmetry breaking is implemented by expressing the scalar

field as an expansion around its minimizing value, namely

$$\varphi = \frac{1}{\sqrt{2}}((v+h)+i\rho), \tag{152}$$

where the real part h is identified as the Higgs field and ρ is the (unphysical) Goldstone boson, with $\langle\rho\rangle = 0$. Here we choose to expand around the classical value of the minimizing value, so that $\langle h\rangle$ is zero at the classical level, but receives loop corrections[4] . The action (150) now becomes

$$\begin{aligned} S &= \int d^4x \left\{ \frac{1}{4}F_{\mu\nu}F_{\mu\nu} + \frac{1}{2}\partial_\mu h \partial_\mu h + \frac{1}{2}\partial_\mu\rho\partial_\mu\rho - e\,\rho\,\partial_\mu h\, A_\mu + e\,(h+v)A_\mu\partial_\mu\rho \right. \\ &+ \left. \frac{1}{2}e^2 A_\mu[(h+v)^2+\rho^2]A_\mu + \frac{1}{8}\lambda(h^2+2hv+\rho^2)^2 \right\} \end{aligned} \tag{153}$$

and we notice that both the gauge field and the Higgs field have acquired the following masses

$$m^2 = e^2v^2,\ m_h^2 = \lambda v^2. \tag{154}$$

With this parametrization, the Higgs coupling λ and the parameter v can be fixed in terms of m, m_h and e, whose values will be suitably chosen later on in the text.

Even in the broken phase, the action (153) is left invariant by the following gauge transformations

$$\begin{aligned} \delta A_\mu &= -\partial_\mu\omega,\ \delta\varphi = ie\omega\varphi,\ \delta\varphi^\dagger = -ie\omega\varphi^\dagger, \\ \delta h &= -e\omega\rho,\ \delta\rho = e\omega(v+h). \end{aligned} \tag{155}$$

where ω is the gauge parameter.

3.1.1 Gauge fixing

Quantization of the theory (153) requires a proper gauge fixing. We shall employ the gauge fixing term

$$S_{gf} = \int d^4x \left\{ \frac{1}{2\xi}\left(\partial_\mu A_\mu + \xi m\rho\right)^2 \right\}, \tag{156}$$

[4] There is of course an equivalent procedure of fixing $\langle h\rangle$ to zero at all orders, by expanding φ around the full minimizing value: $\varphi = \frac{1}{\sqrt{2}}((\langle\varphi\rangle + h) + i\rho)$. In the Appendix E we explicitly show that—as expected—both procedures give the same final results up to a given order.

known as the 't Hooft or R_ξ-gauge, which has the pleasant property of cancelling the mixed term $\int d^4x(ev\ A_\mu\partial_\mu\rho)$ in the expression (153). Of course, (156) breaks the gauge invariance of the action. As is well known, the latter is replaced by the BRST invariance. In fact, introducing the FP ghost fields $\bar{c}, c$ as well as the auxiliary field b, for the BRST transformations we have

$$\begin{aligned}
sA_\mu &= -\partial_\mu c, \\
sc &= 0, \\
s\varphi &= iec\varphi, \\
s\varphi^\dagger &= -iec\varphi^\dagger, \\
sh &= -ec\rho, \\
s\rho &= ec(v+h), \\
s\bar{c} &= ib, \\
sb &= 0.
\end{aligned} \tag{157}$$

Importantly, the operator s is nilpotent, i.e. $s^2 = 0$, allowing to work with the so-called BRST cohomology, a useful concept to prove unitarity and renormalizability of the Abelian Higgs model (BECCHI; ROUET; STORA, 1975; BECCHI; ROUET; STORA, 1974; KUGO; OJIMA, 1979).

We can now introduce the gauge fixing in a BRST invariant way via

$$\mathcal{S}_{gf} = s\int d^dx\left\{-i\frac{\xi}{2}\bar{c}b + \bar{c}(\partial_\mu A_\mu + \xi m\rho)\right\}, \tag{158}$$

$$= \int d^dx\left\{\frac{\xi}{2}b^2 + ib\partial_\mu A_\mu + ib\xi m\rho + \bar{c}\partial^2 c - \xi m^2\bar{c}c - \xi me\bar{c}hc\right\}. \tag{159}$$

Notice that the ghosts $(\bar{c}, c)$ get a gauge parameter dependent mass, while interacting directly with the Higgs field.

The total gauge fixed BRST invariant action then becomes

$$\begin{aligned}
S &= \int d^4x\left\{\frac{1}{4}F_{\mu\nu}F_{\mu\nu} + \frac{1}{2}\partial_\mu h\partial_\mu h + \frac{1}{2}\partial_\mu\rho\partial_\mu\rho - e\,\rho\,\partial_\mu h\,A_\mu + e\,hA_\mu\partial_\mu\rho + \frac{1}{2}m^2A_\mu A_\mu\right. \\
&+ \frac{1}{2}e^2A_\mu[h^2 + 2vh + \rho^2]A_\mu + \frac{1}{8}\lambda(h^2+\rho^2)(h^2+\rho^2+4hv) + \frac{1}{2}m_h^2h^2 2b^2 \\
&+ \left. mA_\mu\partial_\mu\rho + \frac{\xi}{+}ib\partial_\mu A_\mu + ib\xi m\rho + \bar{c}(\partial^2)c - m^2\xi c\bar{c} - m\xi e\bar{c}ch\right\},
\end{aligned} \tag{160}$$

with

$$sS = 0\ . \tag{161}$$

In Appendix C and D we collect the propagators and vertices corresponding to the action

(160) of the Abelian Higgs model in the R_ξ gauge.

3.2 Photon and Higgs propagators at one-loop

In this section we obtain the one-loop corrections to the photon propagator, as well as to the propagator of the Higgs boson. This requires the calculation[5], in section 3.2.1 and 3.2.2, of the Feynman diagrams as shown in Figure 6 and Figure 7. Notice that the last four diagrams in Figure 6 and Figure 7 vanish for $\langle h \rangle = 0$. Since we have chosen to expand the φ field around its classical minimizing value v (cf. (152)), $\langle h \rangle$ has loop contributions which are nonzero and the resulting tadpole diagrams have to be included in the quantum corrections for the propagators[6]. Of course the final result for the propagators would be the same had we chosen to expand the φ field around its full minimizing value and required $\langle h \rangle = 0$. In fact, including the tadpole diagrams in our formulation has the same effect as shifting the masses of the fields to include the one-loop corrections to the Higgs minimizing value $\langle \varphi \rangle$, calculated by imposing $\langle h \rangle = 0$ (see Appendix E for the technical details). These diagrams can actually be seen as a correction to the tree-level mass term: in the spontaneously broken phase the gauge boson mass is given by $m = e\langle \varphi \rangle$, depending thus on $\langle \varphi \rangle$ that receives quantum corrections order by order. Therefore, the full inverse photon propagator can be written as

$$\begin{aligned} G_{AA}^{-1}(p^2) &= p^2 + e^2 v^2 + (\text{1PI diagrams}) + (\text{diagrams with tadpoles}) \\ &= p^2 + e^2 \langle \varphi \rangle^2 + (\text{1PI diagrams}) \ , \end{aligned} \tag{162}$$

where the equalities are to be understood up to a given order in perturbation theory and a similar reasoning can be drawn for the Higgs propagator. In what follows, we shall proceed with the expansion adopted in eq. (152) and include the tadpole diagrams explicitly in our self-energy results. The calculations are done for arbitrary dimension d. In section 3.2.3 we will analyze the results for $d = 4 - \epsilon$, making use of the techniques of dimensional regularization in the $\overline{\text{MS}}$ scheme.

---

[5] We have used the techniques of modifying integrals into "master integrals" with momentum-independent numerators from (PASSARINO; VELTMAN, 1979).

[6] The diagrams with tadpole balloons are not part of the standard definition of one-particle irreducible diagrams that contribute to the self-energies. However, since the momentum flowing in the vertical h-field (dashed) line is zero, they can be effectively included as a momentum-independent term in the self-energies.

Figure 6 - One-loop photon self-energy

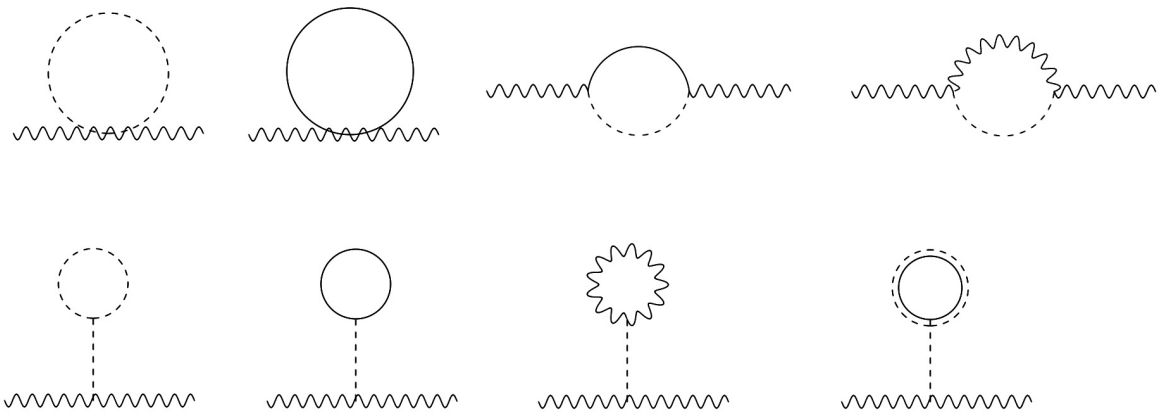

Legend: Contributions to one-loop photon self-energy in the Abelian Higgs Model, including tadpole contributions in the second line. Wavy lines represent the photon field, dashed lines the Higgs field, solid lines the Goldstone boson and double lines the ghost field.

Source: The author, 2020.

3.2.1 Corrections to the photon self-energy

The first diagram contributing to the photon self-energy is the Higgs boson snail (first diagram in the first line of Figure 6) and gives a contribution

$$\Gamma_{A_\mu A_\nu,1}(p^2) = \frac{-4e^2}{(4\pi)^{d/2}} \frac{\Gamma(2-d/2)}{2-d} \frac{m_h^{d-2}}{2} \delta_{\mu\nu}. \tag{163}$$

The second diagram is the Goldstone boson snail (second diagram in the first line of Figure 6)

$$\Gamma_{A_\mu A_\nu,2}(p^2) = \frac{-4e^2}{(4\pi)^{d/2}} \frac{\Gamma(2-d/2)}{2-d} \frac{(\xi m^2)^{d/2-1}}{2} \delta_{\mu\nu}. \tag{164}$$

Being momentum-independent, the only effect of these first two diagrams is to renormalize the mass parameters (m_h^2, m^2).

The third term contributing to the photon propagator is the Higgs-Goldstone sun-

set (third diagram in first line of Figure 6)

$$\Gamma_{A_\mu A_\nu,3}(p^2) = \frac{4e^2}{(4\pi)^{d/2}}\frac{\Gamma(2-d/2)}{2-d}\int_0^1 dx\Bigg[K_{d/2-1}(m_h^2,\xi m^2)P_{\mu\nu} + \Bigg(K_{d/2-1}(m_h^2,\xi m^2) + \frac{(2-d)}{4}(1-4x(1-x))p^2K_{d/2-2}(m_h^2,\xi m^2)\Bigg)\mathcal{L}_{\mu\nu}\Bigg], \quad (165)$$

where we used the definitions

$$K_\alpha(m_1^2,m_2^2) \equiv \Big(p^2x(1-x)+xm_1^2+(1-x)m_2^2\Big)^\alpha, \quad (166)$$

and

$$\mathcal{P}_{\mu\nu} = \delta_{\mu\nu} - \frac{p_\mu p_\nu}{p^2}, \quad (167)$$

$$\mathcal{L}_{\mu\nu} = \frac{p_\mu p_\nu}{p^2}, \quad (168)$$

which are the transversal and longitudinal projectors, respectively. The fourth term contributing to the photon propagator is the Higgs-photon sunset (fourth diagram in first line of Figure 6)

$$\Gamma_{A_\mu A_\nu,4}(p^2) = \frac{4e^2}{(4\pi)^{d/2}}\frac{\Gamma(2-d/2)}{2-d}\int_0^1 dx\Bigg[\Big((2-d)m^2K_{d/2-2}(m_h^2,m^2)+K_{d/2-1}(m_h^2,m^2) - K_{d/2-1}(m_h^2,\xi m^2)\Big)\mathcal{P}_{\mu\nu} + \Big((2-d)m^2K_{d/2-2}(m_h^2,m^2) + K_{d/2-1}(m_h^2,m^2) - K_{d/2-1}(m_h^2,\xi m^2) + (2-d)p^2x^2(K_{d/2-2}(m_h^2,m^2)-K_{d/2-1}(m_h^2,\xi m^2))\Big)\mathcal{L}_{\mu\nu}\Bigg]. \quad (169)$$

Finally, we have four tadpole (balloon) diagrams. The Higgs boson balloon (first diagram of the last line in Figure 6)

$$\Gamma_{A_\mu A_\nu,5}(p^2) = \frac{4e^2}{(4\pi)^{d/2}}\frac{\Gamma(2-d/2)}{(2-d)}\frac{3}{2}m_h^{d/2-1}\delta_{\mu\nu}, \quad (170)$$

the Goldstone boson balloon (second diagram of the last line in Figure 6)

$$\Gamma_{A_\mu A_\nu,6}(p^2) = \frac{4e^2}{(4\pi)^{d/2}}\frac{\Gamma(2-d/2)}{(2-d)}\frac{1}{2}(\xi m)^{d/2-1}\delta_{\mu\nu}, \quad (171)$$

the photon balloon (third diagram of the last line in Figure 6)

$$\Gamma_{A_\mu A_\nu,7}(p^2) = 2e^2\frac{m^2}{m_h^2}\int\frac{d^dk}{(2\pi)^d}\left(\frac{1}{k^2+m^2}(d-1)+\frac{\xi}{k^2+\xi m^2}\right)\delta_{\mu\nu}, \quad (172)$$

and finally, the ghost balloon (fourth diagram of the last line in Figure 6)

$$\Gamma_{A_\mu A_\nu,8}(p^2) = -2e^2\frac{m^2}{m_h^2}\int\frac{d^dk}{(2\pi)^d}\frac{\xi}{k^2+\xi m^2}\delta_{\mu\nu}. \tag{173}$$

Combining all these contributions (163)-(173), we find

$$\begin{aligned}\Gamma_{A_\mu A\nu}(p^2) &= \frac{4e^2}{(4\pi)^{d/2}}\frac{\Gamma(2-d/2)}{2-d}\int_0^1 dx\Big((2-d)m^2K_{d/2-2}(m^2,m_h^2)+K_{d/2-1}(m^2,m_h^2)\\ &+ m_h^{d-2}+\frac{m^d}{m_h^2}(d-1)\Big)\mathcal{P}_{\mu\nu}\\ &+ \frac{4e^2}{(4\pi)^{d/2}}\frac{\Gamma(2-d/2)}{2-d}\int_0^1 dx\Bigg(\frac{2-d}{4}(1-4x)p^2K_{d/2-2}(m_h^2,\xi m^2)\\ &+ (2-d)(m^2+p^2x^2)K_{d/2-2}(m_h^2,m^2)\\ &+ K_{d/2-1}(m_h^2,m^2)+m_h^{d-2}+\frac{m^d}{m_h^2}(d-1)\Bigg)\mathcal{L}_{\mu\nu}.\end{aligned} \tag{174}$$

Defining

$$\Gamma_{A_\mu A_\nu} = \Pi_{AA}^{\perp}(p^2)\mathcal{P}_{\mu\nu}+\Pi_{AA}^{\parallel}(p^2)\mathcal{L}_{\mu\nu}, \tag{175}$$

it follows that

$$\partial_\xi\Pi_{AA}^{\perp}=0. \tag{176}$$

As expected, eq.(176) expresses the gauge parameter independence of the gauge invariant transverse component of the photon propagator (HAUSSLING; KRAUS, 1997).

3.2.2 Corrections to the Higgs self-energy

The first diagrams contributing to the Higgs self-energy are of the snail type, renormalizing the masses of the internal fields.

The Higgs boson snail (first diagram in the first line of Figure 7)

$$\Gamma_{hh,1}(p^2) = -3\frac{\lambda}{(4\pi)^{d/2}}\frac{\Gamma(2-d/2)}{(2-d)}m_h^{d-2}, \tag{177}$$

the Goldstone boson snail (second diagram in the first line of Figure 7)

$$\Gamma_{hh,2}(p^2) = -\frac{\lambda}{(4\pi)^{d/2}}\frac{\Gamma(2-d/2)}{(2-d)}(\xi m^2)^{d/2-1} \tag{178}$$

Figure 7 - One-loop Higgs self-energy

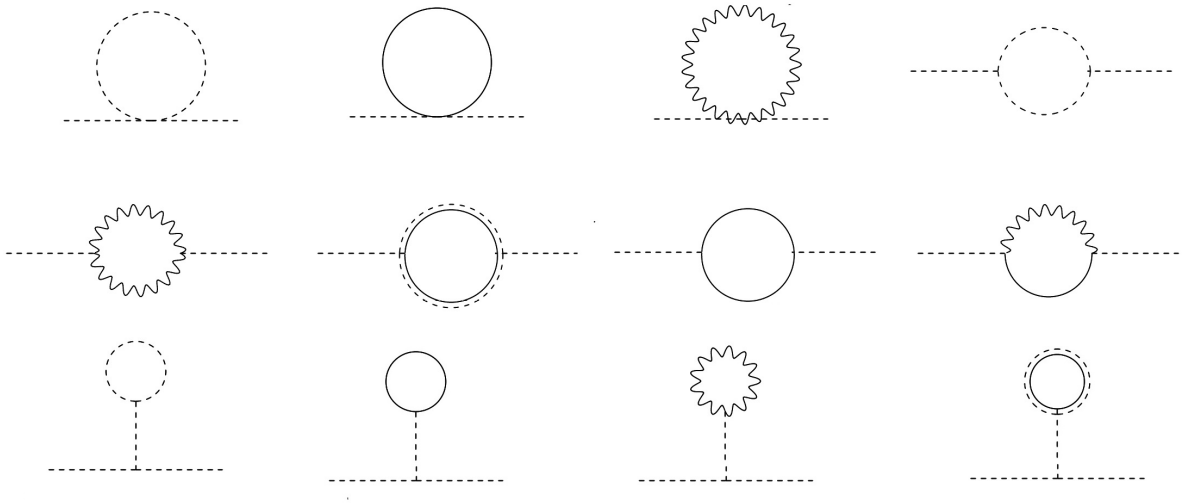

Legend: Contributions to the one-loop Higgs self-energy. Line representations are as in Figure 6.
Source: The author, 2020.

and the photon snail (third diagram in the first line of Figure 7)

$$\Gamma_{hh,3}(p^2) = -2\frac{e^2}{(4\pi)^{d/2}}\frac{\Gamma(2-d/2)}{(2-d)}\Big((d-1)m^{d-2}+\xi(\xi m^2)^{d/2-1}\Big). \tag{179}$$

Next, we meet a couple of sunset diagrams. The Higgs boson sunset (fourth diagram in the first line of Figure 7):

$$\Gamma_{hh,4}(p^2) = \frac{9}{2}\frac{\lambda}{(4\pi)^{d/2}}\frac{\Gamma(2-d/2)}{(2-d)}(2-d)m_h^2\int_0^1 dx K_{d/2-2}(m_h^2,m_h^2), \tag{180}$$

the photon sunset (first diagram in the second line of Figure 7):

$$\Gamma_{hh,5}(p^2) \tag{181}$$

$$\begin{aligned}
&= e^2\frac{\Gamma(2-d/2)}{2-d}\frac{1}{(4\pi)^{d/2}}\int_0^1 dx\Bigg[(2-d)\Big(2m^2(d-1)+2p^2+\frac{p^4}{2m^2}\Big)K_{d/2-2}(m^2,m^2)\\
&- (2-d)\Big(2p^2+\frac{p^4}{m^2}+\xi^2m^2+2p^2\xi-2\xi m^2+m^2\Big)K_{d/2-2}(m^2,\xi m^2)\\
&+ (2-d)\Big(2\xi p^2+2\xi^2m^2+\frac{p^4}{2m^2}\Big)K_{d/2-2}(\xi m^2,\xi m^2)\\
&+ 2(\xi-1)(m^2)^{d/2-1}+2(1-\xi)(\xi m^2)^{d/2-1}\Bigg],
\end{aligned} \tag{182}$$

the ghost sunset (second diagram in the second line of Figure 7):

$$\Gamma_{hh,6}(p^2) = -\frac{e^2}{(4\pi)^{d/2}}\frac{\Gamma(2-d/2)}{(2-d)}(2-d)m^2\xi^2\int_0^1 dx K_{d/2-2}(\xi m^2,\xi m^2), \tag{183}$$

the Goldstone boson sunset (third diagram in the second line of Figure 7):

$$\Gamma_{hh,7}(p^2) = \frac{1}{2}\frac{\lambda}{(4\pi)^{d/2}}\frac{\Gamma(2-d/2)}{(2-d)}(2-d)m_h^2\int_0^1 dx K_{d/2-2}(\xi m^2,\xi m^2)^{d/2-2} \tag{184}$$

and a mixed Goldstone-photon sunset (fourth diagram in the second line of Figure 7):

$$\begin{aligned}\Gamma_{hh,8}(p^2) &= e^2\frac{\Gamma(2-d/2)}{2-d}\frac{1}{(4\pi)^{d/2}}\int_0^1 dx\Bigg[(2-d)\Big(2p^2+\frac{p^4}{m^2}+\xi^2m^2 \qquad (185)\\ &+ 2p^2\xi-2\xi m^2+m^2\Big)K_{d/2-2}(m^2,\xi m^2)\\ &- (2-d)\Big(\xi^2m^2+\frac{p^4}{m^2}+2p^2\xi\Big)K_{d/2-2}(\xi m^2,\xi m^2)\\ &+ 2\Big(1-\xi-\frac{p^2}{m^2}\Big)(m^2)^{d/2-1}\\ &+ 2\Big(2\xi-1+\frac{p^2}{m^2}\Big)(\xi m^2)^{d/2-1}\Bigg]. \qquad (186)\end{aligned}$$

Finally, we have the tadpole diagrams. The Higgs balloon (first diagram on the third line of Figure 7):

$$\Gamma_{hh,9}(p^2) = 9\frac{\lambda}{(4\pi)^{d/2}}\frac{\Gamma(2-d/2)}{(2-d)}m_h^{d-2}, \tag{187}$$

the photon balloon (second diagram on the third line of Figure 7):

$$\Gamma_{hh,10}(p^2) = 6\frac{e^2}{(4\pi)^{d/2}}\frac{\Gamma(2-d/2)}{(2-d)}\Big((d-1)m^{d-2}+\xi(\xi m^2)^{d/2-1}\Big), \tag{188}$$

the Goldstone boson balloon (third diagram on the third line of Figure 7):

$$\Gamma_{hh,11}(p^2) = 3\frac{\lambda}{(4\pi)^{d/2}}\frac{\Gamma(2-d/2)}{(2-d)}(\xi m^2)^{d/2-1} \tag{189}$$

the ghost balloon (fourth diagram on the third line of Figure 7):

$$\Gamma_{hh,12}(p^2) = -6\frac{e^2\xi}{(4\pi)^{d/2}}\frac{\Gamma(2-d/2)}{(2-d)}(\xi m^2)^{d/2-1}. \tag{190}$$

Putting together eqs. (177) to (190) we find the total one-loop correction to the Higgs

boson self-energy,

$$\begin{aligned}
\Pi_{hh}(p^2) &\equiv \\
\Gamma_{hh}(p^2) &= \frac{\Gamma(2-d/2)}{2-d}\frac{1}{(4\pi)^{d/2}}\int_0^1 dx\Bigg[(2-d)e^2\Big(2m^2(d-1)+2p^2+\frac{p^4}{2m^2}\Big)K_{d/2-2}(m^2,m^2) \\
&+ \frac{9}{2}\lambda(2-d)m_h^2K_{d/2-2}(m_h^2,m_h^2) \\
&+ e^2\left(-2\frac{p^2}{m^2}+4(d-1)\right)(m^2)^{d/2-1} \\
&+ 6\lambda(m_h^2)^{d/2-1} \\
&+ (2-d)\Big(-\frac{p^4}{2m^2}e^2+\frac{\lambda}{2}m_h^2\Big)K_{d/2-2}(\xi m^2,\xi m^2) \\
&+ 2(\frac{p^2}{m^2}e^2+\lambda)(\xi m^2)^{d/2-1}\Big]. \qquad (191)
\end{aligned}$$

3.2.3 Results for $d = 4-\epsilon$

For $d=4$, the 2-point functions are divergent. We therefore follow the standard procedure of dimensional regularization, as we have no chiral fermions present. Thus, we choose $d=4-\epsilon$ with ϵ an infinitesimal parameter, and analyze the solution in the limit $\epsilon \to 0$.

Let us start with the photon 2-point function, given for arbitrary dimension d by (174). The mass dimension of the coupling constant e is $[e] = 2-d/2 = \epsilon/2$, and redefining $e \to e\tilde{\mu}^{\epsilon/2} = e\tilde{\mu}^{2-d/2}$ we put the dimension on $\tilde{\mu}$, while e is dimensionless. Using

$$\frac{4e^2}{(4\pi)^{d/2}}\frac{\Gamma(2-d/2)}{2-d} \stackrel{d\to 4-\epsilon}{=} -2\frac{e^2}{(4\pi)^2}\left(\frac{2}{\epsilon}+1+\ln(\mu^2)\right), \qquad (192)$$

where we defined

$$\mu^2 = \frac{4\pi\tilde{\mu}^2}{e^{\gamma_E}}, \qquad (193)$$

we find for the divergent part of the transverse photon 2-point function:

$$\Pi^{\perp}_{AA,div}(p^2) = \frac{2}{\epsilon}\frac{e^2}{(4\pi)^2}\left(\frac{p^2}{3}+6(\frac{g^2}{\lambda}-\frac{1}{2})m^2+3m_h^2\right) \qquad (194)$$

and these infinities are, following the $\overline{\text{MS}}$-scheme, cancelled by the corresponding counterterms. The renormalized correlation function is then finite in the limit $d \to 4$ and we

find the one-loop correction

$$\begin{aligned}\Pi_{AA}(p^2) &= 2\frac{e^2}{(4\pi)^2}\int_0^1 dx\,\Big\{p^2x(1-x)+m^2x \\ &+ m_h^2(1-x)(1-\ln\frac{p^2x(1-x)+m^2x+m_h^2(1-x)}{\mu^2})+m_h^2(1-\ln\frac{m_h^2}{\mu^2}) \\ &+ \frac{m^4}{m_h^2}(1-3\ln\frac{m^2}{\mu^2})+2m^2\ln\frac{p^2x(1-x)+m^2x+m_h^2(1-x)}{\mu^2}\Big\}. \qquad (195)\end{aligned}$$

In the same way, we find the divergent part of the Higgs boson 2-point function:

$$\Pi_{hh,div}(p^2) = -\frac{1}{2\epsilon}\frac{1}{(4\pi)^2}\Big(e^2(12p^2-4\xi p^2)+\lambda(8m_h^2-4\xi m^2)\Big), \qquad (196)$$

which is canceled by the corresponding counterterm. Therefore, the one-loop correction to the Higgs boson propagator reads

$$\begin{aligned}\Pi_{hh}(p^2) &= \frac{1}{(4\pi)^2}\int_0^1 dx\Big\{e^2\Big[p^2(1-\ln\frac{m^2}{\mu^2}-2\ln\frac{p^2x(1-x)+m^2}{\mu^2}) \\ &- \frac{p^4}{2m^2}\ln\frac{p^2x(1-x)+m^2}{\mu^2}-6m^2(1-\ln\frac{m^2}{\mu^2}+\ln\frac{p^2x(1-x)+m^2}{\mu^2})\Big] \\ &+ \lambda\Big[\frac{1}{2}m_h^2(-6+6\ln\frac{m_h^2}{\mu^2}-9\ln\frac{p^2x(1-x)+m_h^2}{\mu^2})\Big] \\ &- \Big[\xi(e^2p^2+\lambda m^2)(1-\ln\frac{\xi m^2}{\mu^2})-(e^2\frac{p^4}{2m^2}-\lambda\frac{m_h^2}{2})\ln\frac{p^2x(1-x)+\xi m^2}{\mu^2}\Big]\Big\} \qquad (197)\end{aligned}$$

3.2.4 One-loop propagators for the elementary fields

For the photon field, the transverse part of the propagator $G^{AA}_{\mu\nu}(p^2)$ up to order $\hbar$ is given in momentum space by

$$\langle A_\mu(p)A_\nu(-p)\rangle = \frac{1}{p^2+m^2}+\frac{1}{(p^2+m^2)^2}\Pi_{AA}(p^2)+\mathcal{O}(\hbar^2) \qquad (198)$$

and we can approach the all-order form factor with the resummed approximation

$$G^T_{AA}(p^2) = \frac{1}{p^2+m^2-\Pi(p^2)}, \qquad (199)$$

shown in Figure 8.

Figure 8 - Resummed photon form factor

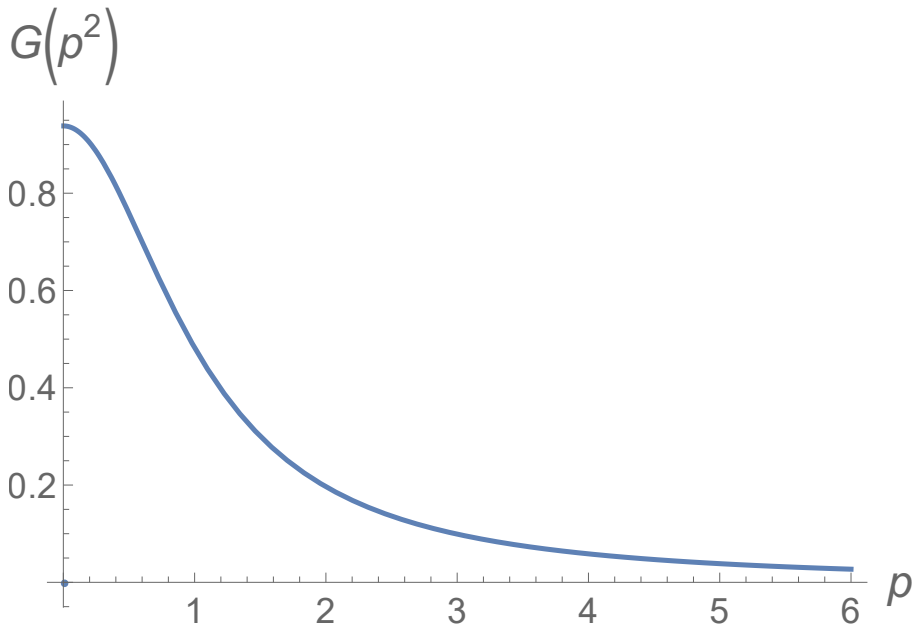

Legend: Resummed form factor for the photon operator, with p given in units of the energy scale μ, for the parameter values $e = 1$, $v = 1\,\mu$, $\lambda = \frac{1}{5}$.

Source: The author, 2020.

For the Higgs field, we find

$$\langle h(p)h(-p)\rangle \;=\; \frac{1}{p^2+m_h^2}+\frac{1}{(p^2+m_h^2)^2}\Pi_{hh}(p^2)+\mathcal{O}(\hbar^2). \tag{200}$$

Before making the resummed approximation, we notice that the resummation is based on the assumption that the second term in (200) is much smaller than the first term. Then, we see that (200) contains terms of the order of $\frac{p^4}{(p^2+m_h^2)^2}\ln\frac{p^2x(1-x)+m_h^2}{\mu^2}$, which cannot be resummed for big values of p. We therefore use the identity

$$p^4 \;=\; (p^2+m_h^2)^2-m_h^4-2p^2m_h^2, \tag{201}$$

to rewrite

$$\frac{p^4}{(p^2+m_h^2)^2}\ln\frac{p^2x(1-x)+m_h^2}{\mu^2} \;=\; \ln\frac{p^2x(1-x)+m_h^2}{\mu^2}-\frac{(m^4+2p^2m^2)}{(p^2+m^2)^2}\ln\frac{p^2x(1-x)+m_h^2}{\mu^2} \tag{202}$$

The last two terms in (202) can be safely resummed. We rewrite

$$\frac{\Pi_{hh}(p^2)}{(p^2+m_h^2)^2} = \frac{\hat{\Pi}_{hh}(p^2)}{(p^2+m_h^2)^2} + C_{hh}(p^2), \tag{203}$$

with

$$\begin{aligned}\hat{\Pi}_{hh}(p^2) &= \frac{1}{(4\pi)^2}\int_0^1 dx\Bigg\{e^2\Bigg[p^2(1-\ln\frac{m^2}{\mu^2}-2\ln\frac{p^2x(1-x)+m^2}{\mu^2}) \\ &+ \frac{(m_h^4+2p^2m_h^2)}{2m^2}\ln\frac{p^2x(1-x)+m_h^2}{\mu^2} - 6m^2(1-\ln\frac{m^2}{\mu^2}+\ln\frac{p^2x(1-x)+m^2}{\mu^2})\Bigg] \\ &+ \lambda\Big[\frac{1}{2}m_h^2(-6+6\ln\frac{m_h^2}{\mu^2}-9\ln\frac{p^2x(1-x)+m_h^2}{\mu^2})\Big] - \Bigg[\xi(e^2p^2+\lambda m^2)(1-\ln\frac{\xi m^2}{\mu^2}) \\ &+ (e^2\frac{(m_h^4+2p^2m_h^2)}{2m^2}+\lambda\frac{m_h^2}{2})\ln\frac{p^2x(1-x)+\xi m^2}{\mu^2}\Bigg]\Bigg\}. \end{aligned}\tag{204}$$

and

$$C_{hh}(p^2) = -\frac{e^2}{2m^2(4\pi)^2}\int_0^1 dx\Big\{\ln\left(\frac{p^2x(1-x)+m_h^2}{\mu^2}\right)-\ln\left(\frac{p^2x(1-x)+\xi m^2}{\mu^2}\right)\Big\} \tag{205}$$

and the resummed approximation becomes

$$G_{hh}(p^2) = \frac{1}{p^2+m^2-\hat{\Pi}(p^2)} + C_{hh}(p^2), \tag{206}$$

which is shown in Figure 9. Notice that the dependence on the Feynman parameter x for all integrals is restricted to functions of the type $\int_0^1 dx \ln\frac{p^2x(1-x)+xm_1^2+(1-x)m_2^2}{\mu^2}$. These functions have an analytical solution, depicted in Appendix F. Since the transverse component A_μ^T of the Abelian gauge field is gauge invariant, it turns out that the transverse photon propagator is independent from the gauge parameter ξ, while the Higgs propagator does depend on ξ, in agreement with the Nielsen identities analyzed in (HAUSSLING; KRAUS, 1997).

3.3 **Spectral properties of the propagators**

In this section we will investigate the spectral properties corresponding to the connected propagators of the last section. Strictly speaking, the calculation of the spectral

Figure 9 - Higgs operator resummed form factor

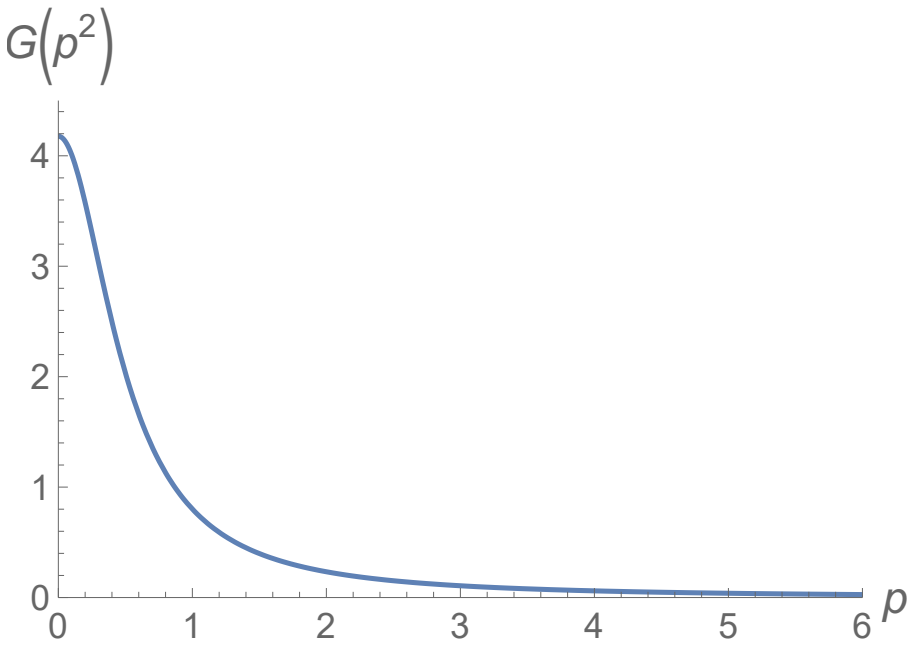

Legend: Resummed form factor for the Higgs operator, with p given in units of the energy scale μ, for the parameter values $e = 1$, $v = 1\,\mu$, $\lambda = \frac{1}{5}$.

Source: The author, 2020.

properties should only be done to first order[7] in $\hbar$, since the one-loop corrections to the propagators have been evaluated up to this order. In practice, however, for small values of the coupling constants the higher-order contributions become negligible, and one could treat the one-loop solution as the all-order solution without a significant numerical difference. Even so, when looking for analytical rather than numerical results—for example a gauge parameter dependence—we should restrict ourselves to the first-order results. We shall see the crucial difference between both approaches.

To plot the spectral properties of our model we choose some specific values of the parameters $\{m, m_h, \mu, e\}$. We want to restrict ourselves to the case where the Higgs particle is a stable particle, so we need $m_h^2 < 4m^2$. Furthermore, given the Abelian nature of the model, and thus a weak coupling regime in the infrared, we can choose an energy scale μ that is sufficiently small w.r.t. the elusive Landau pole (that is exponentially large) and a corresponding small value for the coupling constant e. The particular values chosen per graph are denoted in the figure captions. Notice that by choosing μ and e, we are implicitly fixing the Landau pole Λ, with $\mu \ll \Lambda$, see (IRGES; KOUTROULIS, 2017) for

[7] This would correspond to first order in the gauge coupling e^2 and in the Higgs coupling λ neglecting the implicit coupling dependence in the masses.

more details. We have checked that results are as good as independent from the choice of μ over a very wide range of μ-values.

We start by calculating the pole mass in section 3.3.1. The pole mass is the actual physical mass of a particle that enters the energy-momentum dispersion relation. It is an observable for both the photon and the Higgs boson and should therefore not depend on the gauge parameter ξ. We will also discuss the residue to first order and compare these with the output from the Nielsen identities (HAUSSLING; KRAUS, 1997). In section 3.3.2 we show how to obtain the spectral function to first order from the propagator. In section 3.4 we will discuss some more details about the Higgs spectral function.

3.3.1 Pole mass, residue and Nielsen identities

The pole mass for any massless or massive field excitation is obtained by calculating the pole of the resummed connected propagator

$$G(p^2) = \frac{1}{p^2 + m^2 - \Pi(p^2)}, \tag{207}$$

where $\Pi(p^2)$ is the self-energy correction. The pole of the propagator is thus equivalently defined by the equation

$$p^2 + m^2 - \Pi(p^2) = 0 \tag{208}$$

and its solution defines the pole mass $p^2 = -m^2_{pole}$. As consistency requires us to work up to a fixed order in perturbation theory, we should solve eq.(208) for the pole mass in an iterative fashion. To first order in $\hbar$, we find

$$m^2_{pole} = m^2 - \Pi^{1-loop}(-m^2) + \mathcal{O}(\hbar^2), \tag{209}$$

where Π^{1-loop} is the first order, or one-loop, correction to the propagator.

Next, we also want to compute the residue Z, again up to order $\hbar$. In principle, the residue is given by

$$Z = \lim_{p^2 \to -m^2_{pole}} (p^2 + m^2_{pole}) G(p^2). \tag{210}$$

We write (207) in a slightly different way

$$\begin{aligned} G(p^2) &= \frac{1}{p^2+m^2-\Pi(p^2)} \\ &= \frac{1}{p^2+m^2-\Pi^{1-loop}(-m^2)-(\Pi(p^2)-\Pi^{1-loop}(-m^2))} \\ &= \frac{1}{p^2+m^2_{pole}-\widetilde{\Pi}(p^2)}, \end{aligned} \tag{211}$$

where we defined $\widetilde{\Pi}(p^2) = \Pi(p^2) - \Pi^{1-loop}(-m^2)$. At one-loop, expanding $\widetilde{\Pi}(p^2)$ around $p^2 = -m^2_{pole} = -m^2 + \mathcal{O}(\hbar)$ gives the residue

$$Z = \frac{1}{1-\partial_{p^2}\Pi(p^2)|_{p^2=-m^2}} = 1 + \partial_{p^2}\Pi(p^2)|_{p^2=-m^2} + \mathcal{O}(\hbar^2). \tag{212}$$

In (HAUSSLING; KRAUS, 1997), for the Abelian Higgs model, the Nielsen identities were obtained for both the photon and the Higgs boson. It was found that for the photon propagator, the transverse part is explicitly independent of ξ to all orders of perturbation theory, giving the Nielsen identity:

$$\partial_\xi (G^\perp_{AA})^{-1}(p^2) = 0 \tag{213}$$

and consequently

$$\begin{aligned} \partial_\xi \partial_{p^2}(G^\perp_{AA})^{-1}(p^2)|_{p^2=-m^2_{pole}} &= 0, \\ \partial_\xi (G^\perp_{AA})^{-1}(-m^2_{pole}) &= 0, \end{aligned} \tag{214}$$

confirming the gauge independence of the residue and the pole mass. Of course, this is not unexpected since the transverse part of an Abelian gauge field propagator can be written as

$$\mathcal{P}_{\mu\nu}\langle A_\mu A_\nu\rangle_{conn} \propto \langle A^T_\mu A^T_\mu\rangle\ , \qquad A^T_\mu = \mathcal{P}_{\mu\nu}A_\nu \tag{215}$$

and the transverse component A^T_μ is gauge invariant under Abelian gauge transformations.

We can now compare the outcome of the Nielsen identities with our one-loop calculation (199). Indeed, to the first order, eq.(199) is an explicit demonstration of the identity (213). For the Higgs boson, the Nielsen identity is a bit more complicated, and is given by

$$\partial_\xi G^{-1}_{hh}(p^2) = -\partial_\chi G^{-1}_{Y_1 h}(p^2) G^{-1}_{hh}(p^2), \tag{216}$$

where $G^{-1}_{Y_1 h}(p^2)$ stands for a non-vanishing $1PI$ Green function which can be obtained from the extended BRST symmetry which also acts on the gauge parameter (PIGUET; SIBOLD, 1985). To be more precise, Y_1 is a local source coupled to the BRST variation

Figure 10 - Pole residue gauge dependence

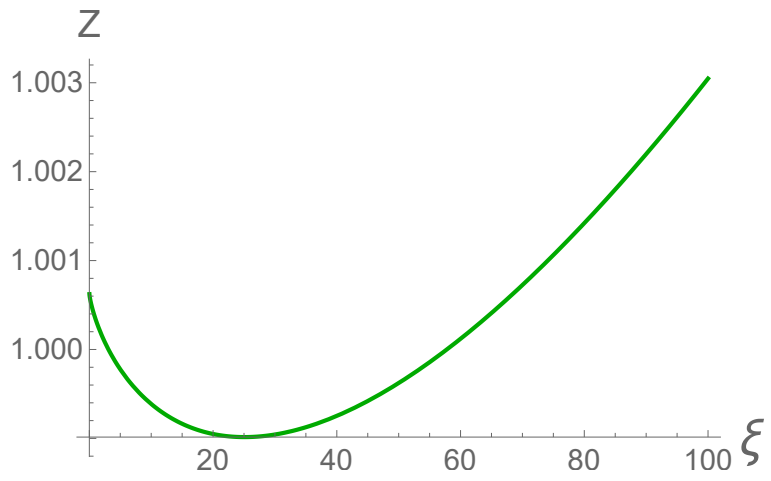

Legend: Gauge dependence of the residue of the pole for the Higgs field, for the parameter values $m = 2$ GeV, $m_h = \frac{1}{2}$ GeV, $\mu = 10$ GeV, $e = \frac{1}{10}$.
Source: The author, 2020.

of the Higgs field (see (157)), while χ is coupled to the integrated composite operator $\int d^4x \left(-\frac{i}{2}\bar{c}b + mc\rho\right)$. Acting with ∂_χ inserts the latter composite operator with zero momentum flow into the $1PI$ Green function $\langle(sh)h\rangle$, see (HAUSSLING; KRAUS, 1997) for the explicit expression of $G^{-1}_{Y_1 h}(p^2)$ in terms of Feynman diagrams. As a consequence, the Higgs propagator $G_{hh}(p^2)$ is not gauge independent, in agreement with our results (197). From (216) we further find

$$\partial_\xi \partial_{p^2} G^{-1}_{hh}(p^2)|_{p^2=-m^2_{pole}} \;=\; -\partial_\chi G^{-1}_{Y_1 h}(-m^2_{pole}) \partial_{p^2} G^{-1}_{hh}(p^2)|_{p^2=-m^2_{pole}}, \tag{217}$$

which means that the residue is not gauge independent, as $G^{-1}_{Y_1 h}(p^2)$ does not necessarily vanish at the pole. We can confirm this for the one-loop calculation, see Figure 34.

Furthermore, we do have

$$\partial_\xi G^{-1}_{hh}(-m^2_{pole}) \;=\; 0, \tag{218}$$

so that the Higgs pole mass is indeed gauge independent, the expected result for the physical (observable) Higgs mass. This can be confirmed to one-loop order by using eq. (209), see also Figure 13. Explicitly, in eq. (206) for $G^{-1}_{hh}(-m^2_h)$ all the gauge parameter dependence drops out, which means that the Higgs pole mass is gauge independent to first order in $\hbar$.

3.3.2 Obtaining the spectral function

We can try to determine the spectral function itself to first order. To do so, we compare the Källén-Lehmann spectral representation for the propagator

$$G(p^2) = \int_0^\infty dt \frac{\rho(t)}{t + p^2}, \tag{219}$$

where $\rho(t)$ is the spectral density function, with the propagator (211) to first order, written as

$$\begin{aligned} G(p^2) &= \frac{Z}{(p^2 + m_{pole}^2 - \widetilde{\Pi}(p^2))Z} \\ &= \frac{Z}{p^2 + m_{pole}^2 - \widetilde{\Pi}(p^2) + (p^2 + m_{pole}^2)\frac{\partial \widetilde{\Pi}(p^2)}{\partial p^2}|_{p^2=-m^2}} \\ &= \frac{Z}{p^2 + m_{pole}^2} + Z\left(\frac{\widetilde{\Pi}(p^2) - (p^2 + m_{pole}^2)\frac{\partial \widetilde{\Pi}(p^2)}{\partial p^2}|_{p^2=-m^2}}{(p^2 + m_{pole}^2)^2}\right), \end{aligned} \tag{220}$$

where in the last line we used a first-order Taylor expansion so that the propagator has an isolated pole at $p^2 = -m_{pole}^2$. In (219) we can isolate this pole in the same way, by defining the spectral density function as $\rho(t) = Z\delta(t - m_{pole}^2) + \widetilde{\rho}(t)$, giving

$$G(p^2) = \frac{Z}{p^2 + m_{pole}^2} + \int_0^\infty dt \frac{\widetilde{\rho}(t)}{t + p^2} \tag{221}$$

and we identify the second term in each of the representations (220) and (221) as the *reduced propagator*

$$\widetilde{G}(p^2) \equiv G(p^2) - \frac{Z}{p^2 + m_{pole}^2}, \tag{222}$$

so that

$$\widetilde{G}(p^2) = \int_0^\infty dt \frac{\widetilde{\rho}(t)}{t + p^2} = Z\left(\frac{\widetilde{\Pi}(p^2) - (p^2 + m_{pole}^2)\frac{\partial \widetilde{\Pi}(p^2)}{\partial p^2}|_{p^2=-m^2}}{(p^2 + m_{pole}^2)^2}\right). \tag{223}$$

Finally, using Cauchy's integral theorem in complex analysis, we can find $\widetilde{\rho}(t)$ as a function of $\widetilde{G}(p^2)$, giving

$$\widetilde{\rho}(t) = \frac{1}{2\pi i} \lim_{\epsilon \to 0^+} \left(\widetilde{G}(-t - i\epsilon) - \widetilde{G}(-t + i\epsilon)\right). \tag{224}$$

3.3.3 Spectral density functions

We are now ready to plot the spectral density function for the photon propagator and the Higgs boson propagator. For this section we shall write all quantities as a function of the renormalization scale μ and choose the parameters $e = 1$, $v = 1\,\mu$, $\lambda = \frac{1}{5}$, so that $m = 1\,\mu$ and $m_h = \frac{1}{\sqrt{5}}\,\mu$. For this choice of parameters, all one-loop corrections computed are within 20% of the tree-level results, indicating that our perturbative approximation is under control.

Since in the Abelian case the transverse component of the gauge field $A^T_\mu(x)$ is gauge invariant, it turns out that the corresponding propagator (199) is independent from the gauge parameter ξ, and so are its pole mass, residue and spectral function. Following the steps from section 3.3.1, we find the first-order pole mass of the transverse photon to be

$$m^2_{pole} \;=\; 1.05417\,\mu^2 \tag{225}$$

and the first-order residue

$$Z = 0.984983. \tag{226}$$

These values are small corrections of the tree-level ones, $m^2 = \mu^2$ and $Z_{\text{tree}} = 1$, so that the one-loop approximation appears to be consistent.

The spectral function is given in Figure 11. We can distinguish a two-particle state threshold at $t = (m + m_h)^2 = 2.09\,\mu^2$, and the spectral density function is positive, adequately describing the physical photon excitation. For the Higgs fields, following the steps from section 3.3.1, we find the pole mass to first order in $\hbar$ to be

$$m^2_{h,pole} \;=\; 0.237987\,\mu^2 = 1.1899\,m_h^2, \tag{227}$$

for all values of the parameter ξ. This means that while the Higgs propagator (197) is gauge-dependent, the pole mass is gauge-independent. This is in full agreement with the Nielsen identities of the Abelian $U(1)$ Higgs model studied in (HAUSSLING; KRAUS, 1997). For the residue, we distinguish three regions:

- $\xi < \frac{1}{20} = \frac{\lambda}{4e^2}$: for these values $m_h > 2\sqrt{\xi}m$, which means the Higgs particle is unstable and can decay into two Goldstone fields $\rho(x)$. Of course, this process is physically impossible because the Goldstone boson itself is not physical. It therefore clearly demonstrates the unphysical nature of the propagator $\langle h(x)h(y)\rangle$. For these values of ξ, the pole mass is a real value inside the branch cut created by the two-particle state of Goldstone excitations. This means that we cannot properly define

Figure 11 - Photon spectral function

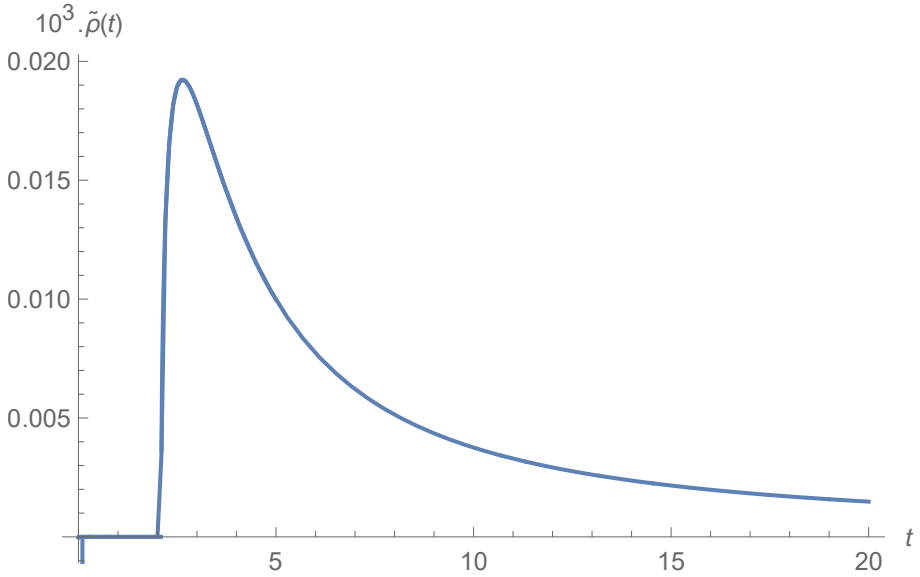

Legend: Spectral function for the transverse part of the reduced photon propagator $\langle A(p)A(-p)\rangle^T$, with t given in units of μ^2, for the parameter values $e = 1$, $v = 1\,\mu$, $\lambda = \frac{1}{5}$.

Source: The author, 2020.

the derivative of the one-loop correction to obtain the corresponding residue through eq. (212).

- $\xi \leq 3$: for these values we find $Z > 1$.
- $\xi > 3$: for these values we find $Z < 1$.

In Figure 12, we find the spectral density functions for three values of $\xi : 2, 3, 5$. For small t, their behaviour is the same, with a two-particle state for the Higgs field at $t = (m_h + m_h)^2 = 0.8\,\mu^2$, and a two-particle state for the photon field, starting at $t = (m + m)^2 = 4\mu^2$. Then, we see that there is a negative contribution, different for each diagram, at $t = (\sqrt{\xi}m + \sqrt{\xi}m)^2$. This corresponds to the threshold for creation of two (unphysical) Goldstone bosons. This negative contribution eventually overcomes the other ones, leading to a negative regime in the spectral function, independently of the value of ξ. This feature is consistent with the large-momentum behaviour of the Higgs propagator (197), for a detailed discussion see Appendix G. As one lowers the value of the gauge parameter ξ, this unphysical threshold is shifted towards lower t's and may occur for momentum values lower than the physical two-particle states of two Higgs or two photons. As discussed above, for $\xi < \frac{\lambda}{4e^2}$ even the one-particle delta peak becomes located within the unphysical Goldstone production region and the standard interpretation of the spectral properties is completely lost. It is therefore clear that this correlation function

Figure 12 - Higgs spectral function

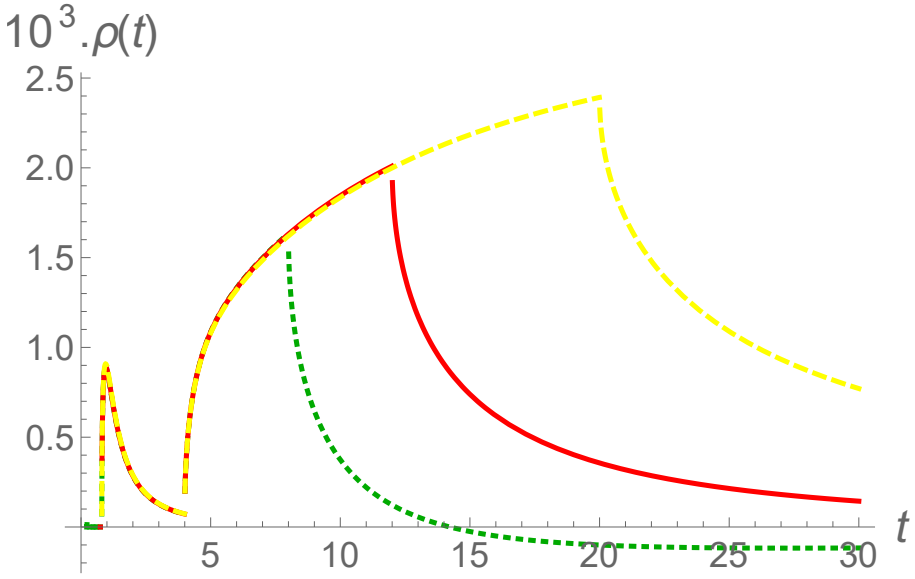

Legend: Spectral function for the reduced Higgs propagator $\langle h(p)h(-p)\rangle$, for gauge parameters $\xi = 2$ (Green, dotted), $\xi = 3$ (Yellow, dashed), $\xi = 5$ (Red, Solid), with t given in units of μ^2, for the parameter values $e = 1$, $v = 1\,\mu$, $\lambda = \frac{1}{5}$.

Source: The author, 2020.

does not display the desired spectral properties to describe the Higgs mode in this theory, indicating the necessity of resorting to another operator as we shall do in what follows.

3.4 **Some subtleties of the Higgs spectral function**

In this section we discuss some subtleties that arose during the analysis of the spectral function of the Higgs boson.

3.4.1 A slightly less correct approximation for the pole mass

In the previous two sections we have obtained strictly first-order expressions. In practice, for small values of the coupling parameter e^2, we could think about making the approximation

$$G(p^2) \;=\; \frac{1}{p^2 + m^2 - \Pi(p^2)} \approx \frac{1}{p^2 + m^2 - \Pi^{1-loop}(p^2)}, \tag{228}$$

Figure 13 - Gauge dependence Higgs pole mass

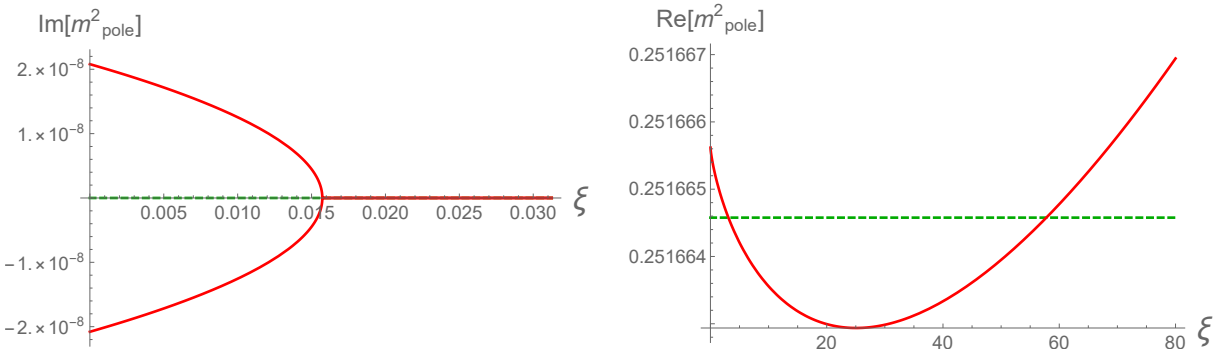

Legend: Gauge dependence of the Higgs pole mass obtained iteratively to first order (Green) and the approximated pole mass (Red), for the parameter values $m = 2$ GeV, $m_h = \frac{1}{2}$ GeV, $\mu = 10$ GeV, $e = \frac{1}{10}$. Up: real part, down: imaginary part.

Source: The author, 2020.

in which case one can fix the pole mass by locating the root of

$$p^2 + m^2 - \Pi^{1-loop}(p^2) = 0. \tag{229}$$

The difference between the pole masses obtained by the iterative method (209) and the approximation (229) is very small, of the order 10^{-6} GeV for our set of parameters. However, it is rather interesting to notice that the pole mass of the Higgs boson becomes gauge dependent in the approximation (229). This is no surprise, as the validity of the Nielsen identities is understood either in an exact way, or in a consistent order per order approximation. The previous approximation is neither.

In Figure 13 one can see the gauge dependence of the approximated pole mass of the Higgs, in contrast with the first order pole mass. Even worse, for very small values of ξ, the approximated pole mass gets complex (conjugate) values. This is due to the fact that the threshold of the branch cut, the branch point, for (191) is ξ-dependent, as we will see in the next section.

3.4.2 Something more on the branch points

The existence of a diagram with two internal Goldstone lines (see Figure 41) leads to a term proportional to $\int_0^1 dx \ln(p^2 x(1-x) + \xi m^2)$ in the Higgs propagator (191). This means that for small values of ξ, the threshold for the branch cut of the propagator will be ξ-dependent too. Let us look at the Landau gauge $\xi = 0$. In this gauge, the above ln-term

Figure 14 - Higgs propagator around pole mass

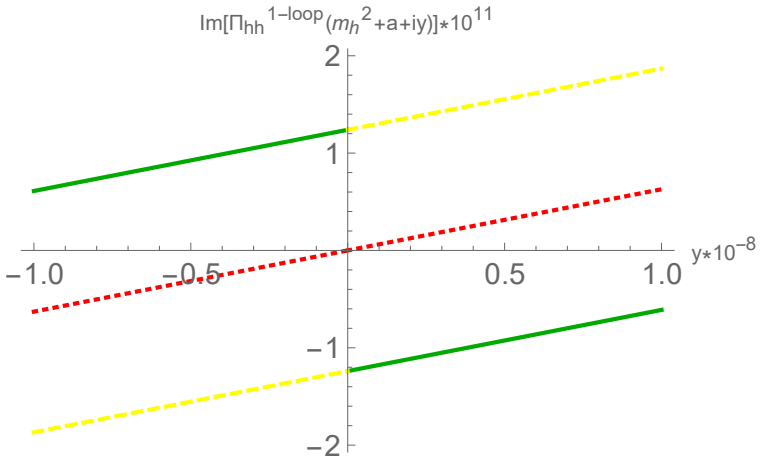

Legend: Behaviour of the one-loop correction of the Higgs propagator $\Pi_{hh}(p^2)$ around the pole mass, for the values $a = -10^{-6}$ (Yellow, dashed), $a = 0$ (Red, dotted), $a = 10^{-6}$ (Green, solid). The value x is a small imaginary variation of the argument in $\Pi_{hh}(p^2)$. Only for $a = 0$ we find a continuous function at $x = 0$, meaning that for any other value, we are on the branch cut.

Source: The author, 2020.

is proportional to $\ln(p^2)$, due to the now massless Goldstone bosons. This logarithm has a branch point at $p^2 = 0$, meaning that the pole mass will be lying on the branch cut. Since the first order pole mass is real and gauge independent, this means that $\Pi_{hh}^{1-loop}(-m_h^2)$ is a singular real point on the branch cut. In the slightly less correct approximation of the last section, we will find complex conjugate poles as in Figure 13. This is explained by the fact that for every real value different from $p^2 = -m_h^2$, we are on the branch cut, see Figure 14 .

Another consequence of the fact that, for small ξ, the pole mass is a real point inside the branch cut is that $\Pi_{hh}(p^2)$ is non-differentiable at $p^2 = -m_h^2$ and we cannot extract a residue for this pole. In order to avoid such a problem, we should move away from the Landau gauge and take a larger value for ξ, so that the threshold for the branch cut will be smaller than $-m_h^2$. For this we need that $4\xi m^2 > m_h^2$, which in the case of our parameters set means to require that $\xi > \frac{1}{64}$, in accordance with Figure 13.

3.4.3 Asymptotics of the spectral function

Away from the Landau gauge, we see on Figure 12 that for e.g. $\xi = 2$ the Higgs spectral function is not non-positive everywhere, while for e.g. $\xi = 4$ it is positive definite, with a turning point at $\xi = 3$. How can we explain this difference? The answer can be related to the UV behaviour of the propagator. For $p^2 \to \infty$, the Higgs boson propagator

at one-loop behaves as

$$G_{hh}(p^2) = \frac{\mathcal{Z}}{p^2 \ln \frac{p^2}{\mu^2}}, \tag{230}$$

with $\mathcal{Z}$ depending on the gauge parameter ξ. Now, one can show (see Appendix G) that for $\mathcal{Z} > 0$, $\rho(t)$ becomes negative for a large value of t. For our parameter set, we find that for large momenta

$$G^{-1}_{hh}(p^2) \to (3-\xi)\frac{p^2 \ln(p^2)}{1600\pi^2}, \quad \text{for} \quad p^2 \to \infty, \tag{231}$$

so that for $\xi < 3$, we indeed find $\mathcal{Z} > 0$. This indicates that the large momentum behaviour of the propagator makes a difference around $\xi = 3$, and determines the positivity of the spectral function, a known fact (OEHME; ZIMMERMANN, 1980; OEHME, 1990; ALKOFER; SMEKAL, 2001). This being said, at the same time we cannot trust the propagator values for $p^2 \to \infty$ without taking into account the renormalization group (RG) effects and in particular the running of the coupling, which is problematic for non-asymptotically free gauge theories as the Abelian Higgs model.

3.5 A non-unitary $U(1)$ model

In this section, we will discuss an Abelian model of the Curci-Ferrari (CF) type (CURCI; FERRARI, 1976b), in order to compare it with the Higgs model (153). Both models are massive $U(1)$ models with a BRST symmetry. However, while the BRST operator s of the Higgs model is nilpotent, this is not true for the CF-like model. We know the that the Higgs model is unitary but, by the criterion of (KUGO; OJIMA, 1979), the CF model is most probably not.

In section 3.5.1 we discuss some essentials for the CF-like model: the action with the modified BRST symmetry, tree-level propagators and vertices. In section 3.5.2 we discuss the one-loop propagators for the photon and scalar field and extract the spectral function. In section 3.5.3 we introduce a local composite field operator that is left invariant by the modified BRST symmetry ot the CF model. The spectral properties of this composite state's propagator will tell us something about the (non-)unitarity of the model, since for unitary models, we expect the propagator of a BRST invariant composite operator to be gauge parameter independent, and the spectral function to be positive definite.

3.5.1 CF-like U(1) model: some essentials

We start with the action of the CF-like $U(1)$ model

$$\begin{aligned} S_{CF} &= \int d^dx \left\{ \frac{1}{4}F_{\mu\nu}F_{\mu\nu} + \frac{m^2}{2}A_\mu A_\mu + (D_\mu\varphi)^\dagger D_\mu\varphi + m_\varphi^2\varphi^\dagger\varphi + \lambda(\varphi\varphi^\dagger)^2 \right. \\ &- \left. \alpha\frac{b^2}{2} + b\partial_\mu A_\mu + \bar{c}\partial^2 c - \alpha m^2\bar{c}c \right\}, \end{aligned} \tag{232}$$

where the mass term $\frac{m^2}{2}A_\mu A_\mu$ is put in by hand rather than coming from a spontaneous symmetry breaking, and we have fixed the gauge in the linear covariant gauge with gauge parameter α. The mass term breaks the BRST symmetry (157) in a soft way. This Abelian CF action is however invariant under the modified BRST symmetry, $s_m S_{CF} = 0$, with[8]

$$\begin{aligned} s_m A_\mu &= -\partial_\mu c, \\ s_m c &= 0, \\ s_m\varphi &= iec\varphi, \\ s_m\varphi^\dagger &= -iec\varphi^\dagger, \\ s_m\bar{c} &= b, \\ s_m b &= -m^2 c. \end{aligned} \tag{233}$$

As noticed before in our Introduction, this modified BRST symmetry is not nilpotent since $s_m^2\bar{c} \neq 0$.

From the quadratic part of (232) we find the following propagators at tree-level

$$\begin{aligned} \langle A_\mu(p)A_\nu(-p)\rangle &= \frac{1}{p^2+m^2}P_{\mu\nu} + \frac{\alpha}{p^2+\alpha m^2}\mathcal{L}_{\mu\nu}, \\ \langle A_\mu(p)b(-p)\rangle &= i\frac{p_\mu}{p^2+\alpha m^2}, \\ \langle b(p)b(-p)\rangle &= -\frac{m^2}{p^2+\alpha m^2}, \\ \langle\varphi^\dagger(p)\varphi(-p)\rangle &= \frac{1}{p^2+m_\varphi^2}, \\ \langle\bar{c}(p)c(-p)\rangle &= -\frac{1}{p^2+\alpha m^2}, \end{aligned} \tag{234}$$

[8] This is the Abelian version of the variation (157). For computational purposes, we have also made a rescaling $ib \to b$. Notice that higher order α-dependent terms present in the CF model are absent in the Abelian limit (CURCI; FERRARI, 1976a; DELDUC; SORELLA, 1989).

Figure 15 - Photon self-energy

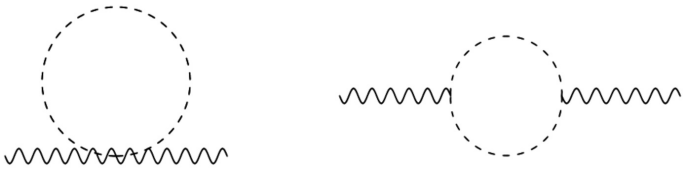

Legend: Contributions to one-loop CF photon self-energy. Wavy lines represent the photon field and dashed lines represent the scalar field.
Source: The author, 2020.

Figure 16 - Scalar self-energy

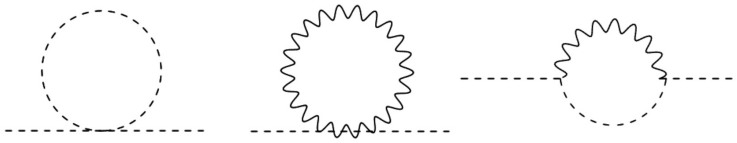

Legend: Contributions to the one-loop CF scalar self-energy. Line representation as in Figure 15.
Source: The author, 2020.

while from the interaction terms we find the vertices

$$\begin{aligned}
\Gamma_{A_\mu\varphi^\dagger\varphi}(-p_1,-p_2,-p_3) &= e(p_{3,\mu}-p_{2,\mu})\delta(p_1+p_2+p_3),\\
\Gamma_{A_\mu A_\nu\varphi^\dagger\varphi}(-p_1,-p_2,-p_3,-p_4) &= -2e^2\delta_{\mu\nu}\delta(p_1+p_2+p_3+p_4),\\
\Gamma_{\varphi^\dagger\varphi\varphi^\dagger\varphi}(-p_1,-p_2,-p_3,-p_4) &= -4\lambda\delta(p_1+p_2+p_3+p_4). \qquad (235)
\end{aligned}$$

3.5.2 Propagators and spectral functions

The one-loop corrections to the photon and scalar self-energies are given in Figure 15 and 16. Without going through the calculational details, we will directly give here the propagators in $d = 4$ and discuss some curiosities. The inverse connected photon propagator,

$$(G^{\perp}_{AA})^{-1}(p^2) = p^2 + m^2 + \frac{e^2}{(4\pi)^2}\int_0^1 dx K(m_\varphi^2, m_\varphi^2)(1 - \ln\frac{K(m_\varphi^2, m_\varphi^2)}{\mu^2}) - m_\varphi^2(1 - \ln\frac{m_\varphi^2}{\mu^2}), \qquad (236)$$

is independent of the gauge parameter. The threshold of the branch cut is given by $t^* = -4m_\varphi^2$, and to avoid a pole mass lying on the branch cut, we need to choose here $m^2 < 4m_\varphi^2$. Choosing $m = \frac{1}{2}$ GeV, $m_\varphi = 2$ GeV, $\mu = 10$ GeV, $e = \frac{1}{10}$, we find a positive

Figure 17 - Photon spectral function

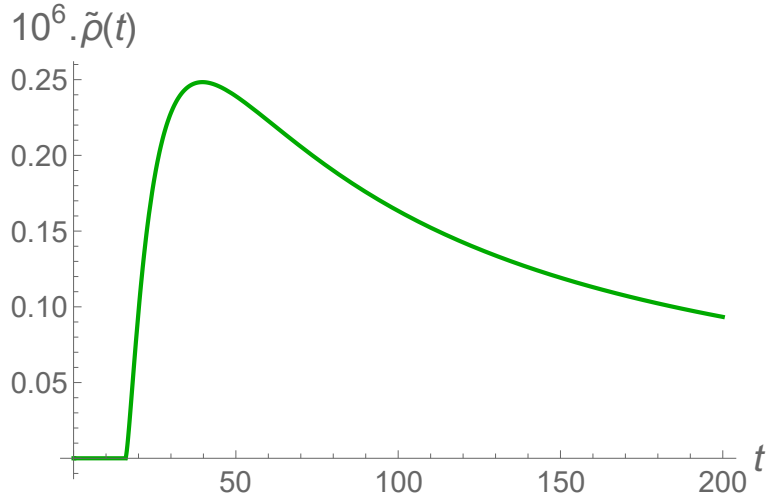

Legend: The reduced spectral function of the photon field in the Abelian CF model, with t given in GeV^2, for the parameter values $m = 2$ GeV, $m_h = \frac{1}{2}$ GeV, $\mu = 10$ GeV, $e = \frac{1}{10}$. The first-order pole mass lies at $t = 0.25151\,\mathrm{GeV}^2$. The photon two-particle state starts at $t^* = 4m_\varphi^2 = 16\,\mathrm{GeV}^2$.

Source: The author, 2020.

spectral function, see Figure 17.

More interestingly, the scalar propagator

$$\begin{aligned}
G^{-1}_{\varphi\varphi}(p) &= p^2 + m_\varphi^2 - \frac{e^2}{(4\pi)^2}\int_0^1 dx m^2 - \alpha^2 m^2 - \alpha K(m_\varphi^2, m^2)(1 - 2\ln\frac{K(m_\varphi^2, \alpha m^2)}{\mu^2}) \\
&+ 4K(m_\varphi^2, 0)\frac{p^2}{m^2}(1 - \ln\frac{K(m_\varphi^2, 0)}{\mu^2}) - 2K(m_\varphi^2, m^2)\frac{p^2}{m^2}(1 - \ln\frac{K(m_\varphi^2, m^2)}{\mu^2}) \\
&- 2K(m_\varphi^2, \alpha m^2)\frac{p^2}{m^2}(1 - \ln\frac{K(m_\varphi^2, \alpha m^2)}{\mu^2}) + 8\frac{p^4}{m^2}x^2\ln\frac{K(m_\varphi^2, 0)}{\mu^2} \\
&- 4\frac{p^4}{m^2}x^2\ln\frac{K(m_\varphi^2, m^2)}{\mu^2} - 4p^2\ln\frac{K(m_\varphi^2, m^2)}{\mu^2} \\
&- (4\alpha p^2 x - \alpha p^2 x^2 + 4\frac{p^2}{m^2}x^2)\ln\frac{K(m_\varphi^2, \alpha m^2)}{\mu^2} \\
&- 3m^2\ln\frac{m^2}{\mu^2} + \alpha m^2\ln\frac{\alpha m^2}{\mu^2} + \frac{\lambda}{(4\pi)^2}m_\varphi^2(1 - \ln\frac{m_\varphi^2}{\mu^2}),
\end{aligned} \tag{237}$$

is α-dependent, and so is the iterative first-order pole mass $m^2_{\varphi,pole} = m_\varphi^2 - \Pi^{1-loop}(-m_\varphi^2)$. This field can thus not represent a physical particle. For any value other than the Landau gauge $\alpha = 0$ we furthermore get complex poles, see Figure 18.

From the fact that we find gauge dependent (complex) pole masses for the scalar field, we can already draw the conclusion that the CF model does not describe a physical scalar field. In the next section we will explicitly verify the non-unitary of this model

Figure 18 - Scalar pole mass gauge dependence

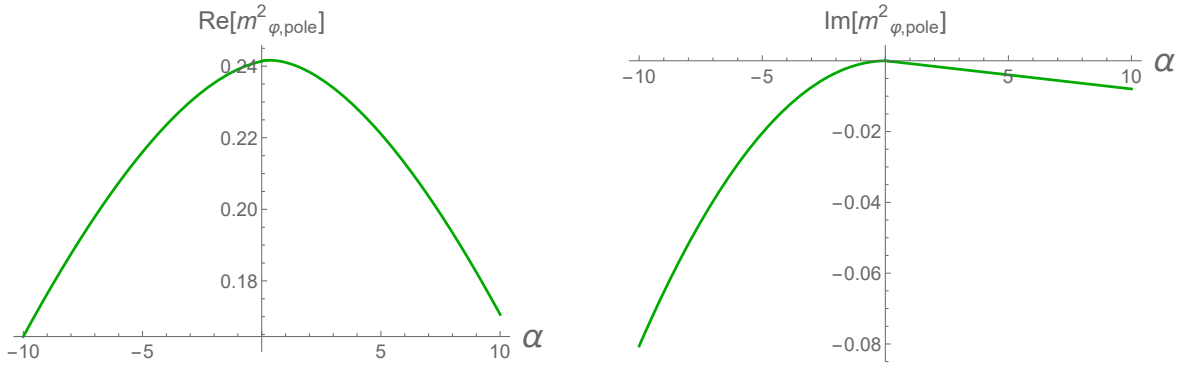

Legend: Gauge dependence of the first order pole mass for the scalar field. Left: Real part, Right: Imaginary part. The chosen parameter values are $m = 2$ GeV, $m_\varphi = \frac{1}{2}$ GeV, $\mu = 10$ GeV, $e = \frac{1}{10}$.

Source: The author, 2020.

in yet another way. Essentially, our findings so far mean that in the CF setting, the unphysical gauge parameter α plays here a quite important role, just like the coupling: different values of the gauge parameter label dfferent theories. This can also be seen from another example: the one-loop vacuum energy of the model will now not only depend on m, but also on α.

3.5.3 Gauge invariant operator

The Abelian CF model allows us to construct a BRST invariant composite operator $\left(\frac{b^2}{2} + m^2\bar{c}c\right)$, with

$$s_m\left(\frac{b^2}{2} + m^2\bar{c}c\right) = 0. \tag{238}$$

Although $s_m^2 \neq 0$ and we can therefore no longer introduce the BRST cohomology classes, we can still use the fact that s_m is a symmetry generator, thereby defining a would-be physical subspace as the one being annihilated by s_m. A Fock space analogue of this operator was introduced in (OJIMA, 1982), where it was established that it has negative norm. As a consequence, it was shown that the physical subspace relating to the symmetry generator s_m was not well-defined, as it contains ghost states. Several more such states were identified later on in (BOER et al., 1996). Up to leading order, the connected

propagator of the composite operator in eq.(238) reads

$$G_{\frac{b^2}{2}+m^2\bar{c}c}(p^2) = \left\langle \left(\frac{b^2}{2} + m^2\bar{c}c\right), \left(\frac{b^2}{2} + m^2\bar{c}c\right) \right\rangle = \frac{1}{4}\langle b^2, b^2\rangle + m^4\langle \bar{c}c, \bar{c}c\rangle, \tag{239}$$

We thus find the propagator (239) to be

$$\begin{aligned} G_{\frac{b^2}{2}+m^2\bar{c}c}(p^2) &= -\frac{3}{4}m^2 \int \frac{d^dk}{(2\pi)^d} \frac{1}{k^2+\alpha m^2} \frac{1}{(k-p)^2+\alpha m^2} \\ &= -\frac{3}{4}m^2 \frac{1}{(4\pi)^{d/2}} \Gamma(2-d/2) \int_0^1 dx K_{d/2-2}(\alpha m^2, \alpha m^2) \end{aligned} \tag{240}$$

and this gives for $d = 4$, using the $\overline{\text{MS}}$-scheme

$$G_{\frac{b^2}{2}+m^2\bar{c}c}(p^2) = \frac{3}{4}\frac{m^2}{(4\pi)^2} \int_0^1 dx \ln\left(\frac{K(\alpha m^2, \alpha m^2)}{\mu^2}\right). \tag{241}$$

Clearly, the propagator is depending on the gauge parameter α, a not so welcome feature for a presumably physical object.

We can also find the spectral function immediately from the propagator by again relying on (224). In Figure 19, one sees that the spectral function is negative for different values of α. Both the α-dependence and the negative-definiteness of the spectral functions demonstrate the non-unitarity of the Abelian CF model. To our knowledge, this is the first time that ghost-dependent invariant operators in the physical subspace of a CF model have been constructed from the functional viewpoint[9], complementing the (asymptotic) Fock space analyses of (OJIMA, 1982; BOER et al., 1996).

3.6 **Conclusion**

In this chapter we have studied the Källén-Lehmann spectral properties of the $U(1)$ Abelian Higgs model in the R_ξ gauge, and that of a $U(1)$ Curci-Ferrari (CF) like model. Our main aim was to disentangle in this analytical, gauge-fixed setup what is physical and what is not at the level of the elementary particle propagators, in conjunction with the Nielsen identities. Special attention was given to the role played by gauge (in)dependence of different quantities and by the correct implementation of the results up to a given order in perturbation theory. In particular, calculating the spectral function for the Higgs propagator in the $U(1)$ model, it became apparent that an unphysical

[9] A similar result can be checked to hold for the original non-Abelian CF model, by adding a few higher order terms to the here introduced Abelian operator. This means that a non-Abelian version of the operator (238), invariant under the BRST transformation (157), can be written down.

Figure 19 - Composite operator $\frac{b^2}{2} + m^2\bar{c}c$ spectral function

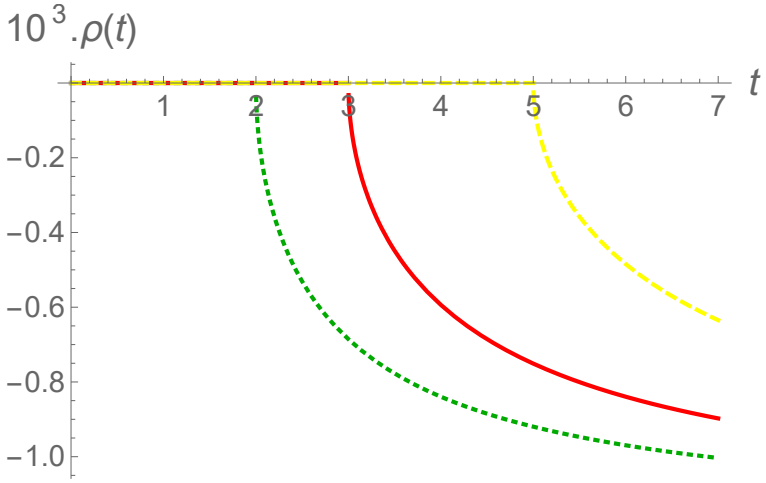

Legend: The spectral function of the composite operator $\frac{b^2}{2} + m^2\bar{c}c$, for $\alpha = 2$ (Green, dotted), $\alpha = 3$ (Red, solid), $\alpha = 5$ (Yellow, dashed). The chosen parameter values are $m = \frac{1}{2}$ GeV, $\mu = 10$ GeV. The treshold for the branch cut of the propagator is given by $t^* = (\sqrt{\alpha}m + \sqrt{\alpha}m)^2$, being $t^* = (2\,\mathrm{GeV}^2, 3\,\mathrm{GeV}^2, 5\,\mathrm{GeV}^2)$ for $\xi = (2, 3, 5)$.

Source: The author, 2020.

occurrence of complex poles, as well as a gauge-dependent pole mass, are caused by the use of the resummed (approximate) propagator as being exact. Indeed, for small coupling constants, the one-loop correction gives a good approximation of the all-order loop correction, and this is a much used method to find numerical results (TISSIER; WSCHEBOR, 2010; TISSIER; WSCHEBOR, 2011; HAYASHI; KONDO, 2019). However, for analytical purposes, one should stick to the order at which one has calculated the propagator. As we have illustrated, at least in the $U(1)$ Abelian Higgs model case, one will then find a real and gauge independent pole mass for the Higgs boson, in accordance with what the Nielsen identities dictate (HAUSSLING; KRAUS, 1997).

Another issue faced here was the fact that the branch point for the Higgs propagator is ξ-dependent, being located at $p^2 = 0$ for the Landau gauge $\xi = 0$. For small values of ξ, the pole mass has a real value. However, its value is located on the branch cut, making it impossible to define a residue at this point, and therefore a spectral function. This means that in order to formulate a spectral function, we should move away from the Landau gauge. These issues with unphysical (gauge-variant) thresholds are nothing new, see for example (BINOSI; PAPAVASSILIOU, 2009). They reinforce in a natural way the need to work with gauge-invariant field operators to correctly describe the observable excitations of a gauge theory.

For the photon, the (transverse) propagator is gauge independent (even BRST invariant), and consequently so are the pole mass, residue and spectral function. For the

Higgs boson, the propagator, residue and spectral function are gauge dependent, while the pole mass is gauge independent, in line with the latter being an observable quantity. Notice that the residue of the two-point function does not need to be gauge independent, since this does not follow from the Nielsen identities, as we discussed in our main text. Rather, the Nielsen identities can be used to show that the residues of the pole masses in S-matrix elements are gauge independent, that is the residues of the singularities in observable scattering amplitudes, see (GRASSI; KNIEHL; SIRLIN, 2001; GRASSI; KNIEHL; SIRLIN, 2002). These residues can evidently be different per scattering process (and per different mass pole). The fact that the Higgs propagator is gauge dependent is not surprising, given that the Higgs field is not invariant under the Abelian gauge transformation.

Concluding, in this chapter several tools have been worked out to determine spectral properties in perturbation theory. We worked up to first order in $\hbar$, but everything can be consistently extended to higher orders. We paid attention how to avoid problems with complex poles and to the pivotal important role of the Nielsen identities, which are intimately related to the exact nilpotent BRST invariance of the model. These tools will turn out to be quite useful for forthcoming work on the spectral properties of HYM theories. For these theories, the Nielsen identities are well established (GAMBINO; GRASSI, 2000), with supporting lattice data (MAAS; MUFTI, 2014), providing thus a solid foundation to compare any results with.

In the next chapters we will consider gauge-invariant operators and study their spectral properties using the same techniques of this paper. If the elementary fields are not gauge invariant (like the Higgs field, but also the gluon field in QCD), these aforementioned gauge-invariant operators will turn out to be composite in nature. Such an approach has recently been addressed in (MAAS; SONDENHEIMER; TOREK, 2019; MAAS, 2019), based on the seminal observations of Fröhlich-Morchio-Strocchi (FROHLICH; MORCHIO; STROCCHI, 1980; FROHLICH; MORCHIO; STROCCHI, 1981), in which composite operators with the same global quantum numbers (parity, spin, ...) as the elementary particles are constructed.[10] These composite states will enable us to access directly the physical spectrum of the theory. Moreover, we notice that the spectral properties and the behaviour in the complex momentum plane of a (gauge-invariant) composite operator will nontrivially depend on the spectral properties of its gauge-variant constituents. This gives another motivation why it is meaningful to study spectral properties of gauge-variant propagators. Another nice illustrative example of this interplay is the Bethe-Salpeter study of glueballs in pure gauge theories (SANCHIS-ALEPUZ et

[10] For a recent discussion of the renormalization properties of higher dimensional gauge invariant operators in HYM models see the recent results by (BINOSI; TRIPOLT, 2020).

al., 2015), based on spectral properties of constituent gluons and ghosts (STRAUSS; FISCHER; KELLERMANN, 2012).

4 GAUGE-INVARIANT SPECTRAL DESCRIPTION OF THE $U(1)$ HIGGS MODEL FROM LOCAL COMPOSITE OPERATORS

4.1 Introduction

An essential aspect of gauge theories is that all physical observable quantities have to be gauge invariant (PESKIN; SCHROEDER, 1995; HOOFT et al., 1980). Therefore, a formulation of the properties of the elementary excitations in terms of gauge-invariant variables is very welcome. Such an endeavour has been addressed by several authors[11] (HOOFT et al., 1980; HOOFT et al., 2012; FROHLICH; MORCHIO; STROCCHI, 1980; FROHLICH; MORCHIO; STROCCHI, 1981), who have been able to construct, out of the elementary fields, a set of local gauge invariant composite operators which can effectively implement a gauge invariant framework by using the tools of quantum gauge field theories: renormalizability, locality, Lorentz covariance and BRST exact symmetry. The aim of this chapter is that of discussing the features of two local gauge invariant operators within the framework of the $U(1)$ Abelian Higgs model discussed in chapter 3. Following (HOOFT et al., 1980; HOOFT et al., 2012), we shall consider the two local composite operators $O(x)$ and $V_\mu(x)$ invariant under (155), given by

$$\begin{aligned} O(x) &= 1/2(h^2(x) + 2vh(x) + \rho^2(x)) = \varphi^\dagger(x)\varphi(x) - \frac{v^2}{2} \,, \\ V_\mu(x) &= -i\varphi^\dagger(x)(D_\mu\varphi)(x) \,. \end{aligned} \tag{242}$$

The relevance of these operators can be understood by using the expansion (152) and retaining the first order terms. For the two-point correlator of the scalar operator one finds (cf. eq. (248) for the full expression):

$$\langle O(x)O(y)\rangle \sim v^2\langle h(x)h(y)\rangle_{(\text{tree-level})} + O(\hbar) + \langle O\left(h^3; h\rho^2; \rho^4\right)\rangle \,, \tag{243}$$

while the contributions to the vector operator at lowest order in the fields read

$$V_\mu(x) \sim \frac{ev^2}{2}A_\mu(x) + \text{total derivative} + \text{higher orders} \,. \tag{244}$$

We see therefore that the gauge-invariant operator $O(x)$ is related to the Higgs excitation, while $V_\mu(x)$ is associated with the photon.

In this chapter, we shall compute the BRST-invariant two-point correlation func-

[11] See (MAAS, 2019; MAAS; SONDENHEIMER; TÖREK, 2019) for a general review on this matter.

tions

$$\langle O(x)O(y)\rangle \, , \qquad \langle V_\mu(x)V_\nu(y)\rangle \, , \tag{245}$$

at one-loop order in the 't Hooft R_ξ-gauge and discuss the differences with respect to the corresponding one-loop elementary propagators $\langle h(x)h(y)\rangle$ and $\langle A_\mu(x)A_\nu(y)\rangle$ already evaluated in the last chapter. Let us point out that the two local operators $(V_\mu(x), O(x))$ belong to the cohomology of the BRST operator (PIGUET; SORELLA, 1995), i.e.

$$\begin{aligned} sV_\mu(x) &= 0 \, , \qquad & V_\mu(x) \neq s\Delta_\mu(x) \\ sO(x) &= 0 \, , \qquad & O(x) \neq s\Delta(x) \, , \end{aligned} \tag{246}$$

for any local quantities $(\Delta_\mu(x), \Delta(x))$. As expected, both correlation functions of eq. (245) turn out to be independent from the gauge parameter ξ. Moreover, we shall show that the one-loop pole masses of $\langle V_\mu(x)V_\nu(y)\rangle_T$ and $\langle O(x)O(y)\rangle$ are exactly the same as those of the elementary propagators $\langle A_\mu(x)A_\nu(y)\rangle_T$ and $\langle h(x)h(y)\rangle$, where $\langle A_\mu(x)A_\nu(y)\rangle_T$ stands for the transverse component of $\langle A_\mu(x)A_\nu(y)\rangle$, i.e.

$$\langle A_\mu(x)A_\nu(y)\rangle_T = \left(\delta_{\mu\rho} - \frac{\partial_\mu\partial_\rho}{\partial^2}\right)\langle A_\rho(x)A_\nu(y)\rangle \, . \tag{247}$$

This important feature makes apparent the fact that the operators $V_\mu(x)$ and $O(x)$ give a gauge invariant picture for the photon and Higgs modes. In addition, the correlation functions $\langle V_\mu(x)V_\nu(y)\rangle_T$ and $\langle O(x)O(y)\rangle$ exhibit a spectral KL representation with positive spectral densities, allowing for a physical interpretation in terms of particles. This property is in sharp contrast with the one-loop spectral density of the elementary non gauge invariant Higgs propagator $\langle h(x)h(y)\rangle$, which displays an explicit dependence on the gauge parameter ξ, as established in the last chapter. Moreover, the longitudinal part of the correlator $\langle V_\mu(x)V_\nu(y)\rangle$ – which is independently gauge invariant – is shown to exhibit the pole mass of the Higgs excitation. This last feature reinforces the consistency of the present description of the physical degrees of freedom of the theory, since the only physically expected elementary excitations are indeed the Higgs and the photon ones. Let us also underline that, to our knowledge, this is the first explicit one-loop calculation of the gauge-invariant correlators (245) and of their analytical properties.

This chapter is organized as follows. In section 4.2 we compute at one-loop order the two-point functions for the composite operators in. In section J, we provide the detailed analysis of the spectral properties of the composite operators, and compare them with the spectral properties of the elementary fields. The unitary limit, in which the gauge parameter ξ tends to infinity, is investigated in section 4.4. Section 5.5 collects our conclusion and outlook. The final Appendices contain the derivation of the Feynman rules and of the diagrams contributing to (245).

4.2 The correlation functions $\langle O(x)O(y)\rangle$ and $\langle V_\mu(x)V_\nu(y)\rangle$ at one loop order

We study the two-point correlation functions of the local gauge invariant operators $(V_\mu(x), O(x))$. For the correlator of the scalar composite operator we get:

$$\begin{aligned}\langle O(x)O(y)\rangle &= v^2\,\langle h(x)h(y)\rangle + v\,\langle h(x)\rho(y)^2\rangle + v\,\langle h(x), h(y)^2\rangle + \\ &\quad +\frac{1}{4}\Big(\,\langle h(x)^2\rho(y)^2\rangle + \langle h(x)^2 h(y)^2\rangle + \langle \rho(x)^2\rho(y)^2\rangle\,\Big).\end{aligned} \tag{248}$$

Individually, the terms in the expansion (248) are not gauge invariant, but their sum is. We can now analyze the connected diagrams for each term, up to one-loop order, through the action (153). We calculated the one-loop diagrams in Appendix G.1. Looking at the diagrams in Figure 39, we can see that the correlation function $\langle O(p)O(-p)\rangle$ will have the following structure

$$\begin{aligned}\langle O(p)O(-p)\rangle^{1-loop} &= \frac{A_{fin}(p^2)+\delta A_{div}(p^2)}{(p^2+m_h^2)^2} + \frac{B_{fin}(p^2)+\delta B_{div}(p^2)}{(p^2+m_h^2)} \\ &+ \; C_{fin}(p^2)+\delta C_{div}(p^2),\end{aligned} \tag{249}$$

where $(A_{fin}, B_{fin}, C_{fin})$ stand for the finite parts and $(\delta A_{div}, \delta B_{div}, \delta C_{div})$ for the purely divergent terms, i.e. the pole terms in $\frac{1}{\epsilon}$ obtained by means of the dimensional regularization, namely

$$\begin{aligned}\delta A_{div}(p^2) &\overset{\epsilon\to 0}{=} \frac{v^2}{8\pi^2\epsilon}\Big(2v^2\lambda^2 - e^2(p^2(-3+\xi)+v^2\lambda\xi)\Big) \\ \delta B_{div}(p^2) &\overset{\epsilon\to 0}{=} \frac{v^2(6e^4-\lambda^2+e^2\lambda\xi)}{8\pi^2\epsilon\lambda} \\ \delta C_{div}(p^2) &\overset{\epsilon\to 0}{=} \frac{1}{8\pi^2\epsilon}\end{aligned} \tag{250}$$

while

$$
\begin{aligned}
A_{fin}(p^2) &= \frac{v^2}{(4\pi)^2}\int_0^1 dx\Bigg\{e^2\Bigg[p^2(1-\ln\frac{m^2}{\mu^2}-2\ln\frac{p^2x(1-x)+m^2}{\mu^2}) \\
&- \frac{p^4}{2m^2}\ln\frac{p^2x(1-x)+m^2}{\mu^2}-6m^2(1-\ln\frac{m^2}{\mu^2}+\ln\frac{p^2x(1-x)+m^2}{\mu^2})\Bigg] \\
&+ \lambda\Big[\frac{1}{2}m_h^2(-6+6\ln\frac{m_h^2}{\mu^2}-9\ln\frac{p^2x(1-x)+m_h^2}{\mu^2})\Big] \\
&- \Bigg[\xi(e^2p^2+\lambda m^2)(1-\ln\frac{\xi m^2}{\mu^2})-(e^2\frac{p^4}{2m^2}-\lambda\frac{m_h^2}{2})\ln\frac{p^2x(1-x)+\xi m^2}{\mu^2}\Bigg]\Bigg\} \\
B_{fin}(p^2) &= \frac{1}{(4\pi)^2m_h^2}\int_0^1 dx\Bigg\{-m^2\xi m_h^2\ln\left(\frac{m^2\xi}{\mu^2}\right) \\
&+ m^2\xi m_h^2+m_h^4\Big(3\ln\left(\frac{m_h^2+p^2(1-x)x}{\mu^2}\right)+\ln\left(\frac{m^2\xi+p^2(1-x)x}{\mu^2}\right)\Big) \\
&- 3m_h^4\ln\left(\frac{m_h^2}{\mu^2}\right)+3m_h^4+2m^4-6m^4\ln\left(\frac{m^2}{\mu^2}\right)\Bigg\} \\
C_{fin}(p^2) &= -\frac{1}{2(4\pi)^2}\int_0^1 dx\Bigg\{\ln\left(\frac{m_h^2+p^2(1-x)x}{\mu^2}\right)+\ln\left(\frac{m^2\xi+p^2(1-x)x}{\mu^2}\right)\Bigg\}. \qquad (251)
\end{aligned}
$$

The divergent terms $(\delta A_{div}, \delta B_{div}, \delta C_{div})$ can be eliminated by means of the Lagrangian counterterms as well as by suitable counterterms in the external part of the action S_J accounting for the introduction of the composite operator $O(x)$, i.e.

$$
S_J = S+\int d^4x\left[(1+\delta Z^0_{div})J(x)O(x)+(1+\delta Z_{div})\frac{(J(x))^2}{2}\right], \qquad (252)
$$

where $J(x)$ is a BRST invariant dimension two source needed to define the generator $Z^c(J)$ of the connected Green function $\langle O(x)O(y)\rangle$:

$$
\langle O(x)O(y)\rangle = \frac{\delta^2 Z^c(J)}{\delta J(x)\delta J(y)}|_{J=0}. \qquad (253)
$$

It is worth emphasizing here that we have the freedom of introducing a pure contact BRST invariant term in the external source $J(x)$:

$$
\int d^4x\,\frac{\alpha}{2}\,J^2(x), \qquad (254)
$$

which can be arbitrarily added to the action (252). Including such a term in (252) will have the effect of adding a dimensionless constant to $G_{OO} = \langle O(p)O(-p)\rangle$, i.e.

$$G_{OO}(p^2) \to G_{OO}(p^2) + \alpha. \tag{255}$$

In particular, α can be chosen to be equal to $-G_{OO}(0)$, implying then that the modified Green's function

$$G_{OO}(p^2) - G_{OO}(0) \tag{256}$$

will obey a one substracted KL representaion .

Inserting the unity

$$1 = (p^2 + m_h^2)/(p^2 + m_h^2) = ((p^2 + m_h^2)/(p^2 + m_h^2))^2, \tag{257}$$

for the finite part of $\langle O(p)O(-p)\rangle$, we write

$$\langle O(p)O(-p)\rangle_{fin} = \frac{v^2}{p^2 + m_h^2} + \frac{\hbar v^2}{(p^2 + m_h^2)^2}\Pi(p^2) + \mathcal{O}(\hbar^2) \tag{258}$$

where

$$\begin{aligned}
\Pi_{OO}(p^2) &= \frac{1}{v^2}\Big((A_{fin}(p^2)) + (p^2 + m_h^2)(B_{fin}(p^2)) + (C_{fin}(p^2))(p^2 + m_h^2)^2\Big), \\
&= \frac{1}{32\pi^2 v^2 m_h^2}\int_0^1 dx\Big\{ - 8m_h^2 m^4 - 2m^2p^2(m_h^2 + 6m^2)\ln\left(\frac{m^2}{\mu^2}\right) + \\
&\quad + m_h^2\Big[- (p^2 - 2m_h^2)^2\ln\left(\frac{m_h^2 + p^2(1-x)x}{\mu^2}\right) \\
&\quad - (12m^4 + 4m^2p^2 + p^4)\ln\left(\frac{m^2 + p^2(1-x)x}{\mu^2}\right)\Big] + \\
&\quad + 2p^2(3m_h^4 + m_h^2m^2 + 2m^4) - 6m_h^4p^2\ln\left(\frac{m_h^2}{\mu^2}\right)\Big\},
\end{aligned} \tag{259}$$

and since (259) contains terms of the order of $\frac{p^4}{p^2+m^2}\ln(p^2)$, we follow the steps (201)-(203) to find the resummed form factor in the one-loop approximation

$$G_{OO}(p^2) = \frac{v^2}{p^2 + m_h^2 - \hat{\Pi}_{OO}(p^2)} + C_{OO}(p^2) \tag{260}$$

with

$$\hat{\Pi}_{OO}(p^2) = \frac{1}{32\pi^2 v^2 m_h^2}\int_0^1 dx\Bigg\{ -8m_h^2 m^4 - 2m^2p^2(m_h^2+6m^2)\ln\left(\frac{m^2}{\mu^2}\right) + \\ +m_h^2\Big[3(m_h^4+2m_h^2p^2)\ln\left(\frac{m_h^2+p^2(1-x)x}{\mu^2}\right) \\ -(12m^4+4m^2p^2-m_h^4-2p^2m_h^2)\ln\left(\frac{m^2+p^2(1-x)x}{\mu^2}\right)\Big] + \\ +2p^2(3m_h^4+m_h^2m^2+2m^4)-6m_h^4p^2\ln\left(\frac{m_h^2}{\mu^2}\right)\Bigg\}, \tag{261}$$

and

$$C_{OO}(p^2) = -\frac{1}{32\pi^2}\int_0^1 dx\Bigg\{\ln\left(\frac{m_h^2+p^2x(1-x)}{\mu^2}\right)+\ln\left(\frac{m^2+p^2x(1-x)}{\mu^2}\right)\Bigg\}. \tag{262}$$

The form factor is depicted in Figure 20. Notice that the Green function $G_{OO}(p^2)$ becomes negative for large enough values of the momentum p. As one realizes from expression (261), this feature is due to the growing in the UV region of the logarithms contained in the term $C_{OO}(p^2)$, see eq. (262). It is worth mentioning that this behaviour is also present when the parameter v is completely removed from the theory. In fact, setting $v=0$, the action S_0 in eq. (150), reduces to that of massless scalar QED, namely

$$S_0|_{v=0} = \int d^4x\left(\frac{F_{\mu\nu}^2}{4}+(D_\mu\varphi)^\dagger(D_\mu\varphi)+\frac{\lambda}{2}(\varphi^\dagger\varphi)^2\right), \tag{263}$$

with

$$\varphi|_{v=0} = \frac{1}{\sqrt{2}}(h+i\rho). \tag{264}$$

Of course, when $v=0$, the operators $O=\varphi^\dagger\varphi$ and $V_\mu=-i\varphi^\dagger D_\mu\varphi$ are still gauge invariant. Though, from eqs. (261)-(262), computing $\langle O(p)O(-p)\rangle_{v=0}$, one immediately gets

$$\langle O(p)O(-p)\rangle_{v=0} = C_{OO}|_{v=0} = -\frac{1}{16\pi^2}\int_0^1 dx\ln\frac{p^2x(1-x)}{\mu^2}. \tag{265}$$

This equation precisely shows that the term C_{OO0}, and thus the negative behaviour

Figure 20 - Scalar composite operator form factor

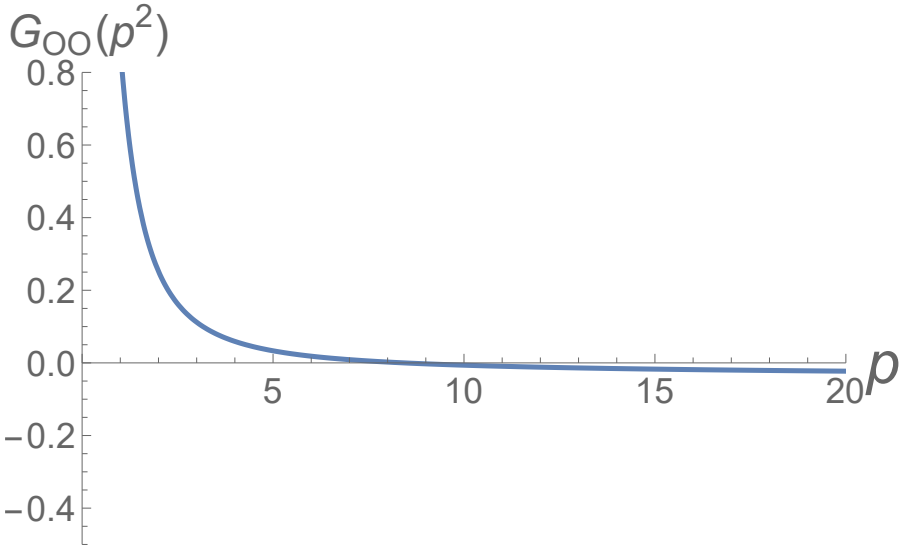

Legend: Resummed form factor for the scalar composite operator. The momentum p is given in units of the energy scale μ, for the parameter values $e = 1$, $v = 1\,\mu$, $\lambda = \frac{1}{5}$.

Source: The author, 2020.

for large enough values of p, is what one usually obtains in a theory for which $v = 0$, making evident that the presence of C_{OO} is not peculiarity of the $U(1)$ Higgs model in the $U(1)$ Higgs model, on the contrary. However, in addition to the term C_{OO} and unlike massless scalar QED, the correlation function $\langle O(p)O(-p)\rangle$ of the $U(1)$ Higgs model exhibits the term $\frac{v^2}{p^2+m_h^2-\tilde{\Pi}_{OO}}$, which will play a pivotal role. Indeed, as we shall see later on, this term, originating from the expansion of φ around the minimum of the Higgs potential, $\phi = \frac{1}{\sqrt{2}}(v+h+i\rho)$, will enable us to devise a gauge invariant description of the elementary excitations of the model.

Let us end the analysis of the correlation function $G_{OO}(p^2)$ by displaying the behaviour of its first derivative, $\frac{\partial G_{OO}(p^2)}{\partial p^2}$, as well as of the one subtracted correlator $G_{OO}(p^2) - G_{OO}(0)$, see Figure 21. The first derivative, as expected, is negative while, unlike $G_{OO}(p^2)$, decays to zero for $p^2 \to \infty$. The quantity $\frac{\partial G_{OO}(p^2)}{\partial p^2}$ will be helpful when discussing the spectral representation corresponding to $\langle O(p)O(-p)\rangle$. Then, for the vectorial composite operator $V_\mu(x)$, we first observe that

$$\begin{aligned} V_\mu(x) &= -i\varphi^\dagger(x)(D_\mu\varphi)(x) \\ &= e\varphi^\dagger(x)A_\mu(x)\varphi(x) - \frac{1}{2}i\varphi^\dagger(x)\partial_\mu\varphi(x) + \frac{1}{2}i\varphi(x)\partial_\mu\varphi^\dagger(x) - i\partial_\mu O(x), \end{aligned} \tag{266}$$

and since we know that the last term is gauge-invariant, the first three terms together are also gauge-invariant. We thus define a new gauge-invariant operator

Figure 21 - Form factor - one subtraction

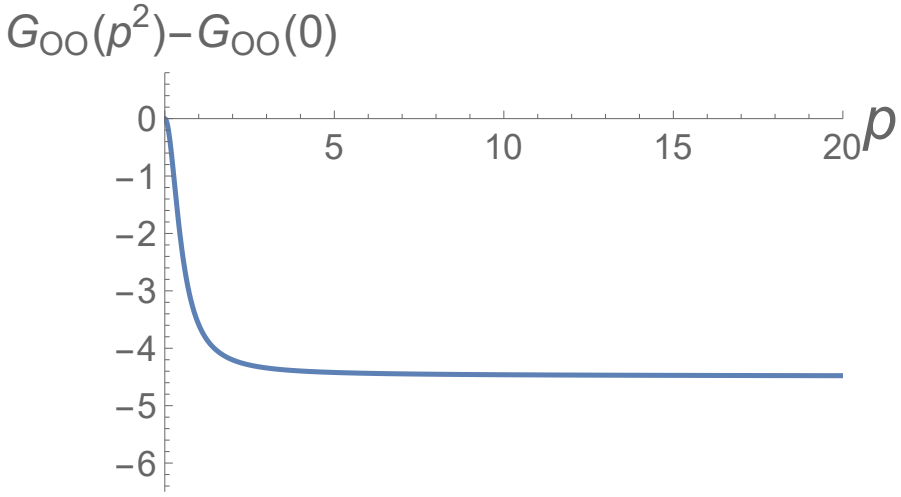

Legend: The resummed form factor with one subtraction. The momentum p is given in units of the energy scale μ, for the parameter values $e = 1$, $v = 1\,\mu$, $\lambda = \frac{1}{5}$.

Source: The author, 2020.

Figure 22 - Form factor first derivative

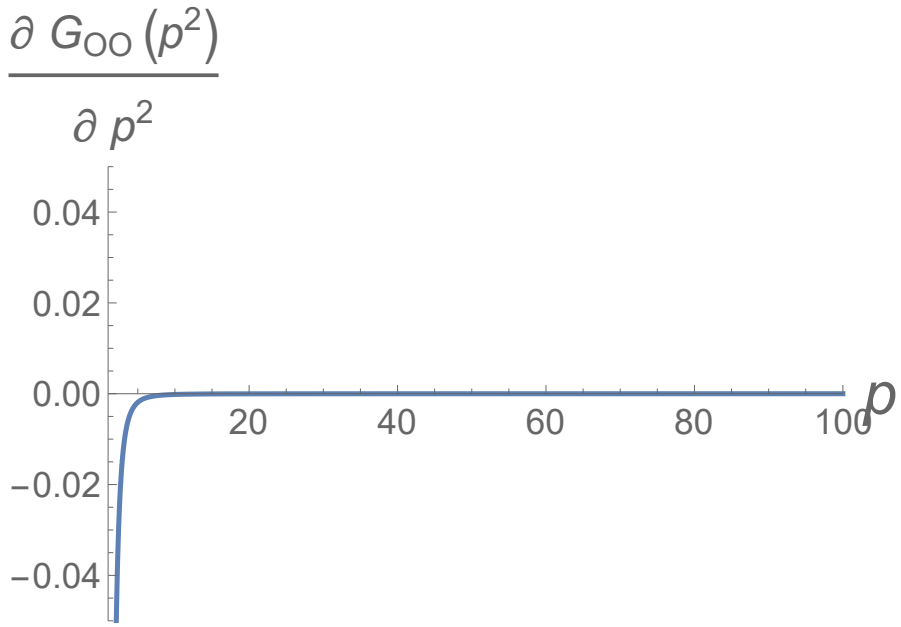

Legend: The first derivative of the form factor (left). The momentum p is given in units of the energy scale μ, for the parameter values $e = 1$, $v = 1\,\mu$, $\lambda = \frac{1}{5}$.

Source: The author, 2020.

$$V'_\mu(x) = e\varphi^\dagger(x)A_\mu(x)\varphi(x) - \frac{1}{2}i\varphi^\dagger(x)\partial_\mu\varphi(x) + \frac{1}{2}i\varphi(x)\partial_\mu\varphi^\dagger(x), \tag{267}$$

expanding the scalar field $\varphi(x)$ we find

$$V'_\mu(x) = \frac{1}{2}e(v+h(x))^2A_\mu(x) + \frac{1}{2}e\rho^2(x)A_\mu(x) + (v+h(x))\partial_\mu\rho(x) - \rho(x)\partial_\mu h(x) \tag{268}$$

so that

$$\begin{aligned}\langle V'_\mu(x)V'_\nu(y)\rangle \overset{\varphi\to\frac{1}{\sqrt{2}}(v+h+i\rho)}{=} & -\frac{1}{4}\Big\{ - e^2v^4\langle A_\mu(x)A_\nu(y)\rangle - 4e^2v^3\langle h(x)A_\mu(x)A_\nu(y)\rangle \\ & -2e^2v^2\langle h(x)^2A_\mu(x)A_\nu(y)\rangle - 4e^2v^2\langle h(x)A_\mu(x)h(y)A_\nu(y)\rangle \\ & -2e^2v^2\langle \rho(x)^2A_\mu(x)A_\nu(y)\rangle - 2ev^2\partial^x{}_\mu\langle h(x)\rho(x)A_v(y)\rangle \\ & +4ev^2\langle \partial^x{}_\mu h(x)\rho(x)A_\nu(y)\rangle - 2ev^3\partial^x{}_\mu\langle \rho(x)A_\nu(y)\rangle \\ & -4ev^2\partial^x{}_\mu\langle \rho(x)h(y)A_v(y)\rangle - 2v\partial^x{}_\mu\partial^y{}_\nu\langle h(x)\rho(x)\rho(y)\rangle \\ & +4v\partial^y{}_\nu\langle \partial^x{}_\mu h(x)\rho(x)\rho(y)\rangle - \partial^x{}_\mu\partial^y{}_\nu\langle h(x)\rho(x)h(y)\rho(y)\rangle \\ & +4\langle \partial^x{}_\mu h(x)\rho(x)h(y)\partial^y{}_\nu\rho(y)\rangle - v^2\partial^x{}_\mu\partial^y{}_\nu\langle \rho(x)\rho(y)\rangle\Big\} \\ & +O(\hbar^2),\end{aligned} \tag{269}$$

where we have discarded the terms that do not have one-loop contributions. In momentum space, we can split the two-point function into transverse and longitudinal parts in the usual way:

$$\langle V'_\mu(p)V'_\nu(-p)\rangle = \langle V'(p)V'(-p)\rangle^T\mathcal{P}_{\mu\nu} + \langle V'(p)V'(-p)\rangle^L\mathcal{L}_{\mu\nu}\,, \tag{270}$$

where we have introduced the transverse and longitudinal projectors, given respectively by

$$\begin{aligned}\mathcal{P}_{\mu\nu}(p) &= \delta_{\mu\nu} - \frac{p_\mu p_\nu}{p^2}\,, \\ \mathcal{L}_{\mu\nu}(p) &= \frac{p_\mu p_\nu}{p^2}\,.\end{aligned} \tag{271}$$

At tree-level, we find in momentum space

$$\begin{aligned}\langle V'_\mu(p)V'_\nu(-p)\rangle_{\rm tree} &= -\frac{1}{4}\left(-e^2v^4\langle A_\mu(p)A_\nu(-p)\rangle - v^2p_\mu p_\nu\langle\rho(p)\rho(-p)\rangle\right)\\ &= \frac{1}{4}\left(e^2v^4\frac{1}{p^2+m^2}\mathcal{P}_{\mu\nu}+e^2v^4\frac{\xi}{p^2+\xi m^2}\mathcal{L}_{\mu\nu}+v^2\frac{p^2}{p^2+\xi m^2}\mathcal{L}_{\mu\nu}\right)\\ &= \frac{e^2v^4}{4}\frac{1}{p^2+m^2}\mathcal{P}_{\mu\nu}+v^2\mathcal{L}_{\mu\nu}. \end{aligned} \tag{272}$$

We can now analyze the connected diagrams for each term, up to one-loop order, through the action (153). We calculated the one-loop diagrams in Appendix G.2. Let us start with the transverse part. Looking at the diagrams in Figure 40, we can see that the one-loop correlation function will have the following structure

$$\begin{aligned}\langle V'(p)V'(-p)\rangle^{T,1-loop} &= \frac{A^V_{fin}(p^2)+\delta A^V_{div}(p^2)}{(p^2+m^2)^2}+\frac{B^V_{fin}(p^2)+\delta B^V_{div}(p^2)}{(p^2+m^2)}\\ &+ C^V_{fin}(p^2)+\delta C^V_{div}(p^2)\end{aligned} \tag{273}$$

where $(A^V_{fin}, B^V_{fin}, C^V_{fin})$ stand for the finite parts and $(\delta A^V_{div}, \delta B^V_{div}, \delta C^V_{div})$ for the purely divergent terms, i.e. the pole terms in $\frac{1}{\epsilon}$ obtained by means of the dimensional regularization, namely

$$\begin{aligned}\delta A^V_{div} &\overset{\epsilon\to0}{=} \frac{e^4v^4}{2(4\pi)^2\epsilon}\Big(\frac{1}{3}p^2-6(\frac{e^2}{\lambda}-\frac{1}{2})e^2v^2+3\lambda v^2\Big)\\ \delta B^V_{div} &\overset{\epsilon\to0}{=} \frac{v^2}{(4\pi)^2\epsilon}(6\frac{e^6v^2}{\lambda}-3e^4v^2-\frac{e^2p^2}{3}+3e^2\lambda v^2)\\ \delta C^V_{div} &\overset{\epsilon\to0}{=} \frac{1}{6(4\pi)^2\epsilon}(9e^2v^2-p^2-3\lambda v^2)\end{aligned} \tag{274}$$

and

$$
\begin{aligned}
A^V_{fin} &= \frac{e^4v^4}{2(4\pi)^2}\int_0^1 dx\,\Bigg\{p^2x(1-x)+m^2x \\
&+ m_h^2(1-x)(1-\ln\frac{p^2x(1-x)+m^2x+m_h^2(1-x)}{\mu^2})+m_h^2(1-\ln\frac{m_h^2}{\mu^2}) \\
&+ \frac{m^4}{m_h^2}(1-3\ln\frac{m^2}{\mu^2})+2m^2\ln\frac{p^2x(1-x)+m^2x+m_h^2(1-x)}{\mu^2}\Bigg\} \\
B^V_{fin} &= \frac{m^2}{18m_h^2p^2(4\pi)^2}\int_0^1 dx\Bigg\{3m_h^4\left(m_h^2-m^2-7p^2\right)\ln\left(\frac{m_h^2}{\mu^2}\right) \\
&- 3m_h^2\left(2p^2\left(m_h^2-5m^2\right)+\left(m_h^2-m^2\right)^2+p^4\right)\ln\left(\frac{xm_h^2+m^2(1-x)+p^2(1-x)x}{\mu^2}\right) \\
&- 3\left(m_h^3-m^2m_h\right)^2+9p^2\left(m^2m_h^2+3m_h^4+2m^4\right)+2p^4m_h^2 \\
&- 3m^2\left(m_h^2\left(p^2-m^2\right)+m_h^4+18m^2p^2\right)\ln\left(\frac{m^2}{\mu^2}\right)\Bigg\} \\
C^V_{fin} &= \frac{1}{36(4\pi)^2p^2}\int_0^1 dx\Bigg\{3m^2\left(m_h^2-m^2+p^2\right)\ln\left(\frac{m^2}{\mu^2}\right) \\
&+ 3m_h^2\left(-m_h^2+m^2+p^2\right)\ln\left(\frac{m_h^2}{\mu^2}\right)+6m_h^2\left(p^2-m^2\right)-5p^2\left(3m_h^2-9m^2+p^2\right) \\
&+ 3\left(2m_h^2\left(p^2-m^2\right)+m_h^4+m^4-10m^2p^2+p^4\right)\ln\left(\frac{p^2x(1-x)+xm^2+(1-x)m_h^2}{\mu^2}\right) \\
&+ 3m_h^4+3m^4-54m^2p^2+3p^4\Bigg\}. \qquad (275)
\end{aligned}
$$

The divergent terms $(\delta A^V_{div}, \delta B^V_{div}, \delta C^V_{div})$ can be eliminated by means of the Lagrangian counterterms as well as by suitable counterterms in the external part of the action S^V_J accounting for the introduction of the composite operator $V'_\mu(x)$, i.e.

$$
S^V_J = S+\int d^4x\left[(1+\delta Z^{V,0}_{div})J_\mu(x)V_\mu(x)+(1+\delta Z^V_{div})\frac{J_\mu(x)J_\mu(x)}{2}\right], \qquad (276)
$$

where $J_\mu(x)$ is a BRST invariant dimension one source needed to define the generator $Z^c(J)$ of the connected Green function $\langle V'_\mu(x)V'_\nu(y)\rangle$:

$$
\langle V'_\mu(x)V'_\nu(y)\rangle = \frac{\delta^2Z^c(J)}{\delta J_\mu(x)\delta J_\nu(y)}|_{J=0}, \qquad (277)
$$

and like in the scalar case, we have the freedom of introducing a pure contact BRST invariant term in the external source $J_\mu(x)$:

$$\int d^4x\,\frac{1}{2}(\beta v^2\,J_\mu(x)J_\mu(x)+\gamma J_\mu(x)\partial^2 J_\mu(x)+\sigma(\partial_\mu J_\mu(x))^2), \tag{278}$$

which can be arbitrarily added to the action (276). Including such a term in (276) will have the effect of adding a dimensionless constant to $G^T_{VV}(p^2)=\langle V'(p)V'(-p)^T\rangle$, i.e.

$$G^T_{VV}(p^2)\to G^T_{VV}(p^2)+\beta v^2+\gamma p^2, \tag{279}$$

where we notice that the last term in (278) does not contribute to the transversal part of the propagator. In particular, β and γ can be choosen so that (279) becomes

$$G^T_{VV}(p^2)-G^T_{VV}(0)-p^2\frac{\partial G^T_{VV}(p^2)}{\partial p^2}|_{p=0}, \tag{280}$$

see Figure 24. It is a Green's function that obeys a two substracted KL representation, see section J. Following the steps in the same way as for the scalar composite field, (252)-(351), we find

$$\langle V'(p)V'(-p)\rangle^T \;=\; \frac{e^2v^4}{4}\frac{1}{p^2+m^2}+\frac{\hbar e^2v^4}{4}\frac{\Pi^T_{VV}(p^2)}{(p^2+m^2)^2}+\mathcal{O}(\hbar^2), \tag{281}$$

with

$$\begin{aligned}
&\Pi^T_{VV}(p^2)=\\
-\;&\frac{1}{9(4\pi)^2e^2v^4m_h^2}\int_0^1 dx\Big\{-18m^4(m_h^4+m^4)+9m_h^2p^4(m_h^2+m^2)\\
-\;&3m_h^2p^2\big[2p^2(m_h^2-5m^2)+(m_h^2-m^2)^2+p^4\big]\ln\left(\frac{m_h^2(1-x)+m^2x+p^2(1-x)x}{\mu^2}\right)\\
+\;&2m_h^2p^6+3m_h^4\ln\left(\frac{m_h^2}{\mu^2}\right)\big[p^2(m_h^2+11m^2)+6m^4-p^4\big]\\
+\;&3m^2\big[-m_h^2p^4+p^2(-m_h^4+m_h^2m^2+36m^4)+18m^6\big]\ln\left(\frac{m^2}{\mu^2}\right)\\
-\;&3p^2(m_h^6+10m_h^4m^2+m_h^2m^4+12m^6)\Big\},
\end{aligned} \tag{282}$$

and following the steps (201)-(203), we find

$$G^T_{VV}\;=\;\frac{e^2v^4}{4}\Big(\frac{1}{p^2+m^2-\Pi^T_{VV}(p^2)}\Big)+C_{VV}(p^2) \tag{283}$$

with

$$\begin{aligned}
\hat{\Pi}^T_{VV}(p^2) &= -\frac{1}{9(4\pi)^2 e^2 v^4 m_h^2}\int_0^1 dx\Big\{ -18m^4(m_h^4+m^4)+9m_h^2p^4(m_h^2+m^2)\\
&- 3m_h^2\big[2(-2m^2p^2-m^4)(m_h^2-5m^2)\\
&+ p^2(m_h^2-m^2)^2-2m^2p^2-m^4\big]\ln\left(\frac{m_h^2(1-x)+m^2x+p^2(1-x)x}{\mu^2}\right)\\
&+ 2m_h^2p^6+3m_h^4\ln\left(\frac{m_h^2}{\mu^2}\right)\left[p^2(m_h^2+11m^2)+6m^4-p^4\right]\\
&+ 3m^2\big[-m_h^2p^4+p^2(-m_h^4+m_h^2m^2+36m^4)+18m^6\big]\ln\left(\frac{m^2}{\mu^2}\right)\\
&- 3p^2(m_h^6+10m_h^4m^2+m_h^2m^4+12m^6)\Big\}, \qquad (284)
\end{aligned}$$

and

$$C_{VV}(p^2) = \frac{1}{12(4\pi)^2}\int_0^1 dx\left\{(2m_h^2+p^2)\ln\left(\frac{m_h^2(1-x)+m^2x+p^2(1-x)x}{\mu^2}\right)\right\}. \qquad (285)$$

The resummed form factor (283) is depicted in Figure 23, as well as the modified version (280) and their second derivative, which is imported for the spectral analysis in section J.

For the longitudinal part of the propagator (see appendix G.2 for details) , we find the divergent part

$$\langle V'(p)V'(-p)\rangle^L_{div} \overset{\epsilon\to 0}{=} -\frac{v^2\,(3e^4+\lambda^2)}{(4\pi)^2\lambda\epsilon} \qquad (286)$$

and the total finite correction up to first order in $\hbar$ is given by

$$\langle V'(p)V'(-p)\rangle^L_{fin} = v^2-\left(\frac{m_h^4-m_h^4\ln\left(\frac{m_h^2}{\mu^2}\right)+m^4-3m^4\ln\left(\frac{m^2}{\mu^2}\right)}{32\pi^2m_h^2}\right) \qquad (287)$$

which means the longitudinal part of the propagator $\langle V'_\mu(x), V'_\nu(y)\rangle$ is not propagating.

Figure 23 - Vector composite operator form factor I

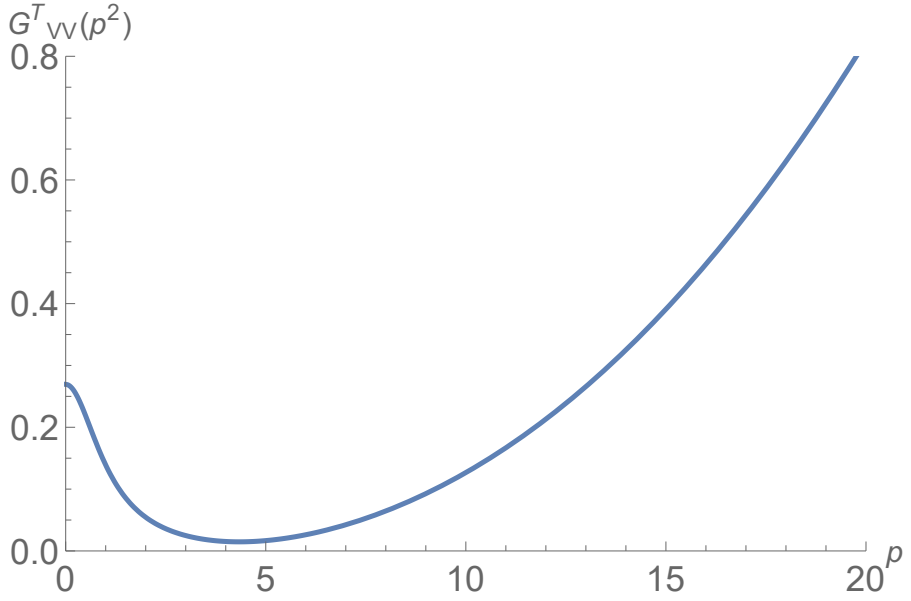

Legend: Resummed form factor for the vector composite operator (left), the resummed form factor with one subtraction (middle), and the first derivative of the form factor (left). The momentum p is given in units of the energy scale μ, for the parameter values $e = 1$, $v = 1\,\mu$, $\lambda = \frac{1}{5}$.

Source: The author, 2020.

Figure 24 - Vector composite operator form factor II

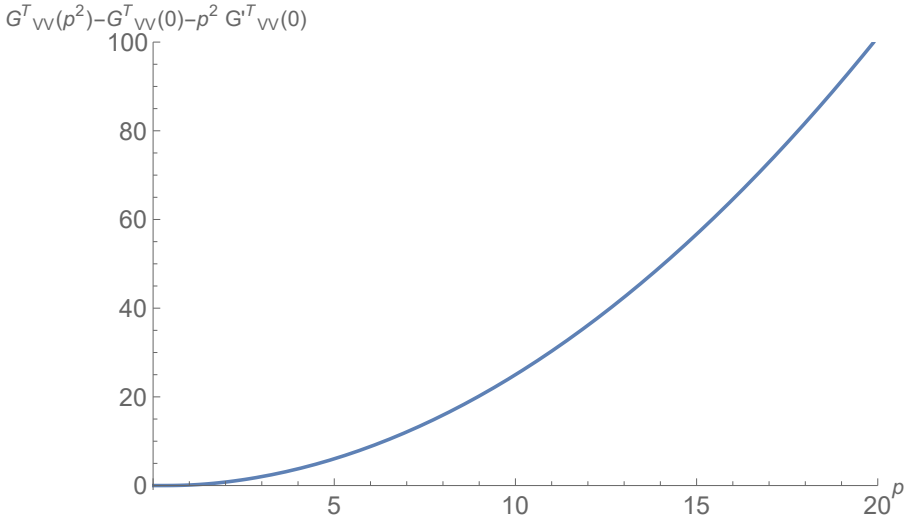

Legend: Resummed form factor for the vector composite operator. The momentum p is given in units of the energy scale μ, for the parameter values $e = 1$, $v = 1\,\mu$, $\lambda = \frac{1}{5}$.

Source: The author, 2020.

Figure 25 - Form factor second derivative

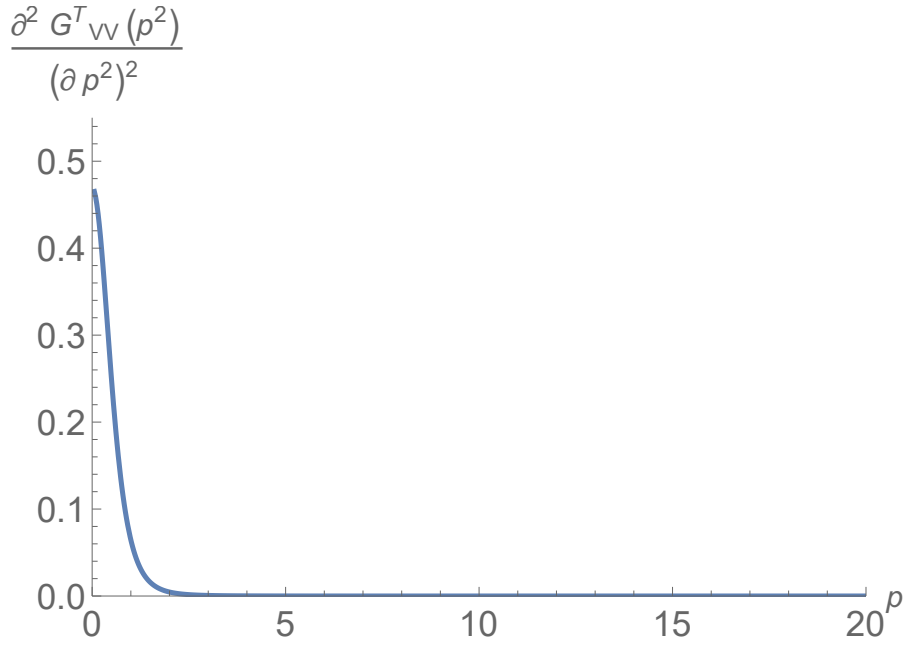

Legend: Second derivative of the form factor. The momentum p is given in units of the energy scale μ, for the parameter values $e = 1$, $v = 1\,\mu$, $\lambda = \frac{1}{5}$.

Source: The author, 2020.

4.3 **Spectral properties of the gauge-invariant local operators** $(V_\mu(x), O(x))$

In this section, we will calculate the spectral properties associated with the correlation function obtained in the last section. In 4.3.1, we will shortly review the techniques employed in the last chapter to obtain the pole mass, residue and spectral density up to first order in $\hbar$. In 4.3.2, the spectral properties of the composite operators $(V_\mu(x), O(x))$ are discussed.

4.3.1 Obtaining the spectral function

For elementary fields we obtained the spectral density function by comparing the Källén-Lehmann spectral representation for the propagator of a generic field $\widetilde{O}(p)$

$$\langle \widetilde{O}(p)\widetilde{O}(-p)\rangle = G(p^2) = \int_0^\infty dt \frac{\rho(t)}{t+p^2}, \tag{288}$$

where $\rho(t)$ is the spectral density function and $G(p^2)$ stands for the resummed propagator

$$G(p^2) \;=\; \frac{1}{p^2 + m^2 - \Pi(p^2)}. \tag{289}$$

For higher-dimensional operators, the resummed propagator acquires an overall (dimensionful) factor identical to the one appearing in its tree level result, as we have seen in section 4.2. We also note that in the case of higher dimensional operators, the spectral representation, eq.(288), might require appropriate subtraction terms in order to ensure convergence. A standard way to cure this problem is to subtract from $G(p^2)$ the first few terms of its Taylor expansion at $p = 0$ (COLANGELO; KHODJAMIRIAN, 2001), making the integral more and more convergent. These subtraction terms are directly related to the renormalization of the composite operators, and one can see that the modified Green's functions for the composite scalar field (256) and for the composite vector field (280) are in fact subtractions of the Taylor series to first and second order, respectively. In our theory we can make use of the subtracted equations at $p = 0$ because all fields are massive in the R_ξ-gauge, so there are no divergences at zero momentum. Also, we stress that the spectral function $\rho(t)$ is not affected by the subtraction procedure. Moreover, we can see that these subtractions do not have an influence on the (second) derivative of the propagator. For the scalar composite operator

$$\frac{\partial(G_{OO}(p^2) - G_{OO}(0))}{\partial p^2} = \frac{\partial G_{OO}(p^2)}{\partial p^2} = -\int_0^\infty dt \frac{\rho(t)}{(t+p^2)^2}, \tag{290}$$

which means that for a positive spectral function the first derivative of G_{OO} is strictly negative, as is confirmed in Figure 22. For the vector composite operator

$$\frac{\partial^2(G_{VV}(p^2) - G_{VV}(0) - p^2 G'_{VV}(0))}{(\partial p^2)^2} = \frac{\partial^2 G_{VV}(p^2)}{(\partial p^2)^2} = 2\int_0^\infty dt \frac{\rho(t)}{(t+p^2)^3}, \tag{291}$$

which should be strictly positive for a positive spectral function, as is shown in Figure 25. Remember, however, that we can also obtain the spectral function directly, by the methods developed in section (3.3.2).

4.3.2 Spectral properties of the gauge-invariant composite operators $V_\mu(x)$ and $O(x)$

For the scalar composite operator $O(x)$ with two-point function given by expression (261), we find the first-order pole mass for our set of parameter values to be

$$m^2_{h,pole} = 0.213472\,\mu^2, \tag{292}$$

which is exactly equal to the pole mass of the elementary Higgs field correlator. Following the steps from 3.3.1, we find the first-order residue to correct the tree-level result $Z_{\text{tree}} = v^2$

Figure 26 - Spectral function of the scalar composite operator

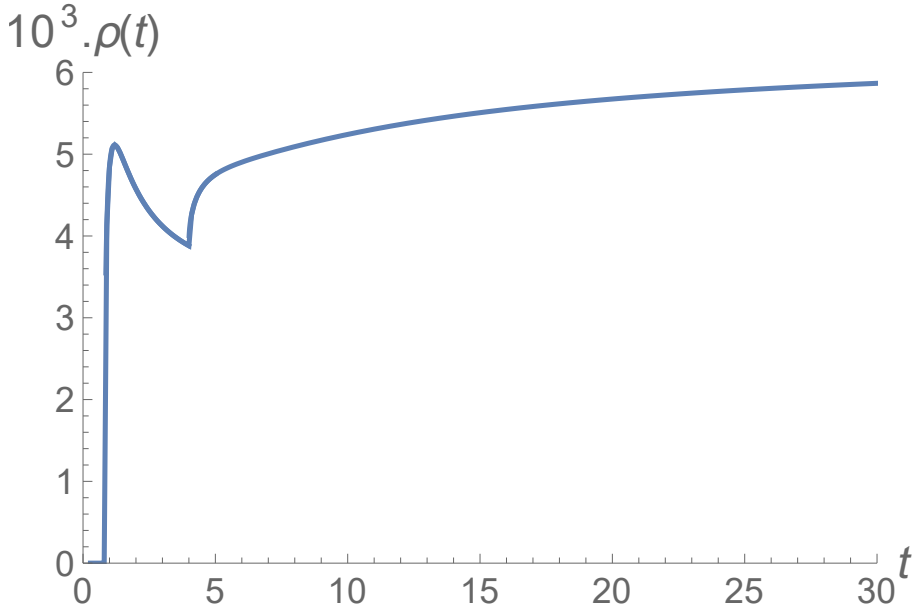

Legend: Spectral function for the reduced propagator of the scalar composite operator, $\langle O(p)O(-p)\rangle$, with t given in units of μ^2, for the parameter values $e = 1$, $v = 1\,\mu$, $\lambda = \frac{1}{5}$.

Source: The author, 2020.

by $\sim 7\%$:

$$Z = v^2(1 + \partial_{p^2}\Pi_{OO}(p^2)_{p^2=-m_h^2}) = 1.06577v^2\,, \tag{293}$$

while the first-order spectral function is shown in Figure 26. Similarly as for the spectral function of the Higgs field in Figure 12, one finds a two-particle threshold for Higgs pair production at $t = (m_h + m_h)^2 = 0.8\,\mu^2$, and a two-photon state starting at $t = (m + m)^2 = 4\,\mu^2$. The difference is that for this gauge-invariant correlation function we no longer have the unphysical Goldstone two-particle state. Due to the absence of this negative contribution, the spectral function is always positive. Therefore, this quantity is suitable for describing a physical Higgs excitation spectrum as opposed to the elementary propagator $\langle hh\rangle$.

Finally, it is interesting to note that below the unphysical threshold the elementary correlator displays the same qualitative spectral properties as this gauge-invariant approach. This means that spectral description of the physical Higgs mode could in principle be successfully encoded in the elementary propagator in the unitary gauge, in which $\xi \to \infty$ and the Goldstone bosons are infinitely heavy. We shall make an explicit comparison in section 4.4.

For the transverse vector composite operator $V_\mu^T(x)$, with our set of parameters

Figure 27 - Spectral function of the vector composite ooperator

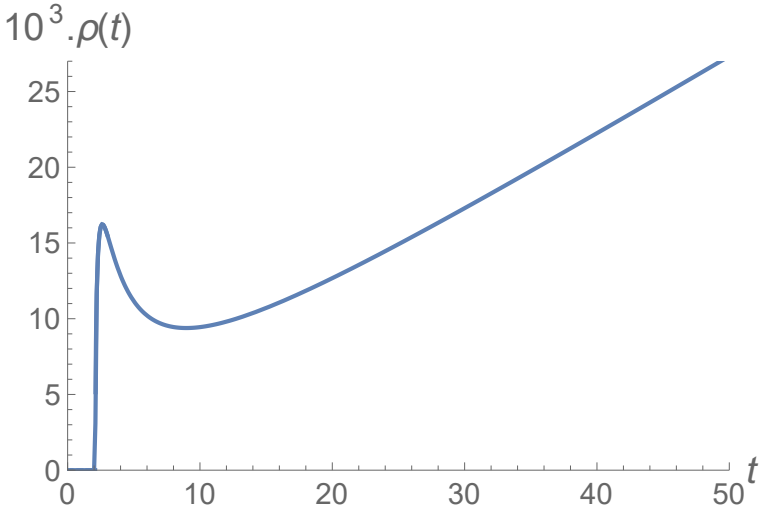

Legend: Spectral function for reduced transverse propagator of the vector composite operator $\langle V(p)V(-p)\rangle^T$, with t given in units of μ^2, for the parameter values $e = 1$, $v = 1\,\mu$, $\lambda = \frac{1}{5}$.
Source: The author, 2020.

we find the first-order pole mass

$$m^2_{pole} = 1.05417\mu^2, \tag{294}$$

which is – as expected from the Nielsen identities – exactly the same as the pole mass of the transverse photon field correlator (225). Furthermore, we find the first-order residue

$$Z = \frac{e^2v^4}{4}(1 + \partial_{p^2}\Pi^T_{VV}(p^2)_{p^2=-m^2}) = 1.09332\frac{e^2v^4}{4}\,, \tag{295}$$

and the first order spectral density for the reduced propagator is displayed in Figure 27. Like the photon spectral density in Figure 11, we find a photon-Higgs two-particle state at $t = (m_h + m)^2 = 2.09\,\mu^2$, and the spectral density is positive for all values of t.

4.3.3 Pole masses

We can explain the fact that the pole mass of the elementary propagator equals that of its gauge-invariant extension in a qualitative way by looking at the definition of a first-order pole mass, eq. (209). When calculating one-loop corrections to the two-point function of the composite operators $O(p)$ and $R^a_\mu(p)$, we find that

$$\Pi_{\text{composite}}(p^2) \;=\; \Pi_{\text{elementary}}(p^2) + \Pi_{1-\text{leg}}(p^2)(p^2+m^2) + \Pi_{0-\text{leg}}(p^2)(p^2+m^2)^2, \tag{296}$$

where $\Pi_{1-\text{leg}}(p^2)$ and $\Pi_{0-\text{leg}}(p^2)$ are the composite one-loop contributions to the correction of the composite field's two-point functions, with one external leg and zero external legs, respectively. From this, we see immediately that

$$\Pi_{\text{composite}}(-m^2) \;=\; \Pi_{\text{elementary}}(-m^2) \tag{297}$$

and therefore, up to first order in $\hbar$, we find

$$m^2_{\text{pole,composite}} \;=\; m^2_{\text{pole,elementary}} \tag{298}$$

which means that the elementary operators and their composite extensions share the same mass. This is an important feature, providing an alternative way to the Nielsen identities, to understand why the pole masses of the elementary particles are gauge invariant and not just gauge parameter independent.

4.4 **Unitary limit**

It is well-known (PESKIN; SCHROEDER, 1995) that for the Higgs model, the unitary gauge represents the physical gauge, as it decouples the unphysical fields, i.e. the ghost field and the Goldstone field. The unitary gauge can be formally obtained in the R_ξ-gauges by taking $\xi \to \infty$. However, this gauge is non-renormalizable, as one can see by looking at this limit for the tree-level propagator of the photon field

$$\langle A_\mu(p) A_\nu(-p)\rangle_{\text{tree}} \;\overset{\xi\to\infty}{=}\; \frac{1}{p^2+m^2}\mathcal{P}_{\mu\nu} + \frac{1}{m^2}\mathcal{L}_{\mu\nu}. \tag{299}$$

Nonetheless, we can approximate the unitary gauge by taking large values of ξ. This is especially interesting when looking at the spectral function of the elementary Higgs field, which is ξ-dependent. In Figure 28 one finds the spectral function for $\xi = 1000$ for small and large ranges of t. In Figure 29 we show the spectral function of the scalar composite field $O(x)$ for the same ranges of t. As one can see, the pictures are qualitatively very similar. This means that when approximating the unitary gauge, the spectral function of the gauge-dependent, elementary field $h(x)$ approximates that of its composite, gauge-invariant counterpart.

Figure 28 - Spectral function of the elementary propagator

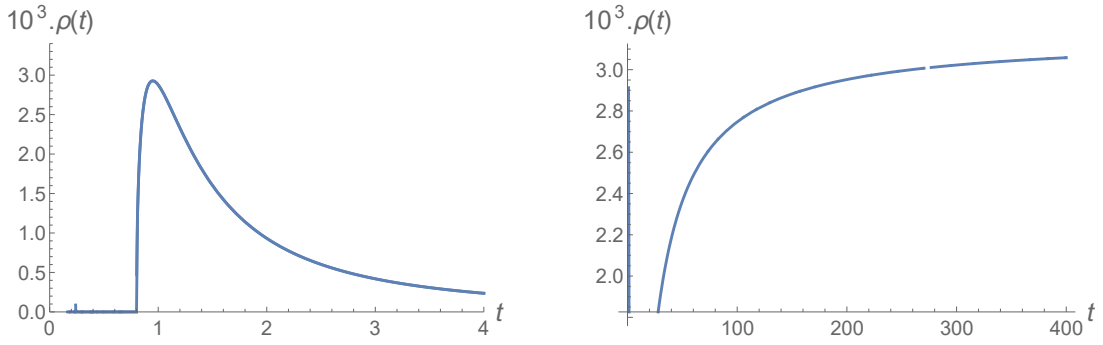

Legend: Spectral function for the reduced elementary propagator $\langle h(p)h(-p)\rangle$ for small values of t (left) and large values of t (right), with t given in units of μ^2, for $\xi = 1000$ the parameter values $e = 1$, $v = 1\,\mu$, $\lambda = \frac{1}{5}$.

Source: The author, 2020.

Figure 29 - Spectral function of the composite propagator

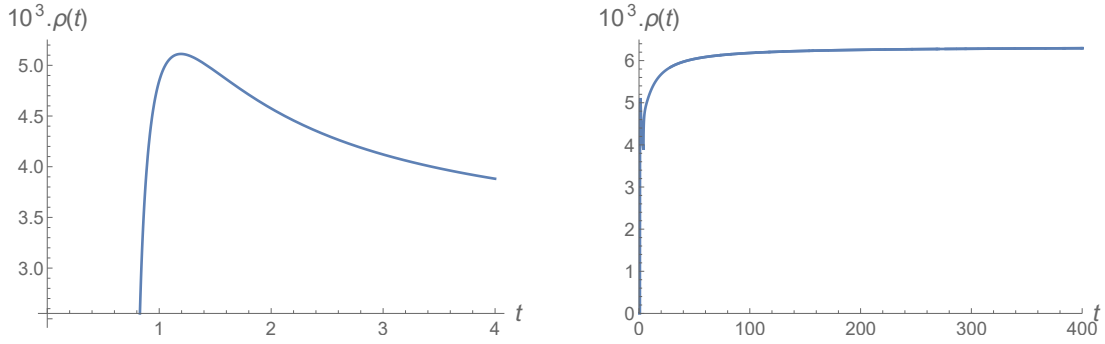

Legend: Spectral function for the reduced composite propagator $\langle O(p), O(-p)\rangle$ for small values of t (left) and large values of t (right), with t given in units of μ^2, for the parameter values $e = 1$, $v = 1\,\mu$, $\lambda = \frac{1}{5}$.

Source: The author, 2020.

4.5 Conclusion

In the present chapter, following the local gauge-invariant setup of (HOOFT et al., 1980; HOOFT et al., 2012; FROHLICH; MORCHIO; STROCCHI, 1980; FROHLICH; MORCHIO; STROCCHI, 1981), we have evaluated at one-loop order the two-point correlation functions $\langle V'_\mu(x)V'_\nu(y)\rangle$, $\langle O(x)O(y)\rangle$ of the two local gauge-invariant operators $V'_\mu(x) = -i\varphi^\dagger(x)D_\mu\varphi(x) + i\partial_\mu O(x)$ and $O(x) = \varphi^\dagger(x)\varphi(x) - \frac{v}{2}$ in the $U(1)$ Abelian Higgs model quantized in the R_ξ gauge. Our results can be summarized as follows:

- both $\langle V'_\mu(x)V'_\nu(y)\rangle$ and $\langle O(x)O(y)\rangle$ do not depend on the gauge parameter ξ, as expected;
- the pole masses of $\langle V'_\mu(x)V'_\nu(y)\rangle^T$ and $\langle O(x)O(y)\rangle$ are exactly the same as those of the correlation functions of the elementary fields $\langle A_\mu(x)A_\nu(y)\rangle^T$ and $\langle h(x)h(y)\rangle$, respectively, where $\langle\cdots\rangle_T$ stands for the transverse component of the corresponding propagator;
- the spectral densities of the Källén-Lehmann representation of the correlation functions $\langle V'_\mu(x)V'_\nu(y)\rangle$ and $\langle O(x)O(y)\rangle$ turn out to be always positive, in contrast to the one associated with the (gauge-dependent) elementary Higgs field.

These important features give us a fully gauge-invariant picture in order to describe the spectrum of elementary excitations of the model, i.e. the massive photon and the Higgs mode.

5 SPECTRAL PROPERTIES OF LOCAL BRST INVARIANT COMPOSITE OPERATORS IN THE $SU(2)$ YANG-MILLS-HIGGS MODEL

In this chapter we will extend the techniques of chapter 3 and 4 to the more complex case of $SU(2)$ Higgs model with a single Higgs field in the fundamental representation. This model is equal to the electroweak model from chapter 1.1 with the coupling constant of the hypercharge interaction taken to zero, $g' \to 0$. As we have seen for the Abelian gauge theory, the direct use of non-gauge invariant fields displays several limitations in the spectral representation, and this will become more severe in the case of a non-Abelian gauge theory. For instance, in the case of the $U(1)$ Higgs model, the transverse component of the Abelian gauge field A_μ is gauge invariant, so that the two-point correlation function $\mathcal{P}_{\mu\nu}(p)\langle A_\mu(p)A_\nu(-p)\rangle$, where $\mathcal{P}_{\mu\nu}(p) = (\delta_{\mu\nu} - \frac{p_\mu p_\nu}{p^2})$ is the transverse projector, turns out to be independent from the gauge parameter ξ. However, this is no more true in the non-Abelian case, where both Higgs and gauge boson two-point functions, *i.e.* $\langle h(p)h(-p)\rangle$ and $\mathcal{P}_{\mu\nu}(p)\langle A^a_\mu(p)A^b_\nu(-p)\rangle$, where h stands for the Higgs field and A^a_μ for the gauge boson field, exhibit a strong gauge dependence from ξ. As a consequence, the understanding of the two-point correlation functions of both Higgs field h and gauge vector boson A^a_μ in terms of the Källén-Lehmann (KL) spectral representation is completely jeopardized by an unphysical dependence from the gauge parameter ξ, obscuring a direct interpretation of the above mentioned correlation functions in terms of the elementary excitations of the physical spectrum, namely the Higgs and the vector gauge boson particles.

We also note here that from a lattice perspective, it is expected that the spectrum of a gauge (Higgs) theory should be describable in terms of local gauge invariant operator correlation functions, with concrete physical information hiding in the various (positive and gauge invariant) spectral functions, not only pole masses, decay widths, but also transport coefficients at finite temperature etc. Clearly, such information will not correctly be encoded in gauge variant, non-positive spectral functions.

As we discussed in section 1.1.5, besides the exact BRST invariance, the quantized theory exhibits a global $SU(2)$ symmetry known as custodial symmetry. In this chapter we will show how the local composite BRST invariant operators corresponding to the gauge bosons transform as a triplet under the custodial symmetry, a property which will imply useful relations for their two-point correlation functions.

This chapter is organized as follows. In section 5.1, we give a review of the $SU(2)$ HYM model with a single Higgs field in the fundamental representation, of the gauge fixing procedure and its ensuing BRST invariance. In section 5.2 we calculate the two-point correlation functions of the elementary fields up to one-loop order. In section 5.3, we define the BRST invariant local composite operators $(O(x), R^a_\mu(x))$ corresponding to the BRST invariant extension of (h, A^a_μ) and calculate their one-loop correlation functions. In

section 5.4, we discuss the spectral properties of both elementary and composite operators. In order to give a more general idea of the behavior of the spectral functions, we shall be using two sets of parameters which we shall refer as to Region I and Region II. To some extent, Region I can be associated to the perturbative weak coupling regime, while in Region II we keep the gauge coupling a little bit larger, while decreasing the minimizing value v of the Higgs field. Section 5.5 is devoted to our conclusion. The technical details are all collected in the appendices.

5.1 The action and its symmetries

The YM action with a single Higgs field in the fundamental representation is given by

$$\begin{aligned} S_0 &= \int d^4x \left\{ \frac{1}{4} F^a_{\mu\nu} F^a_{\mu\nu} + (D^{ij}_\mu \Phi^{\dagger j})(D^{ik}_\mu \Phi^k) + \frac{\lambda}{2}(\Phi^{\dagger i}\Phi^i - \frac{1}{2}v^2)^2 \right\} \\ &= S_{\rm YM} + S_{\rm Higgs} \end{aligned} \tag{300}$$

with

$$F_{\mu\nu} = \partial_\mu A^a_\nu - \partial_\nu A^a_\mu + g\epsilon^{abc} A^b_\mu A^c_\nu \tag{301}$$

and

$$D^{ij}_\mu \Phi^j = \partial_\mu \Phi^i - \frac{i}{2} g (\tau^a)^{ij} A^a_\mu \Phi^j, \;\; (D^{ij}_\mu \Phi^j)^\dagger = \partial_\mu \Phi^{i\dagger} + \frac{i}{2} g \Phi^{j\dagger} (\tau^a)^{ji} A^a_\mu, \tag{302}$$

with the Pauli matrices $\tau^a (a = 1, 2, 3)$ and the Levi-Civita tensor ϵ^{abc} referring to the gauge symmetry group $SU(2)$. The scalar complex field $\Phi^i(x)$ is in the fundamental representation of $SU(2)$, *i.e.* $i, j = 1, 2$. Thus, Φ is an $SU(2)$-doublet of complex scalar fields that can be written as

$$\Phi = \frac{1}{\sqrt{2}} \begin{pmatrix} \phi^+ \\ \phi^0 \end{pmatrix} = \frac{1}{\sqrt{2}} \begin{pmatrix} \phi_1 + i\phi_2 \\ \phi_3 + i\phi_4 \end{pmatrix}. \tag{303}$$

The configuration which minimizes the Higgs potential in the expression (300) is

$$\langle \Phi \rangle = \tfrac{1}{\sqrt{2}} \begin{pmatrix} v \\ 0 \end{pmatrix} \tag{304}$$

and we write down $\Phi(x)$ as an expansion around the configuration (304), so that

$$\Phi = \frac{1}{\sqrt{2}} \begin{pmatrix} v + h + i\rho_3 \\ i\rho_1 - \rho_2 \end{pmatrix}, \tag{305}$$

where h is the Higgs field and ρ^a, $a = 1, 2, 3$, the would-be Goldstone bosons. We can use the matrix notation[12]:

$$\Phi = \frac{1}{\sqrt{2}}((v+h)\mathbf{1} + i\rho^a\tau^a)\cdot\begin{pmatrix}1\\0\end{pmatrix}, \tag{306}$$

so that the second term in eq. (300) becomes

$$\begin{aligned}(D^{ij}_\mu\Phi^j)^\dagger D^{ik}_\mu\Phi^k &= \frac{1}{2}(1,0)\cdot\Bigg[\partial_\mu h\cdot\mathbf{1} - i\partial_\mu\rho^a\tau^a + \frac{ig}{2}\tau^a A^a_\mu\Big((v+h)\mathbf{1}\\ &\quad -i\rho^b\tau^b\Big)\Bigg]\times\Bigg[\partial_\mu h\cdot\mathbf{1} + i\partial_\mu\rho^c\tau^c - \frac{ig}{2}((v+h)\mathbf{1}\\ &\quad -i\rho^d\tau^d\Big)\tau^c A^c_\mu\Bigg]\cdot\begin{pmatrix}1\\0\end{pmatrix}\\ &= \tilde{\mathcal{L}}_0 + \tilde{\mathcal{L}}_1 + \tilde{\mathcal{L}}_2,\end{aligned} \tag{307}$$

with $\tilde{\mathcal{L}}_i$ the ith term in powers of A_μ:

$$\begin{aligned}\tilde{\mathcal{L}}_0 &= \frac{1}{2}\left((\partial_\mu h)^2 + \partial_\mu\rho^a\partial_\mu\rho^a\right),\\ \tilde{\mathcal{L}}_1 &= -\frac{1}{2}\left\{gvA^a_\mu\partial_\mu\rho^a - gA^a_\mu\rho^a\partial_\mu h + gA^a_\mu(\partial_\mu\rho^a)h + g\epsilon^{abc}\partial_\mu\rho^a\rho^b A^c_\mu\right\},\\ \tilde{\mathcal{L}}_2 &= \frac{g^2}{8}A^a_\mu A^a_\mu\left[(v+h)^2 + \rho^b\rho^b\right],\end{aligned} \tag{308}$$

and we have the full action

$$\begin{aligned}S_0 &= \int d^4x\frac{1}{2}\Bigg\{\frac{1}{2}F^a_{\mu\nu}F^a_{\mu\nu} + \frac{1}{4}v^2g^2A^a_\mu A^a_\mu + (\partial_\mu h)^2 + \partial_\mu\rho^a\partial_\mu\rho^a - gvA^a_\mu\partial_\mu\rho^a + gA^a_\mu\rho^a\partial_\mu h\\ &- gA^a_\mu(\partial_\mu\rho^a)h - g\epsilon^{abc}\partial_\mu\rho^a\rho^b A^c_\mu + \frac{g^2}{4}A^a_\mu A^a_\mu\left[2vh + h^2 + \rho^b\rho^b\right] + \lambda v^2h^2 + \lambda vh(h^2 + \rho^a\rho^a)\\ &+ \frac{\lambda}{4}(h^2 + \rho^a\rho^a)^2\Bigg\}.\end{aligned} \tag{309}$$

One sees that both gauge field A^a_μ and Higgs field h have acquired a mass given, respectively, by

$$m^2 = \frac{1}{4}g^2v^2, \quad m_h^2 = \lambda v^2\ . \tag{310}$$

[12] This is of course possible thanks to the fact that Φ counts 3 Goldstone modes and that $SU(2)$ has three generators. This "numerology" is essentially what leads to a large custodial symmetry in the $SU(2)$ case.

5.1.1 Gauge fixing and BRST symmetry

The action (300) is invariant under the local ω-parametrized gauge transformations

$$\delta A^a_\mu = -D^{ab}_\mu \omega^b, \;\; \delta\Phi = -\frac{ig}{2}\omega^a\tau^a\Phi, \;\; \delta\Phi^\dagger = \frac{ig}{2}\omega^a\Phi^\dagger\tau^a, \tag{311}$$

which, when written in terms of the fields (h, ρ^a), become

$$\delta h = \frac{g}{2}\omega^a\rho^a, \;\; \delta\rho^a = -\frac{g}{2}(\omega^a(v+h)\mathbf{1} - \epsilon^{abc}\omega^b\rho^c). \tag{312}$$

As done in the $U(1)$ case, we shall be using the R_ξ-gauge. We add thus need the gauge fixing term

$$\begin{aligned}
\mathcal{S}_{\rm gf} &= s\int d^4x\Big\{-i\frac{\xi}{2}\bar{c}^a b^a + \bar{c}^a(\partial_\mu A^a_\mu - \xi m\rho^a)\Big\} \\
&= \frac{1}{2}\int d^4x\Big\{\xi b^a b^a + 2ib^a\partial_\mu A^a_\mu + 2\bar{c}^a\partial_\mu D^{ab}_\mu c^b - 2i\xi m b^a\rho^a \\
&- 2\xi\bar{c}^a m c^a - g\xi\bar{c}^a m h c^a - \xi g\epsilon^{abc}\bar{c}^a c^b\rho^c\Big\}\,,
\end{aligned} \tag{313}$$

so that the gauge fixed action $S_{\rm full} = S_0 + \mathcal{S}_{\rm gf}$, namely

$$\begin{aligned}
S_{\rm full} &= \int d^4x\frac{1}{2}\Bigg\{\frac{1}{2}F^a_{\mu\nu}F^a_{\mu\nu} + \frac{1}{4}v^2g^2A^a_\mu A^a_\mu \\
&+ (\partial_\mu h)^2 + \partial_\mu\rho^a\partial_\mu\rho^a - gvA^a_\mu\partial_\mu\rho^a + gA^a_\mu\rho^a\partial_\mu h - gA^a_\mu(\partial_\mu\rho^a)h \\
&- g\epsilon^{abc}\partial_\mu\rho^a\rho^b A^c_\mu + \frac{g^2}{4}A^a_\mu A^a_\mu\left[2vh + h^2 + \rho^b\rho^b\right] + \lambda v^2h^2 \\
&+ \lambda vh(h^2 + \rho^a\rho^a) + \frac{\lambda}{4}(h^2 + \rho^a\rho^a)^2 + \xi b^a b^a + 2ib^a\partial_\mu A^a_\mu + 2\bar{c}^a\partial_\mu D^{ab}_\mu c^b - 2i\xi m b^a\rho^a \\
&- 2\xi\bar{c}^a m c^a - g\xi\bar{c}^a m h c^a - \xi g\epsilon^{abc}\bar{c}^a c^b\rho^c\Bigg\}
\end{aligned} \tag{314}$$

turns out to be left invariant by the BRST transformations

$$\begin{aligned}
sA^a_\mu &= -D^{ab}_\mu c^b, \;\; sh = \frac{g}{2}c^a\rho^a, \;\; s\rho^a = -\frac{g}{2}(c^a(v+h)\mathbf{1} - \epsilon^{abc}c^b\rho^c) \\
sc^a &= \frac{1}{2}g\epsilon^{abc}c^b c^c, \;\; s\bar{c}^a = ib^a, \;\; sb^a = 0\,,
\end{aligned} \tag{315}$$

$$sS_{\rm full} = 0\,. \tag{316}$$

5.1.2 Custodial symmetry

As already mentioned, apart from the BRST symmetry, there is an extra global symmetry, which we shall refer to as the custodial symmetry:

$$\begin{aligned}
\delta A^a_\mu &= \epsilon^{abc}\beta^b A^c_\mu, \\
\delta\rho^a &= \epsilon^{abc}\beta^b \rho^c, \\
\delta\overline{c}^a &= \epsilon^{abc}\beta^b \overline{c}^c, \\
\delta c^a &= \epsilon^{abc}\beta^b c^c, \\
\delta b^a &= \epsilon^{abc}\beta^b b^c, \\
\delta h &= 0\ ,
\end{aligned} \tag{317}$$

where β^a is a constant parameter, $\partial_\mu\beta^a = 0$,

$$\delta S_{\rm full} = 0\ . \tag{318}$$

One notices that all fields carrying the index $a = 1, 2, 3$, *i.e.* $(A^a_\mu, b^a, c^a, \bar{c}^a, \rho^a)$, undergo a global transformation in the adjoint representation of $SU(2)$. The origin of this symmetry is an $SU(2)_{\rm gauge} \times SU(2)_{\rm global}$ symmetry of the action in the unbroken phase, see section 1.1.5. The exception is the Higgs field h, which is left invariant, *i.e.* it is a singlet. As we shall see in the following, this additional global symmetry will provide useful relationships for the two-point correlation functions of the BRST invariant composite operators.

5.2 One-loop evaluation of the correlation function of the elementary fields

For the elementary fields $h(x)$ and A^a_μ, the correlation functions are calculated in Appendices I.0.1 and I.0.2. For the Higgs field, for the one-loop propagator we get

$$\langle h(p)h(-p)\rangle = \frac{1}{p^2+m_h^2} + \frac{1}{(p^2+m_h^2)^2}\Pi_{hh}(p^2) + \mathcal{O}(\hbar^2) \tag{319}$$

where

$$\begin{aligned}\Pi_{hh}(p^2) &= \frac{3g^2}{8(4\pi)^2}\int_0^1 dx\left\{2\xi\left(m_h^2+p^2\right)\ln\left(\frac{m^2\xi}{\mu^2}\right)-2\xi m_h^2+2\left(6m^2-p^2\right)\ln\left(\frac{m^2}{\mu^2}\right)\right.\\ &- (12m^2+\frac{p^4}{m^2}+4p^2)\ln\left(\frac{m^2+p^2(1-x)x}{\mu^2}\right)\\ &+ \left(\frac{p^4}{m^2}-\frac{m_h^4}{m^2}\right)\ln\left(\frac{m^2\xi+p^2(1-x)x}{\mu^2}\right)\\ &- 12m^2-2\xi p^2+2p^2\\ &- \left.\frac{m_h^4}{m^2}\left(-2\ln\left(\frac{m_h^2}{\mu^2}\right)+3\ln\left(\frac{m_h^2+p^2(1-x)x}{\mu^2}\right)+2\right)\right\}. \end{aligned} \tag{320}$$

Before trying to resum the self-energy $\Pi_{hh}(p^2)$, we notice that this resummation is tacitly assuming that the second term in (319) is much smaller than the first term. However, we see that eq. (319) contains terms of the order of $\frac{p^4}{(p^2+m_h^2)^2}\ln\left(\frac{m^2+p^2(1-x)x}{\mu^2}\right)$ which cannot be resummed for big values of p^2. We therefore proceed as in eq. (201)-(203) and use the identity

$$p^4=(p^2+m_h^2)^2-m_h^4-2p^2m_h^2 \tag{321}$$

to rewrite

$$\begin{aligned}\frac{p^4}{(p^2+m_h^2)^2}\ln\frac{p^2x(1-x)+m^2}{\mu^2} &= \ln\frac{p^2x(1-x)+m^2}{\mu^2}\\ &- \underline{\frac{(m_h^4+2p^2m_h^2)}{(p^2+m_h^2)^2}\ln\frac{p^2x(1-x)+m^2}{\mu^2}}. \end{aligned} \tag{322}$$

The term which has been underlined in eq. (322) can be safely resummed, as it decays fast enough for large values of p^2. We thence rewrite

$$\frac{\Pi_{hh}(p^2)}{(p^2+m_h^2)^2} = \frac{\hat{\Pi}_{hh}(p^2)}{(p^2+m_h^2)^2}+C_{hh}(p^2)\ , \tag{323}$$

with

$$\begin{aligned}\hat{\Pi}_{hh}(p^2) &= \frac{3g^2}{8(4\pi)^2}\int_0^1 dx\left\{2\xi\left(m_h^2+p^2\right)\ln\left(\frac{m^2\xi}{\mu^2}\right)-2\xi m_h^2+2\left(6m^2-p^2\right)\ln\left(\frac{m^2}{\mu^2}\right)\right.\\ &- (12m^2-\frac{(m_h^4+2p^2m_h^2)}{m^2}+4p^2)\ln\left(\frac{m^2+p^2(1-x)x}{\mu^2}\right)\\ &- \frac{(2m_h^4+2p^2m_h^2)}{m^2}\ln\left(\frac{m^2\xi+p^2(1-x)x}{\mu^2}\right)\\ &- 12m^2-2\xi p^2+2p^2-\frac{m_h^4}{m^2}\Big(-2\ln\left(\frac{m_h^2}{\mu^2}\right)\\ &+ \left.3\ln\left(\frac{m_h^2+p^2(1-x)x}{\mu^2}\right)+2\Big)\right\} \end{aligned} \tag{324}$$

and

$$C_{hh}(p^2) = -\frac{3g^2}{8m^2(4\pi)^2}\int_0^1 dx\left(\ln\frac{p^2x(1-x)+m^2}{\mu^2}-\ln\frac{p^2x(1-x)+\xi m^2}{\mu^2}\right)\ . \tag{325}$$

Thus, for the one-loop Higgs propagator, we get

$$\langle h(p)h(-p)\rangle = \frac{1}{p^2+m_h^2-\hat{\Pi}_{hh}(p^2)}+C_{hh}(p^2)+\mathcal{O}(\hbar^2)\ . \tag{326}$$

For the gauge field, we split the two-point function into transverse and longitudinal parts in the usual way

$$\langle A_\mu^a(p)A_\nu^b(-p)\rangle = \langle A_\mu^a(p)A_\nu^b(-p)\rangle^T\mathcal{P}_{\mu\nu}(p)+\langle A_\mu^a(p)A_\nu^b(-p)\rangle^L\mathcal{L}_{\mu\nu}(p), \tag{327}$$

where we have introduced the transverse and longitudinal projectors, given respectively by

$$\mathcal{P}_{\mu\nu}(p) = \delta_{\mu\nu}-\frac{p_\mu p_\nu}{p^2}\,,\qquad \mathcal{L}_{\mu\nu}(p) = \frac{p_\mu p_\nu}{p^2}\,. \tag{328}$$

We find

$$\langle A_\mu^a(p)A_\nu^b(-p)\rangle^T = \frac{\delta^{ab}}{p^2+m^2}+\frac{\delta^{ab}}{(p^2+m^2)^2}\Pi_{AA^T}(p^2)+\mathcal{O}(\hbar^2), \tag{329}$$

$$
\begin{aligned}
\Pi_{AA^T}(p^2) &= -\frac{\delta^{ab}g^2}{36(4\pi)^2 m^4 p^2 m_h^2}\int_0^1 dx\Bigg\{ -27m^4p^2m_h^4\ln\left(\frac{m_h^2}{\mu^2}\right)\\
&- 27m^6\xi p^2 m_h^2\ln\left(\frac{m^2\xi}{\mu^2}\right)\\
&+ 3m^4m_h^4\left(m_h^2-m^2+2p^2\right)\ln\left(\frac{m_h^2}{\mu^2}\right)+27m^4p^2m_h^2\left(m_h^2+m^2\xi\right)\\
&- 3m^4\xi m_h^2\left(2m^4(\xi-1)+m^2(4\xi+7)p^2+2(\xi+9)p^4\right)\ln\left(\frac{m^2\xi}{\mu^2}\right)\\
&+ 3m^4\ln\left(\frac{m^2}{\mu^2}\right)(-m^2m_h^4+m_h^2(m^4(2\xi-1)+m^2(4\xi+45)p^2\\
&+ 2(\xi+9)p^4)-54m^4p^2)\\
&+ m^4\Big(6m^2m_h^4\\
&+ m_h^2\left(3m^4(2(\xi-2)\xi+1)+3m^2(\xi-1)(4\xi-1)p^2+2(3\xi(\xi+4)-17)p^4\right)\\
&- 3m_h^6+54m^4p^2\Big)\\
&- 3m_h^2\Big[m^4(2p^2\left(m_h^2-5m^2\right)\\
&+ \left(m_h^2-m^2\right)^2+p^4)\ln\left(\frac{p^2(1-x)x+m_h^2(1-x)+m^2x}{\mu^2}\right)\\
&- 2\left(m^2+p^2\right)^2(m^4(\xi-1)^2\\
&+ 2m^2(\xi-5)p^2+p^4)\ln\left(\frac{p^2(1-x)x+\xi m^2(1-x)+m^2x}{\mu^2}\right)\\
&+ p^2\left(p^4-m^4\right)\left(4m^2\xi+p^2\right)\ln\left(\frac{p^2(1-x)x+\xi m^2}{\mu^2}\right)\\
&+ p^2\left(4m^2+p^2\right)\left(12m^4-20m^2p^2+p^4\right)\ln\left(\frac{p^2(1-x)x+m^2}{\mu^2}\right)\Big]\Bigg\}. \qquad (330)
\end{aligned}
$$

We see that (329) contains again terms of the order $\frac{p^4}{(p^2+m^2)^2}\ln\left(\frac{m^2+p^2(1-x)x}{\mu^2}\right)$ and $\frac{p^6}{(p^2+m^2)^2}\ln\left(\frac{m^2+p^2(1-x)x}{\mu^2}\right)$, which cannot be resummed for big values of p^2. We use

$$
\begin{aligned}
\frac{p^4}{(p^2+m^2)^2}\ln\frac{p^2x(1-x)+m^2}{\mu^2} &= \ln\frac{p^2x(1-x)+m^2}{\mu^2}\\
&- \underline{\frac{(m^4+2p^2m^2)}{(p^2+m^2)^2}\ln\frac{p^2x(1-x)+m^2}{\mu^2}} \qquad (331)
\end{aligned}
$$

and

$$
\begin{aligned}
\frac{p^6}{(p^2+m^2)^2}\ln\frac{p^2x(1-x)+m^2}{\mu^2} &= (p^2-2m^2)\ln\frac{p^2x(1-x)+m^2}{\mu^2}\\
&+ \underline{\frac{2m^6+3p^2m^4}{(p^2+m^2)^2}\ln\frac{p^2x(1-x)+m^2}{\mu^2}}. \qquad (332)
\end{aligned}
$$

The underlined terms in (331) and (332) can be safely resummed. We rewrite

$$\frac{\Pi_{AA^T}(p^2)}{(p^2+m^2)^2} = \frac{\hat{\Pi}_{AA^T}(p^2)}{(p^2+m_h^2)^2} + C_{AA^T}(p^2), \tag{333}$$

with

$$\begin{aligned}
&\hat{\Pi}_{AA^T}(p^2) = \\
&- \frac{\delta^{ab}g^2}{36(4\pi)^2 m^4 p^2 m_h^2}\int_0^1 dx\Bigg\{ -27m^4p^2m_h^4\ln\left(\frac{m_h^2}{\mu^2}\right) - 27m^6\xi p^2 m_h^2\ln\left(\frac{m^2\xi}{\mu^2}\right) \\
&+ 3m^4m_h^4\left(m_h^2-m^2+2p^2\right)\ln\left(\frac{m_h^2}{\mu^2}\right) + 27m^4p^2m_h^2\left(m_h^2+m^2\xi\right) \\
&- 3m^4\xi m_h^2\left(2m^4(\xi-1)+m^2(4\xi+7)p^2+2(\xi+9)p^4\right)\ln\left(\frac{m^2\xi}{\mu^2}\right) \\
&+ 3m^4\left(-m^2m_h^4+m_h^2\left(m^4(2\xi-1)+m^2(4\xi+45)p^2+2(\xi+9)p^4\right)-54m^4p^2\right)\ln\left(\frac{m^2}{\mu^2}\right) \\
&+ m^4(6m^2m_h^4+m_h^2(3m^4(2(\xi-2)\xi+1)+3m^2(\xi-1)(4\xi-1)p^2 \\
&+ 2(3\xi(\xi+4)-17)p^4)-3m_h^6+54m^4p^2) \\
&- 3m_h^2\Big[m^4\left(2p^2\left(m_h^2-5m^2\right)+\left(m_h^2-m^2\right)^2+p^4\right)\ln\left(\frac{p^2(1-x)x+(1-x)m_h^2+m^2x}{\mu^2}\right) \\
&- 2m^4(\xi-1)^2\left(m^2+p^2\right)^2\ln\left(\frac{p^2(1-x)x+\xi m^2(1-x)+m^2x}{\mu^2}\right) \\
&+ \left(-2m^4(4\xi-1)p^2\left(m^2+p^2\right)\right)\ln\left(\frac{p^2(1-x)x+\xi m^2}{\mu^2}\right) \\
&+ (66m^6p^2-33m^4p^4)\ln\left(\frac{p^2(1-x)x+m^2}{\mu^2}\right)\Big]\Bigg\}.
\end{aligned} \tag{334}$$

and

$$\begin{aligned}
C_{AA^T}(p^2) &= \frac{\delta^{ab}g^2}{12(4\pi)^2m^4}\int_0^1 dx\Bigg\{(-4m^2(\xi-5)-2p^2) \\
&\times \ln\left(\frac{p^2(1-x)x+\xi m^2(1-x)+m^2x}{\mu^2}\right) \\
&+ \left(4\,\xi m^2+p^2-2m^2\right)\ln\left(\frac{p^2(1-x)x+\xi m^2}{\mu^2}\right) \\
&+ (-18m^2+p^2)\ln\left(\frac{p^2(1-x)x+m^2}{\mu^2}\right)\Bigg\}.
\end{aligned} \tag{335}$$

Finally

$$\langle A_\mu^a(p)A_\nu^b(-p)\rangle^T = \delta^{ab}\left(\frac{1}{p^2+m^2-\hat{\Pi}_{AA^T}(p^2)}+C_{AA^T}(p^2)\right)+\mathcal{O}(\hbar^2)\,. \tag{336}$$

5.3 One-loop evaluation of the correlation function of the local BRST invariant composite operators

5.3.1 Correlation function of the scalar BRST invariant composite operator $O(x)$

The BRST invariant local scalar composite operator $O(x)$ is given by

$$O(x) = \Phi^\dagger\Phi - \frac{v^2}{2}\,, \qquad s\,O(x) = 0\,, \tag{337}$$

which, after using the expansion (306), becomes

$$\begin{aligned} O(x) &= \frac{1}{2}\Big[\begin{pmatrix}1 & 0\end{pmatrix}((v+h)\mathbf{1} - i\rho^a\tau^a))((v+h)\mathbf{1} + i\rho^b\tau^b))\begin{pmatrix}1\\0\end{pmatrix}\Big] - \frac{v^2}{2} \\ &= \frac{1}{2}\Big(h^2(x) + 2vh(x) + \rho^a(x)\rho^a(x)\Big)\,, \end{aligned} \tag{338}$$

so that

$$\begin{aligned} \langle O(x)O(y)\rangle &= v^2\,\langle h(x)h(y)\rangle + v\,\langle h(x)\rho^b(y)\rho^b(y)\rangle + v\,\langle h(x)h(y)^2\rangle + \frac{1}{4}\,\langle h(x)^2\rho^b(y)\rho^b(y)\rangle \\ &+ \frac{1}{4}\,\langle h(x)^2h(y)^2\rangle + \frac{1}{4}\,\langle \rho^a(x)\rho^a(x)\rho^b(y)\rho^b(y)\rangle\,. \end{aligned} \tag{339}$$

Looking at the tree level expression of eq. (339), one easily obtains

$$\langle O(p)O(-p)\rangle_{\rm tree} = v^2\,\langle h(p)h(-p)\rangle_{\rm tree} = v^2\frac{1}{p^2+m_h^2}\,, \tag{340}$$

showing that the BRST invariant scalar operator $O(x)$ is directly linked to the Higgs propagator.

Concerning now the one-loop calculation of expression (339), after evaluating each term, see Appendix J for details, we find that the two-point correlation function of the scalar composite operator $O(x)$ develops a geometric series in the same way as the elementary field $h(x)$. This allows us the make a resummed approximation. Using dimensional regularization in the $\overline{MS}bar$-scheme, we find

$$\langle O(p)O(-p)\rangle\,(p^2) = \frac{v^2}{p^2+m_h^2} + \frac{v^2}{(p^2+m_h^2)^2}\Pi_{OO}(p^2) + \mathcal{O}(\hbar^2), \tag{341}$$

$$\begin{aligned} \Pi_{OO}(p^2) &= \frac{1}{32v^2\pi^2m_h^2}\int_0^1 dx\Big\{ -24m_h^2m^4 - 6m^2p^2\left(m_h^2+6m^2\right)\ln\left(\frac{m^2}{\mu^2}\right) \\ &- m_h^2\left(p^2-2m_h^2\right)^2\ln\left(\frac{m_h^2+p^2x(1-x)}{\mu^2}\right) \\ &- 3m_h^2\left(12m^4+4m^2p^2+p^4\right)\ln\left(\frac{m^2+p^2x(1-x)}{\mu^2}\right) \end{aligned}$$

$$+ \quad 6p^2\left(m_h^4+m_h^2m^2+2m^4\right)-6m_h^4p^2\ln\left(\frac{m_h^2}{\mu^2}\right)\Bigg\}. \tag{342}$$

Since (341) contains terms of the order of $\frac{p^4}{(p^2+m^2)^2}\ln(p^2)$, we follow the steps (201)-(203) to find the resummed correlation function in the one-loop approximation

$$G_{OO}(p^2) = \frac{v^2}{p^2+m_h^2-\hat{\Pi}_{OO}(p^2)}+C_{OO}(p^2) \tag{343}$$

with

$$\begin{aligned}\hat{\Pi}_{OO}(p^2) &= \frac{1}{32v^2\pi^2m_h^2}\int_0^1 dx\Bigg\{-24m_h^2m^4-6m^2p^2\left(m_h^2+6m^2\right)\ln\left(\frac{m^2}{\mu^2}\right)\\ &- m_h^2(3m_h^4-6m_h^2p^2)\ln\left(\frac{m_h^2+p^2x(1-x)}{\mu^2}\right)\\ &- 3m_h^2\left(12m^4+4m^2p^2-m_h^4-2p^2m_h^2\right)\ln\left(\frac{m^2+p^2x(1-x)}{\mu^2}\right)\\ &+ 6p^2\left(m_h^4+m_h^2m^2+2m^4\right)-6m_h^4p^2\ln\left(\frac{m_h^2}{\mu^2}\right)\Bigg\}\end{aligned} \tag{344}$$

and

$$C_{OO}(p^2) = -\frac{1}{32\pi^2}\int_0^1 dx\Bigg\{\ln\left(\frac{m_h^2+p^2x(1-x)}{\mu^2}\right)+3\ln\left(\frac{m^2+p^2x(1-x)}{\mu^2}\right)\Bigg\}. \tag{345}$$

Expressions (343) and (345) show that, as expected, and unlike the Higgs propagator, eq. (326), the correlator $\langle O(p)O(-p)\rangle$ is independent from the gauge parameter ξ.

5.3.2 A little digression on the unitary gauge

Of course, since the composite operator $O(x)$ is BRST invariant, any choice for the gauge parameter ξ should give the same expression for the correlation function $G_{OO}(p^2)$. One convenient choice is the so-called unitary gauge, which is formally attained by taking $\xi\to\infty$ at the end of the calculation. Though, we take here a different route and perform the same calculation done before for $G_{OO}(p^2)$ by employing the tree level propagators and other Feynman rules which follow by taking the limit $\xi\to\infty$ at the beginning. In doing this, for the tree level propagators one finds

$$\begin{aligned}\langle A_\mu^a(p)A_\nu^b(-p)\rangle &= \frac{\delta^{ab}}{p^2+m^2}\mathcal{P}_{\mu\nu}(p)+\delta^{ab}\frac{1}{m^2}\mathcal{L}_{\mu\nu}(p)=\frac{\delta^{ab}}{p^2+m^2}\Big(\delta_{\mu\nu}+\frac{p_\mu p_\nu}{m^2}\Big),\\ \langle h(p)h(-p)\rangle &= \frac{1}{p^2+m_h^2}\end{aligned} \tag{346}$$

with all other propagators, *i.e.* the Goldstone and Faddeev-Popov ghost propagators, vanishing. Then, eq. (339) simplifies to

$$\begin{aligned}\langle O(x)O(y)\rangle_{\text{unitary}} &= v^2\,\langle h(x)h(y)\rangle_{\text{unitary}} + v\,\langle h(x)h(y)^2\rangle_{\text{unitary}} \\ &+ \frac{1}{4}\,\langle h(x)^2h(y)^2\rangle_{\text{unitary}}\,, \end{aligned} \tag{347}$$

with the contributing diagrams shown in Figure 30. Making use of the dimensional regularization in the $\overline{MS}bar$-scheme and switching to momentum space, we get

$$\begin{aligned} v^2\,\langle h(p)h(-p)\rangle_{\text{unitary}} &= \frac{3}{32\pi^2}\int_0^1 dx\Bigg\{\frac{1}{\epsilon}\left(2m_h^4+12m^2p^2+2p^4\right)+2m_h^4\ln\left(\frac{m_h^2}{\mu^2}\right) \\ &+ 2\left(6m^4-m^2p^2\right)\ln\left(\frac{m^2}{\mu^2}\right)-3m_h^4\ln\left(\frac{p^2(1-x)x+m_h^2}{\mu^2}\right) \\ &- \left(12m^4+4m^2p^2+p^4\right)\ln\left(\frac{p^2(1-x)x+m^2}{\mu^2}\right) \\ &- 2m_h^4+2m^2\left(p^2-6m^2\right)\Bigg\}\frac{1}{(m_h^2+p^2)^{\,2}}, \end{aligned} \tag{348}$$

$$\begin{aligned} v\,\langle h(p)h(-p)^2\rangle_{\text{unitary}} &= \frac{3}{16\pi^2m_h^2}\int_0^1 dx\Bigg\{\frac{12}{\epsilon}m^4-6m^4\ln\left(\frac{m^2}{\mu^2}\right)-m_h^4\ln\left(\frac{m_h^2}{\mu^2}\right) \\ &+ m_h^4\ln\left(\frac{m_h^2+p^2(1-x)x}{\mu^2}\right)+m_h^4+2m^4\Bigg\}\frac{1}{(m_h^2+p^2)}, \end{aligned} \tag{349}$$

$$\frac{1}{4}\,\langle h(p)^2h(p)^2\rangle_{\text{unitary}} = \frac{1}{16\pi^2}\int_0^1 dx\Bigg\{\frac{1}{\epsilon}-\frac{1}{2}\ln\left(\frac{m_h^2+p^2(1-x)x}{\mu^2}\right)\Bigg\}. \tag{350}$$

Inserting now the unity

$$1=(p^2+m_h^2)/(p^2+m_h^2)=((p^2+m_h^2)/(p^2+m_h^2))^2, \tag{351}$$

we find indeed that $\langle O(x)O(y)\rangle_{\text{unitary}}=\langle O(x)O(y)\rangle$, showing that the same expression has been re-obtained by starting directly from the tree level propagators of the unitary gauge, $\xi\to\infty$, despite the fact that this gauge is known to be non-renormalizable. Though, at one-loop order, a simple explanation can be found for the previous result, which is due in part to the BRST invariant nature of the correlation function $\langle O(x)O(y)\rangle$ and to the fact that, at one-loop order, the handling of the overlapping divergences is not required. From two-loop onward these divergences will show up, requiring a fully renormalizable setup. More specifically, in this case, one would need to keep ξ finite and use all Feynman rules of the R_ξ-gauge, while taking $\xi\to\infty$ only at the end. Nevertheless, having checked that the one-loop result for $G_{OO}(p^2)$ is the same by using both procedures, in the next section, we will use the same simplifying second trick to evaluate the two-point function of the vectorial composite operator at one-loop order.

Figure 30 - Propagator in unitary gauge

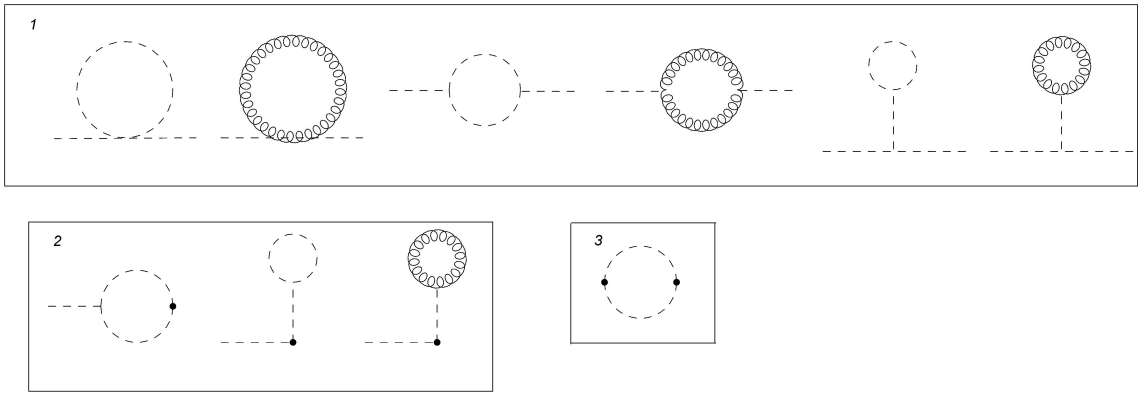

Legend: One-loop contributions for the propagator $\langle O(x)O(y)\rangle$ in the unitary gauge: $\langle h(x)h(y)\rangle$ (first line),$\langle h(x)h(y)^2\rangle$ (second line) and $\langle h(x)^2h(y)^2\rangle$ (third line) . Wavy lines represent the gauge field, dashed lines the Higgs field, solid lines the Goldstone boson and double lines the ghost field. The $\bullet$ indicates the insertion of a composite operator.

Source: The author, 2020.

5.3.3 Vectorial composite operators

We identify three gauge invariant vector composite operators, following the definitions of 't Hooft in (HOOFT et al., 1980), namely

$$\begin{aligned} O^3_\mu &= i\phi^\dagger D_\mu \phi, \\ O^+_\mu &= \phi^T \begin{pmatrix} 0 & 1 \\ -1 & 0 \end{pmatrix} D_\mu \phi, \\ O^-_\mu &= (O^+_\mu)^\dagger. \end{aligned} \tag{352}$$

The gauge invariance of O^3_μ is apparent. For O^+_μ, we can show the gauge invariance by using the following 2×2 matrix representation of a generic $SU(2)$ transformation,

$$U = \begin{pmatrix} a & -b^\star \\ b & a^\star \end{pmatrix} \tag{353}$$

with determinant $|a|^2 + |b|^2 = 1$. Thus, we find that under a $SU(2)$ transformation

$$\begin{aligned} O^+_\mu &\to (U\phi)^T \begin{pmatrix} 0 & 1 \\ -1 & 0 \end{pmatrix} D_\mu (U\phi) \\ &= \phi^T U^T \begin{pmatrix} 0 & 1 \\ -1 & 0 \end{pmatrix} U D_\mu \phi \end{aligned}$$

$$= \phi^T \begin{pmatrix} 0 & 1 \\ -1 & 0 \end{pmatrix} D_\mu \phi = O^+_\mu, \tag{354}$$

which shows the gauge invariance of O^+_μ and, subsequently, of O^-_μ. After using the expansion (306), the first composite operator reads

$$\begin{aligned}
& O^3_\mu \\
= \; & i\phi^\dagger D_\mu \phi \\
= \; & i\phi^\dagger \partial_\mu \phi + \frac{1}{2} g \phi^\dagger \tau^a A^a_\mu \phi \\
= \; & \frac{i}{2}\Big[(v+h)\partial_\mu h + i(v+h)\partial_\mu \rho^3 - i\rho^3 \partial_\mu h + \rho^a \partial_\mu \rho^a + i\rho^1 \partial_\mu \rho^2 - i\rho^2 \partial_\mu \rho^1 \\
- \; & \frac{i}{2} g (v+h)^2 A^3_\mu + ig(v+h)(A^1_\mu \rho^2 - A^2_\mu \rho^1) + \frac{i}{2} g \rho^a A^3_\mu \rho^a - ig\rho^3 A^b_\mu \rho^b \Big] \\
= \; & \frac{1}{2}\Big[- (v+h)\partial_\mu \rho^3 + \rho^3 \partial_\mu h - \rho^1 \partial_\mu \rho^2 + \rho^2 \partial_\mu \rho^1 + \frac{1}{2} g (v+h)^2 A^3_\mu \\
- \; & g(v+h)(A^1_\mu \rho^2 - A^2_\mu \rho^1) \\
- \; & \frac{1}{2} g \rho^a A^3_\mu \rho^a + g\rho^3 A^b_\mu \rho^b \Big] + \frac{i}{2} \partial_\mu O,
\end{aligned} \tag{355}$$

and since the last term, *i.e.* $\frac{i}{2}\partial_\mu O$, is BRST invariant, the sum of the others terms has to be BRST invariant too. Therefore, we can introduce the following three "reduced" vector composite operators R^a_μ with $a = 1, 2, 3$:

$$\begin{aligned}
R^1_\mu &= \frac{i}{2}\Big(O^+_\mu - O^-_\mu \Big), \\
R^2_\mu &= \frac{1}{2}\Big(O^+_\mu + O^-_\mu \Big), \\
R^3_\mu &= O^3_\mu - \frac{i}{2}\partial_\mu O_\mu,
\end{aligned} \tag{356}$$

so that

$$\begin{aligned}
R^a_\mu = \; & \frac{1}{2}\Big[- (v+h)\partial_\mu \rho^a + \rho^a \partial_\mu h - \varepsilon^{abc} \rho^b \partial_\mu \rho^c + \frac{1}{2} g (v+h)^2 A^a_\mu - g(v+h)\varepsilon^{abc}(\rho^b A^c_\mu) \\
- \; & \frac{1}{2} g A^a_\mu \rho^m \rho^m + g \rho^a A^m_\mu \rho^m \Big],
\end{aligned} \tag{357}$$

with

$$sR^a_\mu(x) = 0 \; . \tag{358}$$

Remarkably, the BRST invariant operators R^a_μ transform like a triplet under the custodial symmetry (317), namely

$$\delta R^a_\mu = \varepsilon^{abc}\beta^b R^c_\mu \,, \tag{359}$$

and since the only rank two invariant tensor is δ^{ab}, we can write, moving to momentum space,

$$\langle R^a_\mu(p)\, R^b_\nu(-p)\rangle = \delta^{ab} R_{\mu\nu}(p^2) \;\to\; R_{\mu\nu}(p^2) = \frac{1}{3}\,\langle R^a_\mu(p)\, R^a_\nu(-p)\rangle\,, \tag{360}$$

as well as

$$R_{\mu\nu}(p^2) = R(p^2)\mathcal{P}_{\mu\nu}(p) + L(p^2)\mathcal{L}_{\mu\nu}(p), \tag{361}$$

so that in d dimensions,

$$R(p^2) = \frac{1}{3}\frac{\mathcal{P}_{\mu\nu}(p)}{(d-1)}\,\langle R^a_\mu(p)\, R^a_\nu(-p)\rangle\,, \tag{362}$$

and

$$L(p^2) = \frac{1}{3}\mathcal{L}_{\mu\nu}(p)\,\langle R^a_\mu(p)\, R^a_\nu(-p)\rangle\,. \tag{363}$$

One recognizes that eqs.(360)-(363) display exactly the same structure of the gauge vector boson correlation function $\langle A^a_\mu(p) A_\nu(-p)\rangle$.

In the R_ξ-gauge, the non-vanishing contributions, up to first order in $\hbar$, to the correlation function $\langle R^a_\mu(p)\, R^b_\nu(-p)\rangle$ are

$$\begin{aligned}
\langle R^a_\mu(p)\, R^a_\nu(-p)\rangle \;&=\; \frac{1}{16}g^2v^4\langle A^a_\mu(p)\, A^a_\nu(-p)\rangle - \langle(\rho^a\partial_\mu h)(p)\,(\partial_\nu\rho^a h)(-p)\rangle \\
&+\; \frac{1}{4}p_\mu p_\nu\langle(\rho^a h)(p)\,(\rho^a h)(-p)\rangle \\
&+\; \frac{1}{8}\partial_\mu\partial_\nu\langle(\rho^a\rho^b)(p)\,(\rho^a\rho^b)(-p)\rangle - \frac{1}{2}\langle(\rho^a\partial_\mu\rho^b)(p)\,(\partial_\nu\rho^a\rho^b)(-p)\rangle \\
&+\; \frac{1}{4}g^2v^3\langle A^a_\mu(p)\,(A^a_\nu h)(-p)\rangle - \frac{i}{4}gv^3p_\nu\langle A^a_\mu(p)\,\rho^a(-p)\rangle \\
&+\; \frac{1}{4}v^2p_\mu p_\nu\langle\rho^a(x)\rho^a(y)\rangle + \frac{1}{6}g^2v^2\langle(\rho^a A^b_\mu)(p)\,(\rho^a A^b_\nu)(-p)\rangle \\
&-\; \frac{1}{24}g^2v^2\langle(\rho^a\rho^a A^b_\mu)(p)\, A^b(-p)\rangle + \frac{1}{8}g^2v^2\langle(h^2A^a_\mu)(p)\, A^a_\nu(-p)\rangle \\
&+\; \frac{1}{4}g^2v^2\langle(hA^a_\mu)(p)\,(hA^a_\nu)(-p)\rangle + \frac{i}{4}v^2gp_\mu\langle(h\rho^a)(p)\, A^a_\nu(-p)\rangle \\
&+\; \frac{1}{2}gv^2\langle(\partial_\mu h\rho^a)(p)\, A^a_\nu(-p)\rangle + \frac{i}{2}gv^2p_\mu\langle\rho^a(p)\,(hA^a_\nu)(-p)\rangle \\
&-\; \frac{1}{4}gv^2\varepsilon^{abc}\langle A^a(p)\,(\rho^b\partial_\mu\rho^c)(-p)\rangle - \frac{igv^2}{2}\varepsilon^{abc}p_\mu\langle\rho^a(p)\,(\rho^b A^c_\nu)(-p)\rangle
\end{aligned}$$

$$+ \quad \frac{1}{2} v p_\mu p_\nu \langle (h\rho^a)(p)\, \rho^a(-p)\rangle - ivp_\nu \langle (\partial_\mu h\rho^a)(p)\, \rho^a(-p)\rangle \tag{364}$$

where we have used the notation $\partial_\mu = \frac{\partial}{\partial x^\mu}$ and $\partial_\nu = \frac{\partial}{\partial y^\nu}$ [13]. The first term in expression (364) is the gauge field propagator $\langle A^a_\mu(p) A^a_\mu(-p)\rangle$, which means that R^a_μ can be thought as a kind of BRST invariant extension of the elementary gauge field A^a_μ. At tree-level, we find in fact

$$\begin{aligned} \langle R^a_\mu(x)\, R^a_\nu(y)\rangle_{tree} &= \frac{1}{16} g^2 v^4 \langle A^a_\mu(p), A^a_\nu(-p)\rangle + \frac{1}{4} v^2 \partial_\mu \partial_\nu \langle \rho^a(p), \rho^a(-p)\rangle \\ &= \frac{3}{16} g^2 v^4 \frac{1}{p^2+m^2} \mathcal{P}_{\mu\nu}(p) + \frac{3}{4} v^2 \mathcal{L}_{\mu\nu}(p), \end{aligned} \tag{365}$$

where we can see that, apart from the constant factor $\frac{3}{4}v^2$ appearing in the longitudinal sector, the transverse component reproduces exactly the transverse gauge tree-level propagator.

Since the correlation function $\langle R^a_\mu(p), R^a_\nu(-p)\rangle$ is independent from the gauge parameter ξ, due to the BRST invariant nature of the operator $R^a_\mu(x)$, we shall proceed as in the previous example by making use of $\langle R^a_\mu(p)\, R^a_\nu(-p)\rangle_{\text{unitary}} = \langle R^a_\mu(p), R^a_\nu(-p)\rangle$ and evaluating the correlator at the one-loop order with the propagators given in (346), so that

$$\begin{aligned} \langle R^a_\mu(p)\, R^a_\nu(-p)\rangle &= \frac{1}{16} g^2 v^4 \langle A^a_\mu(p)\, A^a_\nu(-p)\rangle_{\text{unitary}} + \frac{1}{4} g^2 v^3 \langle A^a_\mu(p)\, (A^a_\nu h)(-p)\rangle_{\text{unitary}} \\ &+ \frac{1}{8} g^2 v^2 \langle (h^2 A^a_\mu)(p)\, A^a_\nu(-p)\rangle_{\text{unitary}} \\ &+ \frac{1}{4} g^2 v^2 \langle (hA^a_\mu)(p)\, (hA^a_\nu)(-p)\rangle_{\text{unitary}} \end{aligned} \tag{366}$$

with the contributing diagrams shown in Figure 31. Using dimensional regularization in the $\overline{MS}bar$-scheme with $(d = 4-\epsilon)$ and switching to momentum space, we find

$$\begin{aligned} &\frac{1}{16} g^2 v^4 \langle A^a_\mu(p)\, A^a_\nu(-p)\rangle_{\text{unitary}} = \\ &\frac{g^4 v^4}{32(4\pi)^2} \int_0^1 dx \Bigg\{ - \frac{1}{\epsilon 6 m^4 m_h^2} (9m^4 m_h^4 + m_h^2(-9m^6 - 83m^4 p^2 \\ - \;& 14m^2 p^4 + p^6) + 54m^8) \\ &+ \frac{m_h^2}{2p^2} \left(-m_h^2 + m^2 + 7p^2\right) \ln\left(\frac{m_h^2}{\mu^2}\right) \\ &+ \frac{1}{2m^2 p^2 m_h^2} \left(m^4 m_h^4 - m_h^2 \left(m^6 + 47m^4 p^2 + 16m^2 p^4 - 2p^6\right) + 54m^6 p^2\right) \ln\left(\frac{m^2}{\mu^2}\right) \end{aligned}$$

[13] The derivative here is not expressed in momentum space because for composite operators, the derivative will bring down different momenta depending on the configuration of the Feynman diagram.

$$
\begin{aligned}
&+\frac{1}{2p^2}\left(-2m_h^2\left(m^2-p^2\right)+m_h^4+m^4-10m^2p^2+p^4\right)\\
\times\;&\ln\left(\frac{p^2(1-x)x+(1-x)m_h^2+m^2x}{\mu^2}\right)\\
&+\frac{1}{2m^4}\left(4m^2+p^2\right)\left(12m^4-20m^2p^2+p^4\right)\\
\times\;&\ln\left(\frac{m^2+p^2(1-x)x}{\mu^2}\right)\\
&+\frac{1}{6m^4p^2m_h^2}\Big(3m^4m_h^6-3m_h^4\left(2m^6+9m^4p^2\right)\\
&+m_h^2\left(3m^8-9m^6p^2-2m^4p^4-26m^2p^6-2p^8\right)-54m^8p^2\Big)\Bigg\}\frac{\mathcal{P}_{\mu\nu}(p)}{(p^2+m^2)^2}\\
&+\frac{g^4v^4}{32(4\pi)^2m^4}\int_0^1 dx\Bigg\{\frac{1}{\epsilon}\frac{3}{m_h^2}\left(m_h^2\left(3m^2+p^2\right)-3m_h^4-18m^4\right)\\
&-\frac{3m^2}{2p^2m_h^2}\left(m_h^2\left(p^2-m^2\right)+m_h^4-18m^2p^2\right)\ln\left(\frac{m^2}{\mu^2}\right)\\
+\;&\frac{3m_h^2}{2p^2}\left(m_h^2-m^2+5p^2\right)\ln\left(\frac{m_h^2}{\mu^2}\right)\\
-\;&\frac{3}{2p^2}\left(\left(m_h-m\right)^2+p^2\right)\left(\left(m_h+m\right)^2+p^2\right)\\
\times\;&\ln\left(\frac{p^2(1-x)x+(1-x)m_h^2+m^2x}{\mu^2}\right)\\
-\;&\frac{3}{2p^2m_h^2}\left(m_h^4\left(5p^2-2m^2\right)+m_h^2\left(m^4-m^2p^2\right)+m_h^6+6m^4p^2\right)\Bigg\}\mathcal{L}_{\mu\nu}(p),
\end{aligned}
\tag{367}
$$

$$
\begin{aligned}
&\frac{1}{4}g^2v^3\left\langle A_\mu^a(p)\left(A^ah\right)(-p)\right\rangle_{\text{unitary}}\\
=\;&\frac{1}{16\pi^2}\int_0^1 dx\Bigg\{\frac{1}{\epsilon}\frac{m^2}{m_h^2}\left(m_h^2\left(p^2-9m^2\right)+12m_h^4+54m^4\right)\\
-\;&\frac{m^2m_h^2}{2p^2}\left(-m_h^2+m^2+10p^2\right)\ln\left(\frac{m_h^2}{\mu^2}\right)\\
-\;&\frac{m^4}{2p^2m_h^2}\left(m_h^2\left(p^2-m^2\right)+m_h^4+54m^2p^2\right)\ln\left(\frac{m^2}{\mu^2}\right)\\
-\;&\frac{m^2}{2p^2}\left(2p^2\left(m_h^2-5m^2\right)+\left(m^2-m_h^2\right)^2+p^4\right)\ln\left(\frac{p^2(1-x)x+(1-x)m_h^2+xm^2}{\mu^2}\right)\\
+\;&\frac{m^2}{6p^2m_h^2}\left(6m_h^4\left(m^2+6p^2\right)+m_h^2\left(-3m^4+9m^2p^2+2p^4\right)-3m_h^6+54m^4p^2\right)\Bigg\}\\
\times\;&\frac{\mathcal{P}_{\mu\nu}(p)}{(m^2+p^2)}\\
+\;&\frac{1}{16\pi^2}\int_0^1 dx\Bigg\{\frac{1}{\epsilon}\frac{3}{m_h^2}\left(-m_h^2\left(3m^2+p^2\right)+m_h^4+18m^4\right)
\end{aligned}
$$

$$
\begin{aligned}
&+ \frac{3m^2}{2p^2m_h^2}\left(m_h^2\left(p^2-m^2\right)+m_h^4-18m^2p^2\right)\ln\left(\frac{m^2}{\mu^2}\right)\\
&- \frac{3m_h^2}{2p^2}\left(m_h^2-m^2+3p^2\right)\ln\left(\frac{m_h^2}{\mu^2}\right)\\
&+ \frac{3}{2p^2m_h^2}\left(m_h^2\left(\left(m-m_h\right)^2+p^2\right)\left(\left(m_h+m\right)^2+p^2\right)\right)\\
&\times \ln\left(\frac{p^2(1-x)x+(1-x)m_h^2+xm^2}{\mu^2}\right)\\
&+ \frac{3}{2p^2m_h^2}\left(\left(m_h^3-m^2m_h\right)^2+p^2\left(-m^2m_h^2+3m_h^4+6m^4\right)\right)\Bigg\}\mathcal{L}_{\mu\nu}(p), \qquad (368)
\end{aligned}
$$

$$
\begin{aligned}
&\frac{1}{8}g^2v^2\langle(h^2A_\mu^a)(p)\,A_\nu^a(-p)\rangle_{\text{unitary}}\\
&= -\frac{3m_h^2m^2}{32\pi^2}\int_0^1 dx\left\{\frac{2}{\epsilon}-\ln\left(\frac{m_h^2}{\mu^2}\right)+1\right\}\left(\frac{1}{p^2+m^2}\mathcal{P}_{\mu\nu}(p)+\frac{1}{m^2}\mathcal{L}_{\mu\nu}(p)\right), \qquad (369)
\end{aligned}
$$

$$
\begin{aligned}
&\frac{1}{4}g^2v^2\langle(hA_\mu^a)(p)\,(hA_\nu^a)(-p)\rangle_{\text{unitary}} =\\
&\frac{1}{32\pi^2}\int_0^1 dx\Bigg\{\frac{1}{\epsilon}(-3m_h^2+9m^2-p^2)\\
&+ \frac{m_h^2}{2p^2}\left(m^2+p^2-m_h^2\right)\ln\left(\frac{m_h^2}{\mu^2}\right)+\frac{m^2}{2p^2}\left(m_h^2-m^2+p^2\right)\ln\left(\frac{m^2}{\mu^2}\right)\\
&+ \frac{1}{2p^2}\left(2p^2\left(m_h^2-5m^2\right)+\left(m^2-m_h^2\right)^2+p^4\right)\\
&\times \ln\left(\frac{p^2(1-x)x+(1-x)m_h^2+xm^2}{\mu^2}\right)\\
&+ \frac{1}{6p^2}\left(3\left(m^2-m_h^2\right)^2-9p^2\left(m_h^2+m^2\right)-2p^4\right)\Bigg\}\mathcal{P}_{\mu\nu}(p)\\
&+ \frac{3}{32\pi^2}\int_0^1 dx\Bigg\{\frac{1}{\epsilon}\left(-m_h^2+3m^2+p^2\right)\\
&+ \frac{m^2}{2p^2}\left(-m_h^2+m^2-p^2\right)\ln\left(\frac{m^2}{\mu^2}\right)+\frac{m_h^2}{2p^2}\left(m_h^2-m^2+3p^2\right)\ln\left(\frac{m_h^2}{\mu^2}\right)\\
&- \frac{1}{2p^2}\left(\left(m-m_h\right)^2+p^2\right)\left(\left(m_h+m\right)^2+p^2\right)\\
&\times \ln\left(\frac{p^2x(1-x)+(1-x)m_h^2+xm^2}{\mu^2}\right)\\
&- \frac{1}{2p^2}\left(\left(m^2-m_h^2\right)^2+3p^2m_h^2-p^2m^2\right)\Bigg\}\mathcal{L}_{\mu\nu}(p)\,. \qquad (370)
\end{aligned}
$$

Using the unity (351), we find that the transverse part of the propagator is given by

$$R(p^2) = \frac{1}{16}g^2v^4\left(\frac{1}{p^2+m^2}+\frac{1}{(p^2+m^2)^2}\left(\Pi_R(p^2)+\Pi_{\rm div}(p^2)\right)\right)+\mathcal{O}(\hbar^2) \quad (371)$$

where the divergent part is, see also the comments in the Appendix K,

$$\Pi_{\rm div}(p^2) = \frac{g^2}{\epsilon\pi^2}\Big(-\frac{h^2p^4}{32m^4}+\frac{9m^4}{16h^2}+\frac{9m^2p^2}{8h^2}+\frac{h^2p^2}{8m^2}+\frac{h^2}{16}-\frac{p^6}{48m^4}+\frac{23p^4}{96m^2}+\frac{7p^2}{8}\Big), \quad (372)$$

while for the finite part we get

$$\begin{aligned}
\Pi_R(p^2) &= \frac{3}{36\pi^2g^2v^4m_h^2}\int_0^1 dx\Big\{6m^4\left(m_h^4+3m^4\right)-\frac{p^4m_h^2}{3}\left(9m_h^2+35m^2+4p^2\right)\\
&+ p^2\left(m^4m_h^2+10m^2m_h^4+m_h^6+36m^6\right)\\
&+ m_h^4\left(-p^2\left(m_h^2+11m^2\right)-6m^4+p^4\right)\ln\left(\frac{m_h^2}{\mu^2}\right)\\
&+ m_h^2\left(2p^4\left(m_h^2-5m^2\right)+\left(m^2-m_h^2\right)^2p^2+p^6\right)\\
&\times \ln\left(\frac{p^2(1-x)x+(1-x)m_h^2+xm^2}{\mu^2}\right)\\
&+ m_h^2\left(48m^6-68m^4p^2-16m^2p^4+p^6\right)\ln\left(\frac{p^2(1-x)x+m^2}{\mu^2}\right)\\
&+ m^2(m_h^2\left(-48m^4-17m^2p^2+3p^4\right)\\
&+ p^2m_h^4-54\left(m^6+2m^4p^2\right))\ln\left(\frac{m^2}{\mu^2}\right)\Big\}. \quad (373)
\end{aligned}$$

Since (373) contains terms of the order of $\frac{p^4}{(p^2+m^2)^2}\ln(p^2)$ and $\frac{p^6}{(p^2+m^2)^2}\ln(p^2)$, we follow the steps (201)-(203) to find the resummed propagator in the one-loop approximation, namely

$$G_R(p^2) = \frac{1}{16}g^2v^4\Big(\frac{1}{p^2+m_h^2-\hat{\Pi}_R(p^2)}\Big)+C_R(p^2) \quad (374)$$

with

$$\begin{aligned}
\hat{\Pi}_R(p^2) &= \frac{3}{36\pi^2g^2v^4m_h^2}\int_0^1 dx\Big\{6m^4\left(m_h^4+3m^4\right)-\frac{p^4m_h^2}{3}\left(9m_h^2+35m^2+4p^2\right)\\
&+ p^2\left(m^4m_h^2+10m^2m_h^4+m_h^6+36m^6\right)\\
&+ m_h^4\left(-p^2\left(m_h^2+11m^2\right)-6m^4+p^4\right)\ln\left(\frac{m_h^2}{\mu^2}\right)\\
&+ m_h^2(m_h^4p^2-2m_h^2m^4-6m_h^2m^2p^2\\
&+ 12m^6+24m^4p^2)\ln\left(\frac{x\left(m^2-p^2(x-1)\right)-(x-1)m_h^2}{\mu^2}\right)
\end{aligned}$$

$$
\begin{aligned}
&+ \quad 33m_h^2\left(2m^6 - m^4p^2\right)\ln\left(\frac{m^2 - p^2(x-1)x}{\mu^2}\right) \\
&+ \quad m^2m_h^2\left(-48m^4 - 17m^2p^2 + 3p^4\right) \\
&+ \quad p^2m_h^4 - 54\left(m^6 + 2m^4p^2\right)\Big)\ln\left(\frac{m^2}{\mu^2}\right)\Bigg\} \qquad (375)
\end{aligned}
$$

and

$$
\begin{aligned}
C_R(p^2) &= \frac{1}{12(4\pi)^2}\int_0^1 dx\Bigg\{\left(-18m^2 + p^2\right)\ln\left(\frac{p^2(1-x)x + m^2}{\mu^2}\right) \\
&+ \quad \left(\left(2\left(m_h^2 - 6m^2\right) + p^2\right)\ln\left(\frac{p^2x(1-x) + (1-x)m_h^2 + xm^2}{\mu^2}\right)\right\}. \qquad (376)
\end{aligned}
$$

Looking now at the longitudinal part $L(p^2)$, it turns out to be

$$
\begin{aligned}
L(p^2) &= \frac{1}{4}v^2 \\
&- \quad \frac{1}{(4\pi)^2}\left(\frac{m_h^4 - 3m_h^4\ln\left(\frac{m_h^2}{\mu^2}\right) + 9m^4 - 27m^4\ln\left(\frac{m^2}{\mu^2}\right)}{2m_h^2} - \frac{1}{\epsilon}\left(m_h^2 - 9\frac{m^4}{m_h^2}\right)\right). \qquad (377)
\end{aligned}
$$

As it happens in the tree-level case, expression (377) is independent from the momentum p^2, meaning that it does not correspond to the propagation of some physical mode, a feature which is expected to persist at higher orders.

5.4 **Spectral properties**

In this section, we will calculate the spectral properties associated with the correlation function obtained in the last section. For the employed techniques in obtaining the pole mass, residue and spectral density up to first order we refer to section 4.3.1. In subsection 5.4.1, we analyze the spectral properties of the elementary fields. In 5.4.3, the spectral properties of the composite operators $O(x)$ and $R_\mu^a(x)$ are discussed.

5.4.1 Spectral properties of the elementary fields

We first discuss the spectral properties of the elementary fields: the scalar Higgs field $h(x)$ and the transverse part of the gauge field $A_\mu^a(x)$. We will work with two sets of parameters, set out in Table 3. All values are given in units of the energy scale μ. Also, we have that $m^2 = \frac{1}{4}g^2v^2$ and $m_h^2 = \lambda v^2$, so that $m^2 = 0.23\,\mu^2$ and $m_h^2 = 0.192\,\mu^2$ in Region I and $m^2 = 0.625\,\mu^2$ and $m_h^2 = 0.205\,\mu^2$ in Region II.

Figure 31 - Correlation function of composite operator

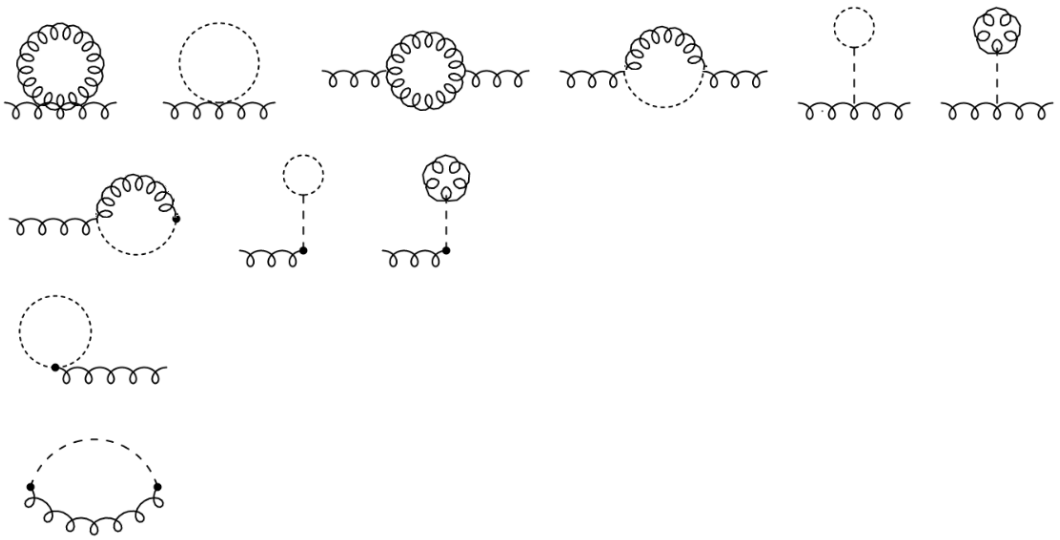

Legend: One-loop contributions for the correlation function $\langle OO \rangle$ in the unitary gauge: $\langle A^a_\mu(x) A^a_\nu(y) \rangle$ (first two lines), $\langle A(x)(Ah)(y) \rangle$ (third line), $\langle h(x)^2 A^a_\mu \rangle$ (fourth line) and $\langle (A^a_\mu h)(x)(A^a_\nu h)(y) \rangle$. Wavy lines represent the gauge field, dashed lines the Higgs field, solid lines the Goldstone boson and double lines the ghost field. The $\bullet$ indicates the insertion of a composite operator.

Source: The author, 2020.

Table 3 - Spectral density functions parameter values

	Region I	**Region II**
v	0.8 μ	1 μ
g	1.2	0.5
λ	0.3	0.205

Legend: Parameter values used in the spectral density functions.

Source: The author, 2020.

Figure 32 - Gauge dependence of Higgs residue

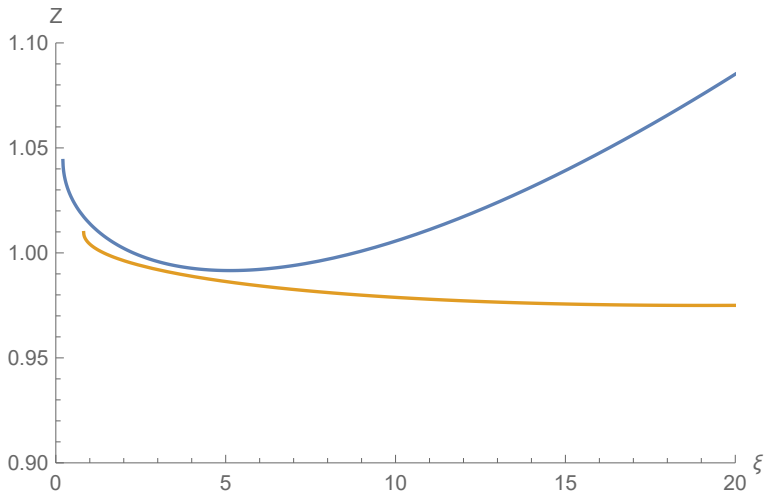

Legend: Dependence of the residue Z for the Higgs field propagator on the gauge parameter ξ, for Region I (Blue), and Region II (Orange).

Source: The author, 2020.

For the Higgs fields, following the steps from section 4.3.1, we find the pole mass to first order in $\hbar$ to be: for Region I

$$m^2_{h,\text{pole}} = 0.207\,\mu^2, \tag{378}$$

and for Region II

$$m^2_{h,\text{pole}} = 0.206\,\mu^2, \tag{379}$$

for all values of the parameter ξ. This means that while the Higgs propagator (320) is gauge dependent, the pole mass is gauge independent. This is in full agreement with the Nielsen identities of the $SU(2)$ Higgs model studied in (GAMBINO; GRASSI; MADRICARDO, 1999). The residue, however, is gauge dependent, as is depicted in Figure 32. For small values of ξ, including the Landau gauge $\xi = 0$, the residue is not well-defined, and we cannot determine the spectral density function, as we will explain further in the next section.

In Figure 33, we find the spectral density functions both regions, for three values of $\xi : 1, 2, 5$. Looking at Region I, we see the first two-particle state appearing at $t = (m_h + m_h)^2 = 0.768\,\mu^2$, followed by another two-particle state at $t = (m+m)^2 = 0.922\,\mu^2$. Then, we see that there is a negative contribution, different for each diagram, at $t = (\sqrt{\xi}m + \sqrt{\xi}m)^2$. This corresponds to the (unphysical) two-particle state of two Goldstone bosons. For $\xi < 3$, this leads to a negative contribution for the spectral function, probably due to the large-momentum behaviour of the Higgs propagator (320), for a detailed discussion

Figure 33 - Higgs spectral function

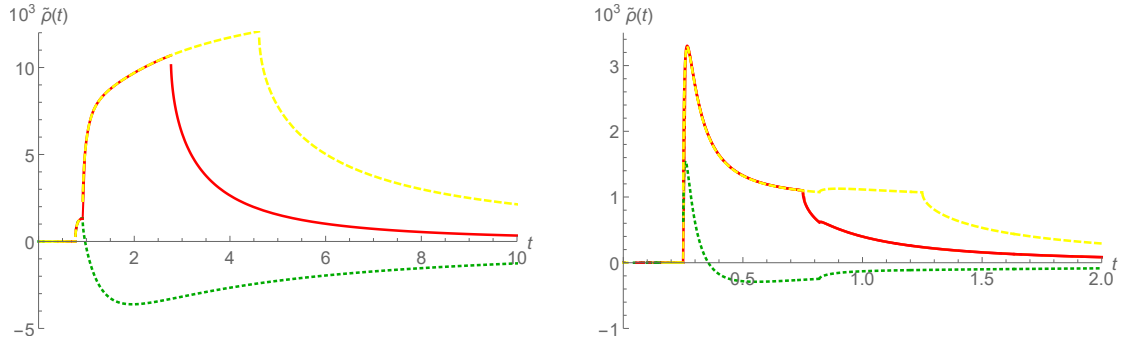

Legend: Spectral functions for the propagator $\langle h(p)h(-p)\rangle$, for $\xi = 1$ (Green, Dotted), $\xi = 3$ (Red, Solid), $\xi = 5$ (Yellow, Dashed), with t given in units of μ^2, for Region I (left) and Region II (right) with the parameter values given in Table 3.

Source: The author, 2020.

see Appendix G . For Region II, we find essentially the same behaviour: a Higgs two-particle state at $t = (m_h + m_h)^2 = 0.81\,\mu^2$, and a gauge field two-particle state at $t = (m + m)^2 = 0.25\,\mu^2$. We also see a negative contribution different for each diagram at $t = (\sqrt{\xi}m + \sqrt{\xi}m)^2$, corresponding to the (unphysical) two-particle state of two Goldstone bosons.

For the gauge field propagator, following the steps from section 4.3.1, we find the first-order pole mass of the transverse gauge field to be: for Region I

$$m^2_{\text{pole}} = 0.274\,\mu^2 \tag{380}$$

and for Region II

$$m^2_{\text{pole}} = 0.065\,\mu^2 \tag{381}$$

for all values of the parameter ξ, so that the pole mass is gauge independent. The residue is, however, gauge dependent as is depicted in Figure 34. For small values of ξ the residue is not well-defined, as we will explain further in the next section.

In Figure 35, we find the spectral density functions for both regions, for three values of ξ: $1, 2, 5$. Looking at Region I, we see the first two-particle state appearing at $t = (m_h + m)^2 = 0.843\,\mu^2$, followed by a two-particle state at $t = (m + m)^2 = 0.922\,\mu^2$. Then, we see that there is a negative contribution, different for each diagram, at $t = (m + \sqrt{\xi}m)^2$. This corresponds to the (unphysical) two-particle state of a gauge and Goldstone boson. For Region II, we find a gauge field two-particle state at $t = (m + m)^2 = 0.25\,\mu^2$. We also see a negative contribution different for each diagram at $t = (m + \sqrt{\xi}m)^2$, corresponding to the (unphysical) two-particle state of two Goldstone bosons.

Figure 34 - Residue gauge dependence

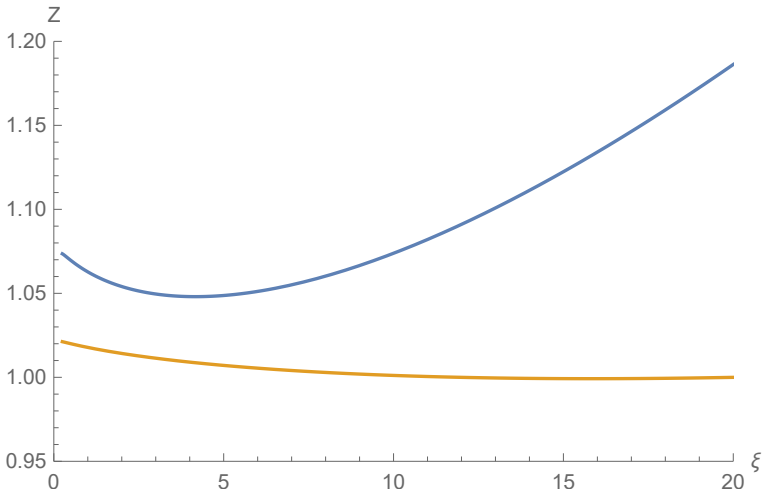

Legend: Dependence of the residue Z for the gauge field propagator from the gauge parameter ξ, for Region I (Blue), and Region II (Orange).

Source: The author, 2020.

Figure 35 - Spectral functions for transverse gluon propagator

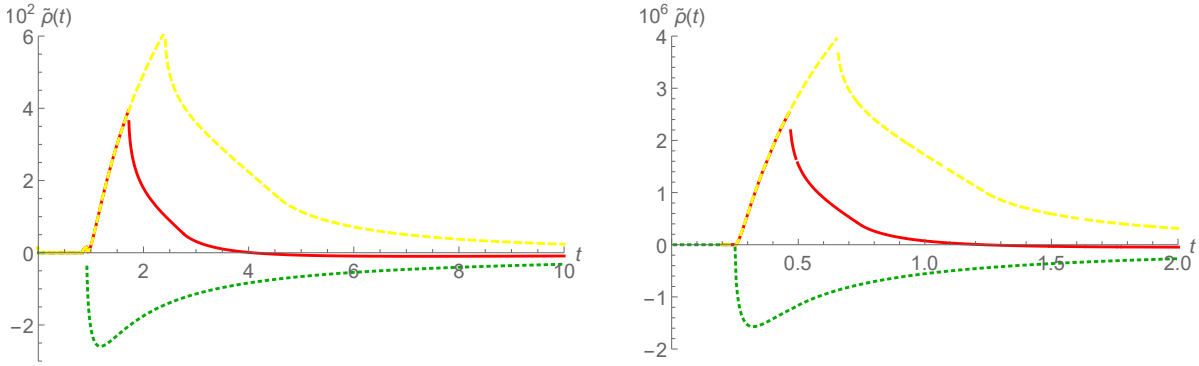

Legend: Spectral functions for the propagator $\langle A^a_\mu(p)A^b_\nu(-p)\rangle^T$, for $\xi = 1$ (Green, Dotted), $\xi = 3$ (Red, Solid), $\xi = 5$ (Yellow, Dashed), with t given in units of μ^2, for Region I (left) and Region II (right) with the parameter values given in Table 3.

Source: The author, 2020.

Figure 36 - Boson decays

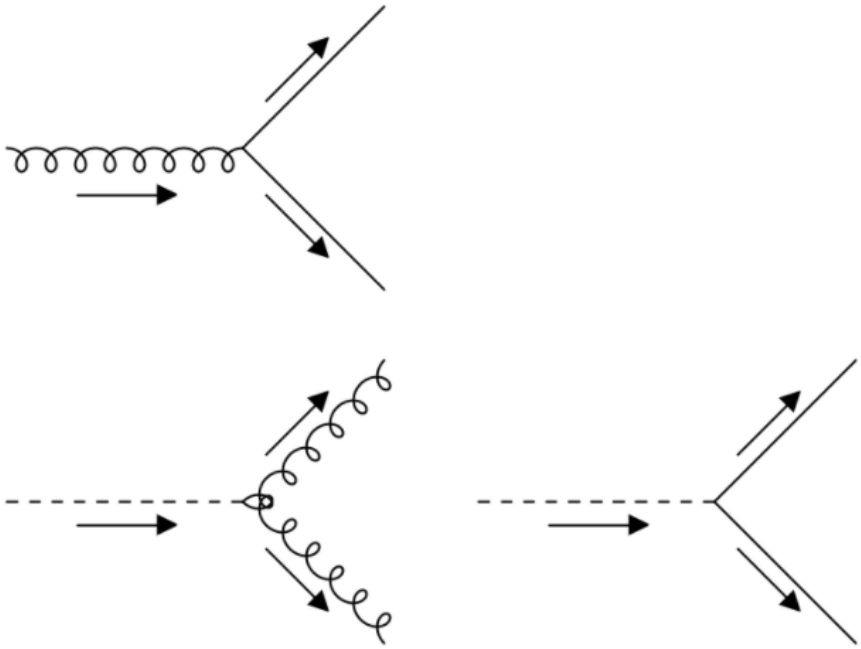

Legend: Possible decays of the gauge boson (above) and the Higgs boson (below).
Source: The author, 2020.

5.4.2 Unphysical threshold effects

From the Feynman vertex rules given in Appendix H, for certain values of the masses, unphysical threshold effects can occur. These effects imply that for certain values of the (physical and unphysical) parameters, a "decay" occurs of a gauge and Higgs boson into two other particles, see Figure 36. We distinguish three cases:

(1.) Decay of a gauge vector boson in two Goldstone bosons: this happens when $m > 2\sqrt{\xi}m$.

(2.) Decay of a Higgs boson in two gauge vector bosons: this happens when $m_h > 2m$.

(3.) Decay of a Higgs boson in two Goldstone bosons: this happens when $m_h > 2\sqrt{\xi}m$.

In order to guarantee the stability of the gauge boson, we therefore need from (1.) that $\xi > \frac{1}{4}$. This means that for the Landau gauge $\xi = 0$, the elementary gauge boson is not stable. For the Higgs particle, to guarantee stability we need from (2.) that $m_h < 2m$. Then, from (3.) we find that $\xi > \frac{m_h^2}{4m^2}$. This is the window in which we can work with a stable model. We can have a look at what happens when we go outside of this window. For the Higgs particle, we see that for $m_h > 2m$, or $\lambda < g^2$, we will find a complex value for the first order pole mass, calculated through (208). For $\lambda \geq g^2$, we will always find

a real pole mass. Since the pole mass is gauge invariant, we find that this is true for all values of ξ. However, we do find that for $\xi > \frac{m_h^2}{4m^2}$ and $\lambda > g^2$, the real value of the pole mass is a real point inside the branch cut. This means that we cannot achieve the usual differentiation around this point. As a consequence, we cannot consistently construct the residue, so that we are unable to obtain a first-order spectral function. For the gauge field, we find the same problem when $\xi < \frac{1}{4}$.

The foregoing mathematically correct observations clearly show that there is something physically wrong with using the elementary fields' spectral functions. Luckily, all of these shortcomings are surpassed by using the gauge invariant composite operators.

5.4.3 Spectral properties for the composite fields

For the scalar composite operator $O(x)$ we find the first-order pole mass for Region I

$$m^2_{OO,\text{pole}} = 0.207\,\mu^2, \tag{382}$$

and for Region II

$$m^2_{OO,\text{pole}} = 0.206\,\mu^2, \tag{383}$$

which is equal to the pole mass of the elementary Higgs field in (378), as we expect from eq. (298). Following the steps from section 4.3.1, we find the first-order residue

$$Z = 1.11\,v^2 \tag{384}$$

for Region I and

$$Z = 1.01\,v^2 \tag{385}$$

for Region II. The first order spectral function for $\langle O(x)\,O(y)\rangle$ is shown in Figure 37. Comparing this result with that of the spectral function of the Higgs field in Figure 35, we see a two-particle state for the Higgs field at $t = (m_h + m_h)^2$, and a two-particle state for the gauge vector field, starting at $t = (m + m)^2$. The difference is that for the gauge invariant correlation function $\langle O(x)\,O(y)\rangle$ we no longer have the unphysical Goldstone two-particle state. Due to the absence of this negative contribution, the spectral function is positive throughout the spectrum. In fact, we see that for bigger values of ξ, we find that the spectral function of the elementary Higgs field resembles more and more the spectral function of the composite operator $O(x)$. This makes sense, since for $\xi \to \infty$, we are approaching the unitary gauge which has a more direct link with the physical

Figure 37 - Spectral function for $\langle O(p)O(-p)\rangle$

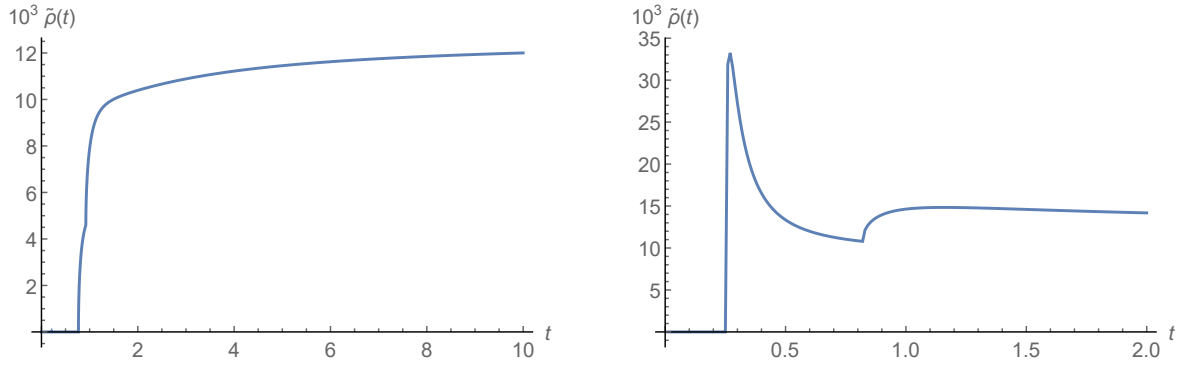

Legend: Spectral function for the two-point correlation function $\langle O(p)O(-p)\rangle$, with t given in units of μ^2, for the Region I (left) and Region II (right) with parameter values given in Table 3.
Source: The author, 2020.

spectrum of the elementary excitations. In Appendix K, one finds a detailed discussion about the unitary gauge limit $\xi \to \infty$ as well as the calculation of the spectral function. The asymptotic (constant) behaviour is directly related to the (classical) dimension of the used composite operator.

For the transverse part of the two-point correlation function $G_R(p^2)$, eq. (375), for our set of parameters we find the first-order pole mass: in Region I

$$m^2_{R,\text{pole}} = 0.274\,\mu^2 \tag{386}$$

and Region II

$$m^2_{R,\text{pole}} = 0.065\,\mu^2 \tag{387}$$

which is the same as the pole mass of the transverse gauge field, eq. (380), in agreement with eq. (298). Following the steps from 4.3.1, we find the first-order residue

$$Z = \frac{1}{16} g^2 v^4\,(1.27) \tag{388}$$

for Region I and

$$Z = \frac{1}{16} g^2 v^4\,(1.05) \tag{389}$$

for Region II. The first order spectral function for $G_R(p^2)$ is shown in Figure 38. Comparing this to the spectral function of the gauge vector field in Figure 35, we see a two-particle state at $t = (m_h{+}m)^2$, and a two-particle state for the gauge field, starting at $t = (m{+}m)^2$.

Figure 38 - Spectral function for $G_R(p^2)$

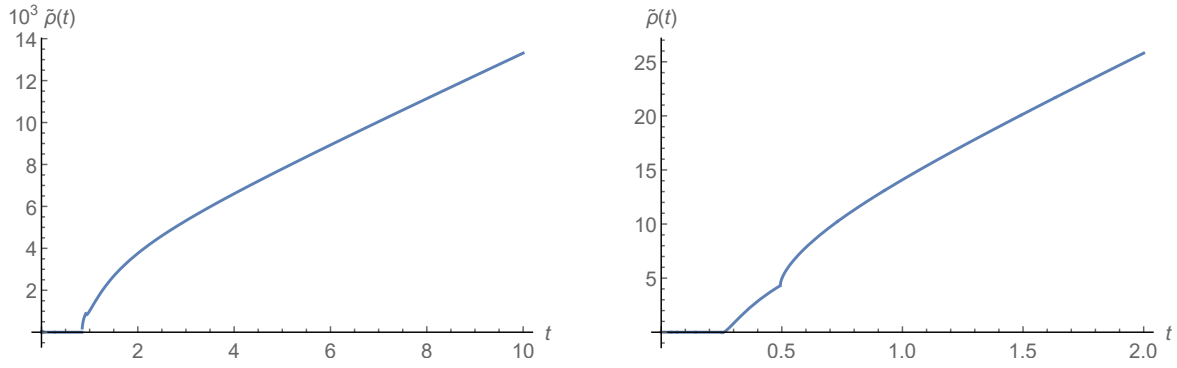

Legend: Spectral function for the transverse two-point correlation function $G_R(p^2)$, with t given in units of μ^2, for the Region I (left) and Region II (right) with parameter values given in Table 3.

Source: The author, 2020.

Again, as in the case of the two-point correlation function of the scalar operator $O(x)$, the difference is that for this gauge invariant correlation function we no longer have the unphysical Goldstone/gauge boson two-particle state. Due to the absence of this negative contribution, the spectral function is positive throughout the spectrum. In fact, we see that for bigger values of ξ, we find that the spectral function of the elementary gauge field resembles more and more the spectral function of the composite operator $R^a_\mu(x)$. As already mentioned previously, this relies on the fact that in the limit $\xi \to \infty$ we are approaching the unitary gauge, see Appendix K. Also here, the linear increase at large t follows from the operator dimension.

5.5 **Conclusion**

This chapter is the natural extension of chapter 3 and 4, where the Abelian $U(1)$ Higgs model has been scrutinized by employing two local composite BRST invariant operators whose two-point correlation functions provide a fully gauge independent description of the elementary excitations of the model, namely the Higgs and the massive gauge boson. This formulation generalizes to the non-Abelian Higgs model as, for example, the $SU(2)$ YM theory with a single Higgs in the fundamental representation (HOOFT et al., 1980; FROHLICH; MORCHIO; STROCCHI, 1980; FROHLICH; MORCHIO; STROCCHI, 1981). This is the model which has been considered in the present analysis. The local BRST invariant composite operators $(O(x), R^a_\mu(x))$ which

generalize their $U(1)$ counterparts are given in eq. (338) and in eqs. (356),(357). The two-point correlation functions $\langle O(x)O(y)\rangle$ and $\langle R^a_\mu(x)R^b_\nu(y)\rangle^T$, where the superscript T stands for the transverse component, have been evaluated at one-loop order in the R_ξ-gauge and compared with the corresponding correlation functions of the elementary fields $\langle h(x)h(y)\rangle$ and $\langle A^a_\mu(x)A^b_\nu(y)\rangle^T$. It turns out that both $\langle O(x)O(y)\rangle$ and $\langle h(x)h(y)\rangle$ share the same gauge independent pole mass, eqs.(378),(379),(382),(383), in agreement with both Nielsen identities (NIELSEN, 1975; PIGUET; SIBOLD, 1985; GAMBINO; GRASSI; MADRICARDO, 1999; GAMBINO; GRASSI, 2000; GRASSI; KNIEHL; SIRLIN, 2001; AITCHISON; FRASER, 1984; ANDREASSEN; FROST; SCHWARTZ, 2015) and the BRST invariant nature of $O(x)$. Nevertheless, unlike the residue and spectral function of the elementary correlator $\langle h(x)h(y)\rangle$, which exhibit a strong unphysical dependence from the gauge parameter ξ, Figure (33), the spectral density of $\langle O(x)O(y)\rangle$ turns out to be ξ-independent and positive over the whole p^2 axis, Figure (37). The same features hold for $\langle A^a_\mu(x)A^b_\nu(y)\rangle^T$ and $\langle R^a_\mu(x)R^b_\nu(y)\rangle^T$. Again, both correlation function share have the same ξ-independent pole mass, eqs. (381),(381),(386),(387). Though, unlike the ξ-dependent spectral function associated to $\langle A^a_\mu(x)A^b_\nu(y)\rangle^T$, Figure (35), that corresponding to $\langle R^a_\mu(x)R^b_\nu(y)\rangle^T$, Figure (38), turns out to be independent from the gauge parameter ξ and positive. As such, the local composite operators $(O(x), R^a_\mu(x))$ provide a fully BRST consistent description of the observable scalar (Higgs) and vector boson particles.

It is worth mentioning here that, besides the BRST invariance of the gauge fixed action, the model exhibits an additional global custodial symmetry, eqs.(317),(318), according to which all fields carrying the index $a = 1, 2, 3$, *i.e.* $(A^a_\mu, b^a, c^a, \bar{c}^a, \rho^a)$, undergo a global transformation in the adjoint representation of $SU(2)$. The same feature holds for the composite operators $(O(x), R^a_\mu(x))$ which transform exactly as h and A^a_μ. More precisely, the operator $O(x)$ is a singlet under the custodial symmetry, while the operators R^a_μ transform like a triplet, eq. (359), so that the correlation function $\langle R^a_\mu(p)R^b_\nu(-p)\rangle$ displays the same $SU(2)$ structure of the elementary two-point function $\langle A^a_\mu(p)A_\nu(-p)\rangle$, eqs.(360)-(363). Although not being the aim of the present analysis, we expect that the existence of a global custodial symmetry will imply far-reaching consequences for the renormalization properties of the composite operators $(O(x), R^a_\mu(x))$ encoded in the corresponding Ward identities. The renormalization properties of the local gauge-invariant composite operators for the $U(1)$ Higgs model have been reported recently in (CAPRI et al., 2020).

CONCLUSION

In this work, we have evaluated different BRST-invariant solutions for the introduction of a mass term in YM theories. More specifically, we have looked at gauge-invariant extensions of the elementary gauge field and Higgs boson, and we evaluated the two-point functions and spectral properties for these gauge-invariant local composite fields. While the proposed solutions differ in methods and levels at which the BRST invariance is introduced, they serve a common goal: to access the physical spectrum for the nuclear forces.

For the composite field $A^h(x)$, we have shown that a renormalizable gauge class can be developed for this field, which introduces a mass μ for the Stueckelberg-like field ξ^a, which is used in the localization procedure for the composite gauge field. This mass ensures the infrared safety of the propagator for this field. The gauge class, with μ as the gauge parameter, gives the opportunity to investigate physical objects related to the gauge field propagator outside of the Landau gauge. For example, in (MINTZ et al., 2019) it was shown, by analyzing dimension two condensates, that the instability of the GZ action observed in the Landau gauge persists in this larger gauge class, suggesting a physical meaning for the refinement of the GZ action in the infrared regime. This indicates an important role for the RGZ action in the IR description of the YM theories.

For the gauge-invariant local composite operators in the Higgs model, we have investigated spectral properties of the field propagators. The most important conclusion here is that for truly gauge-invariant objects, we have not observed any non-physical behavior. In particular, we have not observed any non-physical behaviour of the kind that is commonly associated with confinement, such as positivity violation of the spectral density function. We immediately add that this does not mean that positivity violation, as has been observed for the spectral density function of the elementary gauge field operator, should be solely ascribed to a lack of gauge-invariance. Even though we were able to make a direct comparison between gauge-invariant composite operators and the gauge-dependent elementary operators, and we concluded that the first always shows a positive spectral density function, while the second for some values of the gauge parameter shows a negative spectral density function, our methods are not suited to reach the non-perturbative region in which positivity violation has been observed in other studies. Since our study consisted of perturbative loop calculations in the Higgs model, we are far from the IR region where we expect this confinement-like behavior. It is therefore our hope that this work will encourage others to investigate the spectral properties of the gauge-invariant composite local operators developed in this work with non-perturbative methods, such as lattice simulations. The composite gauge-invariant local operators have already led to some preliminary lattice results (MAAS; SONDENHEIMER; TÖREK,

2019; MAAS, 2015).

A direct comparison between the two methods of developing gauge-invariant composite fields discussed in this thesis can be made in the Landau gauge. In this gauge, the composite gauge field $A^h_\mu(x)$ is equal to the elementary field $A_\mu(x)$, and the action will be equal to the action of the massive YM model discussed in section 1.3.1. The appearance of complex poles for the propagator of the gauge field, even at a perturbative level, means that there is no physical interpretation for these propagators. Thus, while BRST invariance is established by the configuration of $A^h_\mu(x)$, this does not seem to ensure the usual features of the definition of physical space that are associated with BRST invariance. Possibly, this is because the BRST invariance is introduced at a non-local level. In contrast, the local composite BRST invariant operators developed for the Higgs model always have a real pole mass. However, for the Landau gauge the residue is not well-defined, and we are unable to subtract a spectral density function of the gauge field for this gauge choice. Therefore, the Landau gauge might not be the most suitable gauge to work with for massive non-Abelian models.

If we want to access the non-perturbative region to investigate further the local composite gauge-invariant operators in the Higgs model, the continuum offers some ways to access this region besides numerical methods. The BRST invariant nature of $(O(x), R^a_\mu(x))$ makes them natural candidates to an attempt at facing the challenge of investigating the infrared non-perturbative behaviour of the model, trying to make contact with the analytical lattice predictions of Fradkin and Shenker (FRADKIN; SHENKER, 1979). For the $SU(2)$ HYM theory one may for example introduce a horizon term, in its BRST-invariant formulation encoded in the RGZ action (cf. (VANDERSICKEL; ZWANZIGER, 2012; DUDAL et al., 2008a; CAPRI et al., 2015; CAPRI et al., 2018a) and refs. therein) implementing the restriction to the Gribov region Ω (GRIBOV, 1978) in order to take into account the existence of the Gribov copies plaguing the FP quantization procedure. As a consequence, the gauge-invariant pole masses of the non-Abelian generalization of the correlation functions $\langle R^a_\mu(x) R^a_\nu(y)\rangle$ and $\langle O(x)O(y)\rangle$ will now show an explicit dependence on the Gribov mass parameter as well as on the dimension-two condensates present in the RGZ action (VANDERSICKEL; ZWANZIGER, 2012; DUDAL et al., 2008a; CAPRI et al., 2015; CAPRI et al., 2018a). Thus, extending the framework already outlined in (CAPRI et al., 2013), the aforementioned pole masses and further spectral properties could be employed as gauge-invariant probing quantities in order to extract non-perturbative information about the behaviour of the elementary excitations of HYM theories in the light of the Fradkin-Shenker results.

The employment of an order parameter to distinguish between the confinement/deconfinement region can also be done in a YM model with finite temperature. In recent years, much valuable progress has been made towards the understanding of non-abelian gauge theories at finite temperature using background field gauge (BFG)

methods (ABBOTT, 1981; ABBOTT, 1982) in the Landau-DeWitt gauge. BFG methods provide an efficient way to describe the confinement/deconfinement order parameter (the Polyakov loop or any of its proxies (BRAUN; GIES; PAWLOWSKI, 2010)) because the related center symmetry is explicit at the quantum level and is easily maintained in approximation schemes (HERBST; LUECKER; PAWLOWSKI, 2015; REINOSA et al., 2016; REINOSA, 2019). Several models have been put forward in order to implement the BFG formalism in the Landau-deWitt gauge while restricting the number of Gribov copies. In (REINOSA et al., 2015b; REINOSA et al., 2015a; REINOSA et al., 2016; REINOSA; SERREAU; TISSIER, 2015; MAELGER; REINOSA; SERREAU, 2018), the formalism was used within the massive YM model to compute the background potential and Polyakov loop up to two-loop order, both in pure YM theories and in heavy-quark QCD. Recently, results on the BFG method in the Landau-DeWitt gauge for the GZ model have been reported (CANFORA et al., 2015; DUDAL; VERCAUTEREN, 2018; KROFF; REINOSA, 2018; EGMOND; REINOSA, 2020). It would be interesting to see if this method could be combined with the gauge-invariant composite operators developed in this work.

But even without accessing the non-perturbative region, the gauge-invariant composite operators offer several interesting lines of investigation. For example, we could compare different gauge classes that leave different remnant global gauges, such as the R_ξ gauge and the Linear Covariant Gauges (LCG). The R_ξ gauges break the global gauge symmetry of the model, in contrast to the LCG. We could compare the pole masses of the elementary fields for these two gauge classes. Then, they can be compared with the pole mass of their gauge-invariant composite extensions, which should of course be the same in every gauge class. This is a very interesting exercise as in a sense it will reveal which class of gauges is physical. Another line of investigation is given by the gauge-invariant quadratic Higgs condensate $\varphi\varphi^\dagger$, similar to the Coleman-Weinberg condensate (COLEMAN; WEINBERG, 1973; KNECHT; VERSCHELDE, 2001). In particular, we are curious to see what is the influence of this condensate on the propagators of the gauge-invariant operators, including their pole structure.

Finally, a most promising avenue to further explore is the $SU(2) \times U(1)$ setting of the electroweak theory. This sector is of course of special interest because of the experimental data that are available for the masses of the W and Z bosons. We would be the first to ever calculate these masses analytically in a gauge-invariant way.

REFERENCES

AAD, G. et al. Observation of a new particle in the search for the Standard Model Higgs boson with the ATLAS detector at the LHC. *Phys. Lett. B,* [s.l], v. 716, p. 1–29, 2012.

ABBOTT, L. The Background Field Method Beyond One Loop. *Nucl. Phys. B,* [s.l], v. 185, p. 189–203, 1981.

ABBOTT, L. Introduction to the Background Field Method. *Acta Phys. Polon. B,* [s.l], v. 13, p. 33, 1982.

AGUILAR, A.; BINOSI, D.; PAPAVASSILIOU, J. Gluon and ghost propagators in the Landau gauge: Deriving lattice results from Schwinger-Dyson equations. *Phys. Rev. D,* [s.l], v. 78, p. 025010, 2008.

AGUILAR, A.; BINOSI, D.; PAPAVASSILIOU, J. Yang-Mills two-point functions in linear covariant gauges. *Phys. Rev. D,* [s.l], v. 91, n. 8, p. 085014, 2015.

AGUILAR, A.; BINOSI, D.; PAPAVASSILIOU, J. The Gluon Mass Generation Mechanism: A Concise Primer. *Front. Phys. (Beijing),* [s.l], v. 11, n. 2, p. 111203, 2016.

AGUILAR, A. C.; BINOSI, D.; PAPAVASSILIOU, J. Renormalization group analysis of the gluon mass equation. *Phys. Rev.,* [s.l], D89, n. 8, p. 085032, 2014.

AITCHISON, I.; FRASER, C. Gauge Invariance and the Effective Potential. *Annals Phys. ,* [s.l], v. 156, p. 1, 1984.

ALKOFER, R. et al. Analytic properties of the landau gauge gluon and quark propagators. *Physical Review D,* [s.l], American Physical Society (APS), v. 70, n. 1, Jul 2004. ISSN 1550-2368.

ALKOFER, R.; SMEKAL, L. von. The Infrared behavior of QCD Green's functions: Confinement dynamical symmetry breaking, and hadrons as relativistic bound states. *Phys. Rept.,* [s.l], v. 353, p. 281, 2001.

ANDERSON, P. Theory of flux creep in hard superconductors. *Physical Review Letters,* [s.l], APS, v. 9, n. 7, p. 309, 1962.

ANDREASSEN, A.; FROST, W.; SCHWARTZ, M. D. Consistent Use of Effective Potentials. *Phys. Rev. D,* [s.l], v. 91, n. 1, p. 016009, 2015.

BAAL, P. van. More (thoughts on) Gribov copies. *Nucl. Phys. B,* [s.l], v. 369, p. 259–275, 1992.

BAULIEU, L. et al. Gribov horizon and i-particles: About a toy model and the construction of physical operators. *Phys. Rev.,* [s.l], D82, p. 025021, 2010.

BECCHI, C.; PIGUET, O. On the Renormalization of Two-dimensional Chiral Models. *Nucl. Phys. B,* [s.l], v. 315, p. 153–165, 1989.

BECCHI, C.; ROUET, A.; STORA, R. The Abelian Higgs-Kibble Model. Unitarity of the S Operator. *Phys. Lett.,* [s.l], v. 52B, p. 344–346, 1974.

BECCHI, C.; ROUET, A.; STORA, R. Renormalization of the Abelian Higgs-Kibble Model. *Commun. Math. Phys.,* [s.l], v. 42, p. 127–162, 1975.

BERNARD, C. W. Monte Carlo Evaluation of the Effective Gluon Mass. *Phys. Lett.,* [s.l], v. 108B, p. 431–434, 1982.

BICUDO, P. et al. Lattice gluon propagator in renormalizable ξ gauges. *Phys. Rev. D,* [s.l], v. 92, n. 11, p. 114514, 2015.

BINOSI, D.; IBANEZ, D.; PAPAVASSILIOU, J. The all-order equation of the effective gluon mass. *Phys. Rev.,* [s.l], D86, p. 085033, 2012.

BINOSI, D.; PAPAVASSILIOU, J. Pinch Technique: Theory and Applications. *Phys. Rept.,* [s.l], v. 479, p. 1–152, 2009.

BINOSI, D.; TRIPOLT, R.-A. Spectral functions of confined particles. *Phys. Lett. B,* [s.l], v. 801, p. 135171, 2020.

BLASI, A.; DELDUC, F.; SORELLA, S. The Background Quantum Split Symmetry in Two-dimensional σ Models: A Regularization Independent Proof of Its Renormalizability. *Nucl. Phys. B,* [s.l], v. 314, p. 409–424, 1989.

BOER, J. de et al. On the renormalizability and unitarity of the Curci-Ferrari model for massive vector bosons. *Phys. Lett.,* [s.l], B367, p. 175–182, 1996.

BOGOLUBSKY, I. L. et al. Lattice gluodynamics computation of Landau gauge Green's functions in the deep infrared. *Phys. Lett.,* [s.l], B676, p. 69–73, 2009.

BORNYAKOV, V. G.; MITRJUSHKIN, V. K.; MULLER-PREUSSKER, M. SU(2) lattice gluon propagator: Continuum limit, finite-volume effects and infrared mass scale m(IR). *Phys. Rev.,* [s.l], D81, p. 054503, 2010.

BOUCAUD, P. et al. The Infrared Behaviour of the Pure Yang-Mills Green Functions. *Few Body Syst.,* [s.l], v. 53, p. 387–436, 2012.

BOUCAUD, P. et al. Discretization effects on renormalized gauge-field Green's functions, scale setting, and the gluon mass. *Phys. Rev.,* [s.l], D98, n. 11, p. 114515, 2018.

BOWMAN, P. O. et al. Scaling behavior and positivity violation of the gluon propagator in full QCD. *Phys. Rev. D,* [s.l], v. 76, p. 094505, 2007.

BRAUN, J.; GIES, H.; PAWLOWSKI, J. M. Quark Confinement from Color Confinement. *Phys. Lett. B,* [s.l], v. 684, p. 262–267, 2010.

CANFORA, F. et al. Effect of the Gribov horizon on the Polyakov loop and vice versa. *Eur. Phys. J. C,* [s.l], v. 75, n. 7, p. 326, 2015.

CAPRI, M. et al. Exact nilpotent nonperturbative BRST symmetry for the Gribov-Zwanziger action in the linear covariant gauge. *Phys. Rev. D,* [s.l], v. 92, n. 4, p. 045039, 2015.

CAPRI, M. et al. Local and BRST-invariant Yang-Mills theory within the Gribov horizon. *Phys. Rev. D,* [s.l], v. 94, n. 2, p. 025035, 2016a.

CAPRI, M. et al. The universal character of Zwanziger's horizon function in Euclidean Yang–Mills theories. *Phys. Lett. B,* [s.l], v. 781, p. 48–54, 2018a.

CAPRI, M. et al. Nonperturbative aspects of Euclidean Yang-Mills theories in linear covariant gauges: Nielsen identities and a BRST-invariant two-point correlation function. *Phys. Rev. D,* [s.l], v. 95, n. 4, p. 045011, 2017a.

CAPRI, M. et al. On a renormalizable class of gauge fixings for the gauge invariant operatoramin2. *Annals of Physics,* [s.l], Elsevier BV, v. 390, p. 214–235, 2018b. ISSN 0003-4916.

CAPRI, M. et al. Local and renormalizable framework for the gauge-invariant operator $A^2_{\min}$ in Euclidean Yang-Mills theories in linear covariant gauges. *Phys. Rev. D,* [s.l], v. 94, n. 6, p. 065009, 2016b.

CAPRI, M. et al. Renormalizability of the refined Gribov-Zwanziger action in linear covariant gauges. *Phys. Rev. D,* [s.l], v. 96, n. 5, p. 054022, 2017b.

CAPRI, M. A. L. et al. Semiclassical analysis of the phases of 4d SU(2) Higgs gauge systems with cutoff at the Gribov horizon. *Phys. Rev.,* [s.l], D88, p. 085022, 2013.

CAPRI, M. A. L. et al. Renormalizability of n=1 super yang–mills theory in landau gauge with a stueckelberg-like field. *The European Physical Journal C,* [s.l], Springer Science and Business Media LLC, v. 78, n. 10, 2018c. ISSN 1434-6052.

CAPRI, M. A. L. et al. More on the nonperturbative Gribov-Zwanziger quantization of linear covariant gauges. *Phys. Rev.,* [s.l], D93, n. 6, p. 065019, 2016c.

CAPRI, M. A. L. et al. Study of the renormalization of BRST invariant local composite operators in the $U(1)$ Higgs model. *Phys. Rev. D,* [s.l], v. 102, n. 3, p. 033003, 2020.

CAUDY, W.; GREENSITE, J. On the ambiguity of spontaneously broken gauge symmetry. *Phys. Rev.,* [s.l], D78, p. 025018, 2008.

CHATRCHYAN, S. et al. Observation of a New Boson at a Mass of 125 GeV with the CMS Experiment at the LHC. *Phys. Lett. B,* [s.l], v. 716, p. 30–61, 2012.

COLANGELO, P.; KHODJAMIRIAN, A. Qcd sum rules, a modern perspective. In: *At The Frontier of Particle Physics: Handbook of QCD (In 3 Volumes).* [S.l.]: World Scientific, 2001. p. 1495–1576.

COLEMAN, S. R.; WEINBERG, E. J. Radiative Corrections as the Origin of Spontaneous Symmetry Breaking. *Phys. Rev. D,* [s.l], v. 7, p. 1888–1910, 1973.

CORNWALL, J. M. Dynamical Mass Generation in Continuum QCD. *Phys. Rev.,* [s.l], D26, p. 1453, 1982.

CORNWALL, J. M. Positivity issues for the pinch-technique gluon propagator and their resolution. *Phys. Rev. D,* [s.l], v. 80, p. 096001, 2009.

CORNWALL, J. M. Positivity violations in QCD. *Mod. Phys. Lett.,* [s.l], A28, p. 1330035, 2013.

CUCCHIERI, A. et al. Modeling the gluon propagator in landau gauge: Lattice estimates of pole masses and dimension-two condensates. *Physical Review D,* [s.l], American Physical Society (APS), v. 85, n. 9, May 2012. ISSN 1550-2368.

CUCCHIERI, A. et al. Modeling the Landau-gauge ghost propagator in 2, 3, and 4 spacetime dimensions. *Phys. Rev. D,* [s.l], v. 93, n. 9, p. 094513, 2016.

CUCCHIERI, A.; DUDAL, D.; VANDERSICKEL, N. No-pole condition in landau gauge: Properties of the gribov ghost form factor and a constraint on the2dgluon propagator. *Physical Review D,* [s.l], American Physical Society (APS), v. 85, n. 8, Apr 2012. ISSN 1550-2368.

CUCCHIERI, A.; MENDES, T. What's up with IR gluon and ghost propagators in Landau gauge? A puzzling answer from huge lattices. *PoS,* [s.l], LATTICE2007, p. 297, 2007.

CUCCHIERI, A.; MENDES, T. Constraints on the IR behavior of the gluon propagator in Yang-Mills theories. *Phys. Rev. Lett.,* [s.l], v. 100, p. 241601, 2008.

CUCCHIERI, A.; MENDES, T. Numerical test of the Gribov-Zwanziger scenario in Landau gauge. *PoS,* [s.l], QCD-TNT09, p. 026, 2009.

CUCCHIERI, A.; MENDES, T. Landau-gauge propagators in Yang-Mills theories at beta = 0: Massive solution versus conformal scaling. *Phys. Rev.,* [s.l], D81, p. 016005, 2010.

CUCCHIERI, A.; MENDES, T. *Crossing the Gribov horizon: an unconventional study of geometric properties of gauge-configuration space in Landau gauge.* arXiv preprint arXiv:1311.4699, 2013.

CUCCHIERI, A. et al. Feynman gauge on the lattice: New results and perspectives. *AIP Conf. Proc.,* [s.l], v. 1354, n. 1, p. 45–50, 2011.

CUCCHIERI, A.; MENDES, T.; SANTOS, E. M. Covariant gauge on the lattice: A New implementation. *Phys. Rev. Lett.,* [s.l], v. 103, p. 141602, 2009.

CUCCHIERI, A.; MENDES, T.; TAURINES, A. R. Positivity violation for the lattice Landau gluon propagator. *Phys. Rev.,* [s.l], D71, p. 051902, 2005.

CURCI, G.; FERRARI, R. On a Class of Lagrangian Models for Massive and Massless Yang-Mills Fields. *Nuovo Cim. A,* [s.l], v. 32, p. 151–168, 1976.

CURCI, G.; FERRARI, R. Slavnov Transformations and Supersymmetry. *Phys. Lett.,* [s.l], v. 63B, p. 91–94, 1976.

CYROL, A. K. et al. Landau gauge Yang-Mills correlation functions. *Phys. Rev.,* [s.l], D94, n. 5, p. 054005, 2016.

DELDUC, F.; SORELLA, S. P. A Note on Some Nonlinear Covariant Gauges in Yang-Mills Theory. *Phys. Lett.,* [s.l], B231, p. 408–410, 1989.

DELL'ANTONIO, G.; ZWANZIGER, D. Ellipsoidal Bound on the Gribov Horizon Contradicts the Perturbative Renormalization Group. *Nucl. Phys. B,* [s.l], v. 326, p. 333–350, 1989.

DELL'ANTONIO, G.; ZWANZIGER, D. Every gauge orbit passes inside the Gribov horizon. *Commun. Math. Phys.,* [s.l], v. 138, p. 291–299, 1991.

DIRAC, P. A. M. The quantum theory of the electron. *Proceedings of the Royal Society of London. Series A, Containing Papers of a Mathematical and Physical Character,* [s.l], The Royal Society London, v. 117, n. 778, p. 610–624, 1928.

DRAGON, N.; HURTH, T.; NIEUWENHUIZEN, P. van. Polynomial form of the Stuckelberg model. *Nucl. Phys. B,* [s.l] Proc. Suppl., v. 56B, p. 318–321, 1997.

DUARTE, A. G.; OLIVEIRA, O.; SILVA, P. J. Lattice Gluon and Ghost Propagators, and the Strong Coupling in Pure SU(3) Yang-Mills Theory: Finite Lattice Spacing and Volume Effects. *Phys. Rev.,* [s.l], D94, n. 1, p. 014502, 2016.

DUDAL, D. et al. *Gauge-invariant spectral description of the $SU(2)$ Higgs model from local composite operators*. To be published.

DUDAL, D. et al. Gauge-invariant spectral description of the $U(1)$ Higgs model from local composite operators. *JHEP,* [s.l], v. 02, p. 188, 2020a.

DUDAL, D. et al. Some remarks on the spectral functions of the Abelian Higgs Model. *Phys. Rev. D,* [s.l], v. 100, n. 6, p. 065009, 2019.

DUDAL, D. et al. A Refinement of the Gribov-Zwanziger approach in the Landau gauge: Infrared propagators in harmony with the lattice results. *Phys. Rev.,* [s.l], D78, p. 065047, 2008a.

DUDAL, D. et al. Spectral representation of lattice gluon and ghost propagators at zero temperature. *Nucl. Phys. B,* [s.l], v. 952, p. 114912, 2020b.

DUDAL, D.; OLIVEIRA, O.; SILVA, P. J. Källén-Lehmann spectroscopy for (un)physical degrees of freedom. *Phys. Rev.,* [s.l], D89, n. 1, p. 014010, 2014.

DUDAL, D.; OLIVEIRA, O.; SILVA, P. J. High precision statistical Landau gauge lattice gluon propagator computation vs. the Gribov–Zwanziger approach. *Annals Phys. ,* [s.l], v. 397, p. 351–364, 2018.

DUDAL, D.; OLIVEIRA, O.; VANDERSICKEL, N. Indirect lattice evidence for the refined gribov-zwanziger formalism and the gluon condensate A^2 in the landau gauge. *Phys. Rev. D,* [s.l], American Physical Society, v. 81, p. 074505, Apr 2010.

DUDAL, D.; SORELLA, S.; VANDERSICKEL, N. The dynamical origin of the refinement of the Gribov-Zwanziger theory. *Phys. Rev. D,* [s.l], v. 84, p. 065039, 2011.

DUDAL, D. et al. New features of the gluon and ghost propagator in the infrared region from the Gribov-Zwanziger approach. *Phys. Rev. D,* [s.l], v. 77, p. 071501, 2008b.

DUDAL, D.; VERCAUTEREN, D. Gauge copies in the Landau–DeWitt gauge: A background invariant restriction. *Phys. Lett. B,* [s.l], v. 779, p. 275–282, 2018.

DUDAL, D.; VERSCHELDE, H.; SORELLA, S. The Anomalous dimension of the composite operator A**2 in the Landau gauge. *Phys. Lett. B,* [s.l], v. 555, p. 126–131, 2003.

EDEN, R. J. et al. *The analytic S-matrix*. Cambridge: Cambridge Univ. Press,[s.l], 1966.

EGMOND, D. M. van; REINOSA, U. *The scalar sunset diagram at finite temperature with imaginary square masses*. 2020.

EINSTEIN, A. *Relativity: The Special and the General Theory-100th Anniversary Edition*. [S.l.]: Princeton University Press, 2019.

EINSTEIN, A. et al. On the electrodynamics of moving bodies. *Annalen der physik,* [s.l], v. 17, n. 10, p. 891–921, 1905.

ELITZUR, S. Impossibility of spontaneously breaking local symmetries. *Physical Review D,* [s.l], APS, v. 12, n. 12, p. 3978, 1975.

ENGLERT, F. The Origin and Status of Spontaneous Symmetry Breaking. *Pontif. Acad. Sci. Scr. Varia,* [s.l], v. 119, p. 379–393, 2011.

ENGLERT, F.; BROUT, R. Broken symmetry and the mass of gauge vector mesons. *Physical Review Letters,* [s.l], APS, v. 13, n. 9, p. 321, 1964.

FERRARI, R.; QUADRI, A. Physical unitarity for massive non-Abelian gauge theories in the Landau gauge: Stueckelberg and Higgs. *JHEP,* [s.l], v. 11, p. 019, 2004.

FISCHER, C. S.; HUBER, M. Q. Landau gauge Yang-Mills propagators in the complex momentum plane. *Phys. Rev. D,* [s.l], v. 102, n. 9, p. 094005, 2020.

FISCHER, C. S.; MAAS, A.; PAWLOWSKI, J. M. On the infrared behavior of Landau gauge Yang-Mills theory. *Annals Phys. ,* [s.l], v. 324, p. 2408–2437, 2009.

FISCHER, C. S.; PAWLOWSKI, J. M. Uniqueness of infrared asymptotics in Landau gauge Yang-Mills theory II. *Phys. Rev. D,* [s.l], v. 80, p. 025023, 2009.

FRADKIN, E. H.; SHENKER, S. H. Phase Diagrams of Lattice Gauge Theories with Higgs Fields. *Phys. Rev.,* [s.l], D19, p. 3682–3697, 1979.

FRASCA, M. Infrared Gluon and Ghost Propagators. *Phys. Lett. B,* [s.l], v. 670, p. 73–77, 2008.

FROHLICH, J.; MORCHIO, G.; STROCCHI, F. Higgs phenomenon without a symmetry breaking order parameter. *Phys. Lett.,* [s.l], v. 97B, p. 249–252, 1980.

FROHLICH, J.; MORCHIO, G.; STROCCHI, F. Higgs phenomenon without symmetry breaking order parameter. *Nucl. Phys.,* [s.l], B190, p. 553–582, 1981.

GAMBINO, P.; GRASSI, P. A. The Nielsen identities of the SM and the definition of mass. *Phys. Rev.,* [s.l], D62, p. 076002, 2000.

GAMBINO, P.; GRASSI, P. A.; MADRICARDO, F. Fermion mixing renormalization and gauge invariance. *Phys. Lett.,* [s.l], B454, p. 98–104, 1999.

GEORGI, H.; GLASHOW, S. L. Unified weak and electromagnetic interactions without neutral currents. *Physical Review Letters,* [s.l], APS, v. 28, n. 22, p. 1494, 1972.

GEORGI, H.; GLASHOW, S. L. Unity of all elementary-particle forces. *Physical Review Letters,* [s.l], APS, v. 32, n. 8, p. 438, 1974.

GIERES, F. *About symmetries in physics*. [S.l.: s.n.], 1997.

GLASHOW, S. Partial Symmetries of Weak Interactions. *Nucl. Phys.,* [s.l], v. 22, p. 579–588, 1961.

GOLDSTONE, J. Field Theories with Superconductor Solutions. *Nuovo Cim.,* [s.l], v. 19, p. 154–164, 1961.

GRACEY, J. Three loop MS-bar renormalization of the Curci-Ferrari model and the dimension two BRST invariant composite operator in QCD. *Phys. Lett. B,* [s.l], v. 552, p. 101–110, 2003.

GRACEY, J. A. et al. Two loop calculation of Yang-Mills propagators in the Curci-Ferrari model. *Phys. Rev. D,* [s.l], v. 100, n. 3, p. 034023, 2019.

GRASSI, P. A.; KNIEHL, B. A.; SIRLIN, A. Width and partial widths of unstable particles. *Phys. Rev. Lett.,* [s.l], v. 86, p. 389–392, 2001.

GRASSI, P. A.; KNIEHL, B. A.; SIRLIN, A. Width and partial widths of unstable particles in the light of the Nielsen identities. *Phys. Rev.,* [s.l], D65, p. 085001, 2002.

GRIBOV, V. N. Quantization of Nonabelian Gauge Theories. *Nucl. Phys.,* [s.l], B139, p. 1, 1978. [,1(1977)].

GROSS, D. J.; WILCZEK, F. Ultraviolet behavior of non-abelian gauge theories. *Physical Review Letters,* [s.l], APS, v. 30, n. 26, p. 1343, 1973.

GURALNIK, G. S.; HAGEN, C. R.; KIBBLE, T. W. Global conservation laws and massless particles. *Physical Review Letters,* [s.l], APS, v. 13, n. 20, p. 585, 1964.

HAUSSLING, R.; KRAUS, E. Gauge parameter dependence and gauge invariance in the Abelian Higgs model. *Z. Phys.,* [s.l], C75, p. 739–750, 1997.

HAYASHI, Y.; KONDO, K.-I. Complex poles and spectral function of Yang-Mills theory. *Phys. Rev.,* [s.l], D99, n. 7, p. 074001, 2019.

HERBST, T. K.; LUECKER, J.; PAWLOWSKI, J. M. *Confinement order parameters and fluctuations*. 10 2015.

HIGGS, P. W. Broken symmetries and the masses of gauge bosons. *Physical Review Letters,* [s.l], APS, v. 13, n. 16, p. 508, 1964.

HOLANDA, O. Renormalizabilidade de teorias de yang-mills massivas com um campo tipo stueckelberg. 2019. 99 f. Tese (Doutorado) - Instituto de Física Armando Dias Tavares, Universidade do Estado do Rio de Janeiro, Rio de janeiro . 2019.

HOOFT, G. et al. *Nonperturbative quantum field theory*. [S.l.]: Springer Science & Business Media, 2012. v. 185.

HOOFT, G. 't. Magnetic Monopoles in Unified Gauge Theories. *Nucl. Phys. B,* [s.l], v. 79, p. 276–284, 1974.

HOOFT, G. 't et al. Recent Developments in Gauge Theories, [s.l]". Proceedings, Nato Advanced Study Institute, Cargese, France, August 26 - September 8, 1979. *NATO Sci. Ser. B*, v. 59, p. pp.1–438, 1980.

HUBER, M. Q. Gluon and ghost propagators in linear covariant gauges. *Phys. Rev. D,* [s.l], v. 91, n. 8, p. 085018, 2015.

HUBER, M. Q. *Nonperturbative properties of Yang-Mills theories*. Tese (habilitation) — Graz U., 2018.

IRGES, N.; KOUTROULIS, F. Renormalization of the Abelian–Higgs model in the R_ξ and Unitary gauges and the physicality of its scalar potential. *Nucl. Phys.,* [s.l], B924, p. 178–278, 2017. [Erratum: Nucl. Phys.B938,957(2019)].

ITZYKSON, C.; DROUFFE, J.-M. *Statistical field theory: volume 2, strong coupling, Monte Carlo methods, conformal field theory and random systems*. [S.l.]: Cambridge University Press, 1991. v. 2.

JEGERLEHNER, F.; KALMYKOV, M. Yu.; VERETIN, O. MS versus pole masses of gauge bosons: Electroweak bosonic two loop corrections. *Nucl. Phys.,* [s.l], B641, p. 285–326, 2002.

JEGERLEHNER, F.; KALMYKOV, M. Yu.; VERETIN, O. MS-bar versus pole masses of gauge bosons. 2. Two loop electroweak fermion corrections. *Nucl. Phys.,* [s.l], B658, p. 49–112, 2003.

KNECHT, K.; VERSCHELDE, H. New start for local composite operators. *Physical Review D,* [s.l], APS, v. 64, n. 8, p. 085006, 2001.

KONDO, K.-I. et al. Reflection positivity and complex analysis of the Yang-Mills theory from a viewpoint of gluon confinement. *Eur. Phys. J. C,* [s.l], v. 80, n. 2, p. 84, 2020.

KREIN, G.; ROBERTS, C. D.; WILLIAMS, A. G. On the implications of confinement. *Int. J. Mod. Phys,* [s.l], A7, p. 5607–5624, 1992.

KROFF, D.; REINOSA, U. Gribov-Zwanziger type model action invariant under background gauge transformations. *Phys. Rev. D,* [s.l], v. 98, n. 3, p. 034029, 2018.

KUGO, T.; OJIMA, I. Manifestly Covariant Canonical Formulation of Yang-Mills Field Theories. 1. The Case of Yang-Mills Fields of Higgs-Kibble Type in Landau Gauge. *Prog. Theor. Phys.,* [s.l], v. 60, p. 1869, 1978.

KUGO, T.; OJIMA, I. Local Covariant Operator Formalism of Nonabelian Gauge Theories and Quark Confinement Problem. *Prog. Theor. Phys.,* [s.l], v. 66, p. 1–130, 1979.

LANDAU, L. et al. On the quantum theory of fields. IN: PAULI, W. (Ed.). *Niels Bohr and the development of physics.*, New York: McGraw-Hill, 1955.

LAVELLE, M.; MCMULLAN, D. Constituent quarks from QCD. *Phys. Rept.,* [s.l], v. 279, p. 1–65, 1997.

LOGAN, H. E. *TASI 2013 lectures on Higgs physics within and beyond the Standard Model*. 2014.

LOWDON, P. Non-perturbative constraints on the quark and ghost propagators. *Nucl. Phys.,* [s.l], B935, p. 242–255, 2018.

MAAS, A. More on Gribov copies and propagators in Landau-gauge Yang-Mills theory. *Phys. Rev.,* [s.l], D79, p. 014505, 2009.

MAAS, A. Field theory as a tool to constrain new physics models. *Mod. Phys. Lett.,* [s.l], A30, n. 29, p. 1550135, 2015.

MAAS, A. Brout-Englert-Higgs physics: From foundations to phenomenology. *Prog. Part. Nucl. Phys.,* [s.l], v. 106, p. 132–209, 2019.

MAAS, A.; MUFTI, T. Two- and three-point functions in Landau gauge Yang-Mills-Higgs theory. *JHEP,* [s.l], v. 04, p. 006, 2014.

MAAS, A.; SONDENHEIMER, R.; TÖREK, P. On the observable spectrum of theories with a brout–englert–higgs effect. *Annals of Physics,* [s.l], Elsevier, v. 402, p. 18–44, 2019.

MAAS, A.; SONDENHEIMER, R.; TOREK, P. On the observable spectrum of theories with a Brout–Englert–Higgs effect. *Annals Phys. ,* [s.l], v. 402, p. 18–44, 2019.

MAELGER, J.; REINOSA, U.; SERREAU, J. Perturbative study of the QCD phase diagram for heavy quarks at nonzero chemical potential: Two-loop corrections. *Phys. Rev. D,* [s.l], v. 97, n. 7, p. 074027, 2018.

MARTIN, S. P. Pole Mass of the W Boson at Two-Loop Order in the Pure $\overline{MS}$ Scheme. *Phys. Rev.,* [s.l], D91, n. 11, p. 114003, 2015.

MARTIN, S. P. Z-Boson Pole Mass at Two-Loop Order in the Pure $\overline{MS}$ Scheme. *Phys. Rev.,* [s.l], D92, n. 1, p. 014026, 2015.

MAXWELL, J. C. Viii. a dynamical theory of the electromagnetic field. *Philosophical transactions of the Royal Society of London,* [s.l], The Royal Society London, n. 155, p. 459–512, 1865.

MINTZ, B. W. et al. Infrared massive gluon propagator from a brst-invariant gribov horizon in a family of covariant gauges. *Physical Review D,* [s.l], American Physical Society (APS), v. 99, n. 3, Feb 2019. ISSN 2470-0029.

NAMBU, Y. Quasiparticles and Gauge Invariance in the Theory of Superconductivity. *Phys. Rev.,* [s.l], v. 117, p. 648–663, 1960.

NIELSEN, N. K. On the Gauge Dependence of Spontaneous Symmetry Breaking in Gauge Theories. *Nucl. Phys.,* [s.l], B101, p. 173–188, 1975.

OEHME, R. On superconvergence relations in quantum chromodynamics. *Phys. Lett.,* [s.l], B252, p. 641–646, 1990.

OEHME, R.; ZIMMERMANN, W. Quark and Gluon Propagators in Quantum Chromodynamics. *Phys. Rev.,* [s.l], D21, p. 471, 1980.

OJIMA, I. Comments on Massive and Massless Yang-Mills Lagrangians With a Quartic Coupling of Faddeev-popov Ghosts. *Z. Phys.,* [s.l], C13, p. 173, 1982.

OLIVEIRA, O.; SILVA, P. J. The lattice Landau gauge gluon propagator: lattice spacing and volume dependence. *Phys. Rev.,* [s.l], D86, p. 114513, 2012.

PARISI, G.; PETRONZIO, R. On Low-Energy Tests of QCD. *Phys. Lett.,* [s.l], v. 94B, p. 51–53, 1980.

PASSARINO, G.; VELTMAN, M. J. G. One Loop Corrections for e+ e- Annihilation Into mu+ mu- in the Weinberg Model. *Nucl. Phys.,* [s.l], B160, p. 151–207, 1979.

PESKIN, M. E.; SCHROEDER, D. V. *An Introduction to quantum field theory.* Reading, USA: Addison-Wesley, 1995. ISBN 9780201503975, 0201503972.

PIGUET, O.; SIBOLD, K. Renormalization of $N = 1$ Supersymmetrical Yang-Mills Theories. 2. The Radiative Corrections. *Nucl. Phys. B,* [s.l], v. 197, p. 272–289, 1982.

PIGUET, O.; SIBOLD, K. Gauge Independence in Ordinary Yang-Mills Theories. *Nucl. Phys.,* [s.l], B253, p. 517–540, 1985.

PIGUET, O.; SORELLA, S. P. Algebraic renormalization: Perturbative renormalization, symmetries and anomalies. *Lect. Notes Phys. Monogr.,* [s.l], v. 28, p. 1–134, 1995.

PLANCK, M.; MASIUS, M. *The theory of heat radiation.* [S.l.]: Blakiston, 1914.

POLITZER, H. D. Reliable perturbative results for strong interactions? *Physical Review Letters,* [s.l], APS, v. 30, n. 26, p. 1346, 1973.

REINOSA, U. *Perturbative aspects of the deconfinement transition - Physics beyond the Faddeev-Popov model.* 2019. Habilitation thesis- École Polytechnique, Institut Polytechnique de Paris, 2019.

REINOSA, U.; SERREAU, J.; TISSIER, M. Perturbative study of the QCD phase diagram for heavy quarks at nonzero chemical potential. *Phys. Rev. D,* [s.l], v. 92, p. 025021, 2015.

REINOSA, U. et al. Deconfinement transition in SU(2) Yang-Mills theory: A two-loop study. *Phys. Rev.,* [s.l], D91, p. 045035, 2015a.

REINOSA, U. et al. Deconfinement transition in SU(N) theories from perturbation theory. *Phys. Lett. B,* [s.l], v. 742, p. 61–68, 2015b.

REINOSA, U. et al. Two-loop study of the deconfinement transition in Yang-Mills theories: SU(3) and beyond. *Phys. Rev. D,* [s.l], v. 93, n. 10, p. 105002, 2016.

RIPKA, G. *Dual superconductor models of color confinement.* [S.l.: s.n.], 2004. v. 639.

ROBERTS, C. D.; WILLIAMS, A. G. Dyson-Schwinger equations and their application to hadronic physics. *Prog. Part. Nucl. Phys.,* [s.l], v. 33, p. 477–575, 1994.

RUEGG, H.; RUIZ-ALTABA, M. The Stueckelberg field. *Int. J. Mod. Phys,* [s.l].

SALAM, A. Weak and Electromagnetic Interactions. *Conf. Proc. C,* [s.l], v. 680519, p. 367–377, 1968.

SANCHIS-ALEPUZ, H. et al. Glueballs from the Bethe-Salpeter equation. *Phys. Rev.,* [s.l], D92, p. 034001, 2015.

SCHRÖDINGER, E. An undulatory theory of the mechanics of atoms and molecules. *Physical review,* [s.l], APS, v. 28, n. 6, p. 1049, 1926.

SERREAU, J.; TISSIER, M. Lifting the Gribov ambiguity in Yang-Mills theories. *Phys. Lett.,* [s.l], B712, p. 97–103, 2012.

SIRINGO, F. Analytical study of Yang–Mills theory in the infrared from first principles. *Nucl. Phys. B,* [s.l], v. 907, p. 572–596, 2016.

SMEKAL, L. von; HAUCK, A.; ALKOFER, R. Infrared behavior of gluon and ghost propagators in landau gauge qcd. *Phys. Rev. Lett.,*[s.l], American Physical Society, v. 79, p. 3591–3594, Nov 1997.

SMEKAL, L. von; HAUCK, A.; ALKOFER, R. A Solution to Coupled Dyson–Schwinger Equations for Gluons and Ghosts in Landau Gauge. *Annals Phys. ,* [s.l], v. 267, p. 1–60, 1998. [Erratum: Annals Phys. , [s.l] 269, 182 (1998)].

STRAUSS, S.; FISCHER, C. S.; KELLERMANN, C. Analytic structure of the Landau gauge gluon propagator. *Phys. Rev. Lett.,* [s.l], v. 109, p. 252001, 2012.

TISSIER, M. Gribov copies, avalanches and dynamic generation of a gluon mass. *Phys. Lett. B,* [s.l], v. 784, p. 146–150, 2018.

TISSIER, M.; WSCHEBOR, N. Infrared propagators of Yang-Mills theory from perturbation theory. *Phys. Rev.,* [s.l], D82, p. 101701, 2010.

TISSIER, M.; WSCHEBOR, N. An Infrared Safe perturbative approach to Yang-Mills correlators. *Phys. Rev.,* [s.l], D84, p. 045018, 2011.

VANDERSICKEL, N. *A study of the Gribov-Zwanziger action: from propagators to glueballs.* 2011. Thesis (Ph.D. in Physics) – Faculty of Sciences, Universiteit Gent, Gent, 2011.

VANDERSICKEL, N.; ZWANZIGER, D. The Gribov problem and QCD dynamics. *Phys. Rept.,* [s.l], v. 520, p. 175–251, 2012.

VERLINDE, E. P. Emergent Gravity and the Dark Universe. *SciPost Phys.,* [s.l], v. 2, n. 3, p. 016, 2017.

WEBER, A. Epsilon Expansion for Infrared Yang-Mills theory in Landau Gauge. *Phys. Rev. D,* [s.l], v. 85, p. 125005, 2012.

WEINBERG, S. A Model of Leptons. *Phys. Rev. Lett.,* [s.l], v. 19, p. 1264–1266, 1967.

WINDISCH, A.; HUBER, M. Q.; ALKOFER, R. On the analytic structure of scalar glueball operators at the Born level. *Phys. Rev.,* [s.l], D87, n. 6, p. 065005, 2013.

YANG, C.-N.; MILLS, R. L. Conservation of Isotopic Spin and Isotopic Gauge Invariance. *Phys. Rev.,* [s.l], v. 96, p. 191–195, 1954.

ZWANZIGER, D. Local and Renormalizable Action From the Gribov Horizon. *Nucl. Phys.,* [s.l], B323, p. 513–544, 1989.

ZWANZIGER, D. Quantization of Gauge Fields, Classical Gauge Invariance and Gluon Confinement. *Nucl. Phys. B,* [s.l], v. 345, p. 461–471, 1990.

ZWANZIGER, D. Renormalizability of the critical limit of lattice gauge theory by BRS invariance. *Nucl. Phys.,* [s.l], B399, p. 477–513, 1993.

ZWANZIGER, D. Nonperturbative Landau gauge and infrared critical exponents in QCD. *Phys. Rev.,* [s.l], D65, p. 094039, 2002.

APPENDIX A – Properties of the functional $f_A[u]$.

In this Appendix we recall some useful properties of the functional $f_A[u]$

$$f_A[u] \equiv \mathrm{Tr} \int d^4x \, A^u_\mu A^u_\mu = \mathrm{Tr} \int d^4x \left(u^\dagger A_\mu u + \frac{i}{g} u^\dagger \partial_\mu u \right) \left(u^\dagger A_\mu u + \frac{i}{g} u^\dagger \partial_\mu u \right) . \tag{390}$$

For a given gauge field configuration A_μ, $f_A[u]$ is a functional defined on the gauge orbit of A_μ. Let $\mathcal{A}$ be the space of connections A^a_μ with finite Hilbert norm $||A||$, *i.e.*

$$||A||^2 = \mathrm{Tr} \int d^4x \, A_\mu A_\mu = \frac{1}{2} \int d^4x A^a_\mu A^a_\mu < +\infty , \tag{391}$$

and let $\mathcal{U}$ be the space of local gauge transformations u such that the Hilbert norm $||u^\dagger \partial u||$ is finite too, namely

$$||u^\dagger \partial u||^2 = \mathrm{Tr} \int d^4x \, \left(u^\dagger \partial_\mu u \right) \left(u^\dagger \partial_\mu u \right) < +\infty . \tag{392}$$

The following proposition holds (ZWANZIGER, 1990; DELL'ANTONIO; ZWANZIGER, 1989; DELL'ANTONIO; ZWANZIGER, 1991; BAAL, 1992)

- Proposition
  The functional $f_A[u]$ achieves its absolute minimum on the gauge orbit of A_μ.

This proposition means that there exists a $h \in \mathcal{U}$ such that

$$\delta f_A = 0 , \tag{393}$$

$$\delta^2 f_A \geq 0 , \tag{394}$$

$$f_A \leq f_A[u] , \qquad \forall \, u \in \mathcal{U} . \tag{395}$$

The operator $A^2_{\min}$ is thus given by

$$A^2_{\min} = \min_{\{u\}} \mathrm{Tr} \int d^4x \, A^u_\mu A^u_\mu = f_A . \tag{396}$$

Let us give a look at the two conditions (393) and (394). To evaluate δf_A and $\delta^2 f_A$ we set[14]

$$v = h e^{ig\omega} = h e^{ig\omega^a T^a} , \tag{397}$$

[14] The case of the gauge group $SU(N)$ is considered here.

$$\left[T^a, T^b\right] = i f^{abc}\, T^c \;, \qquad \mathrm{Tr}\left(T^a T^b\right) = \frac{1}{2}\delta^{ab} \;, \tag{398}$$

where ω is an infinitesimal hermitian matrix and we compute the linear and quadratic terms of the expansion of the functional $f_A[v]$ in power series of ω. Let us first obtain an expression for A^v_μ

$$\begin{aligned} A^v_\mu &= v^\dagger A_\mu v + \frac{i}{g} v^\dagger \partial_\mu v \\ &= e^{-ig\omega} h^\dagger A_\mu h e^{ig\omega} + \frac{i}{g} e^{-ig\omega}\left(h^\dagger \partial_\mu h\right) e^{ig\omega} + \frac{i}{g} e^{-ig\omega} \partial_\mu e^{ig\omega} \\ &= e^{-ig\omega} A^h_\mu e^{ig\omega} + \frac{i}{g} e^{-ig\omega} \partial_\mu e^{ig\omega} \;. \end{aligned} \tag{399}$$

Expanding up to the order ω^2, we get

$$\begin{aligned} A^v_\mu &= \left(1 - ig\omega - g^2\frac{\omega^2}{2}\right) A^h_\mu \left(1 + ig\omega - g^2\frac{\omega^2}{2}\right) \\ &+ \frac{i}{g}\left(1 - ig\omega - g^2\frac{\omega^2}{2}\right) \partial_\mu \left(1 + ig\omega - g^2\frac{\omega^2}{2}\right) \\ &= \left(1 - ig\omega - g^2\frac{\omega^2}{2}\right)\left(A^h_\mu + igA^h_\mu\omega - g^2 A^h_\mu \frac{\omega^2}{2}\right) + \\ &+ \frac{i}{g}\left(1 - ig\omega - g^2\frac{\omega^2}{2}\right)\left(ig\partial_\mu\omega - \frac{g^2}{2}\left(\partial_\mu\omega\right)\omega - \frac{g^2}{2}\omega\left(\partial_\mu\omega\right)\right) \\ &= A^h_\mu + igA^h_\mu\omega - \frac{g^2}{2}A^h_\mu\omega^2 - ig\omega A^h_\mu + g^2\omega A^h_\mu\omega - \frac{g^2}{2}\omega^2 A^h_\mu \\ &+ \frac{i}{g}\left(ig\partial_\mu\omega - \frac{g^2}{2}\left(\partial_\mu\omega\right)\omega - \frac{g^2}{2}\omega\partial_\mu\omega + g^2\omega\partial_\mu\omega\right) + O(\omega^3) \;, \end{aligned} \tag{400}$$

from which it follows

$$A^v_\mu = A^h_\mu + ig[A^h_\mu, \omega] + \frac{g^2}{2}[[\omega, A^h_\mu], \omega] - \partial_\mu\omega + i\frac{g}{2}[\omega, \partial_\mu\omega] + O(\omega^3) \;, \tag{401}$$

We now evaluate

$$\begin{aligned} f_A[v] &= \mathrm{Tr}\int d^4x A^u_\mu A^u_\mu \\ &= \mathrm{Tr}\int d^4x \left[\left(A^h_\mu + ig[A^h_\mu, \omega] + \frac{g^2}{2}[[\omega, A^h_\mu], \omega] - \partial_\mu\omega + i\frac{g}{2}[\omega, \partial_\mu\omega] + O(\omega^3)\right) \times \right. \\ &\quad \left. \left(A^h_\mu + ig[A^h_\mu, \omega] + \frac{g^2}{2}[[\omega, A^h_\mu], \omega] - \partial_\mu\omega + i\frac{g}{2}[\omega, \partial_\mu\omega] + O(\omega^3)\right)\right] \\ &= \mathrm{Tr}\int d^4x \left\{A^h_\mu A^h_\mu + igA^h_\mu[A^h_\mu, \omega] + g^2 A^h_\mu\omega A^h_\mu\omega \right. \\ &- \left. \frac{g^2}{2}A^h_\mu A^h_\mu\omega^2 - \frac{g^2}{2}A^h_\mu\omega^2 A^h_\mu - A^h_\mu\partial_\mu\omega \right. \end{aligned}$$

$$
\begin{aligned}
&+ \quad i\frac{g}{2}A^h_\mu[\omega,\partial_\mu\omega] + ig[A^h_\mu,\omega]A^h_\mu - g^2[A^h_\mu,\omega][A^h_\mu,\omega] - ig[A^h_\mu,\omega]\partial_\mu\omega + g^2\omega A^h_\mu\omega A^h_\mu \\
&- \quad \frac{g^2}{2}A^h_\mu\omega^2 A^h_\mu - \frac{g^2}{2}\omega^2 A^h_\mu A^h_\mu - \partial_\mu\omega A^h_\mu - ig\partial_\mu\omega[A^h_\mu,\omega] + \partial_\mu\omega\partial_\mu\omega + i\frac{g}{2}[\omega,\partial_\mu\omega]A^h_\mu\Big\} \\
&+ \quad O(\omega^3) \\
&= \quad f_A - \mathrm{Tr}\int d^4x\ \left\{A^h_\mu,\partial_\mu\omega\right\} \\
&+ \quad \mathrm{Tr}\int d^4x\ \Big(g^2A^h_\mu\omega A^h_\mu\omega - \frac{g^2}{2}A^h_\mu A^h_\mu\omega^2 - \frac{g^2}{2}A^h_\mu\omega^2A^h_\mu \\
&- \quad g^2[A^h_\mu,\omega][A^h_\mu,\omega] + g^2\omega A^h_\mu\omega A^h_\mu - \frac{g^2}{2}A^h_\mu\omega^2A^h_\mu - \frac{g^2}{2}\omega^2A^h_\mu A^h_\mu\Big) \\
&+ \quad \mathrm{Tr}\int d^4x\ (\partial_\mu\omega\partial_\mu\omega \\
&+ \quad i\frac{g}{2}[\omega,\partial_\mu\omega]A^h_\mu - ig\partial_\mu\omega[A^h_\mu,\omega] - ig[A^h_\mu,\omega]\partial_\mu\omega + i\frac{g}{2}A^h_\mu[\omega,\partial_\mu\omega]\Big) \\
&+ \quad O(\omega^3)
\end{aligned}
$$

$$
\begin{aligned}
&= \quad f_A + 2\int d^4x\, tr\left(\omega\partial_\mu A^h_\mu\right) + \int d^4x\, tr\left\{2g^2\omega A^h_\mu\omega A^h_\mu - 2g^2A^h_\mu A^h_\mu\omega^2\right. \\
&- \quad \left. g^2\left(A^h_\mu\omega - \omega A^h_\mu\right)\left(A^h_\mu\omega - \omega A^h_\mu\right)\right\} + \int d^4x\, tr\Big(\partial_\mu\omega\partial_\mu\omega + i\frac{g}{2}\omega\partial_\mu\omega A^h_\mu - i\frac{g}{2}\partial_\mu\omega\omega A^h_\mu \\
&- \quad ig\partial_\mu\omega A^h_\mu\omega + ig\partial_\mu\omega\omega A^h_\mu - igA^h_\mu\omega\partial_\mu\omega + ig\omega A^h_\mu\partial_\mu\omega + i\frac{g}{2}A^h_\mu\omega\partial_\mu\omega - i\frac{g}{2}A^h_\mu\partial_\mu\omega\omega\Big) \\
&+ \quad O(\omega^3) \\
&= \quad f_A + 2\mathrm{Tr}\int d^4x\left(\omega\partial_\mu A^h_\mu\right) + \mathrm{Tr}\int d^4x\ \left(\partial_\mu\omega\partial_\mu\omega + ig\omega\partial_\mu\omega A^h_\mu - ig\partial_\mu\omega\omega A^h_\mu\right. \\
&- \quad \left. 2ig\partial_\mu\omega A^h_\mu\omega + 2ig\partial_\mu\omega\omega A^h_\mu\right) + O(\omega^3)\ . \qquad (402)
\end{aligned}
$$

Thus

$$
\begin{aligned}
f_A[v] \quad &= \quad f_A + 2\mathrm{Tr}\int d^4x\ \left(\omega\partial_\mu A^h_\mu\right) + \mathrm{Tr}\int d^4x\ \left(\partial_\mu\omega\partial_\mu\omega + ig\omega\partial_\mu\omega A^h_\mu - ig\partial_\mu\omega\omega A^h_\mu\right. \\
&- \quad \left. ig\left(\partial_\mu\omega\right)A^h_\mu\omega + ig\left(\partial_\mu\omega\right)\omega A^h_\mu\right) + O(\omega^3) \\
&= \quad f_A + 2\mathrm{Tr}\int d^4x\ \left(\omega\partial_\mu A^h_\mu\right) + \mathrm{Tr}\int d^4x\ \left\{\partial_\mu\omega\left(\partial_\mu\omega - ig\left[A^h_\mu,\omega\right]\right)\right\} + O(\omega^3)\ . \qquad (403)
\end{aligned}
$$

Finally

$$
f_A[v] = f_A + 2\mathrm{Tr}\int d^4x\ \left(\omega\partial_\mu A^h_\mu\right) - \mathrm{Tr}\int d^4x\,\omega\partial_\mu D_\mu(A^h)\omega + O(\omega^3)\ , \qquad (404)
$$

so that

$$
\begin{aligned}
\delta f_A \quad &= \quad 0 \quad \Rightarrow \quad \partial_\mu A^h_\mu \ = \ 0\ , \\
\delta^2 f_A \quad &> \quad 0 \quad \Rightarrow \quad -\partial_\mu D_\mu(A^h) \ > \ 0\ . \qquad (405)
\end{aligned}
$$

We see therefore that the set of field configurations fulfilling conditions (405), *i.e.* defining relative minima of the functional $f_A[u]$, belong to the so called Gribov region Ω, which is defined as

$$\Omega = \{A_\mu |\, \partial_\mu A_\mu = 0 \text{ and } -\partial_\mu D_\mu(A) > 0\} \; . \tag{406}$$

Let us proceed now by showing that the transversality condition, $\partial_\mu A^h_\mu = 0$, can be solved for $h = h(A)$ as a power series in A_μ. We start from

$$A^h_\mu = h^\dagger A_\mu h + \frac{i}{g} h^\dagger \partial_\mu h \; , \tag{407}$$

with

$$h = e^{ig\phi} = e^{ig\phi^a T^a} \; . \tag{408}$$

Let us expand h in powers of ϕ

$$h = 1 + ig\phi - \frac{g^2}{2}\phi^2 + O(\phi^3) \; . \tag{409}$$

From equation (407) we have

$$A^h_\mu = A_\mu + ig[A_\mu, \phi] + g^2 \phi A_\mu \phi - \frac{g^2}{2} A_\mu \phi^2 - \frac{g^2}{2}\phi^2 A_\mu - \partial_\mu \phi + i\frac{g}{2}[\phi, \partial_\mu] + O(\phi^3) \; . \tag{410}$$

Thus, condition $\partial_\mu A^h_\mu = 0$, gives

$$\begin{aligned} \partial^2 \phi &= \partial_\mu A + ig[\partial_\mu A_\mu, \phi] + ig[A_\mu, \partial_\mu \phi] + g^2 \partial_\mu \phi A_\mu \phi + g^2 \phi \partial_\mu A_\mu \phi + g^2 \phi A_\mu \partial_\mu \phi \\ &- \frac{g^2}{2}\partial_\mu A_\mu \phi^2 - \frac{g^2}{2} A_\mu \partial_\mu \phi \phi - \frac{g^2}{2} A_\mu \phi \partial_\mu \phi - \frac{g^2}{2}\partial_\mu \phi \phi A_\mu - \frac{g^2}{2}\phi \partial_\mu \phi A_\mu - \frac{g^2}{2}\phi^2 \partial_\mu A_\mu \\ &+ i\frac{g}{2}[\phi, \partial^2 \phi] + O(\phi^3) \; . \end{aligned} \tag{411}$$

This equation can be solved iteratively for ϕ as a power series in A_μ, namely

$$\phi = \frac{1}{\partial^2}\partial_\mu A_\mu + i\frac{g}{\partial^2}\left[\partial A, \frac{\partial A}{\partial^2}\right] + i\frac{g}{\partial^2}\left[A_\mu, \partial_\mu \frac{\partial A}{\partial^2}\right] + \frac{i}{2}\frac{g}{\partial^2}\left[\frac{\partial A}{\partial^2}, \partial A\right] + O(A^3) \; , \tag{412}$$

so that

$$\begin{aligned} A^h_\mu &= A_\mu - \frac{1}{\partial^2}\partial_\mu \partial A - ig\frac{\partial_\mu}{\partial^2}\left[A_\nu, \partial_\nu \frac{\partial A}{\partial^2}\right] - i\frac{g}{2}\frac{\partial_\mu}{\partial^2}\left[\partial A, \frac{1}{\partial^2}\partial A\right] \\ &+ ig\left[A_\mu, \frac{1}{\partial^2}\partial A\right] + i\frac{g}{2}\left[\frac{1}{\partial^2}\partial A, \frac{\partial_\mu}{\partial^2}\partial A\right] + O(A^3) \; . \end{aligned} \tag{413}$$

Expression (413) can be written in a more useful way, given in eq.(79). In fact

$$\begin{aligned}
A^h_\mu &= \left(\delta_{\mu\nu} - \frac{\partial_\mu\partial_\nu}{\partial^2}\right)\left(A_\nu - ig\left[\frac{1}{\partial^2}\partial A, A_\nu\right] + \frac{ig}{2}\left[\frac{1}{\partial^2}\partial A, \partial_\nu\frac{1}{\partial^2}\partial A\right]\right) + O(A^3) \\
&= A_\mu - ig\left[\frac{1}{\partial^2}\partial A, A_\mu\right] + \frac{ig}{2}\left[\frac{1}{\partial^2}\partial A, \partial_\mu\frac{1}{\partial^2}\partial A\right] - \frac{\partial_\mu}{\partial^2}\partial A + ig\frac{\partial_\mu}{\partial^2}\partial_\nu\left[\frac{1}{\partial^2}\partial A, A_\nu\right] \\
&- i\frac{g}{2}\frac{\partial_\mu}{\partial^2}\partial_\nu\left[\frac{\partial A}{\partial^2}, \frac{\partial_\nu}{\partial^2}\partial A\right] + O(A^3) \\
&= A_\mu - \frac{\partial_\mu}{\partial^2}\partial A + ig\left[A_\mu, \frac{1}{\partial^2}\partial A\right] + \frac{ig}{2}\left[\frac{1}{\partial^2}\partial A, \partial_\mu\frac{1}{\partial^2}\partial A\right] + ig\frac{\partial_\mu}{\partial^2}\left[\frac{\partial_\nu}{\partial^2}\partial A, A_\nu\right] \\
&+ i\frac{g}{2}\frac{\partial_\mu}{\partial^2}\left[\frac{\partial A}{\partial^2}, \partial A\right] + O(A^3) \qquad (414)
\end{aligned}$$

which is precisely expression (413). The transverse field given in eq.(79) enjoys the property of being gauge invariant order by order in the coupling constant g. Let us work out the transformation properties of ϕ_ν under a gauge transformation

$$\delta A_\mu = -\partial_\mu\omega + ig[A_\mu, \omega] \; . \qquad (415)$$

We have, up to the order $O(g^2)$,

$$\begin{aligned}
\delta\phi_\nu &= -\partial_\nu\omega + ig\left[\frac{1}{\partial^2}\partial A, \partial_\nu\omega\right] - i\frac{g}{2}\left[\omega, \partial_\nu\frac{1}{\partial^2}\partial A\right] - i\frac{g}{2}\left[\frac{\partial A}{\partial^2}, \partial_\nu\omega\right] + O(g^2) \\
&= -\partial_\nu\omega + i\frac{g}{2}\left[\frac{1}{\partial^2}\partial A, \partial_\nu\omega\right] + i\frac{g}{2}\left[\partial_\nu\frac{1}{\partial^2}\partial A, \omega\right] + O(g^2) \; . \qquad (416)
\end{aligned}$$

Therefore

$$\delta\phi_\nu = -\partial_\nu\left(\omega - i\frac{g}{2}\left[\frac{\partial A}{\partial^2}, \omega\right]\right) + O(g^2) \; , \qquad (417)$$

from which the gauge invariance of A^h_μ is established.

Finally, let us work out the expression of $A^2_{\rm min}$ as a power series in A_μ.

$$\begin{aligned}
& A^2_{\rm min} = \\
& {\rm Tr}\int d^4x\, A^h_\mu A^h_\mu \\
= \; & {\rm Tr}\int d^4x\, \left[\phi_\mu\left(\delta_{\mu\nu} - \frac{\partial_\mu\partial_\nu}{\partial^2}\right)\phi_\nu\right] \\
= \; & {\rm Tr}\int d^4x\, \left[\left(A_\mu - ig\left[\frac{1}{\partial^2}\partial A, A_\mu\right] + \frac{ig}{2}\left[\frac{1}{\partial^2}\partial A, \partial_\mu\frac{1}{\partial^2}\partial A\right]\right)\times \right. \\
& \left.\left(\delta_{\mu\nu} - \frac{\partial_\mu\partial_\nu}{\partial^2}\right)\left(A_\nu - ig\left[\frac{1}{\partial^2}\partial A, A_\nu\right] + \frac{ig}{2}\left[\frac{1}{\partial^2}\partial A, \partial_\nu\frac{1}{\partial^2}\partial A\right]\right)\right]
\end{aligned}$$

$$
\begin{aligned}
&= \frac{1}{2}\int d^4x \left[A^a_\mu \left(\delta_{\mu\nu} - \frac{\partial_\mu \partial_\nu}{\partial^2} \right) A^a_\nu - 2g f^{abc} \frac{\partial_\nu \partial A^a}{\partial^2} \frac{\partial A^b}{\partial^2} A^c_\nu - g f^{abc} A^a_\nu \frac{\partial A^b}{\partial^2} \frac{\partial_\nu \partial A^c}{\partial^2} \right] \\
&+ O(A^4). \qquad (418)
\end{aligned}
$$

We conclude this Appendix by noting that, due to gauge invariance, $A^2_{\min}$ can be rewritten in a manifestly invariant way in terms of $F_{\mu\nu}$ and the covariant derivative D_μ (ZWANZIGER, 1990).

APPENDIX B – A generalised Slavnov-Taylor identity

In this Appendix we derive the Ward identities for the generalised gauge fixing of eq.(97). Since the quantity $\omega^a(\xi)$ is now a composite operator, *i.e.* a product of fields at the same space-time point, we need to define $\omega^a(\xi)$ by introducing it into the starting action though a suitable external source. In order to maintain BRST invariance, we make use of a BRST doublet of external sources (Q^a, R^a), of dimension four and ghost number $(-1, 0)$,

$$sQ^a = R^a \ , \qquad sR^a = 0 \ , \tag{419}$$

and introduce the term

$$\int d^4x \ s\left(Q^a\omega^a(\xi)\right) = \int d^4x \left(R^a\omega^a(\xi) - Q^a\frac{\partial\omega^a}{\partial\xi^c}g^{cd}(\xi)c^d\right) \ . \tag{420}$$

We start thus with the complete classical action Σ given now by

$$\begin{aligned}
\Sigma &= S_{inv} + \int d^4x \left(\mathcal{J}^a_\mu A^{ah}_\mu + \Xi^a_\mu D^{ab}_\mu(A^h)\eta^b\right) \\
&+ \int d^4x \Big(ib^a\partial_\mu A^a_\mu + \frac{\alpha}{2}b^ab^a - iM^{ab}b^a\omega^b(\xi) - N^{ab}\bar{c}^a\omega^b(\xi) \\
&+ \bar{c}^a\partial_\mu D^{ab}_\mu c^b + M^{ab}\bar{c}^a\frac{\partial\omega^b(\xi)}{\partial\xi^c}g^{cd}(\xi)c^d\Big) \\
&+ \int d^4x \left(-\Omega^a_\mu D^{ab}_\mu c^b + L^a\frac{gf^{abc}}{2}c^bc^c + K^ag^{ab}(\xi)c^d + R^a\omega^a(\xi) - Q^a\frac{\partial\omega^a}{\partial\xi^c}g^{cd}(\xi)c^d\right) ,
\end{aligned} \tag{421}$$

with S_{inv} given by expression (85).

The action Σ, eq.(421), obeys the following Ward identities:

- the Slavnov-Taylor identity

$$\int d^4x \left(\frac{\delta\Sigma}{\delta A^a_\mu}\frac{\delta\Sigma}{\delta\Omega^a_\mu} + \frac{\delta\Sigma}{\delta c^a}\frac{\delta\Sigma}{\delta L^a} + \frac{\delta\Sigma}{\delta\xi^a}\frac{\delta\Sigma}{\delta K^a} + ib^a\frac{\delta\Sigma}{\delta\bar{c}^a} + N^{ab}\frac{\delta\Sigma}{\delta M^{ab}} + R^a\frac{\delta\Sigma}{\delta Q^a}\right) = 0 \ , \tag{422}$$

- the equation of motion of the Lagrange multiplier b^a

$$\frac{\delta\Sigma}{\delta b^a} = i\partial_\mu A^a_\mu + \alpha b^a - iM^{ab}\frac{\delta\Sigma}{\delta R^b} \ , \tag{423}$$

- the anti-ghost equation

$$\frac{\delta\Sigma}{\delta\bar{c}^a} + \partial_\mu \frac{\delta\Sigma}{\delta\Omega^a_\mu} + M^{ab}\frac{\delta\Sigma}{\delta Q^b} - N^{ab}\frac{\delta\Sigma}{\delta R^b} = 0 \,, \tag{424}$$

- the equation of τ^a

$$\frac{\delta\Sigma}{\delta\tau^a} - \partial_\mu \frac{\delta\Sigma}{\delta\mathcal{J}^a_\mu} \;=\; 0 \,, \tag{425}$$

- the equation of the ghost η^a

$$\int d^4x \left(\frac{\delta\Sigma}{\delta\eta^a} + g f^{abc}\bar{\eta}^b \frac{\delta\Sigma}{\delta\tau^c} + g f^{abc}\Xi^b \frac{\delta\Sigma}{\delta\mathcal{J}^c_\mu} \right) \;=\; 0 \,, \tag{426}$$

- the equation of the antighost $\bar{\eta}^a$

$$\frac{\delta\Sigma}{\delta\bar{\eta}^a} - \partial_\mu \frac{\delta\Sigma}{\delta\Xi^a_\mu} \;=\; 0 \,. \tag{427}$$

These Ward identities can be employed for the analysis of the algebraic renormalization when the generalised function $\omega^a(\xi)$ is explicitly present in the gauge-fixing. In this case, the general counterterm will be reabsorbed through a renormalization of $\omega^a(\xi)$, corresponding to a renormalization of the infinite set of unphysical gauge parameters $(a_1^{abc}, a_2^{abcd}, a_3^{abcde}, ..)$ of expression (95).

Repeating the lengthy discussion of the previous sections, for the most general local invariant counterterm we find now

$$\begin{aligned}
\Sigma^{ct} \;=\; & \int d^4x \left\{ - a_0 g^2 \frac{\partial\Sigma}{\partial g^2} + d_2\,(\alpha)\, 2\alpha \frac{\partial\Sigma}{\partial\alpha} + a_7 m^2 \frac{\partial\Sigma}{\partial m^2} \right. \\
& + a_4 \left(\tau^a \frac{\delta\Sigma}{\delta\tau^a} + \mathcal{J}^a_\mu \frac{\delta\Sigma}{\delta\mathcal{J}^a_\mu} + \frac{1}{2}\bar{\eta}^a \frac{\delta\Sigma}{\delta\bar{\eta}^a} + \frac{1}{2}\eta^a \frac{\delta\Sigma}{\delta\eta^a} + \frac{1}{2}\Xi^a_\mu \frac{\delta\Sigma}{\delta\Xi^a_\mu} \right) \\
& + d_2\,(\alpha)\, A^a_\mu \frac{\delta\Sigma}{\delta A^a_\mu} - d_2\,(\alpha)\, \Omega^a_\mu \frac{\delta\Sigma}{\delta\Omega^a_\mu} - d_1\,(\alpha)\, c^a \frac{\delta\Sigma}{\delta c^a} + d_1\,(\alpha)\, L^a \frac{\delta\Sigma}{\delta L^a} \\
& + f_1^{ab}(\xi,\alpha)\xi^a \frac{\delta\Sigma}{\delta\xi^b} - \left(f_1^{ab}(\xi,\alpha) + \frac{\partial f_1^{kb}(\xi,\alpha)}{\partial\xi^a}\xi^k \right) K^b \frac{\delta\Sigma}{\delta K^a} \\
& - d_2(\alpha)\bar{c}\frac{\delta\Sigma}{\delta\bar{c}} + (d_2(\alpha) - f_2(0,\alpha))\, M^{ab}\frac{\delta\Sigma}{\delta M^{ab}} + (d_2(\alpha) - f_2(0,\alpha))\, N^{ab}\frac{\delta\Sigma}{\delta N^{ab}} \\
& \left. - d_2(\alpha) b^a \frac{\delta\Sigma}{\delta b^a} - f_2(0,\alpha) Q^a \frac{\delta\Sigma}{\delta Q^a} - f_2(0,\alpha) R^a \frac{\delta\Sigma}{\delta R^a} \right.
\end{aligned}$$

$$+\Big[\left(f_2(0,\alpha)a_1^{abc}+\tilde{a}_1^{abc}\right)\frac{\delta\Sigma}{\delta a_1^{abc}}+\left(f_2(0,\alpha)a_2^{abcd}+\tilde{a}_2^{abcd}\right)\frac{\delta\Sigma}{\delta a_2^{abcd}}$$
$$+\left(f_2(0,\alpha)a_3^{abcde}+\tilde{a}_3^{abcde}\right)\frac{\delta\Sigma}{\delta a_3^{abcde}}+...\Big]\Bigg\}\,, \tag{428}$$

where the dots ... denote the reamaining, infinite set, of terms of the kind

$$\sum_j\left(f_2(0,\alpha)a_j^{abcde...}+\tilde{a}_j^{abcde...}\right)\frac{\delta\Sigma}{\delta a_j^{abcde...}}\,,\qquad j=4,...,\infty\,, \tag{429}$$

The counterterm Σ^{ct} in eq.(428) can be rewritten as

$$\Sigma^{ct}=\mathcal{R}\Sigma\,, \tag{430}$$

with

$$\begin{aligned}\mathcal{R} &= -a_0g^2\frac{\partial}{\partial g^2}+d_2\left(\alpha\right)2\alpha\frac{\partial}{\partial\alpha}+a_7m^2\frac{\partial}{\partial m^2}\\
&+\int d^4x\Bigg\{a_4\left(\tau^a\frac{\delta}{\delta\tau^a}+\mathcal{J}_\mu^a\frac{\delta}{\delta\mathcal{J}_\mu^a}+\frac{1}{2}\bar{\eta}^a\frac{\delta}{\delta\bar{\eta}^a}+\frac{1}{2}\eta^a\frac{\delta}{\delta\eta^a}+\frac{1}{2}\Xi_\mu^a\frac{\delta}{\delta\Xi_\mu^a}\right)\\
&+d_2\left(\alpha\right)A_\mu^a\frac{\delta}{\delta A_\mu^a}-d_2\left(\alpha\right)\Omega_\mu^a\frac{\delta}{\delta\Omega_\mu^a}-d_1\left(\alpha\right)c^a\frac{\delta}{\delta c^a}+d_1\left(\alpha\right)L^a\frac{\delta}{\delta L^a}\\
&+f_1^{ab}(\xi,\alpha)\xi^a\frac{\delta}{\delta\xi^b}-\left(f_1^{ab}(\xi,\alpha)+\frac{\partial f_1^{kb}(\xi,\alpha)}{\partial\xi^a}\xi^k\right)K^b\frac{\delta}{\delta K^a}\\
&-d_2(\alpha)\bar{c}\frac{\delta}{\delta\bar{c}}+\left(d_2(\alpha)-f_2(0,\alpha)\right)M^{ab}\frac{\delta}{\delta M^{ab}}+\left(d_2(\alpha)-f_2(0,\alpha)\right)N^{ab}\frac{\delta}{\delta N^{ab}}\\
&-d_2(\alpha)b^a\frac{\delta}{\delta b^a}-f_2(0,\alpha)Q^a\frac{\delta}{\delta Q^a}-f_2(0,\alpha)R^a\frac{\delta}{\delta R^a}\\
&+\Big[\left(f_2(0,\alpha)a_1^{abc}+\tilde{a}_1^{abc}\right)\frac{\delta}{\delta a_1^{abc}}+\left(f_2(0,\alpha)a_2^{abcd}+\tilde{a}_2^{abcd}\right)\frac{\delta}{\delta a_2^{abcd}}\\
&+\left(f_2(0,\alpha)a_3^{abcde}+\tilde{a}_3^{abcde}\right)\frac{\delta}{\delta a_3^{abcde}}+...\Big]\Bigg\}\,.\end{aligned} \tag{431}$$

For the renormalization factors, we have now

$$\Sigma(\Phi)+\varepsilon\Sigma^{ct}(\Phi)=\Sigma(\Phi)+\varepsilon\mathcal{R}\Sigma(\Phi)=\Sigma(\Phi_0)+O(\varepsilon^2)\,, \tag{432}$$

with

$$\Phi_0=Z_\Phi\Phi=(1+\varepsilon\mathcal{R})\Phi+O(\varepsilon^2)\,. \tag{433}$$

where

$$A_0 = Z_A^{1/2}A_\mu\,,\ b_0=Z_b^{1/2}\,,\ c_0=Z_c^{1/2}c\,,\ \bar{c}_0=Z_{\bar{c}}^{1/2}\bar{c}\,,$$

$$
\begin{aligned}
\xi_0^a &= Z_\xi^{ab}(\xi)\xi^b,\ \ \tau_0 = Z_\tau^{1/2}\tau\ , \Omega_0 = Z_\Omega\Omega\ ,\ \ L_0 = Z_L L\ ,\\
K_0^a &= Z_K^{ab}(\xi)K^b\ ,\ \ m_0^2 = Z_{m^2}m^2\ ,\ \ \mathcal{J}_0 = Z_{\mathcal{J}}\mathcal{J}\ ,\\
g_0 &= Z_g\ ,\ \ \alpha_0 = Z_\alpha\alpha\ ,\ \ \bar\eta_0 = Z_{\bar\eta}^{1/2}\bar\eta\ ,\ \ \eta_0 = Z_\eta^{1/2}\eta\ ,\\
\Xi_0 &= Z_\Xi\Xi\ ,\ \ M_0 = Z_M M\ ,\\
N_0 &= Z_N N,\ \ Q_0 = Z_Q Q,\ \ R_0 = Z_R R\ ,
\end{aligned}
\tag{434}
$$

and

$$
\begin{aligned}
Z_g &= 1-\varepsilon\frac{a_0}{2}\\
Z_A^{1/2} &= Z_\Omega^{-1} = Z_{\bar c}^{-1/2} = Z_b^{-1/2} = Z_\alpha^{1/2} = 1+\varepsilon d_2(\alpha)\\
Z_\xi^{ab} &= \delta^{ab}+\varepsilon f_1^{ab}(\xi,\alpha)\\
Z_L &= Z_c^{-1/2} = 1+\varepsilon d_1(\alpha)\\
Z_{\bar\eta} &= Z_\eta = Z_\Xi^2 = Z_\tau^{1/2} = Z_{\mathcal{J}} = 1+\varepsilon a_4\\
Z_{m^2} &= 1+\varepsilon a_7\\
Z_M &= Z_N = 1+\varepsilon(d_2 - f_2(0,\alpha))\\
Z_Q &= Z_R = 1-\varepsilon(f_2(0,\alpha))\\
Z_K^{ab} &= \delta^{ab}-\varepsilon\left(f_1^{ab}(\xi,\alpha)+\frac{\partial f_1^{kb}(\xi,\alpha)}{\partial\xi^a}\xi^k\right)\ ,
\end{aligned}
\tag{435}
$$

with the addition of a multiplicative renormalization of the infinite set of gauge parameters $(a_1^{abc}, a_2^{abcd}, a_3^{abcde}, ..)$ of expression (95), namely

$$
\begin{aligned}
(a_1^{abc})_0 &= (1+\varepsilon f_2(0,\alpha))a_1^{abc}+\varepsilon\tilde a_1^{abc}\\
(a_2^{abcd})_0 &= (1+\varepsilon f_2(0,\alpha))a_2^{abcd}+\varepsilon\tilde a_2^{abcd}\\
(a_3^{abcde})_0 &= (1+\varepsilon f_2(0,\alpha))a_3^{abcde}+\varepsilon\tilde a_3^{abcde}\\
&\ ...\quad .
\end{aligned}
\tag{436}
$$

Equations (435) and (436) show that the inclusion of the ambiguity $\omega^a(\xi)$ in the generalised gauge fixing of eq.(97) gives rise to a standard renormalization of the fields, parameters and sources. Clearly, from eq.(436) one sees that the renormalization of $\omega^a(\xi)$ itself is now encoded into a multiplicative renormalization of the infinite set of the unphysical gauge parameters $(a_1^{abc}, a_2^{abcd}, a_3^{abcde}, ..)$.

APPENDIX C – Field propagators of the Abelian Higgs model in the R_ξ gauge

The quadratic part of the action (160) in the bosonic sector is given by

$$\begin{aligned} S_{bos}^{quad} &= \frac{1}{2}\int d^4x\Big\{A_\mu(-\delta_{\mu\nu}(\partial^2-m^2)+\partial_\mu\partial_\nu)A_\nu-\rho\partial^2\rho-h(\partial^2-m_h^2)h \\ &+ \bar{c}(\partial^2-m^2\xi)c+2ib\partial_\mu A_\mu+\xi b^2+2im\xi b\rho+2mA_\mu\partial_\mu\rho\Big\}. \end{aligned} \tag{437}$$

Putting this in a matrix form yields

$$S_{bos}^{quad}=\frac{1}{2}\int d^4x\,\Psi_\mu^T O_{\mu\nu}\Psi_\nu, \tag{438}$$

where

$$\Psi_\mu^T=\begin{pmatrix} A_\mu & b & \rho & h\end{pmatrix},\ \Psi_\nu=\begin{pmatrix} A_\nu \\ b \\ \rho \\ h\end{pmatrix}, \tag{439}$$

and

$$O=\begin{pmatrix} (-\delta_{\mu\nu}(\partial^2-m^2)+\partial_\mu\partial_\nu) & -i\partial_\mu & m\partial_\mu & 0 \\ i\partial_\nu & \xi & im\xi & 0 \\ -m\partial_\nu & im\xi & -\partial^2 & 0 \\ 0 & 0 & 0 & -(\partial^2-m_h^2)\end{pmatrix}, \tag{440}$$

the tree-level field propagators can be read off from the inverse of $\mathcal{O}$, leading to the following expressions

$$\begin{aligned} \langle A_\mu(p)A_\nu(-p)\rangle &= \frac{1}{p^2+m^2}P_{\mu\nu}+\frac{\xi}{p^2+\xi m^2}\mathcal{L}_{\mu\nu}, \\ \langle\rho(p)\rho(-p)\rangle &= \frac{1}{p^2+\xi m^2}, \\ \langle h(p)h(-p)\rangle &= \frac{1}{p^2+m_h^2}, \\ \langle A_\mu(p)b(-p)\rangle &= \frac{p_\mu}{p^2+\xi m^2}, \\ \langle b(p)\rho(-k)\rangle &= \frac{-im}{p^2+\xi m^2}, \end{aligned} \tag{441}$$

where $\mathcal{P}_{\mu\nu}=\delta_{\mu\nu}-\frac{p_\mu p_\nu}{p^2}$ and $\mathcal{L}_{\mu\nu}=\frac{p_\mu p_\nu}{p^2}$ are the transversal and longitudinal projectors, respectively. The ghost propagator is

$$\langle\bar{c}(p)c(-p)\rangle = \frac{1}{p^2+\xi m^2}. \tag{442}$$

APPENDIX D – Field propagators of the Abelian Higgs model in the R_ξ gauge

Vertices of the Abelian Higgs model in the R_ξ gauge From the action (160), we find the following vertices

$$\begin{aligned}
\Gamma_{A_\mu\rho h}(-p_1,-p_2,-p_3) &= ie(p_{\mu,3}-p_{\mu,2})\delta(p_1+p_2+p_3),\\
\Gamma_{A_\mu A_\nu h}(-p_1,-p_2,-p_3) &= -2e^2 v\delta_{\mu\nu}\delta(p_1+p_2+p_3),\\
\Gamma_{A_\mu A_\nu hh}(-p_1,-p_2,-p_3,-p_4) &= -2e^2\delta_{\mu\nu}\delta(p_1+p_2+p_3+p_4),\\
\Gamma_{A_\mu A_\nu \rho\rho}(-p_1,-p_2,-p_3,-p_4) &= -2e^2\delta_{\mu\nu}\delta(p_1+p_2+p_3+p_4),\\
\Gamma_{hhhh}(-p_1,-p_2,-p_3,-p_4) &= -3\lambda\,\delta(p_1+p_2+p_3+p_4),\\
\Gamma_{hh\rho\rho}(-p_1,-p_2,-p_3,-p_4) &= -\lambda\,\delta(p_1+p_2+p_3+p_4),\\
\Gamma_{\rho\rho\rho\rho}(-p_1,-p_2,-p_3,-p_4) &= -3\lambda\,\delta(p_1+p_2+p_3+p_4),\\
\Gamma_{hhh}(-p_1,-p_2,-p_3) &= -3\lambda v\,\delta(p_1+p_2+p_3),\\
\Gamma_{h\rho\rho}(-p_1,-p_2,-p_3) &= -\lambda v\,\delta(p_1+p_2+p_3),\\
\Gamma_{\bar{c}hc}(-p_1,-p_2,-p_3) &= -m\xi e\,\delta(p_1+p_2+p_3).
\end{aligned} \tag{443}$$

APPENDIX E – Equivalence between including tadpole diagrams in the self-energies and shifting $\langle\varphi\rangle$

There is yet another way to come to (191). For this, we do not need to include the balloon type tadpoles in the self-energies, but rather fix the expectation value of the Higgs field $\langle h\rangle = 0$ by shifting the vacuum expectation value of the Higgs field to its proper one-loop value. The h field one-point function has the following contributions at one-loop order :

- the gluon contribution

$$-\frac{1}{m_h^2}\frac{2e^2v}{(4\pi)^{d/2}}\frac{\Gamma(2-d/2)}{(2-d)}(m^{d-2}(d-1)+\xi(\xi m^2)^{d/2-1}), \tag{444}$$

- the Goldstone boson one

$$-\frac{1}{m_h^2}\lambda v\frac{1}{(4\pi)^{d/2}}\frac{\Gamma(2-d/2)}{(2-d)}(\xi m^2)^{d/2-1}, \tag{445}$$

- the ghost loop

$$2\frac{1}{m_h^2}\frac{e^2v\xi}{(4\pi)^{d/2}}\frac{\Gamma(2-d/2)}{(2-d)}(\xi m^2)^{d/2-1} \tag{446}$$

- the Higgs boson one

$$-3\frac{1}{m_h^2}\frac{\lambda v}{(4\pi)^{d/2}}\frac{\Gamma(2-d/2)}{(2-d)}m_h^{d-2}, \tag{447}$$

Together those four contributions yield

$$\begin{aligned}\Gamma_{\langle h\rangle} &= \frac{1}{(4\pi)^{d/2}}\frac{\Gamma(2-d/2)}{(2-d)}\frac{1}{m_h^2}(-2e^2vm^{d-2}(d-1)\\ &- \lambda v(\xi m^2)^{d/2-1}-3\lambda v m_h^{d-2}),\end{aligned} \tag{448}$$

that becomes, for $d=4-\epsilon$,

$$\begin{aligned}&= -\frac{1}{2}\frac{1}{m_h^2}\frac{1}{(4\pi)^2}(\frac{2}{\epsilon}+1+\ln(\mu^2))(-2e^2vm^{2-\epsilon}(3-\epsilon)-\lambda v(\xi m^2)^{1-\epsilon/2}-3\lambda v m_h^{2-\epsilon})\\ &= -\frac{1}{2}\frac{1}{m_h^2}\frac{1}{(4\pi)^2}(\frac{2}{\epsilon}+1+\ln(\mu^2))(-2e^2vm^2(1-\frac{\epsilon}{2}\ln m^2)(3-\epsilon)\\ &- \lambda v\xi m^2(1-\frac{\epsilon}{2}\ln m^2)-3\lambda v m_h^2(1-\frac{\epsilon}{2}\ln m_h^2)).\end{aligned} \tag{449}$$

We can split this in a divergent part

$$\Gamma^{div}_{\langle h\rangle} = \frac{1}{\epsilon}\frac{1}{m_h^2}(6e^2m^2v + 3m_h^2v\lambda + \xi m^2 v), \tag{450}$$

which we can cancel with the counterterms, and a finite part that reads

$$\begin{aligned}\Gamma^{fin}_{\langle h\rangle} &= \frac{1}{m_h^2}\frac{e^2}{(4\pi)^2}v\Big(m^2(1-3\ln\frac{m^2}{\mu^2})\Big) \\ &+ \frac{1}{m_h^2}\frac{\lambda}{(4\pi)^2}\frac{v}{2}\Big(3m_h^2(1-\ln\frac{h^2}{\mu^2}) + \xi m^2(1-\ln\frac{\xi m^2}{\mu^2})\Big).\end{aligned} \tag{451}$$

Now, to see how this reflects on the propagator, we can rewrite our scalar field as

$$\varphi = \frac{1}{\sqrt{2}}((\langle\varphi\rangle + h) + i\rho), \tag{452}$$

where the vacuum expectation value of the Higgs field has tree-level and one-loop terms:

$$\langle\varphi\rangle = v + \hbar v_1. \tag{453}$$

Thus the "classical" potential part of the action becomes

$$\frac{\lambda}{2}\left(\varphi^\dagger\varphi - \frac{v^2}{2}\right)^2 = \frac{\lambda}{8}\left(\langle\varphi\rangle^2 - v^2 + 2h\langle\varphi\rangle + h^2 + \rho^2\right)^2 \tag{454}$$

and expanding this, we find for the shifted tree level Higgs mass

$$m_h^2 = \frac{1}{2}\lambda(3\langle\varphi\rangle^2 - v^2) = \lambda v^2 + 3\hbar\lambda v v_1, \tag{455}$$

while the photon mass is

$$m^2 = e^2\langle\varphi\rangle^2 = e^2v^2 + 2\hbar e^2 v v_1. \tag{456}$$

As now per construction $\langle h\rangle = 0$, we can fix the one-loop correction[15] to the Higgs minimizing value by requiring it to absorb the tadpole contributions:

$$v_1 + \Gamma^{fin}_{\langle h\rangle} = 0, \tag{457}$$

thus

$$v_1 = -\frac{1}{m_h^2}\frac{e^2}{(4\pi)^2}v\Big(m^2(1-3\ln\frac{m^2}{\mu^2})\Big)$$

[15] This procedure is also equivalent to computing $\langle\varphi\rangle$ via an effective potential minimization up to the same order.

$$- \quad \frac{1}{m_h^2}\frac{\lambda}{(4\pi)^2}\frac{v}{2}\Big(3m_h^2(1-\ln\frac{h^2}{\mu^2})+\xi m^2(1-\ln\frac{\xi m^2}{\mu^2})\Big). \tag{458}$$

Implementing this in the transverse $\langle AA\rangle$-propagator, one gets

$$G^{\perp}_{AA}(p^2)=\frac{1}{p^2+e^2(v^2+2\hbar v_1 v)-\Pi^{\perp}_{AA}(p^2)}, \tag{459}$$

where in the correction $\Pi^{\perp}_{AA}$, which is already of $\mathcal{O}(\hbar)$, we only include the $\mathcal{O}(\hbar^0)$ part of $\langle\varphi\rangle$, i.e. v.

We can now verify the ξ-independence of the transverse propagator $\langle AA\rangle$. The ξ-dependent part of $\Pi^{\perp}_{AA}(p^2)$ is

$$\Pi^{\perp}_{AA,\xi}(p^2)=\frac{-2e^2}{(4\pi)^{d/2}}\frac{\Gamma(2-d/2)}{2-d}(\xi m^2)^{d/2-1}, \tag{460}$$

while we find the ξ-dependent part of v_1 to be (using (448))

$$v_{1\xi}=\frac{1}{(4\pi)^{d/2}}\frac{\Gamma(2-d/2)}{(2-d)}\frac{1}{m_h^2}(\lambda v(\xi m^2)^{d/2-1}). \tag{461}$$

In the denominator of (459) we now easily see that

$$2e^2 v_{1\xi}v_0-\Pi^{\perp}_{AA,\xi}(p^2)=0, \tag{462}$$

thereby establishing the gauge independence of the transverse photon propagator.

For the Higgs propagator, we similarly find

$$G_{hh}(p^2)=\frac{1}{p^2+\lambda(v^2+3\hbar v_1 v)-\Pi_{hh}(p^2)}. \tag{463}$$

Here we observe that the ξ-dependent part of v_1 has the same effect as the balloon tadpole of the Goldstone boson, consequently establishing the gauge parameter independence of the Higgs mass pole.

APPENDIX F – Feynman integrals

$$\begin{aligned}
\int_0^1 dx \ln \frac{K(m_1^2, m_2^2)}{\mu^2} &= \frac{1}{2p^2}\Bigg\{ m_1^2 \ln(\frac{m_2^2}{m_1^2}) + m_2^2 \ln(\frac{m_1^2}{m_2^2}) + p^2 \ln(\frac{m_1^2 m_2^2}{\mu^4}) \\
&- 2\sqrt{-m_1^4 + 2m_1^2 m_2^2 - 2m_1^2 p^2 - m_2^4 - 2m_2^2 p^2 - p^4} \\
&\times \tan^{-1}\Big[\frac{-m_1^2 + m_2^2 - p^2}{\sqrt{-m_1^4 + 2m_1^2(m_2^2 - p^2) - (m_2^2 + p^2)^2}}\Big] \\
&+ 2\sqrt{-m_1^4 + 2m_1^2 m_2^2 - 2m_1^2 p^2 - m_2^4 - 2m_2^2 p^2 - p^4} \\
&\times \tan^{-1}\Big[\frac{-m_1^2 + m_2^2 + p^2}{\sqrt{-m_1^4 + 2m_1^2(m_2^2 - p^2) - (m_2^2 + p^2)^2}}\Big] \\
&- 4p^2 \Bigg\} \qquad (464)
\end{aligned}$$

APPENDIX G – Asymptotics of the Higgs propagator

At one-loop, the Higgs propagator behaves like

$$G_{hh}(p^2) = \frac{\mathcal{Z}}{p^2 \ln \frac{p^2}{\mu^2}} \qquad \text{for} \qquad p^2 \to \infty. \tag{465}$$

For $\mathcal{Z} > 0$, this can only be compatible with

$$G_{hh}(p^2) = \int_0^\infty \frac{\rho(t)dt}{t + p^2} \tag{466}$$

if the superconvergence relation (OEHME, 1990; CORNWALL, 2013) $\int dt\rho(t) = 0$ holds, which forbids a positive spectral function. Let us support this non-positivity of $\rho(t)$ by using (465) to show that $\rho(t)$ is certainly negative for very large t. This argument can also be found in the Appendix of (DUDAL et al., 2020b).

Since for a KL representation we have:

$$\rho(t) = \frac{1}{2\pi i} \lim_{\epsilon \to 0^+} \left(G(-t - i\epsilon) - G(-t + i\epsilon) \right), \tag{467}$$

we find for $t \to +\infty$ and $\epsilon \to 0^+$,

$$\begin{aligned}
\rho(t) &= \frac{\mathcal{Z}}{2\pi i} \left[\frac{\left(\ln \frac{-t - i\epsilon}{\mu^2} \right)^{-1}}{-t - i\epsilon} - \frac{\left(\ln \frac{-t + i\epsilon}{\mu^2} \right)^{-1}}{-t + i\epsilon} \right] \\
&= \frac{\mathcal{Z}}{2\pi i t} \left[- \left(\ln \frac{t}{\mu^2} - i\pi \right)^{-1} + \left(\ln \frac{t}{\mu^2} + i\pi \right)^{-1} \right] \\
&= \frac{\mathcal{Z}}{\pi t} \mathrm{Im} \left[\left(\ln \frac{t}{\mu^2} + i\pi \right)^{-1} \right] \\
&= \frac{\mathcal{Z}}{\pi t} \left(\left(\ln \frac{t}{\mu^2} \right)^2 + \pi^2 \right)^{-1/2} \sin \left(- \arctan \frac{\pi}{\ln \frac{t}{\mu^2}} \right).
\end{aligned} \tag{468}$$

From the latter expression, we can indeed infer that $\rho(t)$ becomes negative for t large. We find

$$\rho(t) \overset{t \to \infty}{=} -\frac{\mathcal{Z}}{t} \left(\ln \frac{t}{\mu^2} \right)^{-2} < 0 \tag{469}$$

for $\mathcal{Z} > 0$, and vice versa for $\mathcal{Z} < 0$.

Figure 39 - One-loop contributions to $\langle O(p)O(-p)\rangle$

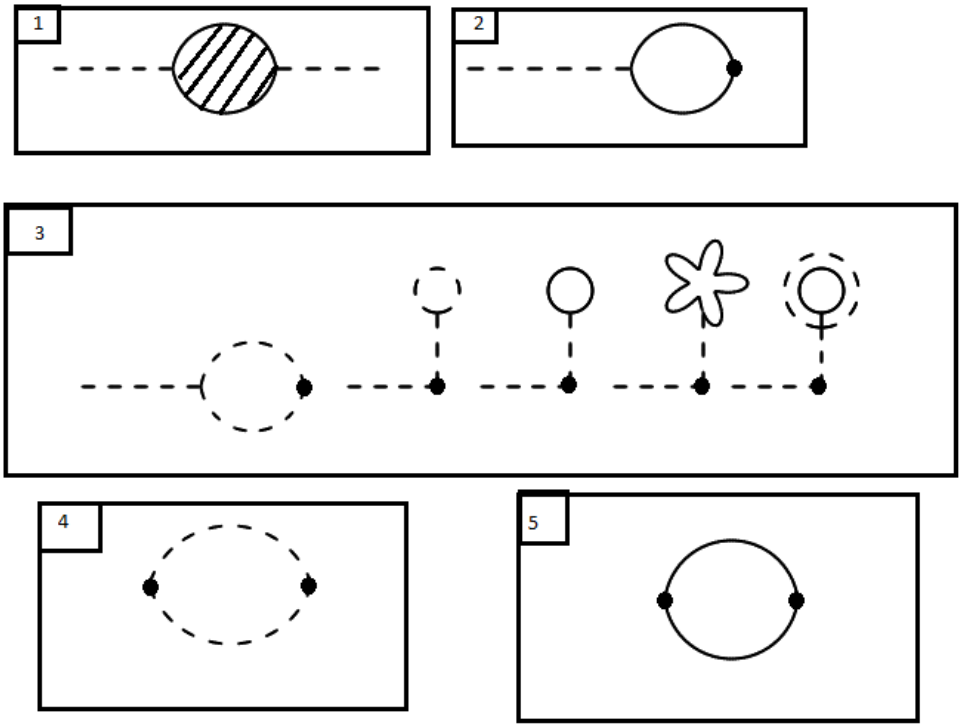

Legend: One-loop contributions to the propagator $\langle O(p)O(-p)\rangle$. Wavy lines represent the photon field, dashed lines the Higgs field, solid lines the Goldstone boson and double lines the ghost field.
Source: The author, 2020.

G.1 **Contributions to** $\langle O(p)O(-p)\rangle$

We consider each term in the two-point function $\langle O(p)O(-p)\rangle$, given by eq. (248). The first term is the one-loop correction to the Higgs propagator $\langle h(p)h(-p)\rangle$ known from the last chapter, shown in frame (1) in Figure 39, which gives

$$\begin{aligned} v^2\langle h(p)h(-p)\rangle &= \frac{v^2}{m_h^2+p^2} + v^2\Big(e^2\eta\left(m^2,m^2\right)\left(2(d-1)m^2+\frac{p^4}{2m^2}+2p^2\right) \\ &+ \eta\left(m^2\xi,m^2\xi\right)\left(\frac{m_h^2\lambda}{2}-\frac{e^2p^4}{2m^2}\right) \\ &+ \frac{9}{2}m_h^2\lambda\eta\left(m_h^2,m_h^2\right)+\frac{1}{2}e^2\chi\left(m^2\right)\left(4(d-1)-\frac{2p^2}{m^2}\right) \end{aligned}$$

$$+ \quad \chi\left(m^2\xi\right)\left(\frac{e^2p^2}{m^2}+\lambda\right)+3\lambda\chi\left(m_h^2\right)\Big)\frac{1}{\left(m_h^2+p^2\right)^2}. \tag{470}$$

The second term, the one-loop correction shown in frame (2) of Figure 39, gives

$$v\langle h(p)\rho(-p)^2\rangle \;=\; -\frac{m_h^2\eta\left(m^2\xi,m^2\xi\right)}{m_h^2+p^2}. \tag{471}$$

The third term, the one-loop correction shown in frame (3) of Figure 39, gives

$$\begin{aligned} v\langle h(p)h(-p)^2\rangle \;=\; & -\frac{3m_h^2\eta\left(m_h^2,m_h^2\right)}{m_h^2+p^2}-\frac{3\chi\left(m_h^2\right)}{m_h^2+p^2}-\frac{\chi\left(m^2\xi\right)}{m_h^2+p^2}-\frac{2(d-1)m^2\chi\left(m^2\right)}{m_h^2\left(m_h^2+p^2\right)} \\ & - \quad \frac{2m^2\xi\chi\left(m^2\xi\right)}{m_h^2\left(m_h^2+p^2\right)}+\frac{2m^2\xi\chi\left(m^2\xi\right)}{m_h^2\left(m_h^2+p^2\right)}. \end{aligned} \tag{472}$$

The fourth term has no 1-loop contributions. The fifth term, the one-loop correction shown in frame (4) of Figure 39, gives

$$\frac{1}{4}\langle h(p)h(p)h(-p)h(-p)\rangle \;=\; \frac{1}{2}\eta\left(m_h^2,m_h^2\right). \tag{473}$$

The sixth term, the one-loop correction shown in frame (5) of Figure 39, gives

$$\frac{1}{4}\langle \rho(p)\rho(p)\rho(-p)\rho(-p)\rangle \;=\; \frac{1}{2}\eta\left(\xi m^2,\xi m^2\right). \tag{474}$$

Using the identity (351) we are able to write the whole one-loop correlation function $\langle O(-p),O(p)\rangle$, up to the order $\hbar$, as

$$\begin{aligned} \langle O(p)O(-p)\rangle \;=\; & \frac{v^2}{p^2+m_h^2}+\frac{1}{(p^2+m_h^2)^2}\int_0^1 dx\Bigg(\frac{1}{2}\eta\left[m^2,m^2\right]\left(4(d-1)m^4+4m^2p^2+p^4\right) \\ & + \quad \frac{1}{2}(p^2-2m_h^2)^2\eta\left[m_h^2,m_h^2\right]-\frac{p^2\chi[m^2](2(d-1)m^2+m_h^2)}{m_h^2} \\ & - \quad 3p^2\chi[m_h^2]\Bigg) \end{aligned} \tag{475}$$

Figure 40 - One-loop contributions for $\langle V_\mu(p)V_\nu(-p)\rangle$

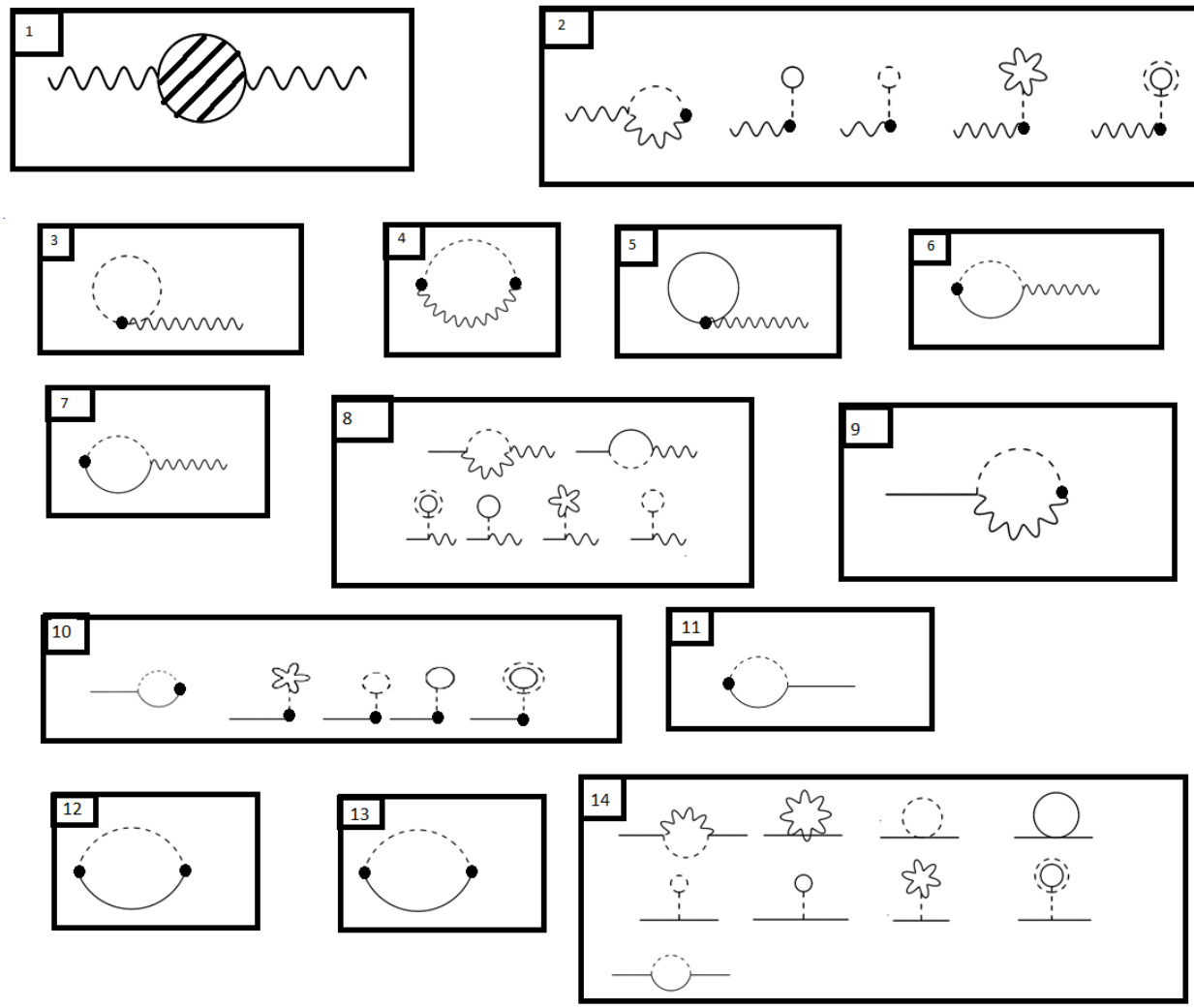

Legend: One-loop contributions for the propagator $\langle V_\mu(p)V_\nu(-p)\rangle$. Wavy lines represent the photon field,
dashed lines the Higgs field, solid lines the Goldstone boson and double lines the ghost field.

Source: The author, 2020.

G.2 Contributions to $\langle V_\mu(x)V_\nu(y)\rangle$

We consider each term in the two-point function $\langle V_\mu(p)V_\nu(-p)\rangle$, given by eq. (269). The first term is the one-loop correction to the photon propagator $\langle A_\mu(p)A_\nu(-p)\rangle$ known from the last chapter, shown in frame (1) in Figure 40, which gives

$$
\begin{aligned}
&\frac{1}{4}e^2v^4\langle A_\mu(p)A_v(-p)\rangle = \\
&\frac{1}{4}e^2v^4\frac{\mathcal{P}_{\mu\nu}(p)}{p^2+m^2} + \frac{1}{4}e^2v^4\Bigg[- \frac{m^2\eta\left(m^2,m_h^2\right)\left(\left(m_h^2-m^2+p^2\right)^2-4(d-2)m^2p^2\right)}{(d-1)p^2v^2} \\
+ \;& \frac{m^2\chi\left(m^2\right)\left(2(d-1)^2m^2p^2+m_h^2\left(p^2-m^2\right)+m_h^4\right)}{(d-1)p^2v^2m_h^2} \\
+ \;& \frac{m^2\chi\left(m_h^2\right)\left((2d-1)p^2-m_h^2+m^2\right)}{(d-1)p^2v^2}\Bigg]\frac{\mathcal{P}_{\mu\nu}(p)}{(p^2+m^2)^2} \\
+ \;& \frac{1}{4}e^2v^4\frac{\xi}{p^2+\xi m^2}\mathcal{L}_{\mu\nu}(p) \\
+ \;& \frac{1}{4}e^2v^4\Bigg[\frac{m^2\xi^2\left(-2m_h^2\left(m^2-p^2\right)+m_h^4+\left(m^2+p^2\right)^2\right)\eta\left(m^2,m_h^2\right)}{p^2v^2} \\
- \;& \frac{m^2\xi^2\left(2m_h^2-2m^2\xi+p^2\right)\eta\left(m_h^2,m^2\xi\right)}{v^2} \\
+ \;& \frac{m^2\xi^2\chi\left(m^2\right)\left(2(d-1)m^2p^2+m_h^2\left(m^2-p^2\right)-m_h^4\right)}{p^2v^2m_h^2} \\
- \;& \frac{m^2\xi^2\left(-m_h^2+m^2-3p^2\right)\chi\left(m_h^2\right)}{p^2v^2} + \frac{2m^2\xi^2\chi\left(m^2\xi\right)}{v^2}\Bigg]\frac{\mathcal{L}_{\mu\nu}(p)}{(p^2+\xi m^2)^2}.
\end{aligned}
\tag{476}
$$

The second term, the one-loop correction shown in frame (2) of Figure 40, gives

$$
\begin{aligned}
&e^2v^3\langle hA_\mu(p)A_v(-p)\rangle = \\
&e^2v^3\Big[- \frac{e\eta\left(m_h^2,m^2\xi\right)\left(2evm_h^4\left(p^2-m^2\xi\right)+evm_h^2\left(m^2\xi+p^2\right)^2+evm_h^6\right)}{2(d-1)m^2p^2m_h^2} \\
- \;& \frac{e\eta\left(m^2,m_h^2\right)\left(evm_h^2\left(-2(3-2d)m^2p^2-m^4-p^4\right)+2evm_h^4\left(m^2-p^2\right)-evm_h^6\right)}{2(d-1)m^2p^2m_h^2} \\
- \;& \frac{e\chi\left(m^2\xi\right)\left(dep^2vm_h^2+em^2\xi vm_h^2-2ep^2vm_h^2-evm_h^4\right)}{2(d-1)m^2p^2m_h^2)} \\
- \;& \frac{e\chi\left(m_h^2\right)\left(3dep^2vm_h^2-em^2\xi vm_h^2+em^2vm_h^2-3ep^2vm_h^2\right.}{2(d-1)m^2p^2m_h^2} \\
- \;& \left.\frac{e\chi\left(m^2\right)\left(2(d-1)^2em^2p^2v-em^2vm_h^2+ep^2vm_h^2+evm_h^4\right)}{2(d-1)m^2p^2m_h^2}\Big]\frac{\mathcal{P}_{\mu\nu}(p)}{(p^2+m^2)} \\
+ \;& e^2v^3\Big[\frac{1}{2p^2v}\xi\Big(\left(m_h^2+m^2(-\xi)+p^2\right)^2\eta\left(m_h^2,m^2\xi\right)
\end{aligned}
$$

$$
\begin{aligned}
&- \Big(-2m_h^2\left(m^2-p^2\right)+m_h^4+\left(m^2+p^2\right)^2\Big)\,\eta\left(m^2,m_h^2\right)\\
&+ \frac{\chi\left(m^2\right)\left(-2(d-1)m^2p^2+m_h^2\left(p^2-m^2\right)+m_h^4\right)}{m_h^2}-\chi\left(m^2\xi\right)\left(m_h^2+m^2(-\xi)+2p^2\right)\\
&- \chi\left(m_h^2\right)\left(m^2(\xi-1)+3p^2\right)\Big)\Big]\frac{\mathcal{L}_{\mu\nu}}{p^2+\xi m^2}. \qquad (477)
\end{aligned}
$$

The third term, the one-loop correction shown in frame (3) of Figure 40, gives

$$
\frac{1}{2}e^2v^2\langle h^2A_\mu(p)A_v(-p)\rangle=\frac{1}{2}e^2v^2\Big[\frac{\chi\left(m_h^2\right)}{m^2+p^2}\Big]\mathcal{P}_{\mu\nu}+\frac{1}{2}e^2v^2\Big[\frac{\xi\chi\left(m_h^2\right)}{m^2\xi+p^2}\Big]\mathcal{L}_{\mu\nu}. \qquad (478)
$$

The fourth term, the one-loop correction shown in frame (4) of Figure 40, gives

$$
\begin{aligned}
&e^2v^2\langle hA_\mu(p)hA_v(-p)\rangle\\
=\;& e^2v^2\Big[\frac{\left(\frac{\left(m_h^2+m^2(-\xi)+p^2\right)^2}{m^2p^2}+4\xi\right)\eta\left(m_h^2,m^2\xi\right)}{4(d-1)}\\
+\;& \frac{\eta\left(m^2,m_h^2\right)\left(4(d-2)-\frac{\left(m_h^2-m^2+p^2\right)^2}{m^2p^2}\right)}{4(d-1)}-\frac{\chi\left(m^2\xi\right)\left(m_h^2+m^2(-\xi)+p^2\right)}{4(d-1)m^2p^2}\\
+\;& \frac{\chi\left(m^2\right)\left(m_h^2-m^2+p^2\right)}{4(d-1)m^2p^2}-\frac{(\xi-1)\chi\left(m_h^2\right)}{4(d-1)p^2}\Big]\mathcal{P}_{\mu\nu}\\
+\;& e^2v^2\Big[\frac{1}{4m^2p^2}\Big(-\left(m_h^2+m^2(-\xi)+p^2\right)^2\eta\left(m_h^2,m^2\xi\right)\\
+\;& \left(\left(m_h^2-m^2+p^2\right)^2+4m^2p^2\right)\eta\left(m^2,m_h^2\right)+m^2(\xi-1)\chi\left(m_h^2\right)\\
+\;& \chi\left(m^2\xi\right)\left(m_h^2+m^2(-\xi)+p^2\right)+\chi\left(m^2\right)\left(-m_h^2+m^2-p^2\right)\Big)\Big]\mathcal{L}_{\mu\nu}. \qquad (479)
\end{aligned}
$$

The fifth term, the one-loop correction shown in frame (5) of Figure 40, gives

$$
\frac{1}{2}e^2v^2\langle\rho^2A_\mu(p),A_v(-p)\rangle=\frac{1}{2}e^2v^2\frac{\chi\left(m^2\xi\right)}{m^2+p^2}\mathcal{P}_{\mu\nu}+\frac{1}{2}e^2v^2\frac{\xi\chi\left(m^2\xi\right)}{m^2\xi+p^2}\mathcal{L}_{\mu\nu}. \qquad (480)
$$

The sixth term, the one-loop correction shown in frame (6) of Figure 40, gives

$$
\begin{aligned}
&-\frac{i}{2}ev^2p_\mu\langle h\rho(p)A_v(-p)\rangle\\
=\;& -\frac{i}{2}ev^2\Big[\frac{ie\xi\left(m^2\xi-m_h^2\right)\eta\left(m_h^2,m^2\xi\right)}{m^2\xi+p^2}-\frac{ie\xi\chi\left(m_h^2\right)}{m^2\xi+p^2}+\frac{ie\xi\chi\left(m^2\xi\right)}{m^2\xi+p^2}\Big]\mathcal{L}_{\mu\nu}. \qquad (481)
\end{aligned}
$$

The seventh term, the one-loop correction shown in frame (7) of Figure 40, gives

$$
\begin{aligned}
& ev^2\langle \partial^x{}_\mu h\rho(p)A_v(-p)\rangle \\
= \;& ev^2\Big[-\frac{e\left(\left(-m_h^2+m^2\xi+p^2\right)^2+4p^2m_h^2\right)\eta\left(m_h^2,m^2\xi\right)}{2(d-1)p^2\left(m^2+p^2\right)} \\
+ \;& \frac{e\chi\left(m^2\xi\right)\left(m_h^2+m^2(-\xi)+p^2\right)}{2(d-1)p^2\left(m^2+p^2\right)}+\frac{e\chi\left(m_h^2\right)\left(-m_h^2+m^2\xi+p^2\right)}{2(d-1)p^2\left(m^2+p^2\right)}\Big]\mathcal{P}_{\mu\nu} \\
+ \;& ev^2\Big[\frac{e\xi\left(-3p^2\left(m_h^2-m^2\xi+p^2\right)+\left(m_h^2-m^2\xi+p^2\right)^2+2p^4\right)\eta\left(m^2\xi,m_h^2\right)}{2p^2\left(m^2\xi+p^2\right)} \\
+ \;& \frac{e\xi\chi\left(m_h^2\right)\left(m_h^2-m^2\xi\right)}{2p^2\left(m^2\xi+p^2\right)}+\frac{e\xi\chi\left(m^2\xi\right)\left(-m_h^2+m^2\xi+2p^2\right)}{2p^2\left(m^2\xi+p^2\right)}\Big]\mathcal{L}_{\mu\nu}.
\end{aligned}
\tag{482}
$$

The eighth term, the one-loop correction shown in frame (11) of Figure 40, gives

$$
\begin{aligned}
& -\frac{1}{2}iev^3p_\mu\langle\rho(p)A_v(-p)\rangle = \\
- \;& \frac{1}{2}iev^3\Bigg[\frac{ie^3\xi v\left(\left(m_h^2-m^2+p^2\right)^2+4m^2p^2\right)\eta\left(m^2,m_h^2\right)}{m^2\left(m^2\xi+p^2\right)^2} \\
+ \;& \eta\left(m_h^2,m^2\xi\right)\left(\frac{ie^3\xi vm_h^2\left(m_h^2-m^2\xi\right)}{m^2\left(m^2\xi+p^2\right)^2}-\frac{ie^3\xi v\left(m_h^2+p^2\right)\left(m_h^2+m^2(-\xi)+p^2\right)}{m^2\left(m^2\xi+p^2\right)^2}\right) \\
+ \;& \chi\left(m^2\right)\left(\frac{i(d-1)e^3\xi p^2v}{m_h^2\left(m^2\xi+p^2\right)^2}-\frac{ie^3\xi v\left(m_h^2-m^2+p^2\right)}{m^2\left(m^2\xi+p^2\right)^2}\right) \\
+ \;& \chi\left(m_h^2\right)\left(\frac{ie^3\xi vm_h^2}{m^2\left(m^2\xi+p^2\right)^2}-\frac{ie^3\xi v}{\left(m^2\xi+p^2\right)^2}+\frac{3ie^3\xi p^2v}{2m^2\left(m^2\xi+p^2\right)^2}\right) \\
+ \;& \chi\left(m^2\xi\right)\left(\frac{ie^3\xi^2p^2v}{m_h^2\left(m^2\xi+p^2\right)^2}+\frac{ie^3\xi v\left(m_h^2+p^2\right)}{m^2\left(m^2\xi+p^2\right)^2}\right. \\
- \;& \left.\frac{ie^3\xi vm_h^2}{m^2\left(m^2\xi+p^2\right)^2}+\frac{ie^3\xi p^2v}{2m^2\left(m^2\xi+p^2\right)^2}-\frac{ie^2m\xi^2p^2}{m_h^2\left(m^2\xi+p^2\right)^2}\right)\Bigg]\mathcal{L}_{\mu\nu}.
\end{aligned}
\tag{483}
$$

The ninth term, the one-loop correction shown in frame (12) of Figure 40, gives

$$
\begin{aligned}
& -iev^2p_\mu\langle\rho(p)hA_v(-p)\rangle \\
= \;& -iev^2\Bigg[-\frac{ie\left(m_h^2+p^2\right)\chi\left(m^2\xi\right)}{2m^2\left(m^2\xi+p^2\right)} \\
- \;& \frac{1}{2m^2\left(m^2\xi+p^2\right)}\Big(ie\left(-\left(m_h^2+p^2\right)\left(m_h^2+m^2(-\xi)+p^2\right)\eta\left(m^2\xi,m_h^2\right)\right. \\
+ \;& \left.\left(\left(m_h^2-m^2+p^2\right)^2+4m^2p^2\right)\eta\left(m^2,m_h^2\right)-m^2\chi\left(m_h^2\right)\right.
\end{aligned}
$$

$$- \quad m_h^2\chi\left(m^2\right) - p^2\chi\left(m^2\right) + m^2\chi\left(m^2\right)\Big)\Big]\mathcal{L}_{\mu\nu}. \tag{484}$$

The tenth term, the one-loop correction shown in frame (14) of Figure 40, gives

$$\begin{aligned}
&-\frac{1}{2}vp_\mu p_\nu\langle h\rho(p)\rho(-p)\rangle = \\
&-\frac{1}{2}v\Big[p^2\Big(-\frac{e^2vm_h^2\eta\left(m^2\xi,m_h^2\right)}{m^2\left(m^2\xi+p^2\right)} - \frac{(d-1)e^2v\chi\left(m^2\right)}{m_h^2\left(m^2\xi+p^2\right)} \\
- \quad &\frac{3e^2v\chi\left(m_h^2\right)}{2m^2\left(m^2\xi+p^2\right)} - \frac{e^2\xi v\chi\left(m^2\xi\right)}{m_h^2\left(m^2\xi+p^2\right)} - \frac{e^2v\chi\left(m^2\xi\right)}{2m^2\left(m^2\xi+p^2\right)} + \frac{em\xi\chi\left(m^2\xi\right)}{m_h^2\left(m^2\xi+p^2\right)}\Big)\Big]\mathcal{L}_{\mu\nu}.
\end{aligned} \tag{485}$$

The eleventh term, the one-loop correction shown in frame (15) of Figure 40, gives

$$\begin{aligned}
&ivp_\nu\langle\partial^x{}_\mu h\rho(p)\rho(-p)\rangle = \\
&iv\Big[\frac{ie^2m_h^2v\chi\left(m^2\xi\right)}{2m^4\xi+2m^2p^2} - \frac{ie^2m_h^2v\left(\left(m_h^2-m^2\xi-p^2\right)\eta\left(m^2\xi,m_h^2\right)+\chi\left(m_h^2\right)\right)}{2m^2\left(m^2\xi+p^2\right)}\Big]\mathcal{L}_{\mu\nu}.
\end{aligned} \tag{486}$$

The twelfth term, the one-loop correction shown in frame (16) of Figure 40, gives

$$\frac{1}{4}p_\mu p_\nu\langle hh(p)\rho\rho(-p)\rangle \quad = \quad p^2\eta\left(m^2\xi,m_h^2\right)\mathcal{L}_{\mu\nu}. \tag{487}$$

The thirteenth term, the one-loop correction shown in frame (17) of Figure 40, gives

$$\begin{aligned}
&-\langle\partial^x{}_\mu h\rho(p)h\partial^y{}_\nu\rho(-p)\rangle \\
= \quad &-\Big[\frac{\left(\frac{\left(-m_h^2+m^2\xi+p^2\right)^2}{p^2}+4m_h^2\right)\eta\left(m_h^2,m^2\xi\right)}{4(d-1)} + \frac{\chi\left(m^2\xi\right)\left(-m_h^2+m^2\xi-p^2\right)}{4(d-1)p^2} \\
- \quad &\frac{\chi\left(m_h^2\right)\left(-m_h^2+m^2\xi+p^2\right)}{4(d-1)p^2}\Big]\mathcal{P}_{\mu\nu} \\
- \quad &\Big[-\frac{\left(m_h^2+m^2(-\xi)-p^2\right)\left(m_h^2+m^2(-\xi)+p^2\right)\eta\left(m^2\xi,m_h^2\right)}{4p^2} \\
+ \quad &\frac{\chi\left(m^2\xi\right)\left(m_h^2+m^2(-\xi)-p^2\right)}{4p^2} - \frac{\chi\left(m_h^2\right)\left(m_h^2+m^2(-\xi)+p^2\right)}{4p^2}\Big]\mathcal{L}_{\mu\nu}.
\end{aligned} \tag{488}$$

The fourteenth term, the one-loop correction shown in frame (18) of Figure 40, gives

$$\begin{aligned}
&\frac{1}{4}v^2p_\mu p_\nu\langle\rho(p)\rho(-p)\rangle = \\
&\Big[p^2\Big(\frac{e^4v^2m_h^4\eta\left(m^2\xi,m_h^2\right)}{m^4\left(m^2\xi+p^2\right)^2} + \frac{e^2\left(\left(m_h^2-m^2+p^2\right)^2+4m^2p^2\right)\eta\left(m^2,m_h^2\right)}{m^2\left(m^2\xi+p^2\right)^2}
\end{aligned}$$

$$
\begin{aligned}
- & \frac{e^2\left(m_h^2+p^2\right)^2\eta\left(m_h^2,m^2\xi\right)}{m^2\left(m^2\xi+p^2\right)^2}+\frac{(d-1)e^4v^2\chi\left(m^2\right)}{m^2\left(m^2\xi+p^2\right)^2}-\frac{(d-1)e^2\chi\left(m^2\right)}{\left(m^2\xi+p^2\right)^2}+\frac{e^4v^2m_h^2\chi\left(m^2\xi\right)}{2m^4\left(m^2\xi+p^2\right)^2} \\
+ & \frac{3e^4v^2m_h^2\chi\left(m_h^2\right)}{2m^4\left(m^2\xi+p^2\right)^2}+\frac{e^4\xi v^2\chi\left(m^2\xi\right)}{m^2\left(m^2\xi+p^2\right)^2}-\frac{e^3\xi v\chi\left(m^2\xi\right)}{m\left(m^2\xi+p^2\right)^2}+\frac{e^2\chi\left(m^2\xi\right)\left(m_h^2+m^2\xi+p^2\right)}{m^2\left(m^2\xi+p^2\right)^2} \\
- & \frac{e^2\chi\left(m_h^2\right)}{\left(m^2\xi+p^2\right)^2}-\frac{e^2\chi\left(m^2\right)\left(m_h^2-m^2+p^2\right)}{m^2\left(m^2\xi+p^2\right)^2}-\frac{3e^2m_h^2\chi\left(m^2\xi\right)}{2m^2\left(m^2\xi+p^2\right)^2}-\frac{e^2m_h^2\chi\left(m_h^2\right)}{2m^2\left(m^2\xi+p^2\right)^2} \\
- & \frac{e^2\xi\chi\left(m^2\xi\right)}{\left(m^2\xi+p^2\right)^2}\Big)\Big]\mathcal{L}_{\mu\nu}. \qquad (489)
\end{aligned}
$$

APPENDIX H – Propagators and vertices of the $SU(2)$ Higgs model in the R_ξ gauge

The tree level elementary propagators of the fields are easily computed, being given by

$$\begin{aligned}
\langle A^a_\mu(p)A^b_\nu(-p)\rangle &= \frac{\delta^{ab}}{p^2+m^2}\mathcal{P}_{\mu\nu}(p) + \delta^{ab}\frac{\xi}{p^2+\xi m^2}\mathcal{L}_{\mu\nu}(p),\\
\langle \rho^a(p)\rho^b(-p)\rangle &= \frac{\delta^{ab}}{p^2+\xi m^2},\\
\langle h(p)h(-p)\rangle &= \frac{1}{p^2+m_h^2},\\
\langle A^a_\mu(p)b^b(-p)\rangle &= \delta^{ab}\frac{p_\mu}{p^2+\xi m^2},\\
\langle b^a(p)\rho^b(-k)\rangle &= \delta^{ab}\frac{im}{p^2+\xi m^2}
\end{aligned} \tag{490}$$

and

$$\langle \bar{c}^a(p)c^b(-p)\rangle = \frac{\delta^{ab}}{p^2+\xi m^2} \tag{491}$$

for the ghost propagator. For all vertices, adopting the convention that the momentum is flowing towards the vertex, we get

- The AAh-vertex: $\Gamma_{A^a_\mu A^b_\nu h}(-p_1,-p_2,-p_3) = -\frac{g^2 v}{2}\delta_{\mu\nu}\delta^{ab}\delta(p_1+p_2+p_3)$.
- The $\rho\rho A$-vertex: $\Gamma_{\rho^a\rho^b A^c_\mu}(-p_1,-p_2,-p_3) = \frac{g}{2}i\epsilon^{abc}(p_{\mu,1}-p_{\mu,2})\delta(p_1+p_2+p_3)$.
- The $A\rho h$-vertex: $\Gamma_{A^a_\mu\rho^b h}(-p_1,-p_2,-p_3) = i\frac{g}{2}\delta^{ab}(p_{\mu,3}-p_{\mu,2})\delta(p_1+p_2+p_3)$.
- The hhh vertex: $\Gamma_{hhh}(-p_1,-p_2,-p_3) = -3\lambda v\ \delta(p_1+p_2+p_3)$.
- The $h\rho\rho$ vertex: $\Gamma_{h\rho^a\rho^b}(-p_1,-p_2,-p_3) = -\lambda v\delta^{ab}\ \delta(p_1+p_2+p_3)$.
- The AAA-vertex: $\Gamma_{A^a_\mu A^b_\nu A^c_\sigma}(-p_1,-p_2,-p_3)$
  $= -igf^{abc}\left[(p_1-p_3)_\nu\delta_{\sigma\mu} + (p_3-p_2)_\mu\delta_{\nu\sigma} + (p_2-p_1)_\sigma\delta_{\nu\mu}\right]\delta(p_1+p_2+p_3)$.
- The $\bar{c}Ac$-vertex: $\Gamma_{\bar{c}^a A^b_\mu c^c}(-p_1,-p_2,-p_3) = igf^{abc}p_{1,\mu}\delta(p_1+p_2+p_3)$.
- The $AAAA$-vertex: $\Gamma_{A^a_\mu A^b_\nu A^c_\rho A^d_\sigma}(-p_1,-p_2,-p_3,-p_4)$
  $= g^2[f^{eab}f^{ecd}(\delta_{\mu\sigma}\delta_{\nu\rho}-\delta_{\mu\rho}\delta_{\nu\sigma}) + f^{eac}f^{ebd}(\delta_{\mu\sigma}\delta_{\nu\rho}-\delta_{\mu\nu}\delta_{\rho\sigma})$
  $+ f^{ead}f^{ebc}(\delta_{\mu\rho}\delta_{\nu\sigma}-\delta_{\mu\nu}\delta_{\rho\sigma})]\delta(p_1+p_2+p_3+p_4)$.
- The $AAhh$-vertex: $\Gamma_{A^a_\mu A^b_\nu hh}(-p_1,-p_2,-p_3,-p_4) = -\frac{1}{2}g^2\delta^{ab}\delta_{\mu\nu}$.
- The $AA\rho\rho$-vertex: $\Gamma_{A^a_\mu A^b_\nu\rho^c\rho^d}(-p_1,-p_2,-p_3,-p_4) = -\frac{1}{2}g^2\delta_{\mu\nu}\delta^{ab}\delta^{cd}$.

APPENDIX I – Elementary propagators of the $SU(2)$ Higgs model in the R_ξ gauge

Here we will calculate the one-loop corrections to the Higgs and gauge field propagator. This requires the calculation [16] of the Feynman diagrams as shown in Figures 41 and 42. We will use the following definitions:

$$\begin{aligned}\eta(m_1,m_2) &\equiv \frac{1}{(4\pi)^{d/2}}\Gamma(2-\frac{d}{2})\int_0^1 dx\left(p^2x(1-x)+xm_1+(1-x)m_2\right)^{d/2-2},\\ \chi(m_1) &\equiv \frac{1}{(4\pi)^{d/2}}\Gamma(1-\frac{d}{2})m_1^{d/2-1}.\end{aligned} \tag{492}$$

Notice that the last four diagrams for both particles are zero for $\langle h\rangle = 0$. In fact, including these diagrams has the same effect as making a shift in the minimizing value of the scalar field Φ to demand $\langle h\rangle = 0$, see the Appendix of (DUDAL et al., 2019) for the technical details. In the context of the FMS operators, we found it more convenient to expand around the (classical) v that is gauge invariant, and thus to include the tadpoles. Expanding the FMS operator around the quantum corrected vev would lead to cancellations in that quantum vev coming from the propagator loop corrections to render it gauge invariant again, indeed the minimum of the quantum corrected effective Higgs potential is not gauge invariant itself.

I.0.1 Higgs propagator

The first diagrams contributing to the Higgs self-energy are of the snail type, renormalizing the masses of the internal fields. The Higgs boson snail (first diagram in the first line of Figure 41):

$$\Gamma_{hh,1}(p^2) = -\frac{3\lambda\chi\left(m_h^2\right)}{2\left(m_h^2+p^2\right)^2}, \tag{493}$$

the Goldstone boson snail (second diagram in the first line of Figure 41):

$$\Gamma_{hh,2}(p^2) = -\frac{3\lambda\chi\left(m^2\xi\right)}{2\left(m_h^2+p^2\right)^2}, \tag{494}$$

[16] We have used from (PASSARINO; VELTMAN, 1979) the technique of modifying integrals into "master integrals" without numerators.

Figure 41 - Propagator $\langle h(p)h(-p)\rangle$

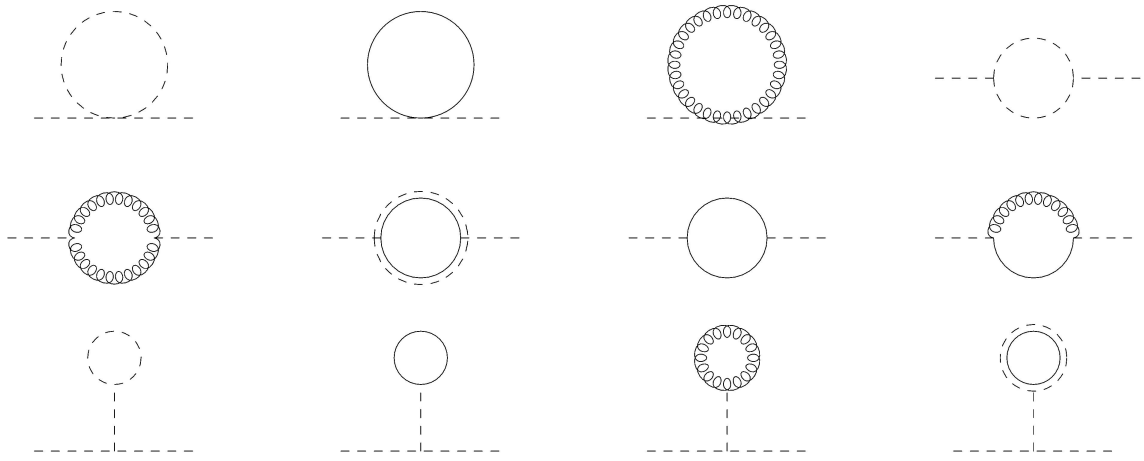

Legend: One-loop contributions to the propagator $\langle h(p)h(-p)\rangle$. Curly lines represent the gauge field, dashed lines the Higgs field, solid lines the Goldstone boson and double lines the ghost field.
Source: The author, 2020.

and the gauge field snail (third diagram in the first line of Figure 41):

$$\Gamma_{hh,3}(p^2) = -\frac{3(d-1)g^2\chi\left(m^2\right)}{4\left(m_h^2+p^2\right)^2} - \frac{3g^2\xi\chi\left(m^2\xi\right)}{4\left(m_h^2+p^2\right)^2}. \tag{495}$$

Next, we meet a couple of sunset diagrams. The Higgs boson sunset (fourth diagram in the first line of Figure 41):

$$\Gamma_{hh,4}(p^2) = \int_0^1 dx\Big\{\frac{9\lambda^2v^2\eta\left(m_h^2,m_h^2\right)}{2\left(m_h^2+p^2\right)^2}\Big\}, \tag{496}$$

the gauge field sunset (first diagram in the second line of Figure 41):

$$\begin{aligned}\Gamma_{hh,5}(p^2) &= \int_0^1 dx\Big\{\frac{3g^2\eta\left(m^2,m^2\right)\left(4(D-1)m^4+4m^2p^2+p^4\right)}{8m^2\left(m_h^2+p^2\right)^2}\\ &+ \frac{3g^2\left(2m^2\xi+p^2\right)^2\eta\left(m^2\xi,m^2\xi\right)}{8m^2\left(m_h^2+p^2\right)^2}\\ &- \frac{3g^2\left(m^4(\xi-1)^2+2m^2\xi p^2+2m^2p^2+p^4\right)\eta\left(m^2,m^2\xi\right)}{4m^2\left(m_h^2+p^2\right)^2}\\ &+ \frac{3g^2(\xi-1)\chi\left(m^2\right)}{4\left(m_h^2+p^2\right)^2}\\ &- \frac{3g^2(\xi-1)\chi\left(m^2\xi\right)}{4\left(m_h^2+p^2\right)^2}\Big\},\end{aligned} \tag{497}$$

the ghost sunset (second diagram in the second line of Figure 41):

$$\Gamma_{hh,6}(p^2) = -\int_0^1 dx\Big\{\frac{3g^2m^2\xi^2\eta\left(m^2\xi,m^2\xi\right)}{4\left(m_h^2+p^2\right)^2}\Big\}, \tag{498}$$

the Goldstone boson sunset (third diagram in the second line of Figure 41):

$$\Gamma_{hh,7}(p^2) = \int_0^1 dx\Big\{\frac{3\lambda^2v^2\eta\left(m^2\xi,m^2\xi\right)}{2\left(m_h^2+p^2\right)^2}\Big\}, \tag{499}$$

and a mixed Goldstone-gauge sunset (fourth diagram in the second line of Figure 41):

$$\begin{aligned}\Gamma_{hh,8}(p^2) &= \int_0^1 dx\Big\{\frac{3g^2\left(\left(m^2(\xi-1)+p^2\right)^2+4m^2p^2\right)\eta\left(m^2,m^2\xi\right)}{4m^2\left(m_h^2+p^2\right)^2}\\ &- \frac{3g^2\left(m^2\xi+p^2\right)^2\eta\left(m^2\xi,m^2\xi\right)}{4m^2\left(m_h^2+p^2\right)^2}\\ &+ \frac{3g^2\chi\left(m^2\xi\right)\left(m^2(2\xi-1)+p^2\right)}{4m^2\left(m_h^2+p^2\right)^2}-\frac{3g^2\chi\left(m^2\right)\left(m^2(\xi-1)+p^2\right)}{4m^2\left(m_h^2+p^2\right)^2}\Big\}.\end{aligned} \tag{500}$$

Finally, we have the tadpole diagrams. The Higgs balloon (first diagram on the third line of Figure 41):

$$\Gamma_{hh,9}(p^2) = \frac{9\lambda^2v^2\chi\left(m_h^2\right)}{2m_h^2\left(m_h^2+p^2\right)^2}, \tag{501}$$

the gauge balloon (second diagram on the third line of Figure 41):

$$\Gamma_{hh,10}(p^2) = \frac{9g\lambda mv\left((d-1)\chi\left(m^2\right)+\xi\chi\left(m^2\xi\right)\right)}{2m_h^2\left(m_h^2+p^2\right)^2}, \tag{502}$$

the Goldstone boson balloon (third diagram on the third line of Figure 41):

$$\Gamma_{hh,11}(p^2) = \frac{9\lambda^2v^2\chi\left(m^2\xi\right)}{2m_h^2\left(m_h^2+p^2\right)^2}, \tag{503}$$

the ghost balloon (fourth diagram on the third line of Figure 41):

$$\Gamma_{hh,12}(p^2) = -\frac{9g\lambda m\xi v\chi\left(m^2\xi\right)}{2m_h^2}. \tag{504}$$

Putting together eqs. (493) to (504) we find the Higgs propagator up to first order in $\hbar$

$$\begin{aligned}\langle h(x)\,h(y)\rangle &= \frac{1}{p^2+m_h^2}+g^2\int_0^1 dx\Big\{\frac{3\left(4(d-1)m^4+4m^2p^2+p^4\right)}{8m^2}\eta\left(m^2,m^2\right)\\ &+ \frac{9m_h^4}{8m^2}\eta\left(m_h^2,m_h^2\right)+\frac{3\left(m_h^4-p^4\right)}{8m^2}\eta\left(m^2\xi,m^2\xi\right)+\frac{\left(6(d-1)m^2-3p^2\right)}{4m^2}\chi\left(m^2\right)\\ &+ \frac{3\left(m_h^2+p^2\right)}{4m^2}\chi\left(m^2\xi\right)+\frac{3m_h^2}{4m^2}\chi\left(m_h^2\right)\Big\}\frac{1}{(p^2+m_h^2)^2}.\end{aligned} \tag{505}$$

The resummed one-loop Higgs propagator can be now approximated by

$$\begin{aligned} G^{-1}_{hh}(p^2) &= p^2 + m_h^2 - g^2 \int_0^1 dx \Big\{ \frac{3\left(4(d-1)m^4 + 4m^2p^2 + p^4\right)}{8m^2} \eta\left(m^2, m^2\right) \\ &+ \frac{9m_h^4}{8m^2}\eta\left(m_h^2, m_h^2\right) + \frac{3\left(m_h^4 - p^4\right)}{8m^2}\eta\left(m^2\xi, m^2\xi\right) + \frac{\left(6(d-1)m^2 - 3p^2\right)}{4m^2}\chi\left(m^2\right) \\ &+ \frac{3\left(m_h^2 + p^2\right)}{4m^2}\chi\left(m^2\xi\right) + \frac{3m_h^2}{4m^2}\chi\left(m_h^2\right) \Big\}. \end{aligned} \tag{506}$$

For $d = 4$, the above expression, eq. (506), is divergent. Employing the procedure of dimensional regularization, *i.e.* setting $d = 4 - \epsilon$, the divergent part for $G_{hh}(p^2)$ is given by:

$$G_{hh,\mathrm{div}}(p^2) = \frac{g^2\left(\frac{3m_h^4}{m^2} - 3\xi m_h^2 - 3\xi p^2 + 9p^2\right)}{32\pi^2\epsilon}, \tag{507}$$

which, following the $\overline{MS}$-scheme, are re-absorbed by the introduction of suitable local counterterms. We remain thus with the finite part of the Higgs propagator, given in eq. (320).

I.0.2 Gauge field propagator

The first diagram contributing to transverse part of the gauge field self-energy is the gauge field snail (first diagram in the first line of Figure 42) and gives a contribution:

$$\begin{aligned} \Pi_{AA^T,1}(p^2) &= \frac{2g^2\left(p^2 - d\left(d^2 - 3d + 3\right)p^2\right)\chi\left(m^2\right)}{(d-1)dp^2\left(m^2 + p^2\right)^2} \\ &- \frac{2g^2\xi\left(\left((d-2)dp^2 + p^2\right)\chi\left(m^2\xi\right)\right)}{(d-1)dp^2\left(m^2 + p^2\right)^2}. \end{aligned} \tag{508}$$

The second diagram is the Goldstone boson snail (second diagram in the first line of Figure 42):

$$\Pi_{AA^T,2}(p^2) = -\frac{3g^2\chi\left(m^2\xi\right)}{4\left(m^2 + p^2\right)^2}. \tag{509}$$

The third diagram is the Higgs boson snail (third diagram in the first line of Figure 42):

$$\Pi_{AA^T,3}(p^2) = -\frac{g^2\chi\left(m_h^2\right)}{4\left(m^2 + p^2\right)^2}. \tag{510}$$

The fourth diagram is the gauge field sunrise (first diagram in the second line of Figure 42):

$$\Pi_{AA^T,4}(p^2) =$$

Figure 42 - One-loop gauge field self-energy

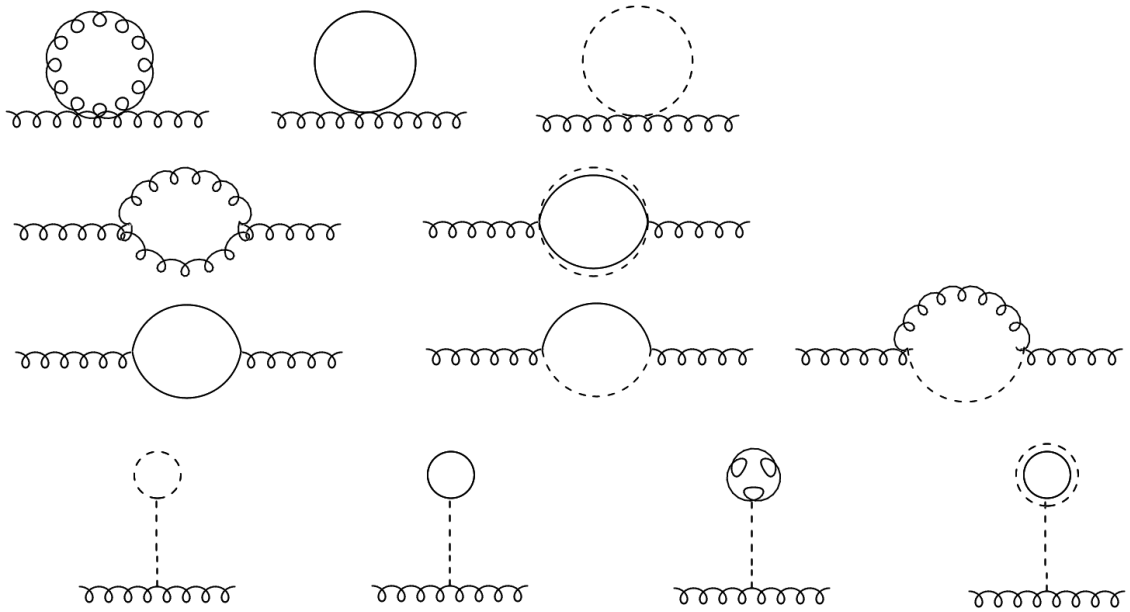

Legend: Contributions to the one-loop gauge field self-energy.
Source: The author, 2020.

$$
\begin{aligned}
& g^2 \int_0^1 dx \Big\{ \frac{\eta\left(m^2, m^2\xi\right)\left(2m^2p^2(-2d+\xi+3)+m^4(\xi-1)^2+p^4\right)}{2(d-1)m^4p^2} \\
- \; & \frac{\left(4m^2+p^2\right)\eta\left(m^2,m^2\right)\left(4(d-1)m^4+4(3-2d)m^2p^2+p^4\right)}{4(d-1)m^4\left(m^2+p^2\right)^2} \\
- \; & \frac{\left(4m^2\xi p^4+p^6\right)\eta\left(m^2\xi, m^2\xi\right)}{4(d-1)m^4\left(m^2+p^2\right)^2} \\
+ \; & \frac{\chi\left(m^2\xi\right)}{2(d-1)dm^2p^2\left(m^2+p^2\right)^2} \\
\times \; & \left(4d^2\left(m^2(\xi+1)p^2+p^4\right)+d\left(m^4(\xi-1)-m^2(6\xi+7)p^2+(\xi-7)p^4\right)+4m^2\xi p^2\right) \\
- \; & \frac{\chi\left(m^2\right)\left(4d^2p^4+d\left(m^4(\xi-1)+m^2(2\xi-5)p^2+(\xi-7)p^4\right)+4m^2p^2\right)}{2(d-1)dm^2p^2\left(m^2+p^2\right)^2} \Big\}. \qquad (511)
\end{aligned}
$$

The fifth diagram is the ghost sunrise (second diagram in the second line of Figure 42):

$$
\begin{aligned}
\Pi_{AA^T,5}(p^2) &= g^2 \int_0^1 dx\eta\left(m^2\xi, m^2\xi\right)\left(\frac{2m^2\xi}{(d-1)\left(m^2+p^2\right)^2}+\frac{p^2}{2(d-1)\left(m^2+p^2\right)^2}\right) \\
&- \frac{\chi\left(m^2\xi\right)}{(d-1)\left(m^2+p^2\right)^2}. \qquad (512)
\end{aligned}
$$

The sixth diagram is the Goldstone sunrise (first diagram in the third line of Figure 42):

$$\begin{aligned}\Pi_{AA^T,6}(p^2) &= g^2\int_0^1 dx\eta\left(m^2\xi,m^2\xi\right)(-\frac{m^2\xi}{(d-1)\left(m^2+p^2\right)^2}\\ &- \frac{p^2}{4(d-1)\left(m^2+p^2\right)^2})\\ &+ \frac{\chi\left(m^2\xi\right)}{2(d-1)\left(m^2+p^2\right)^2}.\end{aligned} \tag{513}$$

The seventh diagram is the mixed Goldstone-Higgs sunrise (second diagram in the third line of Figure 42):

$$\begin{aligned}&\Pi_{AA^T,7}(p^2) =\\ &g^2\int_0^1 dx - \frac{\left(\left(-m_h^2+m^2\xi+p^2\right)^2+4m_h^2p^2\right)\eta\left(m_h^2,m^2\xi\right)}{4(d-1)p^2\left(m^2+p^2\right)^2} + \frac{\chi\left(m_h^2\right)\left(-m_h^2+m^2\xi+p^2\right)}{4(d-1)p^2\left(m^2+p^2\right)^2}\\ &+ \frac{\chi\left(m^2\xi\right)\left(m_h^2-m^2\xi+p^2\right)}{4(d-1)p^2\left(m^2+p^2\right)^2}.\end{aligned} \tag{514}$$

The eighth diagram is the mixed Goldstone-gauge field sunrise (third diagram in the third line of Figure 42):

$$\begin{aligned}\Pi_{AA^T,8}(p^2) &= g^2\int_0^1 dx\frac{\left(\left(m_h^2-m^2\xi+p^2\right)^2+4m^2\xi p^2\right)\eta\left(m_h^2,m^2\xi\right)}{4(D-1)p^2\left(m^2+p^2\right)^2}\\ &- \frac{\eta\left(m^2,m_h^2\right)\left(\left(m_h^2-m^2+p^2\right)^2-4(D-2)m^2p^2\right)}{4(D-1)p^2\left(m^2+p^2\right)^2} - \frac{m^2(\xi-1)\chi\left(m_h^2\right)}{4(D-1)p^2\left(m^2+p^2\right)^2}\\ &- \frac{\chi\left(m^2\xi\right)\left(m_h^2-m^2\xi+p^2\right)}{4(D-1)p^2\left(m^2+p^2\right)^2} + \frac{\chi\left(m^2\right)\left(m_h^2-m^2+p^2\right)}{4(D-1)p^2\left(m^2+p^2\right)^2}.\end{aligned} \tag{515}$$

Finally, we have four tadpole (balloon) diagrams. The Higgs boson balloon (first diagram of the last line in Figure 42):

$$\Pi_{AA^T,5}(p^2) = \frac{3gm\chi\left(m_h^2\right)}{2v\left(m^2+p^2\right)^2}, \tag{516}$$

the Goldstone boson balloon (second diagram of the last line in Figure 42):

$$\Pi_{AA^T,6}(p^2) = \frac{3g\lambda mv\chi\left(m^2\xi\right)}{2m_h^2\left(m^2+p^2\right)^2}, \tag{517}$$

The gauge field balloon (third diagram of the last line in Figure 42):

$$\Pi_{AA^T,7}(p^2) = \frac{3(D-1)g^2m^2\chi\left(m^2\right)}{2m_h^2\left(m^2+p^2\right)^2} + \frac{3g^2m^2\xi\chi\left(m^2\xi\right)}{2m_h^2\left(m^2+p^2\right)^2} \tag{518}$$

and finally, the ghost balloon (fourth diagram of the last line in Figure 42):

$$\Gamma_{AA^T,8}(p^2) \;=\; -\frac{3g^2m^2\xi\chi\left(m^2\xi\right)}{2m_h^2\left(m^2+p^2\right)^2}. \tag{519}$$

Combining all these contributions (508)-(519), we find the total one-loop correction to the gauge field self-energy

$$\begin{aligned}
&\left\langle A^a_\mu(p)A^b_\nu(p)\right\rangle^T = \frac{\delta^{ab}}{p^2+m^2}\\
+\;& \delta^{ab}g^2\int_0^1 dx\Big\{-\frac{(2(3-2d)m^2p^2+m_h^4-2m_h^2\left(m^2-p^2\right)+m^4+p^4)}{4(d-1)p^2}\eta\left(m^2,m_h^2\right)\\
+\;& \frac{\left(m^2+p^2\right)^2\left(2m^2p^2(-2d+\xi+3)+m^4(\xi-1)^2+p^4\right)}{2(d-1)m^4p^2}\eta\left(m^2,m^2\xi\right)\\
+\;& \frac{\left(m^4-p^4\right)\left(4m^2\xi+p^2\right)}{4(d-1)m^4}\eta\left(m^2\xi,m^2\xi\right)\\
-\;& \frac{\left(4m^2+p^2\right)\left(4(d-1)m^4+4(3-2d)m^2p^2+p^4\right)}{4(d-1)m^4}\eta\left(m^2,m^2\right)\\
+\;& \frac{1}{4(d-1)m_h^2m^2p^2}\\
\times\;& \left(m_h^2\left(-m^2p^2\left(8d^2-24d+4\xi+13\right)-2p^4(4d+\xi-7)+m^4(1-2\xi)\right)\right.\\
+\;& \left.6(d-1)^2m^4p^2+m_h^4m^2\right)\chi\left(m^2\right)\\
-\;& \frac{((d-2)p^2+m_h^2-m^2)}{4(d-1)p^2}\chi\left(m_h^2\right)\\
+\;& \frac{(m^2p^2(5d+4\xi-13)+2p^4(4d+\xi-7)+2m^4(\xi-1))}{4(d-1)m^2p^2}\chi\left(m^2\xi\right)\\
+\;& \frac{3}{4}\chi\left(m_h^2\right)+\frac{3}{4}\chi\left(m^2\xi\right)\Big\}\frac{1}{(p^2+m^2)^2}
\end{aligned} \tag{520}$$

and the resummed propagator for the transverse gauge field can be approximated, at one-loop order, by

$$\begin{aligned}
&G^{-1}_{AA^T} = \delta^{ab}\Bigg(p^2+m^2\\
&-g^2\int_0^1 dx\Big\{-\frac{(2(3-2d)m^2p^2+m_h^4-2m_h^2\left(m^2-p^2\right)+m^4+p^4)}{4(d-1)p^2}\eta\left(m^2,m_h^2\right)\\
+\;& \frac{\left(m^2+p^2\right)^2\left(2m^2p^2(-2d+\xi+3)+m^4(\xi-1)^2+p^4\right)}{2(d-1)m^4p^2}\eta\left(m^2,m^2\xi\right)\\
+\;& \frac{\left(m^4-p^4\right)\left(4m^2\xi+p^2\right)}{4(d-1)m^4}\eta\left(m^2\xi,m^2\xi\right)\\
-\;& \frac{\left(4m^2+p^2\right)\left(4(d-1)m^4+4(3-2d)m^2p^2+p^4\right)}{4(d-1)m^4}\eta\left(m^2,m^2\right)\\
+\;& \frac{1}{4(d-1)m_h^2m^2p^2}
\end{aligned}$$

$$
\begin{aligned}
\times \quad & (m_h^2\left(-m^2p^2\left(8d^2-24d+4\xi+13\right)-2p^4(4d+\xi-7)+m^4(1-2\xi)\right) \\
+ \quad & 6(d-1)^2m^4p^2+m_h^4m^2)\chi\left(m^2\right) \\
- \quad & \frac{((d-2)p^2+m_h^2-m^2)}{4(d-1)p^2}\chi\left(m_h^2\right) \\
+ \quad & \frac{(m^2p^2(5d+4\xi-13)+2p^4(4d+\xi-7)+2m^4(\xi-1))}{4(d-1)m^2p^2}\chi\left(m^2\xi\right) \\
+ \quad & \frac{3}{4}\chi\left(m_h^2\right)+\frac{3}{4}\chi\left(m^2\xi\right)\Big\}\Bigg). \qquad (521)
\end{aligned}
$$

For $d = 4 - \epsilon$, following the procedure of dimensional regularization, we find that the divergent part for $G_{AA^T}(p^2)$ is given by:

$$
G_{AA^T,\mathrm{div}}(p^2) \;=\; \frac{g^2}{\pi^2\epsilon}\left(-\frac{9m^4}{16m_h^2}-\frac{3m_h^2}{32}-\frac{m^2\xi}{8}-\frac{3m^2}{32}-\frac{\xi p^2}{8}+\frac{25p^2}{48}\right), \qquad (522)
$$

and these terms can be, following the $\overline{MS}$-scheme, absorbed by means of appropriate counterterms. We remain with the finite part of the propagator, given in eq. (330).

APPENDIX J – Contributions to $\langle O(p)O(-p)\rangle$

The diagrams which contribute to the correlation function $\langle O(p)O(-p)\rangle$ are depicted in Figure(43)

The first term is v^2 times the one-loop correction to the Higgs propagator, given in eq. (506). The second term is

$$v\langle h(p)(\rho^a\rho^a)(-p)\rangle = -3\frac{m_h^2\eta\left(m^2\xi,m^2\xi\right)}{m_h^2+p^2}. \tag{523}$$

The third term is

$$\begin{aligned} v\langle h(p)h^2(-p)\rangle &= -\frac{3m_h^2\eta\left(m_h^2,m_h^2\right)}{m_h^2+p^2}-\frac{3\chi\left(m_h^2\right)}{m_h^2+p^2}-\frac{\chi\left(m^2\xi\right)}{m_h^2+p^2}-\frac{2(D-1)m^2\chi\left(m^2\right)}{m_h^2\left(m_h^2+p^2\right)} \\ &- \frac{2m^2\xi\chi\left(m^2\xi\right)}{m_h^2\left(m_h^2+p^2\right)} \\ &+ \frac{2m^2\xi\chi\left(m^2\xi\right)}{m_h^2\left(m_h^2+p^2\right)}. \end{aligned} \tag{524}$$

The fourth term is

$$\langle m_h^2(p)m_h^2(-p)\rangle = \frac{1}{2}\eta\left(m_h^2,m_h^2\right). \tag{525}$$

The fifth term is

$$\langle(\rho^a\rho^a)(p)(\rho^b\rho^b)(-p)\rangle = \frac{3}{2}\eta\left(\xi m^2,\xi m^2\right) \tag{526}$$

and together these terms give the correlation function of the scalar composite operator O up to first order in $\hbar$

$$\begin{aligned} \langle O(p)O(-p)\rangle &= \frac{v^2}{p^2+m_h^2}+\int_0^1 dx\Big\{\frac{3}{2}\eta\left(m^2,m^2\right)\left(4(d-1)m^4+4m^2p^2+p^4\right) \\ &+ \frac{1}{2}(p^2-2m_h^2)^2\eta\left(m_h^2,m_h^2\right) \\ &- \frac{3p^2\chi(m^2)(2(d-1)m^2+m_h^2)}{m_h^2}-3p^2\chi(m_h^2)\Big\}\frac{1}{(p^2+m_h^2)^2}. \end{aligned} \tag{527}$$

Thus, for the one-loop resummed correlation function, we get

$$\begin{aligned} G_{OO}^{-1}(p^2) &= \frac{p^2+m_h^2}{v^2}-\frac{1}{v^4}\int_0^1 dx\Big\{\frac{3}{2}\eta\left(m^2,m^2\right)\left(4(d-1)m^4+4m^2p^2+p^4\right) \\ &+ \frac{1}{2}(p^2-2m_h^2)^2\eta\left(m_h^2,m_h^2\right) \\ &- \frac{3p^2\chi(m^2)(2(d-1)m^2+m_h^2)}{m_h^2}-3p^2\chi(m_h^2)\Big\}\frac{1}{(p^2+m_h^2)^2}. \end{aligned} \tag{528}$$

Figure 43 - Correlation function $\langle OO \rangle$

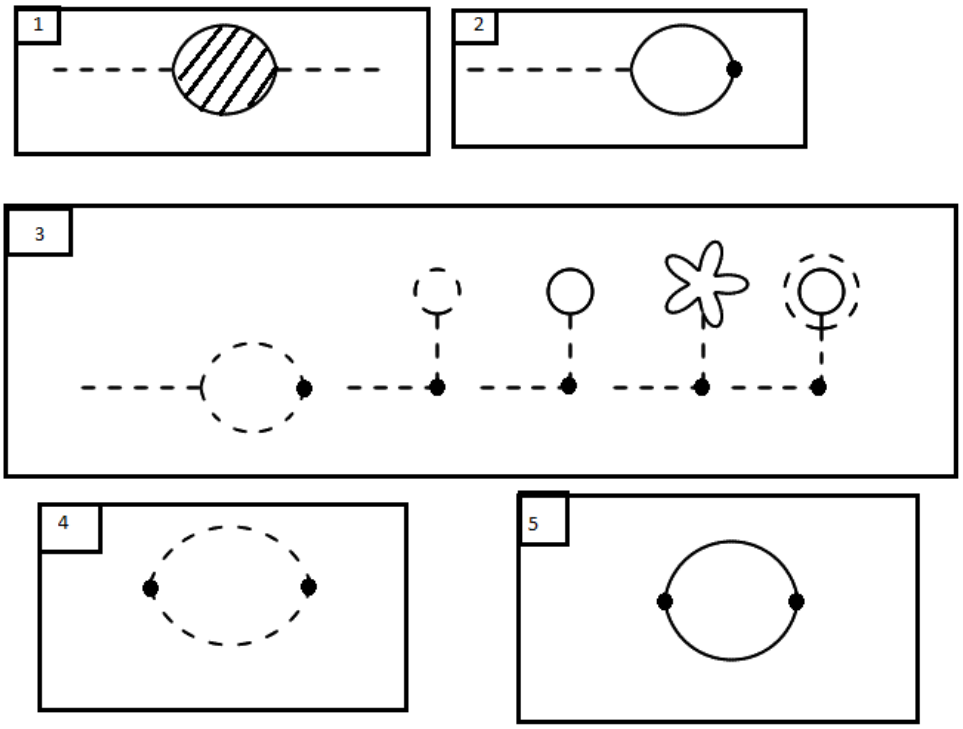

Legend: One-loop contributions to the correlation function $\langle OO \rangle$. Wavy lines represent the gauge field, dashed lines the Higgs field, solid lines the Goldstone boson and double lines the ghost field. The • indicates the insertion of a composite operator.

Source: The author, 2020.

Following the procedure of dimensional regularization for $d = 4 - \epsilon$, we find that the divergent part of the correlator is given by

$$G^{-1}_{OO,\text{div}} = \frac{1}{4v^4\pi^2\epsilon}\Big(\frac{9g^4p^2v^2}{16\lambda} + \frac{9g^4v^4}{16} + \frac{9}{8}g^2p^2v^2 + p^4 + \frac{1}{2}\lambda p^2v^2 + \lambda^2v^4\Big), \tag{529}$$

which can be accounted for by appropriate counterterm, following the $\overline{MS}$-scheme renormalization procedure. We remain with the finite part of the correlator, given in eq. (375).

APPENDIX K – A few comments on the unitary gauge

It is well-known that in the unitary gauge the unphysical fields, like the Goldstone and ghost fields, decouple, a feature which allows for a more direct link with the spectrum of the elementary excitations of the model. However, this gauge is known to be non-renormalizable. In fact, working directly with the elementary tree level propagators taken already in the unitary limit, *i.e.* $\xi \to \infty$, and following the steps of dimensional regularization, we find that the divergent part of the Higgs propagator reads

$$G^{-1}_{hh,\mathrm{div}}(p^2) \;=\; \frac{3g^2\,(m_h^4 + 6m^2p^2 + p^4)}{64\pi^2 m^2 \epsilon}. \tag{530}$$

In expression (530) we clearly see the presence of the term $\sim \frac{p^4}{\epsilon m^2}$, signalling the aforementioned issue of the non-renormalizability. Nevertheless, it is interesting to observe that, if we remove the divergent part (530) anyway, we obtain the spectral function as shown in Figure 44. This spectral function is almost identical to that obtained for the composite operator $O(x)$, see Figure 37.

For the gauge field propagator, proceeding in the same way, we find the divergent part

$$G^{-1}_{AA,\mathrm{div}}(p^2) \;=\; \frac{1}{\epsilon}\Big(-\frac{9g^2m^4}{16\pi^2 m_h^2} - \frac{g^2p^6}{96\pi^2 m^4} + \frac{7g^2p^4}{48\pi^2 m^2} + \frac{3g^2m^2}{32\pi^2} + \frac{83g^2p^2}{96\pi^2} - \frac{3\lambda m^2}{8\pi^2}\Big) \tag{531}$$

which shows again the non-renormalizability of unitary gauge, through the terms $\sim \frac{p^6}{\epsilon m^4}$ and $\sim \frac{p^4}{\epsilon m^2}$. However, if we remove again those terms anyway, we obtain the spectral function as shown in Figure 45. Nevertheless, as already remarked in the previous sections, this nice behaviour of the spectral densities for the Higgs and gauge field obtained by a direct use of the tree level propagators already taken in the unitary limit, $\xi \to \infty$, can be, to some extent, justified by the fact that we are working at the one-loop order in perturbation theory. Since overlapping divergences start from one-loop onward, we can easily figure out that the naive use of the elementary tree level propagators taken already in the unitary limit will run into severe non-renormalizibility issues, making the removal of the (overlapping) divergent parts (530), (531) quite problematic.

Figure 44 - Spectral function of $\langle h(p)h(-p)\rangle$ in the unitary gauge

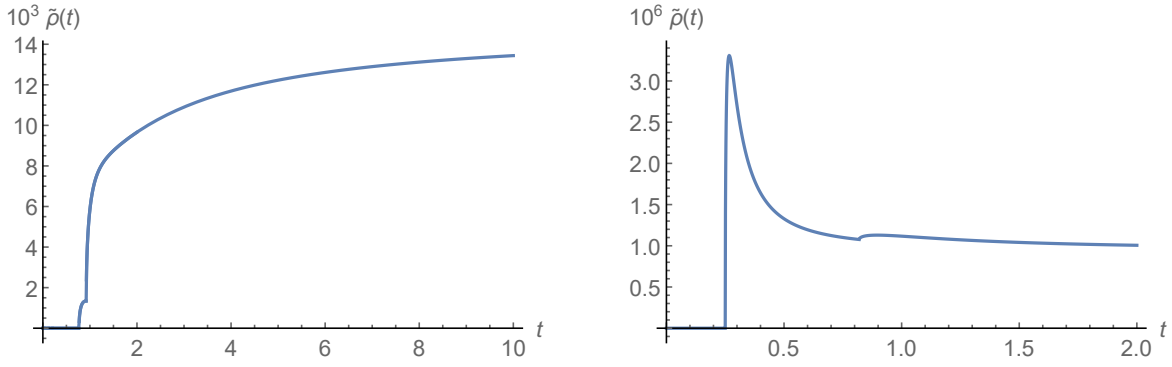

Legend: Spectral function for the propagator $\langle h(p)h(-p)\rangle$ in the unitary gauge, with t given in unity of μ^2, for the Region I (left) and Region II (right), with parameter values given in Table 3.

Source: The author, 2020.

Figure 45 - Spectral function of $\langle A^a_\mu(p)A^b_\nu(-p)\rangle$ in the unitary gauge

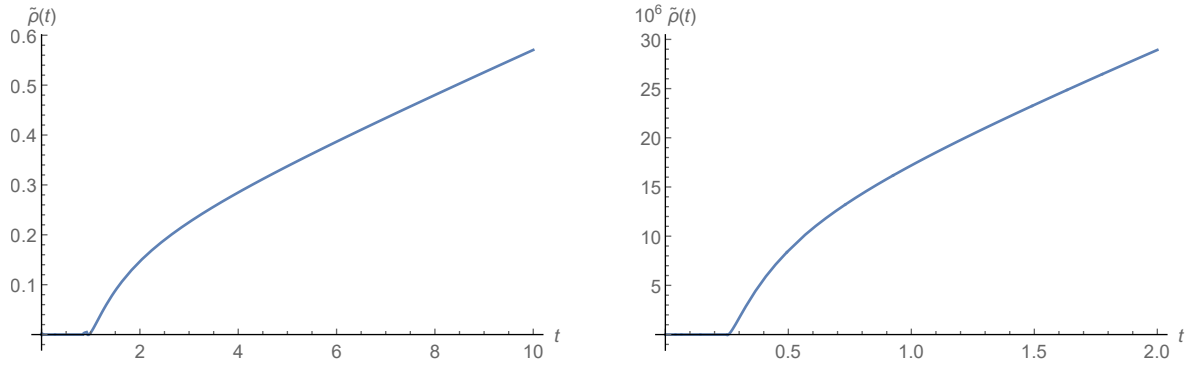

Legend: Spectral function for the propagator $\langle A^a_\mu(p)A^b_\nu(-p)\rangle$ in the unitary gauge, with t given in unity of μ^2, for the Region I (left) and Region II (right), with parameter values given in Table 3.

Source: The author, 2020.